PREDICTIVE ENERGY FUNCTION BASED POWER SYSTEM TRANSIENT STABILITY ASSESSMENT AND IMPROVEMENT

by

Amirreza Sahami

A dissertation submitted to the faculty of
The University of North Carolina at Charlotte
in partial fulfillment of the requirements
for the degree of Doctor of Philosophy in
Electrical Engineering

Charlotte

2019

Approved by:

_____
Dr. Sukumar Kamalasadan

_____
Dr. Valentina Cecchi

_____
Dr. Babak Parkhideh

_____
Dr. Srinivas Pulugurtha

_____
Dr. Zia Salami

ABSTRACT

AMIRREZA SAHAMI. Predictive Energy Function Based Power System Transient Stability Assessment and Improvement. (Under the direction of DR. SUKUMAR KAMALASADAN)

Transient stability assessment and improvement are critical for power grid operation. It deals with the assessment of transient behavior of the power grid (especially the generators) when subjected to large disturbances. State-of-the-art approaches for transient assessment are classified into two: a) numerical methods and b) direct energy functions methods. Numerical methods are computationally expensive and current energy function methods require extensive system knowledge in advance. In this dissertation, two new approaches for transient stability assessment is investigated. First, a new method for predicting the behavior of power system generators is presented. The main advantage of this method is that it helps to find the critical generators, their critical clearing times and angles. Consequently, the system transient stability prediction can be performed. Also, using the Lyapunov theory and energy concept, the prediction can be used to find the unstable equilibrium point of the system. Second, an approach for assessing the potential energy capacity of the power system to prevent and control the transient instability of the power system is proposed. The approach can be used to find the appropriate control strategy so that system instability can be prevented. The proposed methods are tested on IEEE 9 bus, IEEE 39 bus, and North Carolina−South Carolina 500 bus systems. The results and discussions are provided.

DEDICATION

To:

My Parents: Sasan Sahami, Soraya Chamani

My Siblings: Ehsan Sahami, Erfan Sahami

And to all who seek the truth!

ACKNOWLEDGEMENTS

TABLE OF CONTENTS

LIST OF TABLES

LIST OF FIGURES

LIST OF ABBREVIATIONS

BCU: Boundary Controlling Unstable equilibrium point.

CCA: Critical Clearing Angle.

CCT: Critical Clearing Time.

COA: Center of Angle.

COI: Center of Inertia.

DSA: Dynamic Security Assessment.

IEEE: Institute of Electrical and Electronics Engineers.

KE: Kinetic Energy.

PE: Potential Energy.

PEBS: Potential Energy Boundary Surface.

PMU: Phasor Measurement Unit.

SCC: Short Circuit Capacity.

SEP: Stable Equilibrium Point.

TCP/IP: Transmission Control Protocol/Internet Protocol.

TSA: Transient Stability Assessment.

UEP: Unstable Equilibrium Point.

VAR: Volt-Ampere Reactive.

CHAPTER 1: INTRODUCTION

In this chapter, the main concepts used in the stability area are provided. The history of the stability issues is briefly reviewed and the importance of studying the stability of power systems is explained. Then, different types of power system stability are categorized. Afterward, the concept and importance of transient stability, as the main stability issue in power systems, is discussed. Further, the main contribution of this research and dissertation organization are presented.

The power system is a nonlinear, high-order, multi-variable, dynamic system, that changes continually due to changes in loads, generators' output power, or operating parameters. Its dynamic behavior is influenced by a wide array of devices. Maintaining these large systems operational and stable needs comprehensive studies about power systems. The main concepts used in power system stability studies revolve around the following definitions [2, 3, 4]:

Disturbance: A disturbance is a sudden change in the operating parameter or operating condition of a system.

Security: Security is the ability of a power system to endure sudden disturbances, such as faults, unpredicted loss of generation, or large changes in loads.

Steady State: A system is at steady state when the operating parameters of the system can be considered constant during the concerned time frame of the study.

Reliability: Reliability of a power system implies the probability of the satisfactory operation of the system in the long run. It represents the ability to continuously supply enough power into the grid with few interruptions in a long period of time.

Stability: Stability of a system is the continuance of the correct operation of the system, following a disturbance. It depends on the initial operating condition, the

nature of the physical disturbance, and the duration of the disturbance. A system is called synchronously stable, if the system variables settle down to some steady-state values as time approaches infinity following the disturbance is removed. Following, more elaboration about power system stability is provided.

1.1   Power System Stability Importance

Since the 1920s, power system stability has become more important for the secure operation of power grids. Major blackouts happened so far show the importance of this phenomenon. Until about fifty years ago, power system analysis was primarily the area for the system designers, who try to plan and build power networks in a robust way. During this period, power systems were operated below the related limits. In the early 1960s, an average generator had a capacity of about 300 MW. However, today, a single generator, with relatively low inertia constant, has a capacity that exceeds 1000MW. Increasing loads, operating closer to system limits, greater interconnections, new loads and sources interfaced through power electronics, significant integration of distributed energy resources, and severe transmission congestion [5, 6, 7] have made modern power systems very complex. These modern systems are more susceptible to disturbances due to the increased size of generation units with lower inertia constant, demand growth, heavy loads on existing transmission lines, equipment failure, and negative damping effect of controllers, such as fast exciters [8, 9]. The stability of these modern systems and the generators supplying electricity must be maintained in order to provide reliable electric service. The growth and evolution of power systems and the operation of power systems close to their limits resulted in different forms of instability conditions. For instance, voltage stability, frequency stability, and inter-area oscillations have become important concerns in the modern power grid when compared to legacy power systems [10, 11, 12].

Power system stability is the capability of an electric power system, for a given initial operating condition, to regain an equilibrium operating state after undergoing a

physical disturbance with most system variables bounded so that practically the entire system remains stable and operational [8, 13, 14, 15]. The most important ingredient toward stable operation is synchrony. All generators of the network should stabilize at the same frequency after a perturbation followed by seconds-short transients. The second stability goal is maintaining sufficiently high voltages (above 90% of their nominal values). Lower voltage levels cause a byproduct larger current values for the same amount of generated power and higher power transmission losses, which in an extreme case may make it impossible to meet existing loads. A manifestation of this problem is the so-called "voltage collapse". The third stability aim, from an operational perspective, is maintaining line power flows within established bounds [8, 16, 17, 18].

1.2   Power System Stability Classification

In a synchronous stable power system not only all the generators run at the same angular velocity ($\omega = \omega_s$), but also each one is maintained by a local governor that regulates the driving torque via managing energy supplied to the rotor prime mover. This process gives a perfect power balance between generation and demand. Depending on the network topology, system operating condition, and the forms of disturbances, different sets of opposing forces may experience imbalance leading to different forms of instability. Power system stability classification can be done base on three general considerations [8, 19, 20, 21, 22, 23]:

- The physical nature of the resulting mode of instability as indicated by the main system variables, in which instability can be observed.

- The size of the disturbance considered, which influences the method of stability calculation and prediction.

- The devices, processes, and the time span that must be taken into consideration for stability assessment.

The following classification of the power system stability problem is suggested in [8, 24]:

- Rotor Angle Stability (short-term stability):

  - Small-disturbance or small- signal rotor angle stability

  - Large-disturbance rotor angle stability or transient stability

- Voltage Stability (Short-term or long-term phenomenon stability)

  - Small-disturbance voltage stability

  - Large-disturbance voltage stability

- Frequency Stability (short-term or long-term stability)

Different stability types can be classified as shown in Fig. 1.1. The main focus of this research is on transient stability. Therefore, transient stability is more explained in the rest of this chapter.

1.3   Transient Stability Concept

The transient stability of a power system, also discussed as "first-swing" stability, refers to the stability of a power system to reach a stable condition following a large disturbance in the transmission network. Historically, transient stability has been the dominant stability issue in power systems, and the number of papers and reports show that it has been the focus of much of the industry's attention [13, 25, 26]. Transient instability occurs as a disturbance creates a substantial power imbalance between the input power supplied to the generator via the turbine and the electrical output power injected into the grid. It can also happen due to substantial changes in the bus admittance matrix. Under such conditions, generators will swing away from their equilibrium points, and some of them will swing far enough to lose synchronism [8, 27, 28].
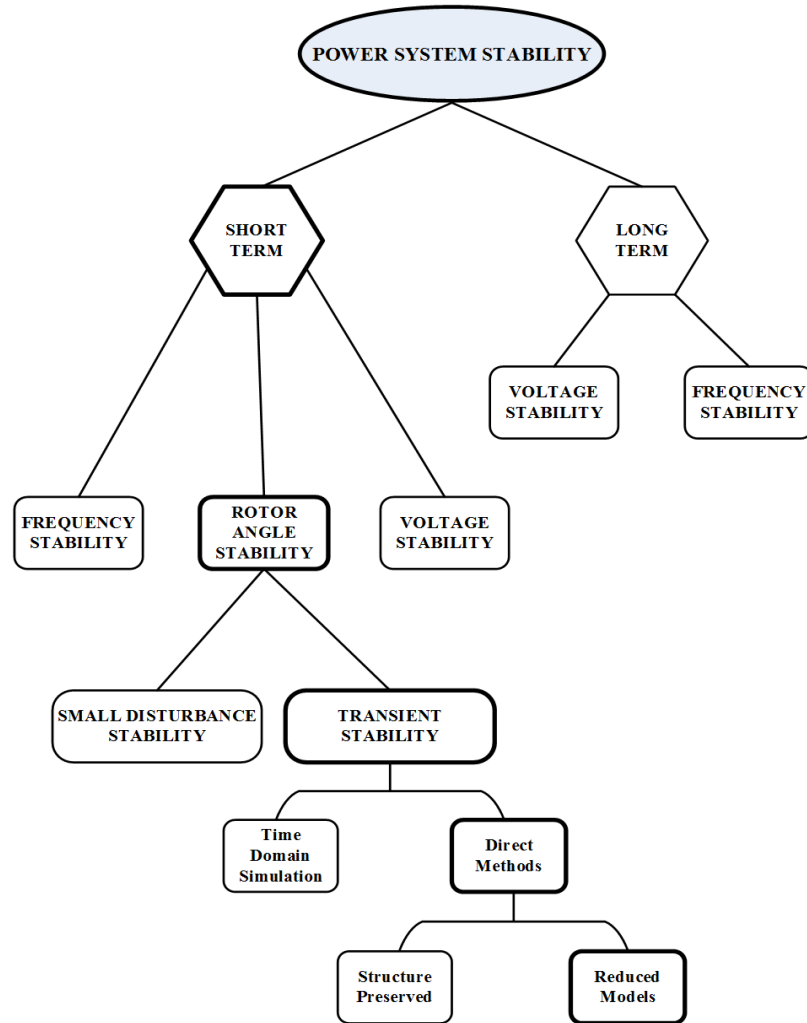
Figure 1.1: Power system stability classification.

A power system is called synchronously stable, if the system variables settle down to some steady-state values as the time approaches infinity after fault removal [13, 14, 15]. Although the stability of the system depends on its initial condition, the Transient Stability (TS) problem is the study of the post-disturbance system [13, 14, 15, 29]. However, it can be used for other purposes, such as investigating the quality of the dynamic behavior of a power system [14, 24, 30]. It should be noted that the post-fault steady state may be different from the pre-fault, depending on the sequence of the disturbances and controllers' actions [8, 31, 32].

The time frame of interest in transient stability investigation is up to a few seconds.

However, a longer period of time can be studied, if the growing oscillations or the behavior of specific controllers are matters of interest [10, 14, 24]. Critical Clearing Time (CCT) refers to the maximum fault duration that the system can tolerate when the post-fault system remains stable after the fault is removed. In transient stability, computing the critical clearing time, for adjusting circuit breakers operating time, is probably the most important part for engineers [33, 34, 35]. The importance of finding the CCT is due to the significant effect of the disturbance duration on the ability of generators to stay in synchronism. So, accurate CCT helps to have a proper protection plan. In case a situation is encountered for which the stability limits and CCT has not been derived off-line, conservative assumptions are made, in order to not endanger the power system stability, and to prevent cascading outages [24, 36].

1.4   Transient Stability Importance

There are many reasons that make transient stability an important issue in modern interconnected power networks. Some of the major ones are [24, 37, 38, 39]:

- Increased size units with lower inertia constant and higher short-circuit ratio. This has a negative effect on system stability.

- Fewer new high voltage transmission lines, which make existing lines to be congested.

- Demand growth in existing load centric areas.

On top of the mentioned issues, there are negative damping effects on power systems due to more dependency of the modern power systems on controllers, such as faster exciters, power system stabilizers, etc. It should be noted that many of these controllers require gentle balancing, which can be easily upset when a disturbance occurs [24, 40, 41].

Paying attention to the importance of transient stability, designers, at the planning level, study the stability of the system for a set of disturbances ranging from a rare

fault, three-phase-to-ground faults for instance, to a single-phase fault, which constitutes about 70 percent of the disturbances. Designers investigate to see if the system has enough safety margin for a potential fault and will not lose synchronism [14, 42]. This study is a time-consuming process, especially with the enormous number of different scenarios to be analyzed in a large interconnected power grid. Therefore, it is an important decision to make a judicious choice between different scenarios, which is becoming more difficult in today's environment. Hence, the contingencies are selected on the basis of having a reasonably high probability of occurrence. It is not practically and economically possible to design a power system that is stable for every possible disturbance. Hence, a stable power system, operating at its stable equilibrium point, has a finite region of attraction if it is disturbed from its normal operating state. A larger region of attraction means that the system is more stable against large disturbances. The region of attraction depends on the operating condition and configuration of the power system [13, 43].

In spite of all the efforts made in the planning level, the system condition might be different from what have been studied while designing the system. Therefore, operators would simulate contingencies in advance and assess the results. The next step is to take preventive control actions so that the security of the system against probable abnormal conditions, due to contingencies, is ensured. This process is called dynamic security assessment (DSA) and preventive control [14, 24, 44, 45]. Fast valving of the steam stream in turbines, tripping generators, using braking resistors, and controlled opening of tie lines are the commonly used actions to prevent system instability after a severe disturbance [7, 46, 47].

1.5   Transient Stability Enhancement

Considering the importance of transient stability, various methods have been used to improve the stability margins in power systems [1, 43, 48, 49, 50, 51, 52]. These methods try to achieve one or more of the following effects:

- Reduction in the disturbing influence by minimizing the fault severity and duration

- Increase in the restoring synchronizing forces

- Reduction in the accelerating torque through control of prime-mover mechanical power

- Reduction in the accelerating torque by applying artificial loads

Some of the methods of achieving these objectives are mentioned below:

1. High-Speed Fault Clearing

2. Regulated Shunt Compensation

3. Reduction of Transmission System Reactance

4. Steam Turbine Fast-Valving

5. Generator Tripping

6. Control of HVDC Transmission Links

7. High-Speed Excitation Systems

8. Dynamic Braking

9. Controlled System Separation and Load Shedding

Choosing the right method depends on the network configuration, operating condition, and available equipment and controllers. In general, a combination of them is utilized to maintain system stability.

1.6   Main Contribution of This Research

As discussed earlier, it is important to predict the system behavior so that necessary controlling actions can be done, in order to prevent a system from going unstable [53, 54, 55, 56]. Different approaches have been studied to achieve this goal. Data-driven methods, artificial intelligence methods, modern and innovative complex control structures are among the hot topics of research in this area [57, 58, 59, 60, 61, 62].

Using direct energy methods, many efforts are done to find the critical clearing time (CCT). All employed techniques of finding the CCT need to have the Unstable Equilibrium Point (UEP) of the post-disturbance system. Hence, different methods, such as Boundary Controlling Unstable equilibrium point (BCU), and Potential Energy Boundary Surface (PEBS) methods, are proposed in the literature to find the UEP [63, 64, 65, 66, 67]. The shortcoming in all proposed methods is that an offline study is required to find the UEP before using direct methods to find the CCT.

As the first contribution of this dissertation, a technique is proposed to overcome the problem of not having the UEP. The method is based on the Taylor series expansion and is used to predict the dynamic behavior of the generators. Being able to predict the generators' behavior, critical generators, critical clearing time, and the critical clearing angles of generators can be found. Having an appropriate TCP/IP infrastructure [68, 69], each generator station can send its data to a central control unit. The data will be processed in the central control unit, and generators that lose synchronism and the moment and the angle of the loss of synchronism will be determined. This makes it possible to find the critical clearing time, and critical clearing angle of the generators for a specific fault once it happens. Accordingly, the due decision can be made in the main control unit.

Another application of generators' behavior prediction, is predicting the energy of the system. This is beneficial when doing transient stability assessment via direct methods. An approximation of the kinetic and potential energy of the system can

be obtained via substituting the predicted values in related equations. This, in turn, helps to introduce a new approach for transient stability enhancement as the second contribution of this research.

The second contribution of this research is introducing a new approach, based on the concept of the potential energy of a power grid, for improving the stability margin of a power system. It is shown that at the critical state of the system, the potential energy of the system reaches a maximum. Hence, increasing the potential energy capacity of the system, even momentarily, can help to improve transient stability. Traditionally, shunt capacitors, reactors, and breaking resistors are utilized for transient stability enhancement. However, the goal for using them was to reduce or consume the kinetic energy of generators, which changed during the disturbance. In contrast, the proposed method here considers the potential energy of the system instead. The advantage of this approach is that it can be used for energy resources without a rotating part. These resources do not have kinetic energy to be controlled or reduced. However, they contribute to the potential energy capacity of a power grid.

1.7   Dissertation Organization

The organization of this thesis is as follows: In chapter 2, dynamics of power systems, and different approaches for system behavior assessment are discussed. Chapter 3 elaborates how the Taylor series can be used for predicting generators' behavior. Related equations and illustrative examples are provided. To show the scalability, more studies and results are provided in Chapter 4. Chapter 5 is about the energy function in a multi-machine system. The concept of potential energy and unstable equilibrium points are also discussed in chapter 5. Chapter 6 talks about combining the prediction method and energy concept to control the system and enhance system stability. Conclusions and suggestions for future works are mentioned in chapter 7. The structure of this thesis is depicted in figure 1.2.
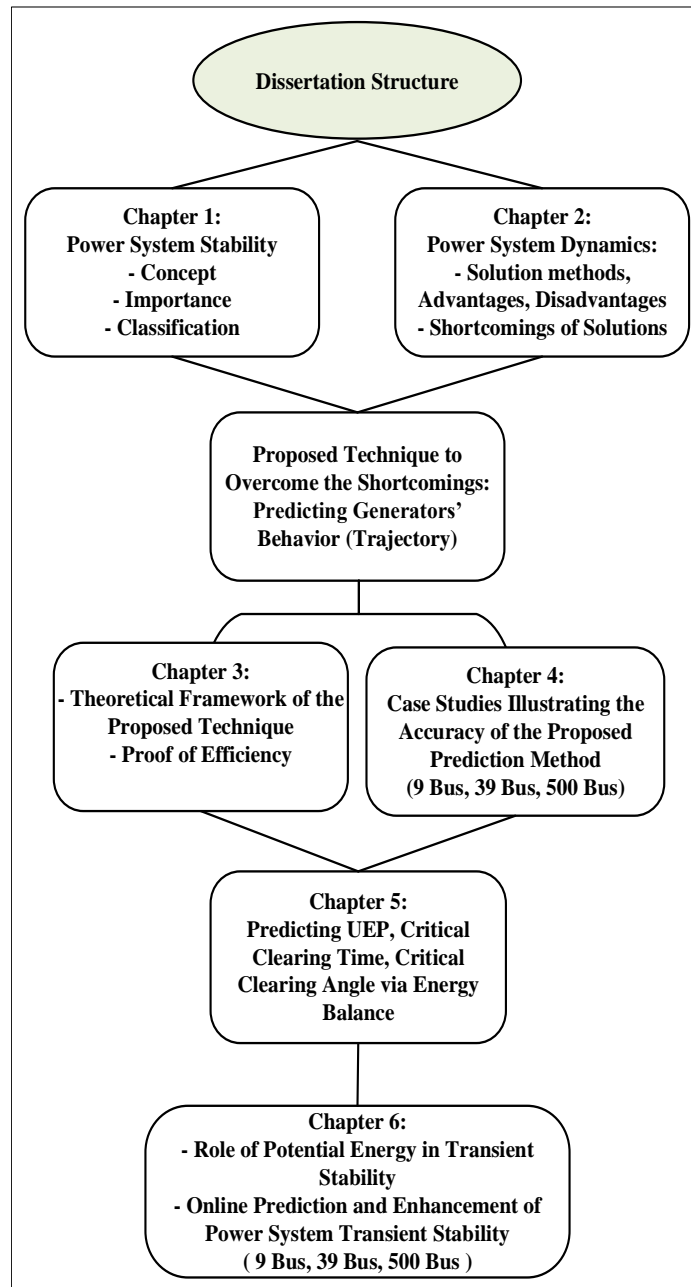
Figure 1.2: Structure of this dissertation.

1.8   Summary

In this chapter, the history and importance of studying the power system stability were reviewed. A classification of different stability issues was presented. Then, the concept and importance of power system transient stability, as the main stability issue in power systems and the focus of this research, were discussed. Finally, the main

contribution of this research, and the organization of this dissertation was explained. Following is chapter 2, where the necessary equations for studying the dynamics of power systems, and different approaches for solving them are elaborated.

CHAPTER 2: POWER SYSTEM DYNAMICS SOLUTIONS

In order to study and solve an engineering problem (usually of a physical nature), first, we have to formulate the problem as a mathematical expression in terms of variables, functions, and equations. Such an expression is known as a mathematical model of the given problem. Many physical concepts, such as velocity and acceleration, are derivatives. Hence, a model is very often an equation containing derivatives of an unknown function. This is called a differential equation. An ordinary differential equation (ODE) is an equation that contains one or several derivatives of an unknown function, which is usually called $y(x)$ or $y(t)$ depending on its variable. The equation may also contain variable y itself, known functions of x (or t), and constants.

2.1   Introduction

In power system transient stability analysis, the main modeling equations are those describing the dynamic behavior of the synchronous generators, such as torque equations related to the generators' rotors and their controllers. The rest of the system is modeled only to the extent that influences the torques of the generators [14, 24, 70, 71]. This chapter initially presents the main equations used for transient stability. Later, two main approaches, numerical and direct methods, for solving differential equations of a dynamic system are explained. Next, the advantages and disadvantages of these methods and more information regarding direct methods of stability assessment and its possible applications are provided.

2.2   Power System Dynamics

Consider the following equations for a power system:

$$\dot{x}(t) = f^I\left(x(t)\right), \quad 0 < t < t_{Disturb} \tag{2.1}$$

$$\dot{x}(t) = f^{Disturbed}\left(x(t)\right), \quad t_{Disturb} < t \le t_{cl} \tag{2.2}$$

$$\dot{x}(t) = f^{Post}\left(x(t)\right), \quad t_{cl} < t < \infty \tag{2.3}$$

Function f represents the dynamic behavior of the system, while Eq. 2.1 describes the pre-fault system, Eq. 2.2 describes the fault-on system, and Eq. 2.3 is for post-disturbance system. The solution of Eq. 2.2 provides the initial condition for Eq. 2.3. Suppose that Eq. 2.3 has a Stable Equilibrium Point (SEP). The transient stability question is whether the trajectory of Eq. 2.3 solution, with initial condition obtained from Eq. 2.2, will converge to an SEP or not, while time goes to infinity [14].

Dynamics of generators are mostly represented by the so-called "swing equation":

$$\frac{2H_i}{\omega_s}\frac{d\omega_i}{dt} + D_i\omega_i = P_{m_i} - P_{e_i} \tag{2.4}$$

$$\frac{d\delta_i}{dt} = \omega_i - \omega_s, \quad i = 1, 2, \ldots, n \tag{2.5}$$

Where δ is the generator angle with respect to the synchronous frame, ω_s is the reference speed, ω_i is the speed of generator i, D_i is the damping factor, and H_i is inertia constant of the generator i. This model is called the classical model, which is the simplest power system model used for stability studies. It is limited to the analysis of the "first swing" transients. The model is based on the following assumptions:

- Input mechanical power is considered constant.

- Asynchronous power and damping are not modeled.

- The generator is modeled via a constant voltage source behind the direct axis transient reactance. This assumption is valid if the exciter (not modeled here) responses much faster than the electromechanical transients under study.

- Angle of the voltage behind the transient reactance represents the mechanical rotor angle of a synchronous generator.

- Loads are modeled by passive impedances, obtained from pre-disturbance conditions and are considered constant during the stability study.

2.3 Transient Stability Assessment

Different approaches for transient stability assessment have been discussed in the literature. They can be studied in two general categories, "Numerical Methods" and "Direct Methods" [72, 73, 74, 75, 76]. These methods are briefly explained in this section.

2.3.1 Numerical Methods

The most straightforward approach to assess the post-fault system stability has been via numerical integration of equations 2.1-2.3 based on direct time simulation of transient dynamics, following a contingency. In this method, iterative integration methods, such as Runge-Kutta, Euler, etc. are used to solve the differential equations modeling the system behavior. Advances in computational hardware have made this methodology fast and accurate even for large scale systems [5, 69, 77, 78, 79, 80].

2.3.2 Advantages and Disadvantages of Numerical Methods

The main advantages of using numerical methods in studying power systems are:

- Understanding the behavior of system variables in desired time frames

- Capability to study the desired variables' behavior, such as voltages and currents of transmission lines

Some of the important disadvantages in employing numerical methods are:

- Inefficient use of computational resources:

  Numerical methods need generators' angles and other variables to be calculated at each time instant and repeating the process after adjusting the parameters. This process is an inefficient use of computational resources, and it is very time-consuming.

- Overall Inefficiency:

  Another disadvantage of numerical methods is their overall inefficiency. Most of the contingencies are safe due to the reliable operation of the system and certifying this via direct simulation is an inefficient use of computational resources. Alternatively, the dynamics following non-critical scenarios could be proven stable using advanced approaches exploiting the mathematical structure of the dynamic systems [14, 24, 81].

It is worth mentioning, while the amount of computational efforts depends on the complexity of the mathematical model used, the only way to have the time solution is by using numerical methods. A comparison between the pros and cons of numerical methods and direct methods is provided in table 2.3.

2.3.3   Direct Methods

An alternative approach for stability assessment is via qualitative methods. Qualitative methods obtain qualitative information on solutions without solving system equations. These methods are particularly valuable to be used for systems with difficult or impossible analytic solutions.

2.3.3.1   History of Direct Methods

Early investigations of using direct methods for transient stability assessment were conducted in 1930s and 1940s [24, 81, 82, 83]. Not much work can be found in the West literature in the 1940s and 1950s. The early 1960s is when the application

of Lyapunov's second method in power systems was considerably used in researches [24, 84]. The first approach for stability analysis, based on the Lyapunov theory, was proposed in 1966 by Gless, El-Abiad, and Nagappan. According to Lyapunov's theory, by using the concept of energy, a function can be defined for a system. This function represents a relationship between the accumulated energy and the dynamics of a system. Based on his theory, a system is stable if the system's energy after a disturbance is continuously decreasing until an equilibrium state is reached [85, 86, 87]. In the 1960s, it was mentioned that direct methods provide a much faster solution for determining critical clearing time compared to conventional time solutions. However, this claim is outdated because first, more advanced computers and solution methods are employed today and second, there are more complex stability-related concerns rather than just finding the critical clearing time of generators.

Early researches on energy criteria were mainly about two issues involved in direct stability analysis: firstly, great emphasis on the development of new Lyapunov functions, and secondly, finding the critical value of the systems' energy. The second issue involves the investigation of equilibrium conditions, i.e., the stable and unstable solutions of dynamic equations of the employed power system model. Achieved results using these functions for power system transient stability problems were conservative, which means smaller critical clearing time was obtained compared to what was obtained by the conventional time simulation method, and what could be the actual case in the real world. Following is a brief summary of the basic efforts in this area [24, 33, 40]:

- Gorev defined an energy criterion for stability represented by T, where T is the summation of the kinetic energy of all the generators. Gorev's second energy criterion of stability states that "a sufficient condition of stability is for the value of T at the highest saddle point of the surface T to be less than zero" [24, 88, 89].

- Magnusson's method, presented in 1947, is similar to the Gorve's. Magnusson's

potential function and Gorve's energy function are similar, and they both use the same procedure for determining the criteria of stability. A region of stability is determined by the potential of the nearest saddle to the equilibrium point [90, 24, 91].

- Aylett studied a multi-machine system based on the classical model. For the multi-machine system, he obtained a set of differential equations in the inter-machine angle coordinates. Aylett states that in the critical case, the potential energy is equal to kinetic energy; in stable situations, the potential energy is greater than kinetic energy, and instability occurs if kinetic energy is greater than the potential energy. An important aspect of Aylett's work is the formulation of the system equations based on inter-machine movements [24, 92].

- In 1972, Tavora and Smith investigated the transient energy of a multi-machine system and equilibrium conditions [4, 79, 93]. They used the classical model of machine and network with considering transfer conductance equal to zero. They suggested confining the fault trajectory of the system to a bounded region for stability studies, after the last phase of the disturbance. An interesting part of their work is defining synchronous equilibrium by conditions that the speed and acceleration of the generators are zero in the COI frame. They also introduced expressions for the total kinetic energy of the system and the transient (or inter-machine) kinetic energy, which can determine the stability according to their claim.

- In 1972, Uyemura suggested approximating the path-dependent term in the Lyapunov functions by path-independent terms [94].

- In 1976, El-Abiad and his colleagues found that the important UEP is not the one with the lowest energy, but the UEP closest to the system trajectory [95].

- The work by Athay, Podmore, and colleagues, in 1976-1979 became the basis for the transient energy function method we use today. Their 1979 report is considered as a benchmark reference for investigating in the TEF area. Their work includes [24, 96]:

  - Search for UEP and critical transient energy in the direction of system trajectory

  - Studying the potential energy boundary surface (PEBS)

  - Linear approximation of path-dependent terms and COI formulation

  - Studying more practical power system sizes than previously used in direct stability analysis research

  - Studying the behavior of the system's energy at different instants using computer simulations.

Tables 2.1 and 2.2 provide a summary of important findings of using direct methods in power system studies, their shortcomings, and the proposed solutions in this dissertation.

2.3.4   Advantages and Disadvantages of Direct Methods

Similar to the numerical approach, there are advantages and disadvantages of using direct methods. Understanding the characteristics of direct methods helps to use them in the most beneficial manner. The main advantages of using direct methods are as follows:

- Avoiding the complicated mathematics of solving differential equations

- Saving computational resources and time

- Gaining qualitative assessment about systems dynamics

The main disadvantages of using direct methods are as follows:

Table 2.1: Summary of important findings of using direct methods in power system studies.

Year Researcher(s)	Contribution
1899 Lyapunov	- Developing a method to define the stability of sets of ordinary differential equations
1930 - 1950 Magnusson	- Claiming the region of stability is determined by the potential of the nearest saddle to the equilibrium point
1958 - 1966 Aylett, Gless, El-Abiad, Nagappan	- Introducing the first energy function for power system stability
1970 - 1980 Tavora, Smith, Uyemura,	- Investigating the transient energy of a multi-machine system and equilibrium conditions - Finding that the important UEP is not the one with the lowest energy - Approximating the path-dependent term in the Lyapunov functions by path-independent terms
1976 - 1979 Athay, Podmore	- Introducing the Center of Inertia - Studying the potential energy boundary surface - Searching for UEP and critical transient energy in the direction of system trajectory - Studying more practical power system sizes
1984 Narasimhamurthi	- Proving that the standard energy function of a lossless system cannot be extended in a general manner to a system
1989 Pai	- Finding an energy function for lossy systems with two generators
1989 Chiang	- Proving that a general Lyapunov function does not exist when losses are considered in the power system model
2000 - Present Different researchers	- Trying to find a new method for finding UEP - Using machine learning for predicting the energy - Studying energy function in structure-preserved power system models

Table 2.2: Shortcomings of the previous researches in using direct methods in power system studies, and the proposed solutions.

Common Shortcomings	1- Requiring numerical solution until the moment of fault removal 2- Having the post-fault UEP prior to using the direct method 3- Impractical for online applications.
Proposed Solution in this dissertation	1- Predicting the system behavior using conditions of the fault moment 2- Predicting the post-fault UEP by using predicted values in PEBS method 3- Using parallel processing for prediction

- The numerical simulation should be used to calculate the initial condition for the post-fault system

- Not delivering the detail of systems behavior

- The requirement of knowledge about the post-disturbance system

- Conservative results

A comparison between the pros and cons of numerical methods and direct methods is provided in table 2.3. More discussions about the shortcomings of using direct methods for power system transient stability assessment is provided in chapter 5, section 2.5.

2.4   Possible Application of Direct Methods

Considering the characteristics of direct methods, the main possible applications of them are as follows [97]:

- A screening tool used before conducting traditional studies

- Online operations dynamic security monitoring

- A method of analyzing the results of traditional transient stability studies and computing the stability margin

Table 2.3: Main advantages and disadvantages of numerical and direct methods.

Advantage	Numerical Methods	Direct Methods
Provide time solution of each variable	Yes	No
Capability of studying different variables	Yes	No
Fast screening tool before comprehensive studies	No	Yes
Qualitative view about system dynamics	No	Yes

Disadvantage	Numerical Methods	Direct Methods
Calculating the system variables at each time step	Yes	No
Time-consuming	Yes	No
Overall inefficiency and waste in computational resources	Yes	No
Requiring numerical solution to find post-disturbance initial condition	Yes	Yes
Conservative stability assessment	No	Yes

- Identifying stability limits for system operations

- A way for adding systems' stability as one of constraint in optimal power-flow

Also, obtaining qualitative information on system stability behavior, identifying critical generators, which are severely affected by disturbances, and studying the sensitivity of systems' parameters are some of the incentives of researches in this area.

2.5   Shortcomings of Using Direct Methods for Transient Stability Assessment

The main problems on the way of direct methods to be reliably applicable are [97]:

- Current energy functions and equations are based on classical generator models and dynamic characteristics of loads, and the effects of controls and stability aids are not represented in these models. Energy functions have been defined for a detailed generator model connected to an infinite bus, but not for a multi-machine model. It seems possible that more detailed generator models can be presented, but probably progress in this will not be fast and easily achievable.

- The response of the system up to the last switching operation should be calculated by conventional time-domain solutions of the system equations. Then the

direct method is used by treating the system as an autonomous system. This limitation is essentially inherent to direct methods because they are based upon the Lyapunov stability theory for autonomous systems.

- The results of an analysis using direct methods do not provide time responses of system variables, which can give us valuable information about the dynamic features of the system.

- Representing automatic switching operations is not possible. For example, automatic switching of reactors and capacitors as a function of bus voltage cannot be represented.

- Direct methods do not indicate how the system loses synchronism if the system is unstable, and do not indicate if the separated parts collapse or survive.

- Monitoring of protective relays is important in stability studies since their operation can lead to cascading system breakups. System operating limits are sometimes dictated by relay margin requirements rather than stability limits. However, apparent impedances, line flows, and bus voltages, required for monitoring and simulating protective relay operations, cannot be computed.

- Using high speed reclosing and switching of reactors and capacitors, the last switching operation may happen beyond 0.5 seconds following the initial disturbance. For such situations, there is not really an advantage in using direct methods.

Direct methods have the potential to be employed for the online derivation of transient stability limits. However, as mentioned earlier in this chapter, the UEP, the path of the angles and the rotor speed of the generators are unknown without numerically solving the system's dynamic equations in the time domain. This is one of the obstacles to achieving utilizing direct methods as an online tool. One way to

overcome this shortcoming is to predict the behavior of the generators' angles and speed. The prediction provides us with the ability to gain a better understanding of the system trajectories during a disturbance, which in turn helps to have a better estimation of the system's energy and stability margin.

In chapter 3, a novel approach for prediction of generators angles and speed is provided.

2.6   Summary

In this chapter, the dynamics of the power system and different approaches for assessment of a system's behavior were discussed. The benefits of using direct methods for transient stability assessment was explained, and its possible applications were mentioned. In order to use direct methods for assessment of system behavior, an appropriate function, which describes the energy of the system should be introduced. To be able to use this function in a more efficient way, having a prediction about the generators' behavior would be beneficial. So, in the next chapter, a method for predicting generators' behavior is proposed.

CHAPTER 3: Theoretical Framework of Prediction of Generator Behavior

Reliable and continuous energy supply is one of the major expectations of a power system. Several studies are conducted on power systems, and many different controllers are employed to meet such an expectation in spite of frequent changes in operating conditions of a real power grid. In addition, due to the significant economic impacts and security consequences, which might happen following a failure in a power system, accurately predicting and controlling the behavior of modern interconnected power systems are of crucial importance [69, 98, 99].

3.1   Introduction

In spite of all the efforts made in the planning level, the system condition might be different from what has been studied during the design process. Therefore, operators would simulate contingencies in advance and assess the results and then take preventive control actions to ensure the security of the power systems against probable abnormal conditions due to contingencies. This process is called dynamic security assessment (DSA) and preventive control [14, 24, 100, 101]. If the behavior of a power system could be predicted real-time or close to real-time, the preventive control actions would be conducted better, and consequently, the reliability of the system would be increased. In the rest of this chapter, the theoretical framework and mathematical discussions for the proposed prediction method followed by illustrative examples are provided. Results and discussions are presented in each part.

3.2   Mathematical Theory of the Proposed Method

Before discussing in detail on the prediction method and the results, some definitions and discussions about analytic functions and representing them by power series are provided.

3.2.1   Analyticity Concept

A function $f(z)$ is said to be analytic in a domain D if $f(z)$ is defined and differentiable at all points in the domain D. The function $f(z)$ is said to be analytic at a point $z = z_0$ in D if $f(z)$ is analytic in a neighborhood of z_0. Also, by an analytic function, we mean a function that is analytic in some domains. Hence, analyticity of $f(z)$ at z_0 means that $f(z)$ has a derivative at every point in vicinity of z_0 (including z_0 itself, since, by definition, z_0 is a point of all its neighborhood). This concept is motivated by the fact that if a function is differentiable merely at a single point z_0 but not throughout some neighborhood of z_0, it will be of no practical interest. Analytic functions can be locally represented by power series. Such functions are usually divided into two important classes: real analytic functions and complex analytic functions, which are commonly called holomorphic functions [102].

The exceptional importance of the class of analytic functions is due to the following reasons. First, the class is sufficiently large; it includes the majority of functions encountered in the principal problems of mathematics and its applications to science and technology. Second, the class of analytic functions is closed with respect to the fundamental operations of arithmetic, algebra, and analysis. Finally, an important property of an analytic function is its uniqueness. Each analytic function is an "organically connected whole", which represents a "unique" function throughout its natural domain of existence [102, 103, 104, 105].

There are different approaches to the concept of analyticity. One definition, which was originally proposed by Cauchy and considerably advanced by Riemann, is based

on structural property of the function, the existence of a derivative with respect to the complex variable, i.e. its complex differentiability. This approach is closely connected with geometric ideas. Another approach, which was systematically developed by Weierstrass, is based on the possibility of representing functions by power series; it is thus connected with the analytic apparatus by means of which a function can be expressed. Several criterions for the analyticity of function f can be established. A popular one is the existence of positive constants C, R and δ such that [102, 103]:

$$\left| f^{(n)}(x) \right| \leq C_n!\, R^n \tag{3.1}$$

$$\forall x \in]x_0 - \delta, x_0 + \delta[, \forall n \in N$$

3.2.2 Power Series for Real Functions

The power series method is the standard method for solving linear ODEs with variable coefficients. It gives solutions in the form of power series. These series can be used for computing values, graphing curves, proving formulas, and exploring properties of solutions. Any real analytic function can be locally extended to a holomorphic (or complex analytic) function [102, 103]:

$$\sum_{m=0}^{\infty} a_m (x - x_0)^m = a_0 + a_1(x - x_0) + a_2(x - x_0)^2 + \cdots \tag{3.2}$$

Here, x is a variable. $a_0, a_1, a_2, \cdots$ are constants, called the coefficients of the series. x_0 is a constant, called the center of the series. More precisely, assume that the left hand side of Eq. 3.2 converges for some x with $|x - x_0| = R$. Then the series converges for any complex value of x with $|x - (x_0 + 0i)| < R$ and defines a holomorphic function, which coincides with f on the interval $]x_0 - R, x_0 + R[$. A power series with a nonzero radius of convergence (R) represents an analytic function at every point interior to its circle of convergence. The derivatives of this function are obtained by differentiating

the original series term by term. All the series thus obtained have the same radius of convergence as the original series. Hence, by the first statement, each of them represents an analytic function. Consider a real (non-complex) power series shown in equation 3.2. In particular, if $x_0 = 0$, we obtain a power series in powers of x, shown in Eq. 3.3:

$$\sum_{m=0}^{\infty} a_m x^m = a_0 + a_1 x + a_2 x^2 + \cdots \tag{3.3}$$

We shall assume that all variables and constants are real. Also, the term "power series" usually refers to a series of the form 3.2 or 3.3, but does not include series of negative or fractional powers of x.

3.2.2.1   Theory of Using Power Series for Approximation

The nth partial sum of Eq. 3.2 is defined as Eq. 3.4:

$$S_n(x) = a_0 + a_1(x - x_0) + a_2(x - x_0)^2 + \cdots + a_n(x - x_0)^n \tag{3.4}$$

Where $n = 0, 1, \cdots$. If we omit the terms of S_n from Eq. 3.2, the remaining expression would be like Eq. 3.5:

$$R_n(x) = a_{n+1}(x - x_0)^{n+1} + a_{n+2}(x - x_0)^{n+2} + \cdots \tag{3.5}$$

This expression is called the remainder of Eq. 3.2 after the term $a_n(x - x_0)^n$.

This way, we have associated with Eq. 3.2 the sequence of the partial sums $s_0(x)$, $s_1(x)$, $s_2(x) \cdots$. If for some $x = x_1$ this sequence converges, $\lim_{n \to \infty} s_n(x_1) = s(x_1)$, then the series Eq. 3.2 is called converged at $x = x_1$. The number $s(x_1)$ is called the value of sum of Eq. 3.2 at x_1, and we write:

$s(x_1) = \sum_{m=0}^{\infty} a_m(x_1 - x_0)^m$

Then, for any value of n:

$$S(x_1) = s_n(x_1) + R_n(x_1) \tag{3.6}$$

If that sequence diverges at $x = x_1$, the series of Eq. 3.2 is called divergent at $x = x_1$. In the case of convergence, for any positive ϵ, there is an N (depending on ϵ) such that:

$$|R_n(x_1)| = |s(x_1) - s_n(x_1)| < \epsilon, \forall n > N \tag{3.7}$$

Geometrically, this means that all $s_n(x_1)$ with $n > N$ lie between $s(x_1) - \epsilon$ and $s(x_1) + \epsilon$ (Fig. 3.1). Practically, this means that in the case of convergence, we can approximate the sum $s(x_1)$ of series of Eq. 3.2 at x_1 by $s_n(x_1)$ as accurately as we please by taking n large enough. Now if we choose $x = x_0$ in Eq. 3.2, the series
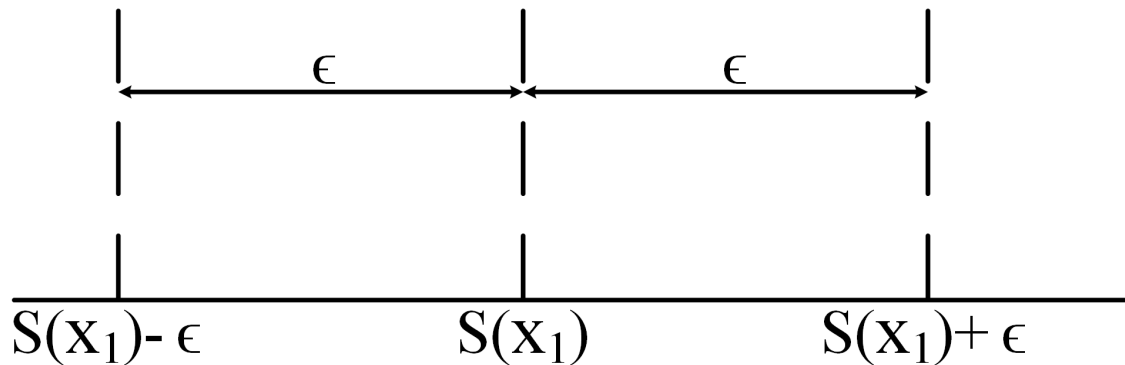
Figure 3.1: Geometric explanation of remainder in a Taylor expansion (Eq. 3.6).

reduces to the single term a_0 since all the other terms are zero. Hence, the series converges at x_0. In some cases, this may be the only value of x for which Eq. 3.2 converges. If there are other values of x for which the series converges, these values form an interval, called the convergence interval. This interval may be finite, as in Fig. 3.2, with midpoint x_0. Then the series Eq. 3.2 converges for all x in the interior of the interval, that is, for all x that:

$$|x - x_0| < R \tag{3.8}$$

and diverges for $|x - x_0| > R$. The interval may also be infinite, that is, the series may converge for all x. The quantity R in Fig. 3.2 is called the "radius" of convergence,
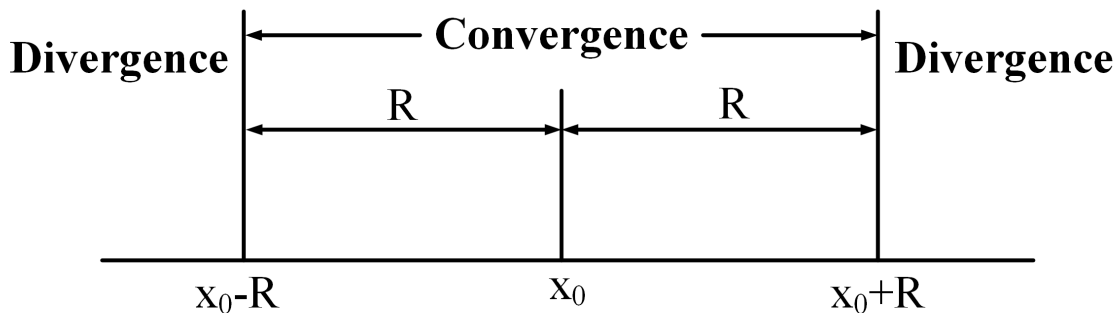
Figure 3.2: Radius of convergence concept.

since for a complex power series R is the radius of the disk of convergence. If the series converges for all x, we set $R = \infty$ (and $\frac{1}{R} = 0$).

The radius of convergence can be determined from the coefficients of the series by
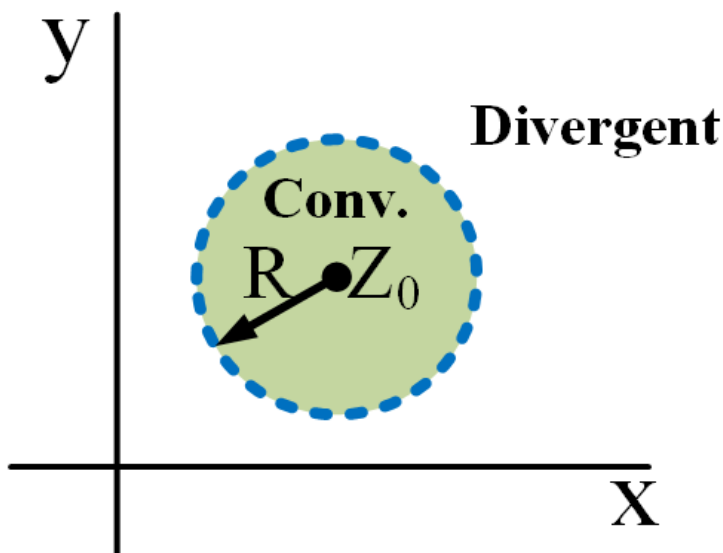
Figure 3.3: Area of convergence concept.

means of each of the formulas below, provided that these limits exist and are not zero.

$$R = \frac{1}{\lim_{m \to \infty} \sqrt[m]{|a_m|}} \tag{3.9}$$

$$R = \frac{1}{\lim_{m\to\infty}\left|\frac{a_{m+1}}{a_m}\right|} \tag{3.10}$$

If these limits are infinite, then Eq. 3.2 converges only at the center x_0. For example, for all three following series let $m \to \infty$. Convergence radius are $R = \infty, 1, 0$ respectively.

$$e^x = \sum_{m=0}^{\infty}\frac{x^m}{m!} = 1 + x + \frac{x^2}{2!} + \dots \quad \left|\frac{a_{m+1}}{a_m}\right|$$

$$= \frac{1/(m+1)!}{1/m!} = \frac{1}{m+1} \to 0, R = \infty \tag{3.11}$$

$$\frac{1}{1-x} = \sum_{m=0}^{\infty}x^m = 1 + x + x^2 + \cdots \quad \left|\frac{a_{m+1}}{a_m}\right| = \frac{1}{1} = 1, R = 1 \tag{3.12}$$

$$\sum_{m=0}^{\infty}m!\,x^m = 1 + x + 2x^2 + \cdots \quad \left|\frac{a_{m+1}}{a_m}\right|$$

$$= \frac{(m+1)!}{m!} = m + 1 \to \infty, R = 0 \tag{3.13}$$

3.3   Taylor Polynomial

Taylor polynomial of degree n, for a function f that is n times differentiable at $x = x_0$ is presented in Eq. 3.14:

$$P_n(x) = \sum_{k=0}^{n}\frac{f^{(k)}(x_0)}{k!}(x - x_0)^k \tag{3.14}$$

The values of the Taylor polynomial and its derivatives up to order n inclusive at the point $x = x_0$ coincide with the values of the function and of its corresponding derivatives at the same point:

$$f^{(k)}(x_0) = P_n^{(k)}(x_0), k = 0, \cdots, n \tag{3.15}$$

The Taylor polynomial is the best polynomial approximation of the function f as $x \to x_0$, in the sense that

$$f(x) - P_n(x) = O((x - x_0)^n), x \to x_0 \tag{3.16}$$

and if some polynomial $Q_n(x)$ of degree not exceeding n has the property that

$$f(x) - Q_n(x) = O((x - x_0)^m), x \to x_0 \tag{3.17}$$

where $m \geq n$, then it coincides with the Taylor polynomial $P_n(x)$. In other words, the polynomial having the property of Eq. 3.15 is unique. If at least one of the derivatives $f^{(k)}(x), k = 0, \cdots, n$ is not equal to 0 at the point x_0, then the Taylor polynomial is the principal part of the Taylor formula. Let U be an open set of $\Re$ and consider a function $f : U \to \Re$. If f is infinitely differentiable at x_0, its Taylor series at x_0 is the power series given by

$$\sum_{n=0}^{\infty} \frac{f^{(n)}(x_0)}{n!}(x - x_0)^n \tag{3.18}$$

where we use the convention that $0^0 = 1$. The partial sums

$$P_k(x) := \sum_{n=0}^{k} \frac{f^{(n)}(x_0)}{n!}(x - x_0)^n \tag{3.19}$$

of a Taylor series are called Taylor polynomial of degree k and the "remainder", $f(x) - P_k(x)$, can be estimated in several ways (see Taylor formula in appendix A).

3.3.1   Approximating a Function via Taylor Series

The most common method of approximating the real-valued function $f : R \to R$ by a simpler function is to use the Taylor series representation. The Taylor series has the form of a polynomial, where the coefficients of the polynomial are derivatives of f evaluated at a point. So long as all derivatives of the function exist at the point

$x = x_0$, $f(x)$ can be expressed in terms of the value of the function and it's derivatives at x_0 as:

$$f(x) = f(x_0) + (x - x_0)f'(x_0) + \frac{(x - x_0)^2}{2!}f''(x_0) + \cdots$$

$$+ \frac{(x - x_0)^k}{k!}f^{(k)}(x_0) + \cdots \tag{3.20}$$

This is known as the Taylor series for f about x_0. It is valid for x "close" to x_0 (strictly, within the "radius of convergence" of the series). This is an infinite series (the sum contains infinitely many terms), so it cannot be directly computed. In practice, we truncate the series after n terms to get the Taylor polynomial of degree n centred at x_0, which we denote $\hat{f}_n(x; x_0)$:

$$f(x) \approx \hat{f}_n(x; x_0) = \sum_{k=0}^{n} \frac{(x - x_0)^k}{k!}f^{(k)}(x_0) \tag{3.21}$$

This is an approximation of f that can be readily calculated so long as the first n derivatives of f evaluated at x_0 can be calculated. The approximation can be made arbitrarily accurate by increasing n. The quality of the approximation also depends on the distance of x from x_0, the closer x is to x_0, the better the approximation would be.

3.4   Approximating the Answer of a Set of Dependant First Order Differential Equation of Functions f and g

As mentioned in chapter 2, dynamic equations ruling the motion of a generator consist of two first order ODEs called the swing equation. In this section, in order to predict the behavior of a system with similar dynamic equations, some feasible scenarios are investigated and the prediction accuracy and the radius of convergence are discussed.

3.4.1   Scenario 1:

When f' Is Always Accurate and Independent of Prediction

Assume that we have the initial points of a function, we have the accurate value of f' at every point, and the derivatives of the function $(f^{(n)}, \forall n \in N)$ are independent of the prediction. It means that the error of prediction will not be affected by the error from approximating f at each time step or iteration. Also, assume that we have derivatives of function g as a coefficient of function f. Mathematically it means:

$$\begin{cases} f^{(n)}(x) & Always\ Accurate \\ & \qquad\qquad\qquad \forall n \in N \\ g^{(n)}(x) = & a f^{(n-1)} \end{cases} \qquad (3.22)$$

Hence, the derivatives of function g will be accurate except for $g' = g^{(1)} = f$, which cause the equation to include the error from approximating f. The total accumulative error after k iterations of prediction, meaning $f(x + kh)$ can be found via following equations [appendix B.1]:

$$\left| Error_k^f \right| \leq k * C_m^f (e^h - \sum_{n=0}^{N} \frac{h^n}{n!}) \qquad (3.23)$$

For 1st order approximation ($N = 1$):

$$\left|Error_k^f\right| \leq k * C_m^f(e^h - 1 - h) \tag{3.24}$$

where h is the prediction step and

$$C_m^f = max(C_i^f) \quad i \in \left\{1, 2, \cdots, k\right\} \tag{3.25}$$

where

$$C_i^f = max(\left|f^{(n)}(t_0 + (i-1)h)\right|) \quad n, i \in N \tag{3.26}$$

Similarly, for function g we will have:

$$C_m^g = aC_m^f \tag{3.27}$$

$$|Error_k^g| \leq (k + h(k-1)^2) * |a| \, C_m^f(e^h - \sum_{n=0}^{N} \frac{h^n}{n!}) \tag{3.28}$$

In power system equations, the maximum change happens in the beginning of a disturbance, hence, in equation 3.25, $C_m^f = C_1^f$.

The limits that are found for $Error_k^f$ and $Error_k^g$ are based on the worst case scenario. Hence, it is guaranteed that the error will not exceed the mentioned limits and in reality, the error will be less than these limits.

3.4.1.1 An Illustrative Example for Scenario 1

(When f' is always accurate and independent of prediction)

Assume functions f, g, and q as:

$$g(t) = 0.1sin(t) + \frac{\pi}{6} \tag{3.29}$$

$$f(t) = 0.1cos(t) \tag{3.30}$$

$$q(t) = \frac{1}{5}(1 + 0.5sin(t)) \tag{3.31}$$

It can be seen that the followings hold true for them:

$$\frac{\mathrm{d}g(t)}{\mathrm{d}t} = f(t) \tag{3.32}$$

$$\frac{\mathrm{d}^2 g(t)}{\mathrm{d}t^2} = \frac{\mathrm{d}f(t)}{\mathrm{d}t} = 1 - q(t) \tag{3.33}$$

The goal is to use the Taylor series to predict the values of the functions f and g in the desired time interval if we have the function q and the initial point of f and g. The initial point refers to their values at the beginning of the time interval of interest. Let us consider the desired time interval as $0 < t < \pi$. The initial value of f and g are:

$g(t_0 = 0) = \frac{\pi}{6}$ and $f(t_0 = 0) = 0.1$

Consider the time steps of the prediction as $h = 0.01$ seconds. The first order Taylor series for prediction is used. So:

$$f(t_0 + kh) = f(t_0 + (k-1)h) + h * f'(t_0 + (k-1)h) + R_k^f \tag{3.34}$$

where,
$$R_k^f = \sum_{n=2}^{\infty} \frac{h^n}{n!} f^{(n)}(t_0 + (k-1)h) \tag{3.35}$$

The maximum error can be calculated from equation 3.23. To do so, we need to find the maximum of $g^{(n)}$, which can be calculated from $q(t)$ as 0.1. Hence, C_m is 0.1. So,

$$Error_k^f \leq k * 0.1(e^{0.01} - \sum_{n=0}^{1} \frac{0.01^n}{n!})$$

$$\left| Error_k^f \right| \leq k * 0.1(e^{0.01} - 1 - 0.01) = k * 5.0167 * 10^{-5}$$

Table 3.1 and figure 3.4 represent the graph of actual and predicted function f and its related errors.

Table 3.1: Function f values when f' is always accurate and independent of prediction.

Iteration (k)	Time (s)	Actual Value	Predicted Value	Absolute of Actual Error	Absolute of Maximum Error
1	0.01	0.1	0.1	4.9999e-6	5.0167e-6
25	0.25	0.0969	0.0968	1.2368e-4	1.2542e-4
50	0.50	0.0878	0.0875	2.3964e-4	2.5084e-4
75	0.75	0.0732	0.0728	3.4060e-4	3.7625e-4
100	1.00	0.0540	0.0536	4.2035e-4	5.0167e-4
150	1.50	0.0071	0.0066	4.9797e-4	7.5752e-4
200	2.00	-0.0416	-0.0421	4.5347e-4	0.001
314	3.14	-0.1	-0.1	8.7034e-7	0.0016
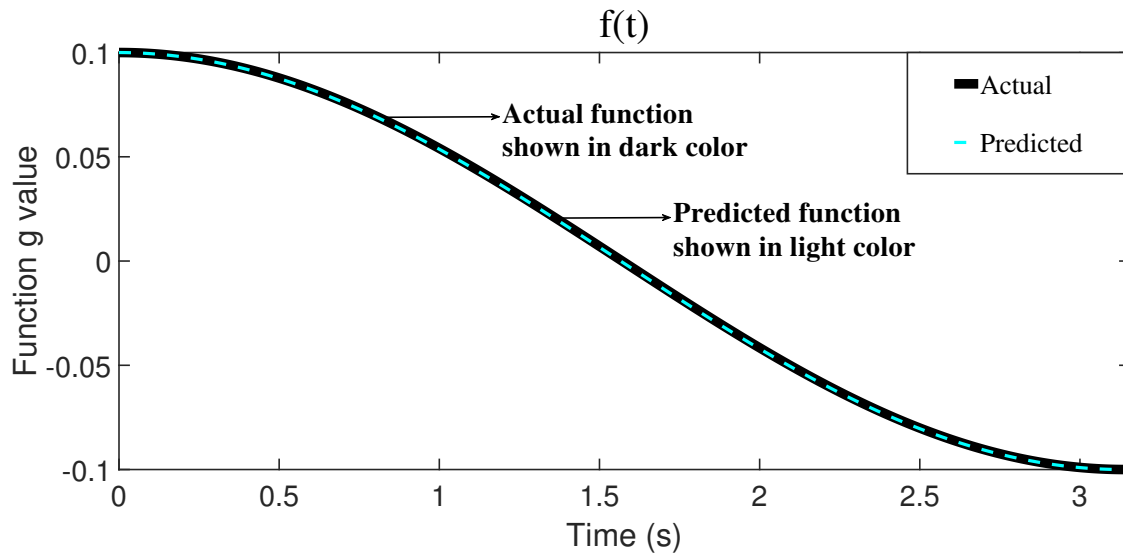
Figure 3.4: Function f(t) when f' is always accurate and independent of prediction.

Let's predict g:

$$g(t_0 + kh) = g(t_0 + (k-1)h) + h * g'(t_0 + (k-1)h) + R_k^g \qquad (3.36)$$

where,

$$R_k^g = \sum_{n=2}^{\infty} \frac{h^n}{n!} g^{(n)}(t_0 + (k-1)h) \qquad (3.37)$$

Table 3.2: Real and Maximum Percentage Error for Function f when f' is always accurate and independent of prediction.

Iteration (k)	Time (s)	Actual Error Percentage	Limit Error Percentage
1	0.01	0.005	0.005
25	0.25	0.1276	0.1294
50	0.5	0.2729	0.2857
75	0.75	0.4653	0.5140
100	1	0.7784	0.9290
150	1.5	7.0137	10.6693
200	2	1.0901	2.4038
314	3.14	0.87	1.6

$$|Error_k^g| \leq (k + 0.01 * (k-1)^2) * 1 * 0.1 * (e^{0.01} - 1 - .01) \qquad (3.38)$$

Table 3.3 and figure 3.5 represent the graph of actual and predicted function g and its related errors.
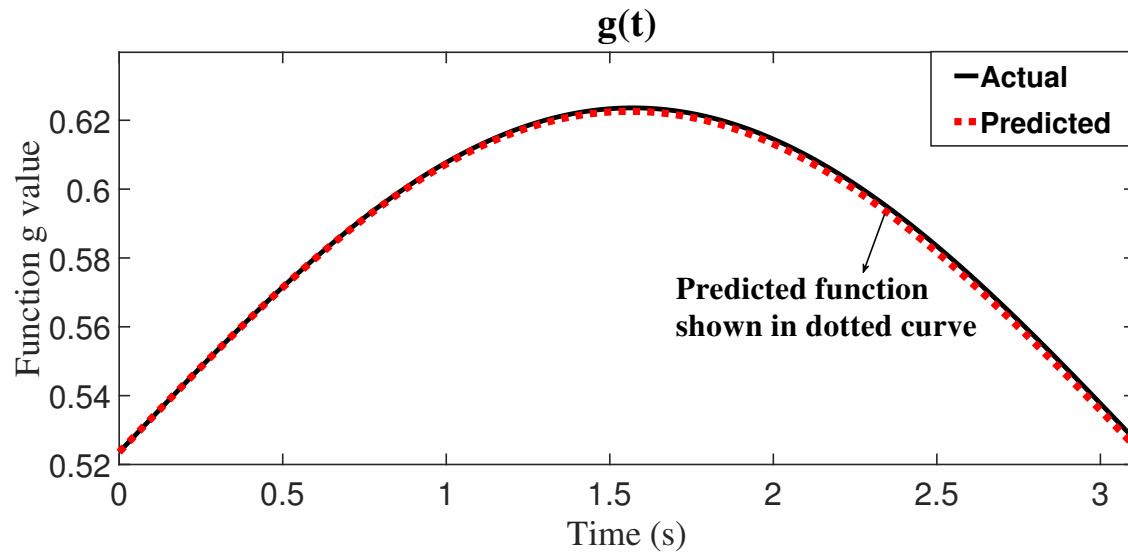
Figure 3.5: Function g(t) when f' is always accurate and independent of prediction.

Table 3.3: Function g values when f' is always accurate and independent of prediction.

Iteration (k)	Time (s)	Actual Value	Predicted Value	Actual Error	Maximum Error
1	0.01	0.5246	0.5246	8.3332e-8	5.0167e-6
25	0.25	0.5483	0.5483	3.1910e-5	1.5431e-4
50	0.50	0.5715	0.5714	1.2400e-4	3.7129e-4
75	0.75	0.5918	0.5915	2.7052e-4	6.5097e-4
100	1.00	0.6077	0.6073	4.6237e-4	9.9336e-4
150	1.50	0.6233	0.6224	9.3216e-4	0.0019
200	2.00	0.6145	0.6131	0.0014	0.003
314	3.14	0.5238	0.5218	0.002	0.0065

Table 3.4: Real and Maximum Percentage Error for Function g when f' is always accurate and independent of prediction.

Iteration (k)	Time (s)	Actual Error Percentage	Limit Error Percentage
1	0.01	0000	0.001
25	0.25	0.0058	0.0281
50	0.5	0.0217	0.0650
75	0.75	0.0457	0.1100
100	1	0.0761	0.1635
150	1.5	0.1496	0.3048
200	2	0.2278	0.4882
314	3.14	0.3818	1.2409

3.4.2   Scenario 2:

When f' Is Not Accurate and Depends on Predicted Value for f

Assume that we have the initial points of a function and the derivative of this function as a function that depends on its value. Then, we want to predict this function and a second function, while the derivative of the second function depends on the first function. In the mathematical expression:

$$
\begin{cases}
f^{(n)}(t) = q(t) - bf^{(n-1)}(t) \\
\\
\hspace{3cm} \forall n \in N \\
\\
g^{(n)}(t) = af^{(n-1)}(t)
\end{cases}
\tag{3.39}
$$

where $q(t)$ is a function that is unlimited times differentiable. The accumulative error of prediction after k iterations can be calculated via the following equations [appendix B.2]:

$$
\sum_{n=1}^{N} \frac{(hb)^n}{n!} = \beta
\tag{3.40}
$$

$$
\left| Error_k^f \right| \leq C_m^f (e^h - 1 - \alpha) \sum_{i=0}^{k-1} (|1 - \beta|)^i
\tag{3.41}
$$

where,

$$
\alpha = \sum_{n=2}^{\infty} \frac{h^n}{n!}
\tag{3.42}
$$

According to geometric progression, if $\alpha\beta \neq 0$, which impose $b \neq 0$, it can be said:

$$
\sum_{i=0}^{k-1} (|1 - \beta|)^i = \frac{1 - (|1 - \beta|)^k}{1 - (|1 - \beta|)}
\tag{3.43}
$$

$$
\left| Error_k^f \right| \leq C_m^f (e^h - 1 - \alpha) * \frac{1 - (|1 - \beta|)^k}{1 - (|1 - \beta|)}
\tag{3.44}
$$

If $|1 - \beta| > 1$, the error will increase in an unacceptable rate after some iterations. However, if $|1 - \beta| \leq 1$, we can say:

$$\sum_{i=0}^{k-1}(|1 - \beta|)^i \leq \sum_{i=0}^{k-1} 1 = k \tag{3.45}$$

Hence:

$$\left| Error_k^f \right| \leq k * C_m^f (e^h - 1 - \alpha) \tag{3.46}$$

Similarly, for function g it can be said that:

$$|Error_k^g| \leq k\,|a|\,C_m^f(e^h - 1 - \alpha) * [1 + h(k - 1)] \tag{3.47}$$

3.4.2.1 An Illustrative Example for Scenario 2
(when f' is not accurate and depends on predicted value for f)

Assume functions f, g, and q as:

$$g(t) = 0.1 sin(t) + \frac{\pi}{6} \tag{3.48}$$

$$f(t) = 0.1 cos(t) \tag{3.49}$$

$$q(t) = \frac{1}{5}(1 + 0.5 sin(t) - cos(t)) \tag{3.50}$$

It is seen that the followings hold true for mentioned functions:

$$\frac{\mathrm{d}g(t)}{\mathrm{d}t} = f(t) \tag{3.51}$$

$$\frac{\mathrm{d}^2 g(t)}{\mathrm{d}t^2} = \frac{\mathrm{d}f(t)}{\mathrm{d}t} = 1 - q(t) - 10f(t) \tag{3.52}$$

The goal is to use the Taylor series to predict the values of the functions f and g in the desired time interval, if we have the function q and the initial point of f and g, meaning their values at the beginning of the time interval. Here, $\frac{\mathrm{d}f(t)}{\mathrm{d}t}$ is not accurate

since it depends on the value of the function f at each time step.

Let us consider the desired time interval as $0 < t < \pi$. The initial value of f and g are:

$g(t_0 = 0) = \frac{\pi}{6}$ and $f(t_0 = 0) = 0.1$

Consider the time steps of the prediction as $h = 0.01$ seconds. The first order Taylor series is used for prediction. So:

$$f(t_0 + 0.01 * k) = f(t_0 + (k-1) * 0.01) + 0.01 * f'(t_0 + (k-1) * 0.01) + R_k^f \quad (3.53)$$

where,

$$R_k^f = \sum_{n=2}^{\infty} \frac{0.01^n}{n!} f^{(n)}(t_0 + (k-1) * 0.01) \quad (3.54)$$

Table 3.5 and figure 3.6 represent the graph of actual and predicted function f and its related errors.
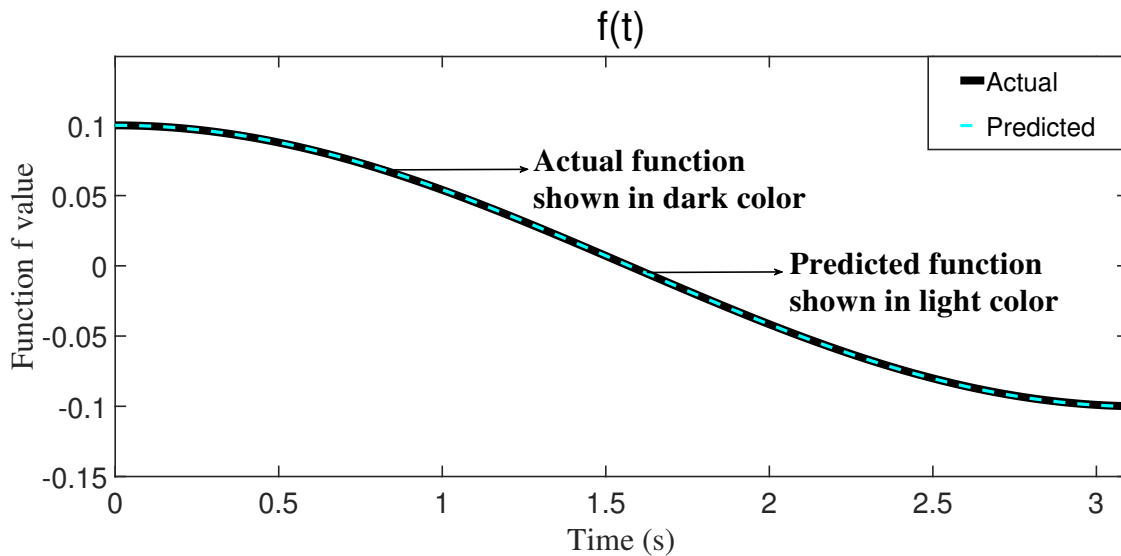
Figure 3.6: Function f(t) when f' is not accurate and depends on predicted value for f.

The graph of actual and predicted function g and its related errors are shown in table 3.6 and figure 3.7.

In the next section, the method for predicting generators behavior is elaborated.

Table 3.5: Function f values when f' is not accurate and depends on predicted value for f.

Iteration (k)	Time (s)	Actual Value	Predicted Value	Absolute of Actual Error	Absolute of Maximum Error
3	0.03	0.1	0.1	-4.9995e-6	1.5050e-5
25	0.25	0.0971	0.0972	-9.1902e-5	1.2542e-4
50	0.50	0.0882	0.0884	-1.4751e-4	2.5084e-4
75	0.75	0.0738	0.0740	-1.6927e-4	3.7625e-4
100	1.00	0.0549	0.0550	-1.6562e-4	5.0167e-4
150	1.50	0.0081	0.0082	-1.0546e-4	7.5251e-4
200	2.00	-0.0407	-.0407	-5.7389e-6	0.0010
314	3.14	-0.1	-0.1002	1.9983e-4	0.0016

Table 3.6: Function g values when f' is not accurate and depends on predicted value for f.

Iteration (k)	Time (s)	Actual Value	Predicted Value	Absolute of Actual Error	Absolute of Maximum Error
3	0.03	0.5256	0.5256	-6.6665e-8	1.5351e-5
25	0.25	0.5474	0.5474	-2.5103e-5	1.5552e-4
50	0.50	0.5707	0.5708	-9.9875e-5	3.7374e-4
75	0.75	0.5910	0.5912	-2.1173e-4	6.5468e-4
100	1.00	0.6072	0.6076	-3.4882e-4	9.9832e-4
150	1.50	0.6233	0.6239	-6.5314e-4	0.0019
200	2.00	0.6149	0.6159	-9.2631e-4	0.0030
314	3.14	0.5248	0.5259	-0.0011	0.0065

Table 3.7: Real and Maximum Percentage Error for Function f when f' is not accurate and depends on predicted value for f.

Iteration (k)	Time (s)	Actual Error Percentage	Limit Error Percentage
1	0.01	0.0000	0.0002
25	0.25	0.0009	0.0013
50	0.5	0.0017	0.0028
75	0.75	0.0023	0.0051
100	1	0.0030	0.0091
150	1.5	0.0130	0.0929
200	2	0.0001	0.0246
314	3.14	0.0020	0.0160
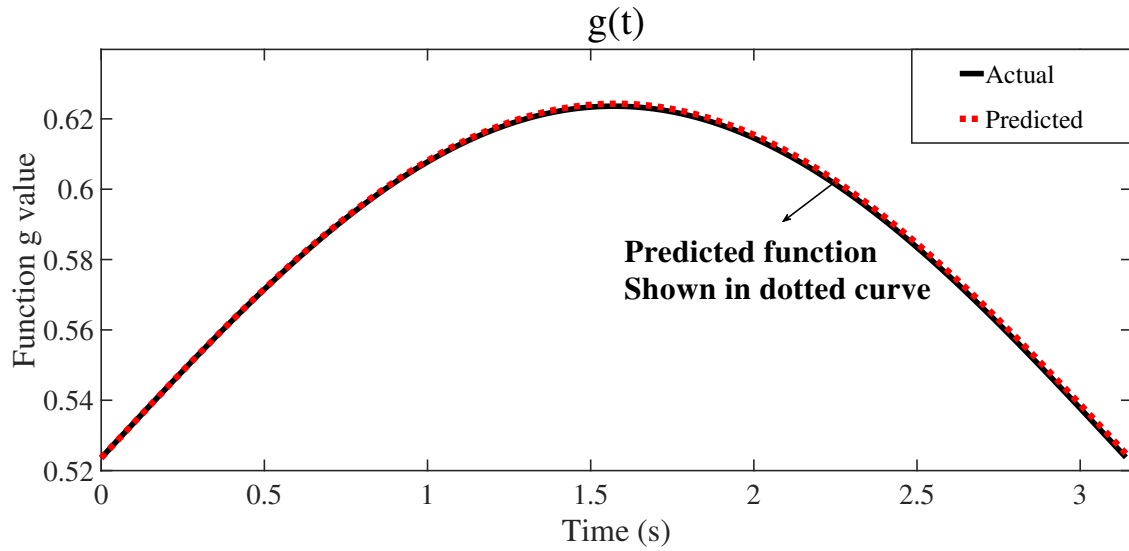
Figure 3.7: Function g(t) when f' is not accurate and depends on predicted value for f.

Table 3.8: Real and Maximum Percentage Error for Function g when f' is not accurate and depends on predicted value for f.

Iteration (k)	Time (s)	Actual Error Percentage	Limit Error Percentage
1	0.01	0.0000	0.0000
25	0.25	0.0000	0.0003
50	0.5	0.0002	0.0007
75	0.75	0.0004	0.0011
100	1	0.0006	0.0016
150	1.5	0.0010	0.0030
200	2	0.0015	0.0049
314	3.14	0.0021	0.0124

3.5   Predicting Generators' Behavior

Phasor Measurement Units (PMUs) are devices that provide real-time phasor measurements at those locations of a power system network, where they are placed. Due to advancements in the field of relay technology, digital relays can now act as PMUs, which has significantly reduced the cost of PMUs [99].

In what follows, it is assumed that there are PMUs or digital relays at all generator buses, which is a realistic assumption. The goal is to predict the values of $\omega(t)$, $\delta(t)$, and $P_e(t)$ using Taylor series. In order to use Taylor series for approximating a function, three concerns should be addressed:

1. Is the function analytic?

2. What is the radius of the convergence?

3. What is the error of approximation?

In the rest of this section, first, the analyticity of the behavior of δ,ω, and P_e is proved. Then the prediction equations are obtained. Finally, the convergence and error of the prediction are discussed.

3.5.1   Analyticity of Variables

Power system main variable, δ, ω, and P_e are analytic, according to the definition of analyticity, and can be approximated via Taylor series. These variables are always defined since they are related to real physical systems. They are unlimited times differentiable since they are sinusoidal in the frequency of power systems operation. However, at switching moments, due to a sudden change in the value of these variables, they are not differentiable. Hence at those moments, Taylor expansion cannot be used for approximating their values.

3.5.2 Predicting Generators' Angle and Speed

Consider that the behavior of any of these variables of power network is represented by a function. We do not know the value of the function at the moment of t_1, but we know it for previous moments. Considering the discussion about approximating a function via Taylor series, we may choose a moment close to t_1, such as $t_1 \pm \Delta t$, $\Delta t > 0$, to approximate the value of each function at the moment of t_1. Since we do not know the value of $f(t_1 + \Delta t)$, we choose $t_1 - \Delta t$ and the value of the function at that moment $f(t_1 - \Delta t)$ for approximation. To make it easier to understand, let's consider $t_1 - \Delta t = t_0$, meaning $t_1 = t_0 + \Delta t$. Therefore, we can approximate the value of $f(t_1)$ using Taylor Series. After approximating $f(t_1)$, it is possible to approximate the value of $f(t_2) = f(t_1 + \Delta t)$; we substitute t_1 in t_0 and consider t_2 as t_1 and this process will be repeated. The error of approximating $f(t_2)$ comes from two sources: the inherent error approximation due to neglecting higher order terms in Taylor expansion, and the error from the approximation of $f(t_1)$. Therefore, the error will be accumulative and it may increase as a longer period of time is predicted. The error is explained and calculated later in this chapter.

Let the dynamics of generators be modeled using (3.55) and (3.56).

$$\frac{2H}{\omega_s}\frac{d\omega}{dt} + D\omega = P_m - P_e \tag{3.55}$$

$$\frac{d\delta}{dt} = \omega - \omega_s \tag{3.56}$$

where ω_s is the synchronous speed, which is equal to 1 p.u.

Let $\frac{2H}{\omega_s} = M$, So, $M = 2H$. Then Eq. (3.55) can be presented as:

$$M\frac{d\omega}{dt} + D\omega = P_m - P_e \tag{3.57}$$

Assume that the behavior of the system between any two consequent time steps is

linear. This is a valid assumption since the waveforms of any stable power system variables are analytic functions, except at switching moments. Hence, Taylor series can be used to linearize the system dynamics, and δ and ω can be expanded as:

$$\delta(t) = \delta(0) + \delta^{'}(0)t + \delta^{''}(0)\frac{t^2}{2!} + ... + \delta^{(n)}(0)\frac{t^n}{n!} + ... \tag{3.58}$$

$$\omega(t) = \omega(0) + \omega^{'}(0)t + \omega^{''}(0)\frac{t^2}{2!} + ... + \omega^{(n)}(0)\frac{t^n}{n!} + ... \tag{3.59}$$

Neglecting terms with order higher than two and considering t_0 as the initial point leads to:

$$\delta(t_0 + \Delta t) = \delta(t_0) + \delta^{'}(t_0)\Delta t + \delta^{''}(t_0)\frac{\Delta t^2}{2!} + O(\Delta t^3) \tag{3.60}$$

$$\delta(t_0 + \Delta t) = \delta(t_0) + \omega(t_0)\Delta t + \omega^{'}(t_0)\frac{\Delta t^2}{2!} + O(\Delta t^3) \tag{3.61}$$

$$\omega(t_0 + \Delta t) = \omega(t_0) + \omega^{'}(t_0)\Delta t + \omega^{''}(t_0)\frac{\Delta t^2}{2!} + O(\Delta t^3) \tag{3.62}$$

where $O(\Delta t^3)$ represents neglected terms. From the swing equation it is known that:

$$M\frac{d\omega}{dt} = P_m - P_e - D\omega = M * a(t) \tag{3.63}$$

Assuming a linear behavior for the system between two consequent moments, leads to:

$$dt = \Delta t = One\ Time\ Step \tag{3.64}$$

So:

$$M\frac{\Delta\omega}{\Delta t} = P_m - P_e - D\omega \tag{3.65}$$

$$M\Delta\omega = (P_m - P_e)\Delta t - D\omega\Delta t \tag{3.66}$$

$$\frac{d\delta}{dt} = \omega - \omega_s \tag{3.67}$$

$$\frac{d\delta}{dt} = \frac{\Delta\delta}{\Delta t} = \omega \Rightarrow \Delta\delta = \omega\Delta t \tag{3.68}$$

$$\Rightarrow M\Delta\omega = (P_m - P_e)\Delta t - D\Delta\delta \tag{3.69}$$

$$\Delta\omega = (\frac{P_m - P_e}{M})\Delta t - \frac{D}{M}\Delta\delta \tag{3.70}$$

$$\omega(t_0 + \Delta t) = \omega(t_0) + (\frac{P_m - P_e}{M})\Delta t - \frac{D}{M}\Delta\delta \tag{3.71}$$

$$\delta(t_0 + \Delta t) = \delta(t_0) + [\omega(t_0)\Delta t + (\frac{P_m - P_e}{M} - \frac{D}{M}\omega(t_0))\frac{\Delta t^2}{2!}] * 2\pi f \tag{3.72}$$

Using (3.71) and (3.72) behaviors of the generators of the system can be predicted. Since the function that shows the variables' behavior is not an analytic function at switching moments, n samples of data at switching moments are required to be known to approximate a function with Taylor series of order n.

As could be seen in the aforementioned discussions, there is a term P_e in prediction formulas. P_e is the electrical output of the understudy generator. The most accurate prediction happens when the actual output electrical power of generators (P_e) is known. This way, the accelerating power can be found accurately (refer to 3.4.1). However, it is not practically possible, since the swing equation should be numerically solved to find P_e at each moment, and it contrasts the prediction. Also, in real-time studies, the actual output of generators cannot be known beforehand to be used for prediction. Therefore, the output of generators for predicting their speed and angle should be found in another way. Three different approaches can be considered for approximating P_e during the fault:

- Assuming P_e of generators equal to zero.

- Assuming P_e as a constant number. This amount is the amount of P_e one moment after the fault.

- Predicting P_e of generators. Because the behavior of the system is predicted for the next time step, Taylor Series can be used. This method is elaborated in

the next session.

Following, a comprehensive discussion about the third assumption is provided. A comparison between the effect of these assumptions in predicting IEEE 9 bus system generator behavior is provided in table 4.4.

3.5.3 Predicting Generators Output Power

In order to predict the generator output power, P_e, the behavior of P_e is considered linear between every two consecutive moments, except at switching times. Hence, the Taylor series of P_e can be employed. The Taylor expansion of P_e is:

$$P(t) = P(0) + P'(0)t + P''(0)\frac{t^2}{2!} + \cdots \tag{3.73}$$

$$M\frac{d\omega}{dt} = P_m - P_e - D\omega \tag{3.74}$$

$$M\frac{d^2\omega}{dt^2} = 0 - \frac{dP_e}{dt} - D\frac{d\omega}{dt} \tag{3.75}$$

$$\frac{d\omega}{dt} = a(t) \tag{3.76}$$

$$\frac{dP_e}{dt} = 0 - M\frac{d^2\omega}{dt^2} - D\frac{d\omega}{dt} = -M\frac{da(t)}{dt} - Da(t) \tag{3.77}$$

Assuming the above equations for one time step and substituting dP_e and dt with ΔP_e and Δt, respectively, leads to:

$$\frac{\Delta P_e}{\Delta t} = -M\frac{\Delta a}{\Delta t} - Da(t) \tag{3.78}$$

$$\Delta P_e = P_e(0) - M\Delta a(0) - Da(0)\Delta t \tag{3.79}$$

So, the first order prediction for P_e will be:

$$P_e(t_0 + \Delta t) = P_e(t_0) - M\Delta a(t_0) - Da(t_0)\Delta t \tag{3.80}$$

This equation has been used for predicting electrical power during the fault. To increase the accuracy, we may have to add a higher order term to the prediction equation:

$$M\frac{d^3\omega}{dt^3} = 0 - \frac{d^2 P_e}{dt^2} - D\frac{d^2\omega}{dt^2} \tag{3.81}$$

Substituting the second term in (3.75) will result in:

$$M\frac{d^2 a}{dt^2} = -\frac{d^2 P_e}{dt^2} - D\frac{da}{dt} \tag{3.82}$$

Assuming above equations for one time step and substituting dP_e and dt with ΔP_e and Δt respectively, leads to:

$$M\frac{\Delta^2 a}{(\Delta t)^2} = -\frac{\Delta^2 P_e}{(\Delta t)^2} - D\frac{\Delta a}{\Delta t} \tag{3.83}$$

$$\frac{\Delta^2 P_e}{(\Delta t)^2} = -M\frac{\Delta^2 a}{(\Delta t)^2} - D\frac{\Delta a}{\Delta t} \tag{3.84}$$

$$P(t) = P(0) + P'(0)t + P''(0)\frac{t^2}{2!} + \cdots \tag{3.85}$$

$$P_e(t_0 + \Delta t) = P_e(t_0) - M\Delta a(t_0) - Da(t_0)\Delta t + \frac{1}{2}(\Delta t)^2\frac{\Delta^2 P_e}{(\Delta t^2)} \tag{3.86}$$

$$P_e(t_0 + \Delta t) = P_e(t_0) - M\Delta a(t_0) - Da(t_0)\Delta t$$

$$+\frac{1}{2}(-M\Delta^2 a(t_0) - D\Delta a(t_0)\Delta t - \frac{D^2}{M}a(t_0)\Delta t^2 + \frac{D^2}{M^2}a(t_0)\Delta t^2) \tag{3.87}$$

$$P_e(t_0 + \Delta t) = P_e(t_0) - M\Delta a(t_0) - Da(t_0)\Delta t$$

$$-\frac{D}{2}\Delta a(t_0)\Delta t + \frac{1}{2}\Delta t^2(\frac{D^2}{M^2}a(t_0) - \frac{D^2}{M}a(t_0)) - \frac{M}{2}(\Delta^2 a(t_0)) \tag{3.88}$$

Considering $\Delta t = TS$ as a constant time step, we have:

$$\Delta a(t_0) = a(t_0) - a(t_0 - \Delta t) = a(t_0) - a(t_0 - TS) \tag{3.89}$$

$$\Delta^2 a(t_0) = \Delta a(t_0) - \Delta a(t_0 - \Delta t) = a(t_0) - 2 * a(t_0 - \Delta t) + a(t_0 - 2\Delta t) \tag{3.90}$$

Hence, (3.88) can be written in discrete form as follows:

$$P_e(i+1) = P_e(i) - M\Delta a(i) - Da(i)\Delta t - \frac{D}{2}\Delta a(i)\Delta t$$

$$+\frac{1}{2}\Delta t^2(\frac{D^2}{M^2}a(i) - \frac{D^2}{M}a(i)) - \frac{M}{2}(\Delta^2 a(i)) \tag{3.91}$$

Substituting (3.89) and (3.90) in (3.91) leads to (3.92).

$$P_e(i+1) = P_e(i) - M(a(i) - a(i-1)) - Da(i)*TS - \frac{D}{2}(a(i) - a(i-1))*TS$$

$$+\frac{1}{2}TS^2(\frac{D^2}{M^2}a(i) - \frac{D^2}{M}a(i)) - \frac{M}{2}(a(i) - 2a(i-1) + a(i-2)) \tag{3.92}$$

Based on (3.92), we can predict the output of electrical power. Using equations (3.71), (3.72), and (3.92), angles, speeds, and output electrical power of generators can be predicted. It is worth reminding that, since 2nd order Taylor series is utilized, the data for the first two moments after the fault or after fault removal is required for predicting the system's variables during the fault and after the fault removal, respectively.

PMUs can be employed to improve the accuracy of the prediction for the post-fault system. It means that we may update the initial point of the prediction using PMU data when the post-fault system is being predicted.

It should be mentioned that the scope of this work is to predict the behavior of the system during the fault so that using direct methods becomes possible without numerically solving the swing equation for during-the-fault system studies. The prediction also helps to apply predictive controllers and have a more stable system. In addition, considering a sustained fault in a system and predicting the system behavior can be employed to find the UEP of a system. Finally, with defining appropriate criteria, prediction can be used for finding the critical clearing time and critical machines, which refer to machines that lose synchronism first. These topics are discussed in

chapters 5 and 6.

3.5.4 Proof of Prediction Convergence in Power Systems

Following, the area of convergence for the prediction equations is discussed. For ease of study, the swing equation is presented again.

$$M\frac{d\omega}{dt} = P_m - P_e - D\omega \tag{3.93}$$

3.5.4.1 Convergence of Generator Speed Prediction

The goal is to prove the convergence of predicted the behavior of generators speed, $\omega(t)$, with Taylor series to its actual values. It is assumed that $\omega(t_1 - \Delta t)$ and $\omega(t_1 - 2\Delta t)$ are known and $\omega(t_1)$ is to be approximated. It means writing the Taylor series of $\omega(t)$ about the point t_0.

$$\omega(t = t_1 = t_0 + \Delta t) = \omega(t_0) + \omega'(t_0)\Delta t + \omega''(t_0)\frac{\Delta t^2}{2!} + ... + \omega^{(n)}(t_0)\frac{\Delta t^n}{n!} + ... \tag{3.94}$$

$$\omega(t) = \sum_{n=0}^{\infty} a_n \Delta t^n \tag{3.95}$$

where

$$a_n = \frac{1}{n!}\omega^{(n)}(t_0) \tag{3.96}$$

Since the process is repeated every time steps, we can assume that P_m and P_e are constant during each step of prediction. Having this assumption, we can differentiate swing equations 3.93 multiple times:

$$\omega^{(1)} = \omega' = \frac{1}{M}(P_m - P_e - D\omega) \tag{3.97}$$

$$\omega^{(2)} = \omega'' = \frac{1}{M}(0 - 0 - D\omega^{(1)}) = \frac{-D}{M}\omega^{(1)} \tag{3.98}$$

$$\omega^{(3)} = \frac{-D}{M}\omega^{(2)} \tag{3.99}$$

$$\vdots$$

$$\omega^{(n)} = \frac{-D}{M}\omega^{(n-1)} \tag{3.100}$$

$$\omega^{(n+1)} = \frac{-D}{M}\omega^{(n)} \tag{3.101}$$

$$\frac{\omega^{(n+1)}}{\omega^{(n)}} = \frac{-D}{M} \tag{3.102}$$

To find the radius of convergence, Eq. 3.10 can be used:

$$\frac{1}{R} = \lim_{n\to\infty}\left|\frac{a_{n+1}}{a_n}\right| = \lim_{n\to\infty}\left|\frac{\frac{1}{(n+1)!}\omega^{(n+1)}}{\frac{1}{(n)!}\omega^{(n)}}\right|$$

$$= \lim_{n\to\infty}\frac{1}{n+1}\left|\frac{\omega^{(n+1)}}{\omega^{(n)}}\right| = \lim_{n\to\infty}\frac{1}{n+1}*\frac{D}{M} = 0 \tag{3.103}$$

So, $R = \infty$.

3.5.4.2   Convergence of Generator Angle Prediction

The goal is to prove that the Taylor series approximation of generators angles, function $\delta(t)$, is convergent.

$$\delta(t = t_1 = t_0 + \Delta t) = \delta(t_0) + \delta'(t_0)\Delta t + \delta''(t_0)\frac{\Delta t^2}{2!} + ... + \delta^{(n)}(t_0)\frac{\Delta t^n}{n!} + ... \tag{3.104}$$

$$\delta(t) = \sum_{n=0}^{\infty}b_n\Delta t^n \tag{3.105}$$

where

$$b_n = \frac{1}{n!}\delta^{(n)}(t_0) \tag{3.106}$$

$$\frac{d\delta}{dt} = \delta' = \omega \Rightarrow \delta^{(1)} = \omega^{(0)} \tag{3.107}$$

$$\delta^{(2)} = \omega^{(1)} = \frac{1}{M}(P_m - P_e - D\omega) \tag{3.108}$$

$$\delta^{(3)} = \omega^{(2)} = \frac{1}{M}(0 - 0 - D\omega^{(1)}) = -\frac{D}{M}\delta^{(2)} \tag{3.109}$$

so:

$$\delta^{(3)} = \omega^{(2)} = -\frac{D}{M}\omega^{(1)} = -\frac{D}{M}\delta^{(2)} \tag{3.110}$$

$$\delta^{(4)} = \omega^{(3)} = -\frac{D}{M}\omega^{(2)} = -\frac{D}{M}\delta^{(3)} \tag{3.111}$$

$$\vdots$$

$$\delta^{(n)} = \omega^{(n-1)} = -\frac{D}{M}\omega^{(n-2)} = -\frac{D}{M}\delta^{(n-2)} \tag{3.112}$$

$$\delta^{(n+1)} = \omega^{(n)} = -\frac{D}{M}\omega^{(n-1)} = -\frac{D}{M}\delta^{(n-1)} \tag{3.113}$$

To find the radius of convergence we can use Eq. 3.10:

$$\frac{1}{R} = \lim_{n\to\infty}\left|\frac{b_{n+1}}{b_n}\right| = \lim_{n\to\infty}\left|\frac{\frac{1}{(n+1)!}\delta^{(n+1)}}{\frac{1}{(n)!}\delta^{(n)}}\right|$$

$$= \lim_{n\to\infty}\frac{1}{n+1}\left|\frac{\delta^{(n+1)}}{\delta^{(n)}}\right| = \lim_{n\to\infty}\frac{1}{n+1}\left|\frac{-\frac{D}{M}\omega^{(n-1)}}{\omega^{(n-1)}}\right| \tag{3.114}$$

$$= \lim_{n\to\infty}\frac{1}{n+1} * \frac{D}{M} = 0 \tag{3.115}$$

So, $R = \infty$.

3.5.4.3   Convergence of Generator Output Power Prediction

Approximating generators output power with Taylor series were discussed earlier. Following, the convergence of this approximation is proved.

$$P(t = t_1 = t_0 + \Delta t) = P(t_0) + P'(t_0)\Delta t + P''(t_0)\frac{\Delta t^2}{2!} + ... + P^{(n)}(t_0)\frac{\Delta t^n}{n!} + ... \tag{3.116}$$

$$P(t) = \sum_{n=0}^{\infty} c_n\Delta t^n \tag{3.117}$$

where

$$c_n = \frac{1}{n!}P^{(n)}(t_0) \tag{3.118}$$

$$P_e = P_m - M\frac{d\omega}{dt} - D\omega \tag{3.119}$$

$$P_e = P_m - M\omega^{(1)} - D\omega \tag{3.120}$$

$$P_e^{(1)} = 0 - M\omega^{(2)} - D\omega^{(1)} \tag{3.121}$$

$$P_e^{(2)} = 0 - M\omega^{(3)} - D\omega^{(2)} \tag{3.122}$$

$$\vdots$$

$$P_e^{(n)} = 0 - M\omega^{(n+1)} - D\omega^{(n)} \tag{3.123}$$

$$P_e^{(n+1)} = 0 - M\omega^{(n+2)} - D\omega^{(n+1)} \tag{3.124}$$

To find the radius of convergence Eq. 3.10 can be used:

$$\frac{1}{R} = \lim_{n\to\infty}\left|\frac{c_{n+1}}{c_n}\right| = \lim_{n\to\infty}\left|\frac{\frac{1}{(n+1)!}P^{(n+1)}}{\frac{1}{(n)!}P^{(n)}}\right|$$

$$= \lim_{n\to\infty}\frac{1}{n+1}\left|\frac{P^{(n+1)}(t_0)}{P^{(n)}(t_0)}\right| = \lim_{n\to\infty}\frac{1}{n+1}\left|\frac{-M\omega^{(n+2)} - D\omega^{(n+1)}}{-M\omega^{(n+1)} - D\omega^{(n)}}\right| \tag{3.125}$$

we know

$$\omega^{(n+1)} = \frac{-D}{M}\omega^{(n)} \tag{3.126}$$

$$= \lim_{n\to\infty}\frac{1}{n+1} * \frac{D}{M} = 0 \tag{3.127}$$

So, $R = \infty$.

3.5.4.4   Discussion about Radius of Convergence

In this section, it was proved that for power system main variables, the radius of convergence is infinity ($R = \infty$). Actually, it will be the case if there is no switching or sudden change in system variables. However, as mentioned at the beginning of the section, these variables are not analytic at the switching moments. This limits the radius of convergence. Figure 3.8 shows the graph of power system variables for a

three-phase fault on a random bus in a 500 bus system. It can be seen that at the switching moments the graphs are not differentiable. However, one time-step after or before the switching moments, the graphs are analytic.

In our studies, the time frame of the prediction is limited between the switching moments. At one time step after the switching, the radius of convergence is equal to time step, $R = \Delta t$. As we continue the prediction, the radius of convergence increases. This increase continues until we are in the middle of switching moments. Afterward, the radius of convergence decreases until we reach the switching moment. This is shown in figure 3.9. In the scope of this research, the radius of convergence equal to one time-step suffices, since the result from each moment is used for the next moment prediction.

3.5.5   Calculating Prediction Error

In previous discussions, it was shown that prediction equations converge to desired functions. However, there will be some errors due to: a) the omission of higher order terms in Taylor series, and b) the accumulative error of prediction of each step in the following steps of prediction.

To study the prediction error, similar to the discussion in 3.4, three possible scenarios for swing equation are discussed:

3.5.5.1   Scenario 1:

The Derivative of ω Is Independent of Prediction

The initial points of a function and the derivative of the first function, which is independent of prediction, are available. The goal is to find the errors when predicting the first function, and predicting the values of a second function, while its derivative depends on the first function.

$$\frac{\mathrm{d}\omega}{\mathrm{d}t} = \frac{P_m - P_e}{M} \tag{3.128}$$

$$\frac{\mathrm{d}\delta}{\mathrm{d}t} = \omega \tag{3.129}$$
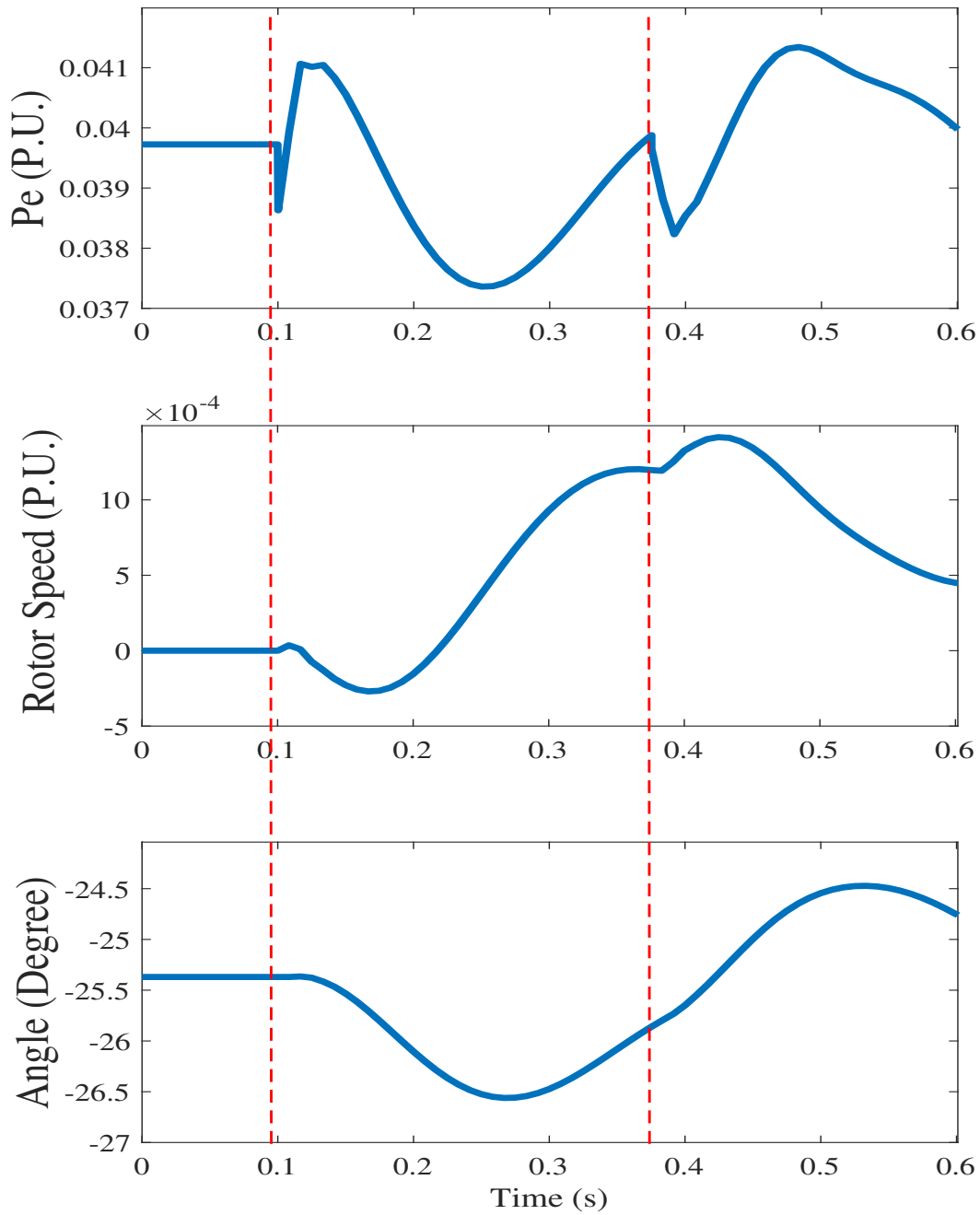
Figure 3.8: Radius of convergence and analyticity concept for power system variables.

Here, $\omega(t)$ is function 1, that its derivatives do not depend on its value explicitly. $\delta(t)$ is the second function that its derivative comes from ω. The goal is to predict both
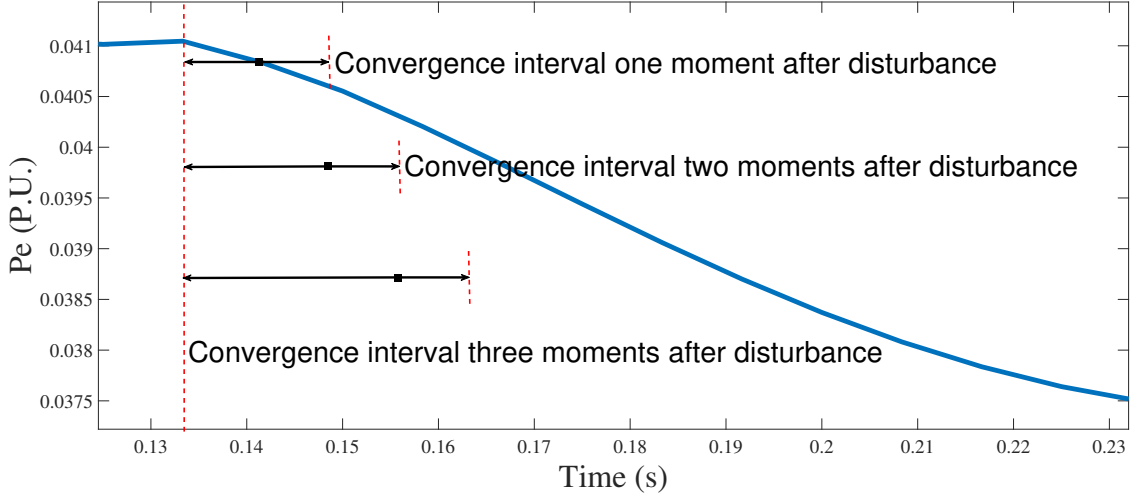
Figure 3.9: Change in radius of convergence between switching moments.

of them and find the prediction error.

R_i^ω and R_i^δ are the remainder of Taylor polynomial at each iteration of prediction for generator i, while E_i^ω and E_i^δ are the accumulative total error after k iterations of prediction.

Iteration 1:

$$\omega(t_0 + h) = \omega(t_0) + \sum_{n=1}^{N} \frac{h^n}{n!} \omega^{(n)}(t_0) + R_1^\omega \tag{3.130}$$

$$E_1^\omega = R_1^\omega \tag{3.131}$$

$$R_1^\omega = \sum_{n=N+1}^{\infty} \frac{h^n}{n!} \omega^{(n)}(t_0) \tag{3.132}$$

$$\delta(t_0 + h) = \delta(t_0) + \sum_{n=1}^{N} \frac{h^n}{n!} \delta^{(n)}(t_0) + R_1^\delta \tag{3.133}$$

$$E_1^\delta = R_1^\delta \tag{3.134}$$

$$R_1^\delta = \sum_{n=N+1}^{\infty} \frac{h^n}{n!} \delta^{(n)}(t_0) \tag{3.135}$$

Iteration 2:

$$\omega(t_0 + 2h) = \omega(t_0 + h) - R_1^\omega + \sum_{n=1}^{N} \frac{h^n}{n!} \omega^{(n)}(t_0 + h) + R_2^\omega \tag{3.136}$$

$$E_2^\omega = R_1^\omega + R_2^\omega \tag{3.137}$$

$$\delta(t_0 + 2h) = \delta(t_0 + h) - R_1^\delta + \sum_{n=1}^{N} \frac{h^n}{n!} \delta^{(n)}(t_0 + h) + R_2^\delta \tag{3.138}$$

$$\delta(t_0 + 2h) = \delta(t_0 + h) - R_1^\delta + h(\omega(t_0 + h) - E_1^\omega)$$

$$+ \sum_{n=2}^{N} \frac{h^n}{n!} \omega^{(n-1)}(t_0 + h) + R_2^\delta \tag{3.139}$$

$$E_2^\delta = R_2^\delta + R_1^\delta + h E_1^\omega \tag{3.140}$$

Iteration 3:

$$\omega(t_0 + kh) = \tilde{\omega}(t_0 + 3h) + E_3^\omega \tag{3.141}$$

$$E_3^\omega = R_1^\omega + R_2^\omega + R_3^\omega \tag{3.142}$$

$$\delta(t_0 + 3h) = \delta(t_0 + 2h) - E_2^\delta + h(\omega(t_0 + 2h) - E_2^\omega)$$

$$+ \sum_{n=2}^{N} \frac{h^n}{n!} \omega^{(n-1)}(t_0 + 2h) + R_3^\delta \tag{3.143}$$

$$E_3^\delta = R_3^\delta + R_2^\delta + R_1^\delta + h E_2^\omega \tag{3.144}$$

$$\vdots$$

Iteration k:

$$\omega(t_0 + kh) = \tilde{\omega}(t_0 + kh) + E_k^\omega \tag{3.145}$$

$$E_k^\omega = \sum_{i=1}^{k} R_i^\omega \tag{3.146}$$

$$R_i^\omega = \sum_{n=N+1}^{\infty} \frac{h^n}{n!} \omega^{(n)}(t_0 + (i-1)h) \tag{3.147}$$

$$\delta(t_0 + kh) = \tilde{\delta}(t_0 + kh) + E_k^\delta \tag{3.148}$$

$$E_k^\delta = \sum_{i=1}^{k} R_i^\delta - h E_{k-1}^\omega \tag{3.149}$$

$$E_k^\delta = \sum_{i=1}^{k} R_i^\delta - h \sum_{i=1}^{k-1} R_i^\omega \tag{3.150}$$

$$R_i^\delta = \sum_{n=N+1}^{\infty} \frac{h^n}{n!} \omega^{(n-1)}(t_0 + (i-1)h) \tag{3.151}$$

3.5.5.2   Scenario 2:

The Derivative of ω Depends Only on Its Value

The initial points of a function and the derivative of it as a function of itself are available. The goal is to find the errors when predicting the first function, and predicting the values of a second function, while its derivative depends on the first function.

$$\frac{d\omega}{dt} = \frac{1}{M}(P_m - P_e - D\omega) \tag{3.152}$$

$$\frac{d\delta}{dt} = \omega \tag{3.153}$$

Iteration 1:

$$\omega(t_0 + h) = \omega(t_0) + \sum_{n=1}^{N} \frac{h^n}{n!} \omega^{(n)}(t_0) + R_1^\omega \tag{3.154}$$

$$E_1^\omega = R_1^\omega \tag{3.155}$$

$$R_1^\omega = \sum_{n=N+1}^{\infty} \frac{h^n}{n!} \omega^{(n)}(t_0) \tag{3.156}$$

$$\delta(t_0 + h) = \delta(t_0) + \sum_{n=1}^{N} \frac{h^n}{n!} \delta^{(n)}(t_0) + R_1^\delta \tag{3.157}$$

$$E_1^\delta = R_1^\delta \tag{3.158}$$

$$R_1^\delta = \sum_{n=N+1}^{\infty} \frac{h^n}{n!} \delta^{(n)}(t_0) \tag{3.159}$$

Iteration 2:

$$\omega(t_0 + 2h) = \omega(t_0 + h) - R_1^\omega + \sum_{n=1}^{N} \frac{h^n}{n!} \omega^{(n)}(t_0 + h)$$

$$-\sum_{n=1}^{N} \frac{h^n}{n!} DR_1^\omega + R_2^\omega \tag{3.160}$$

$$E_2^\omega = R_2^\omega + (1 + \alpha D)R_1^\omega \tag{3.161}$$

$$\delta(t_0 + 2h) = \delta(t_0 + h) - R_1^\delta + \sum_{n=1}^{N} \frac{h^n}{n!} \delta^{(n)}(t_0 + h) + R_2^\delta \tag{3.162}$$

$$\delta(t_0 + 2h) = \delta(t_0 + h) - R_1^\delta + \sum_{n=1}^{N} \frac{h^n}{n!} \omega^{(n-1)}(t_0 + h)$$

$$-\sum_{n=1}^{N} \frac{h^n}{n!} (E_1^\omega)^{(n-1)} + R_2^\delta \tag{3.163}$$

$$E_2^\delta = R_2^\delta + R_1^\delta + \alpha E_1^\omega \tag{3.164}$$

$$E_2^\delta = R_2^\delta + R_1^\delta + \alpha R_1^\omega \tag{3.165}$$

Iteration 3:

$$\omega(t_0 + 3h) = \omega(t_0 + 2h) - E_2^\omega + \sum_{n=1}^{N} \frac{h^n}{n!} \omega^{(n)}(t_0 + 2h)$$

$$-\sum_{n=1}^{N} \frac{h^n}{n!} DE_2^\omega + R_3^\omega \tag{3.166}$$

$$E_3^\omega = R_3^\omega + (1 + \alpha D)E_2^\omega \tag{3.167}$$

$$E_3^\omega = R_3^\omega + (1 + \alpha D)R_2^\omega + (1 + \alpha D)^2 R_1^\omega \tag{3.168}$$

$$\delta(t_0 + 3h) = \delta(t_0 + 2h) - E_2^\delta + \sum_{n=1}^{N} \frac{h^n}{n!} \delta^{(n)}(t_0 + 2h) + R_3^\delta - \alpha E_2^\omega \tag{3.169}$$

$$E_3^\delta = R_3^\delta + E_2^\delta + \alpha E_2^\omega \tag{3.170}$$

$$E_3^\delta = R_3^\delta + R_2^\delta + R_1^\delta + [\alpha(1+\alpha D) + \alpha]R_1^\omega + \alpha R_2^\omega \tag{3.171}$$

$$\vdots$$

Iteration k:

$$\omega(t_0 + kh) = \tilde{\omega}(t_0 + kh) + E_k^\omega \tag{3.172}$$

$$E_k^\omega = \sum_{i=1}^{k}(1+\alpha D)^{k-i}R_i^\omega \tag{3.173}$$

$$E_k^\omega \leq C_m^\omega(e^h - 1 - \alpha)\sum_{i=1}^{k}(1+\alpha D)^i \tag{3.174}$$

$$\delta(t_0 + kh) = \tilde{\delta}(t_0 + kh) + E_k^\delta \tag{3.175}$$

$$E_k^\delta = \sum_{i=1}^{k}R_i^\delta + \alpha\sum_{i=1}^{k-1}E_i^\omega \tag{3.176}$$

$$E_k^\delta = \sum_{i=1}^{k}R_i^\delta + \alpha\sum_{j=1}^{k-1}\sum_{i=1}^{j}(1+\alpha D)^{j-i}R_i^\omega \tag{3.177}$$

$$E_k^\delta \leq kC_m^\delta(e^h - 1 - \alpha) + \alpha C_m^\omega(e^h - 1 - \alpha)\sum_{j=1}^{k-1}\sum_{i=1}^{j}(1+\alpha D)^i \tag{3.178}$$

$$E_k^\delta \leq kC_m^\delta(e^h - 1 - \alpha) + \alpha k C_m^\omega(e^h - 1 - \alpha)\sum_{i=1}^{k}(1+\alpha D)^i \tag{3.179}$$

3.5.5.3   Scenario 3:
The Derivative of ω Depends on Its Value and on P_e

This scenario is similar to scenario 2. The initial points of a function and the derivative of it as a function of itself are available. The difference this time is that P_e, as a term in ω's derivative has an error at every step. However, the amount of the P_e error at each step is unknown. The worst case is when we consider the P_e equal to its value at the moment of the fault, while the actual value is zero. So, the maximum

possible error at each step will be P_{e0}. This is the most general assumption.

$$P_e \leq P_{e0} \tag{3.180}$$

The goal is to find the errors when predicting the first function, and predicting the values of a second function, while its derivative depends on the first function.

$$\frac{\mathrm{d}\omega}{\mathrm{d}t} = \frac{1}{M}(P_m - P_e - D\omega) \tag{3.181}$$

$$\frac{\mathrm{d}\delta}{\mathrm{d}t} = \omega \tag{3.182}$$

Iteration 1:

$$\omega(t_0 + h) = \omega(t_0) + \sum_{n=1}^{N} \frac{h^n}{n!}\omega^{(n)}(t_0) + R_1^{\omega} \tag{3.183}$$

$$E_1^{\omega} = R_1^{\omega} \tag{3.184}$$

$$R_1^{\omega} = \sum_{n=N+1}^{\infty} \frac{h^n}{n!}\omega^{(n)}(t_0) \tag{3.185}$$

$$\delta(t_0 + h) = \delta(t_0) + \sum_{n=1}^{N} \frac{h^n}{n!}\delta^{(n)}(t_0) + R_1^{\delta} \tag{3.186}$$

$$E_1^{\delta} = R_1^{\delta} \tag{3.187}$$

$$R_1^{\delta} = \sum_{n=N+1}^{\infty} \frac{h^n}{n!}\delta^{(n)}(t_0) \tag{3.188}$$

Iteration 2:

$$\omega(t_0 + 2h) = \omega(t_0 + h) - R_1^{\omega} + \sum_{n=1}^{N} \frac{h^n}{n!}\omega^{(n)}(t_0)$$

$$+ \sum_{n=1}^{N} \frac{h^n}{n!}DR_1^{\omega} + \sum_{n=1}^{N} \frac{h^n}{n!}P_{e02}^{(n)}(t_0 + h) + R_2^{\omega} \tag{3.189}$$

$$E_2^{\omega} = R_2^{\omega} + (1 + \alpha D)R_1^{\omega} + \alpha P_{e02} \tag{3.190}$$

$$\vdots$$

Iteration k:

$$E_k^\omega = \sum_{i=1}^{k}(1+\alpha D)^{k-i}R_i^\omega + \sum_{i=2}^{k}\alpha(1+\alpha D)^{i-2}P_{e0i} \qquad (3.191)$$

$$E_k^\omega \le C_m^\omega(e^h-1-\alpha)\sum_{i=1}^{k}(1+\alpha D)^i + \alpha P_{e0}\sum_{i=2}^{k}(1+\alpha D)^i \qquad (3.192)$$

$$E_k^\delta = \sum_{i=1}^{k}R_i^\delta + \alpha\sum_{i=1}^{k-1}E_i^\omega \qquad (3.193)$$

$$E_k^\delta = \sum_{i=1}^{k}R_i^\delta + \alpha\sum_{j=1}^{k-1}(\sum_{i=1}^{j}(1+\alpha D)^{k-i}R_i^\omega)$$

$$+\alpha^2\sum_{j=1}^{k-1}(\sum_{i=1}^{j}(1+\alpha D)^{i-2}P_{e0i}) \qquad (3.194)$$

$$E_k^\delta \le C_m^\delta(e^h-1-\alpha) + k\alpha C_m^\omega(e^h-1-\alpha)\sum_{j=1}^{k}(1+\alpha D)^j$$

$$+k\alpha^2 P_{e0}\sum_{j=2}^{k}(1+\alpha D)^j \qquad (3.195)$$

Tables 3.9 and 3.10 provide a summary of the equations used for predicting generator behavior and related errors in the most general scenario.

Table 3.9: Equations used for predicting generator behavior.

Variable	Prediction Formula	Equation Number
ω	$\omega(t_0+\Delta t) = \omega(t_0) + (\frac{P_m-P_e}{M})\Delta t - \frac{D}{M}\Delta\delta$	3.70
δ	$\delta(t_0+\Delta t) = \delta(t_0) + [\omega(t_0)\Delta t + (\frac{P_m-P_e}{M} - \frac{D}{M}\omega(t_0))\frac{\Delta t^2}{2!}] * 2\pi f$	3.71
P_e	$P_e(i+1) = P_e(i) - M(a(i)-a(i-1))$ $-Da(i)*TS - \frac{D}{2}(a(i)-a(i-1))*TS$ $+\frac{1}{2}TS^2(\frac{D^2}{M^2}a(i) - \frac{D^2}{M}a(i))$ $-\frac{M}{2}(a(i)-2a(i-1)+a(i-2))$	3.91

Table 3.10: Equations used for calculating prediction error.

Variable	Error Formula	Equation Number
ω	$E_k^\omega \leq C_m^\omega(e^h - 1 - \alpha)\sum_{i=1}^{k}(1 + \alpha D)^i$ $+ \alpha P_{e0}\sum_{i=2}^{k}(1 + \alpha D)^i$	3.191
δ	$E_k^\delta \leq C_m^\delta(e^h - 1 - \alpha) + k\alpha C_m^\omega(e^h - 1 - \alpha)\sum_{j=1}^{k}(1 + \alpha D)^j$ $+ k\alpha^2 P_{e0}\sum_{j=2}^{k}(1 + \alpha D)^j$	3.194
P_e	$P_e \leq P_{e0}$	3.179

3.6 An Illustrative Example:

Predicting Generator Behavior in a Single Machine - Infinite Bus System

Consider the network shown in figure 3.10. It is a Single-Machine Infinite-Bus (SMIB). A three-phase symmetrical fault happens at Bus 3 at $t = 0.1$ seconds. According to the numerical simulation, Critically Stable Clearing Time(CSCT) is 0.150 seconds, and Critically Unstable Clearing Time(CUCT) is 0.151 seconds. The goal is to predict the system behavior and compare it with the results of numerically solving the system equations, which is referred as "simulated" or "actual" in this script.
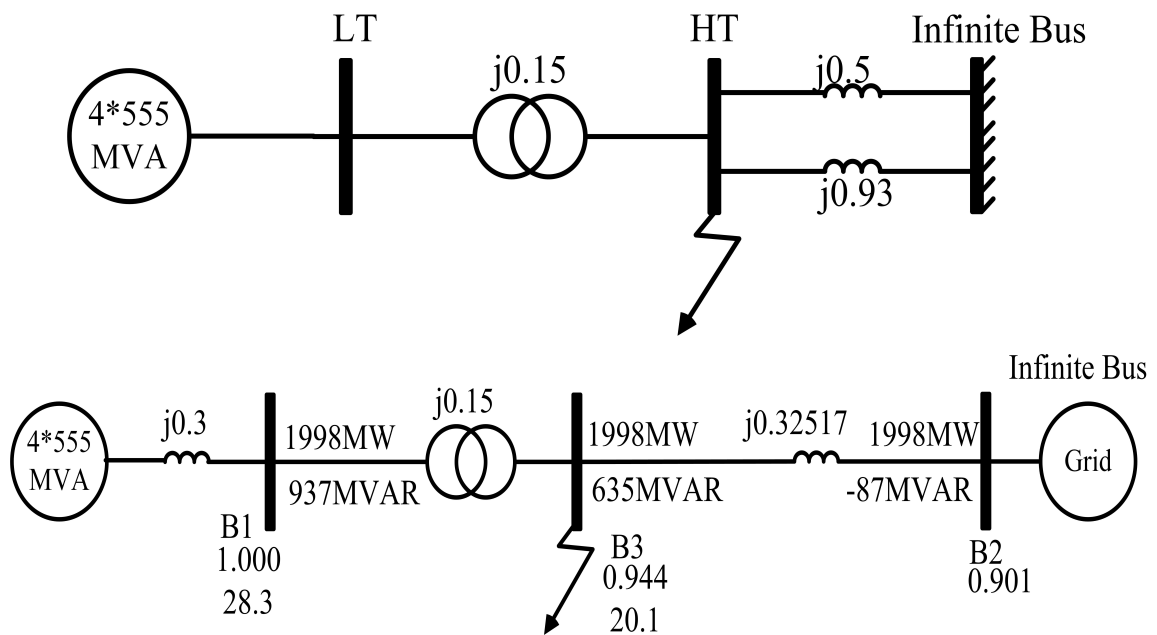
Figure 3.10: SMIB network for illustrating generator behavior prediction [1].

Table 3.11: Prediction results for the SMIB network shown in Fig. 3.10.

Time	ω		δ	
	Predicted	Simulated	Predicted	Simulated
0.11	0.0013	0.0013	0.7310	0.7311
0.20	0.0129	0.0129	0.9310	0.9311

During the fault, the voltage of Bus 3 is zero. So, no active power is transferred from the generator to the grid ($P_e = 0$). The inertia constant of the generator is 3.5 ($H = 3.5$ and $M = 7$), and input mechanical power is 0.9 P.U. ($P_m = 0.9$ P.U.). Assume that the post-fault configuration of the system is the same as the pre-fault. Suppose that the results for $t = 0.13s$ are available, and the goal is to predict δ and ω for fault duration. Two sample calculations are provided below. Table 3.11, and figures 3.11 and 3.12 provide a comparison between the actual and predicted values. The blue curves in figures represent the predicted behavior of the generator if the fault is not cleared (sustained fault).

$\delta(t = 0.13) = 0.74734 radian = 41.77°$

$\omega(t = 0.13) = 0.0039$

$M = 7$

$\omega(t = 0.14)_{predicted} = \omega(t = 0.13) + \frac{0.9-0}{7} * .01 = 0.0052$

$\omega(t = 0.14)_{simulated} = 0.0051$

$\delta(t = 0.14)_{predicted} = 2 * \pi * 50 * \left\{ \frac{0.9-0}{7} \frac{0.01^2}{2!} + 0.0039 * 0.01 \right\} + 0.74734 = 0.7616$

$\delta(t = 0.14)_{simulated} = 0.7615$

$\vdots$

$\omega(t = 0.2)_{predicted} = \omega(t = 0.13) + \frac{0.9-0}{7} * .07 = 0.0129 \quad \omega(t = 0.2)_{simulated} = 0.0129$

$\delta(t = 0.2)_{predicted} = 2 * \pi * 50 * \left\{ \frac{0.9-0}{7} \frac{0.07^2}{2!} + 0.0039 * 0.07 \right\} + 0.74734 = 0.9321$

$\delta(t = 0.2)_{simulated} = 0.9311$

As can be seen in the figures 3.11 and 3.12, the prediction have great accuracy in this simple system and completely matches with the actual results.
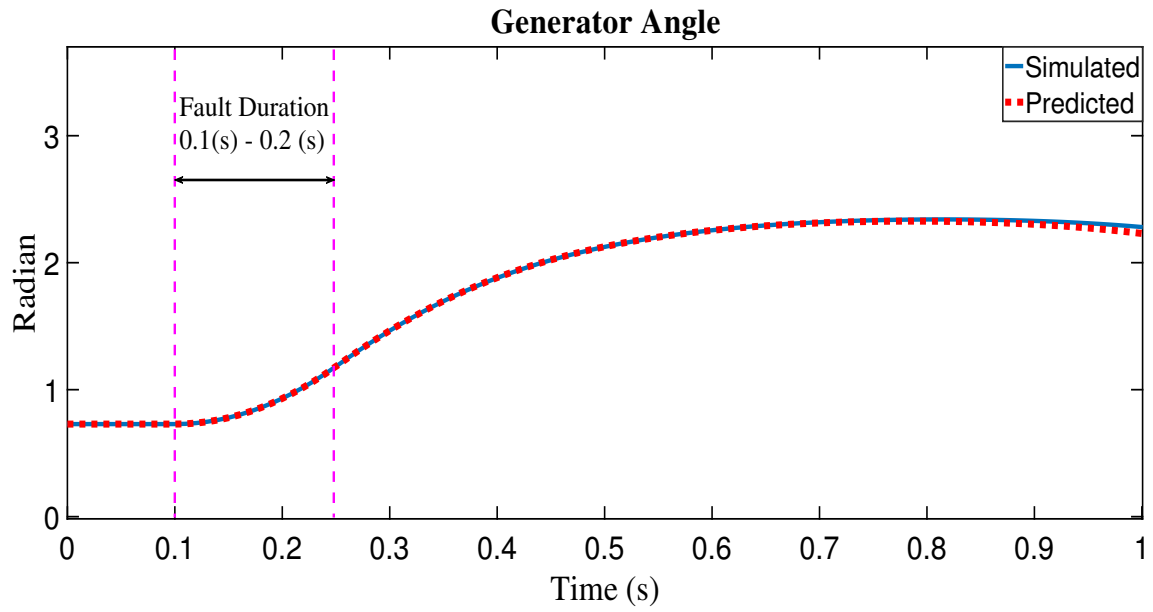
Figure 3.11: Actual and predicted generator angle - SMIB network for transient stability study.
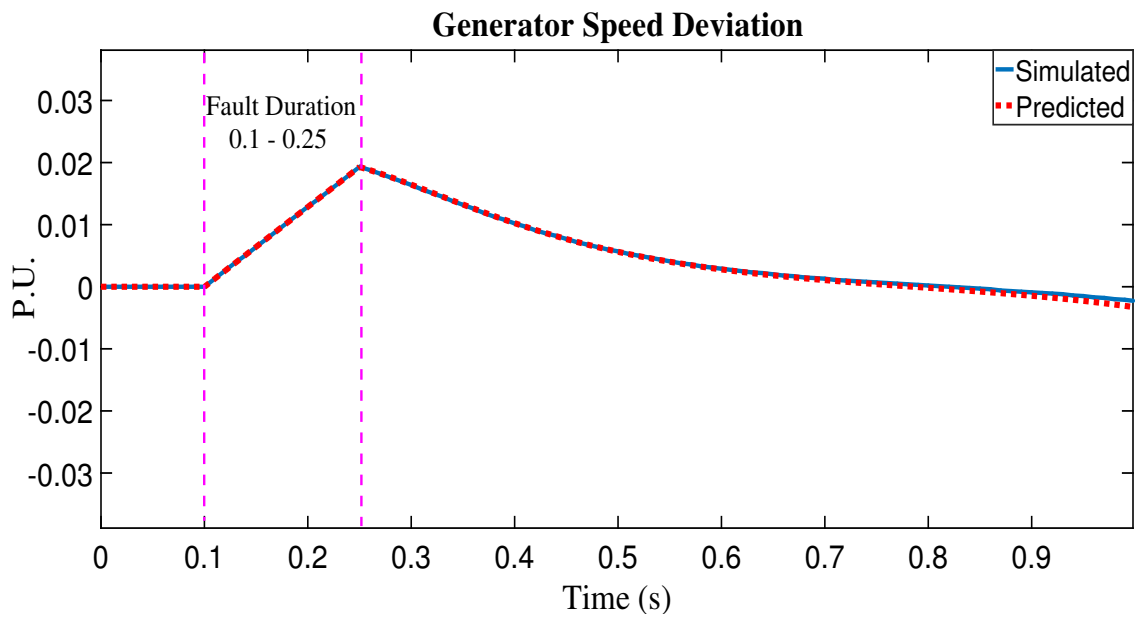
Figure 3.12: Actual and predicted generator speed - SMIB network for transient stability study.

3.7   Summary

In this chapter, the Taylor series fundamental concept was discussed. Later, it was presented how to use Taylor series to predict the speed, angle, and output power of generators. The error of prediction was calculated, and results for testing the proposed prediction method for a SMIB were presented. In the next chapter, chapter 4, the proposed method is applied to multi-machine larger systems and the accuracy of the prediction is discussed.

CHAPTER 4: Generator Behavior Prediction in Multi-Machine Power Systems

In previous chapters, the importance of power systems stability and methods of facing the equations modeling a dynamic system were explained. Later, in chapter 3, a prediction method was proposed and the results for a SMIB case study was shown. In this chapter, the proposed prediction technique is employed for predicting the behavior of larger multi-machine systems. Case studies are IEEE 9 bus system, IEEE 39 bus system, and North Carolina - South Carolina 500 bus system. The results of the studies are presented and discussed.

4.1 Introduction

As mentioned earlier in section 3.5.2, three different assumptions for P_e can be considered when predicting angles and speeds of generators. The most accurate prediction happens when the actual output electrical power of generators (P_e) is known. This way, the accelerating power can be found accurately. However, this is not practically possible, since the swing equation should be numerically solved. Also, in real-time studies, the actual output power of generators cannot be known beforehand to be used for the prediction. Therefore, the output power of generators, for predicting their speed and angle, should be found in another way. Three different approaches can be considered for approximating P_e during the fault:

- Assuming P_e of generators equal to zero

- Assuming P_e as a constant number

  This amount can be the amount of P_e one moment after the fault.

- Predicting P_e of generators

  Because the behavior of the system is predicted for next time step, Taylor's

Series can be used.

In what follows, the prediction has been used to predict the behavior of IEEE 9 bus, IEEE 39 bus, and the 500 bus South Carolina-North Carolina synthetic network. The study is shown for different assumptions of P_e. Also, to show the authenticity of the method, although impractical, prediction of δ and ω with actual values of P_e is shown for post-disturbance graphs. Figures 4.1 and 4.2 show how to use the proposed technique.

The prediction error for desired variable (X), has been calculated and provided using equations 4.1 and 4.2.

$$Error(X_{t_i})(\%) = \frac{X_{t_i}^{actual} - X_{t_i}^{predicted}}{X_{t_i}^{actual}} * 100 \tag{4.1}$$

$$Mean \ \ Error(x) = \frac{\sum_{i=1}^{n} |Error(X_{t_i})|}{n} \tag{4.2}$$

where n is the number of moments that the variables are predicted and can be found using Eq.4.3.

$$n = \frac{t(fault \ removal) - t(fault \ start)}{Time \ Step} \tag{4.3}$$
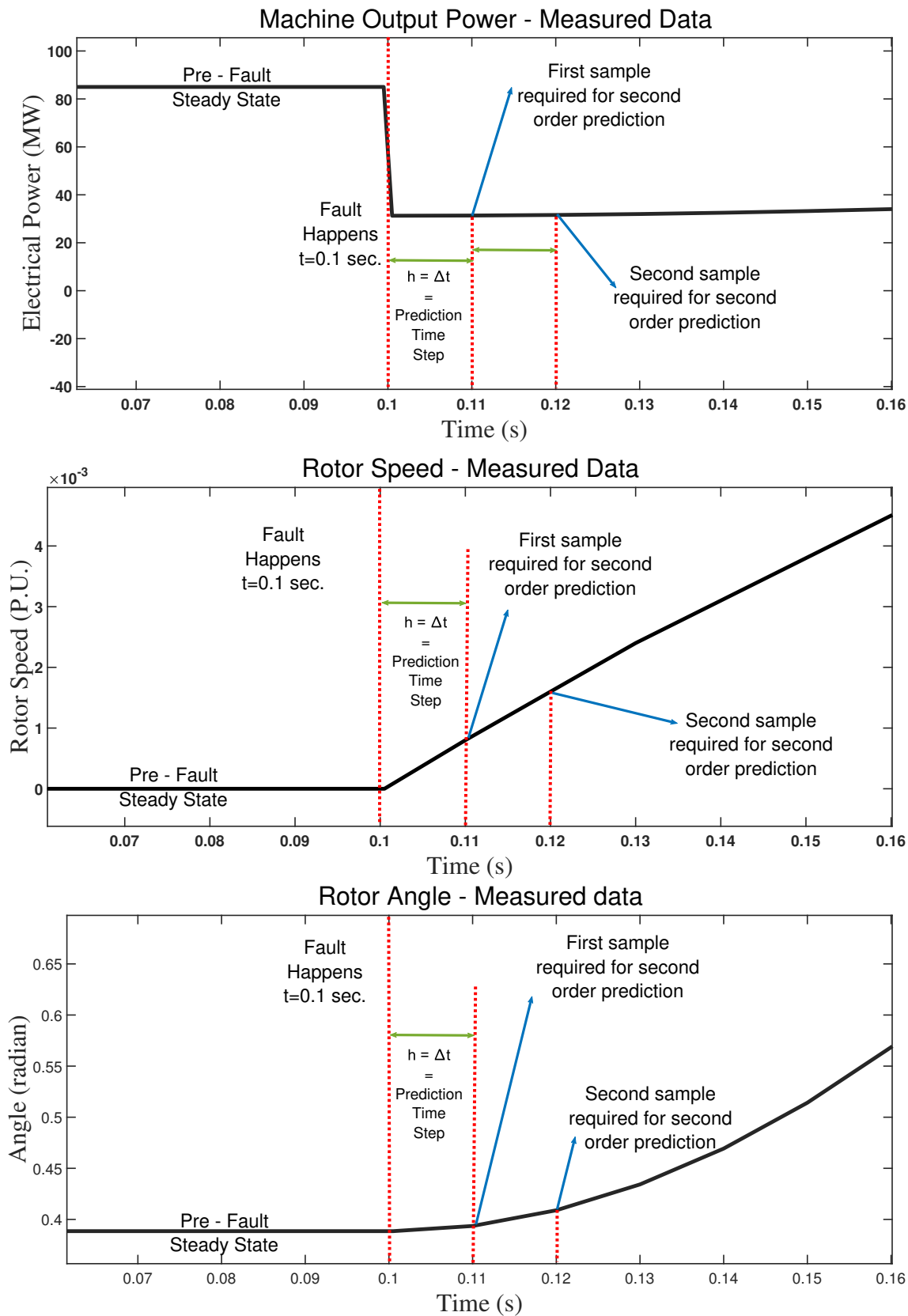
Figure 4.1: Data acquisition for the proposed method.
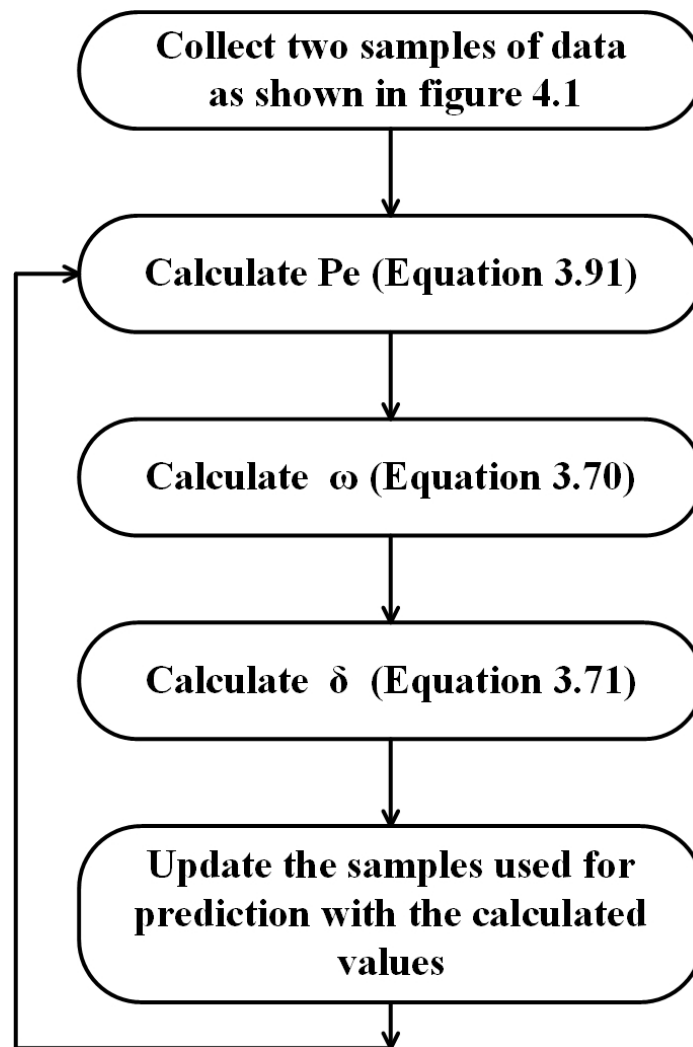
Figure 4.2: Algorithm of proposed prediction method.

4.2   Predicting Generators Angle and Speed in IEEE 9 Bus System

In what follows, the behavior of the IEEE 9 bus test system, shown in figure 4.3, is being predicted based on three different assumptions for P_e during the fault. In this system, generator 1 is the reference machine, meaning $\delta 1 = 0$ during the entire study. A three-phase fault is applied on bus 2 at the terminal of generator 2. Hence, electrical output of generator 2 is zero, $P_{e2} = 0$.

The prediction for system behavior during the fault is only based on the PMU data for two time-steps after the fault. However, the prediction for the post-fault system is corrected by updating the initial point in the related formulas every 8 time-steps (every 0.08 seconds).
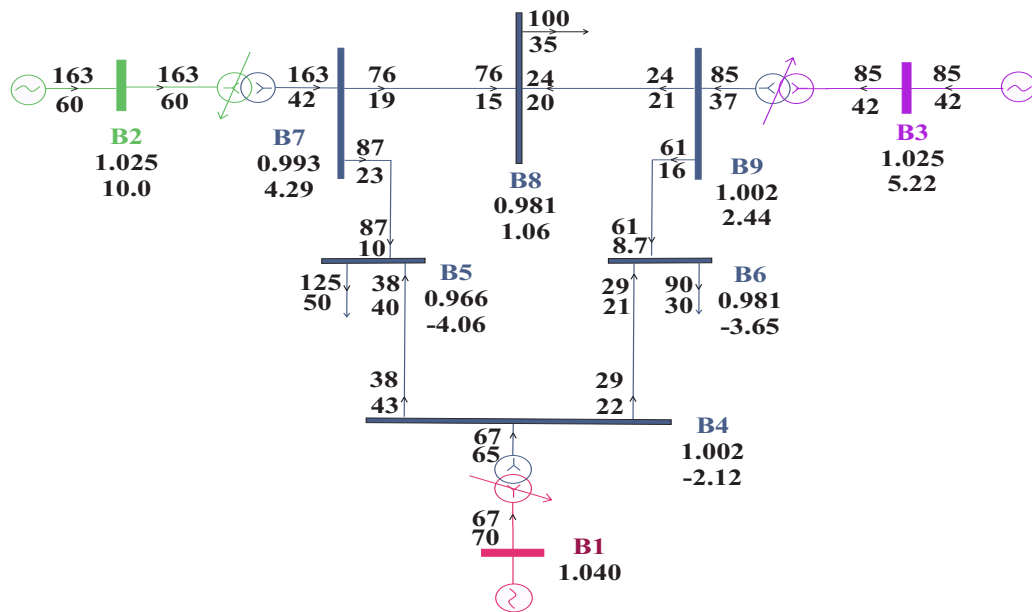
Figure 4.3: IEEE 9 bus system one-line diagram and its load flow result.

4.2.1   Assumption 1: Generators Output Power During the Fault Is Zero

During the fault, generators electrical output, P_e, are considered constant and equal to zero ($P_e(During\ Fault) = 0$). Table 4.1 shows maximum and average errors of predicting generators' rotor speed and angle. Figures 4.4 and 4.5 depict the actual and predicted rotor speed and rotor angle for generators 1 and 2, respectively.
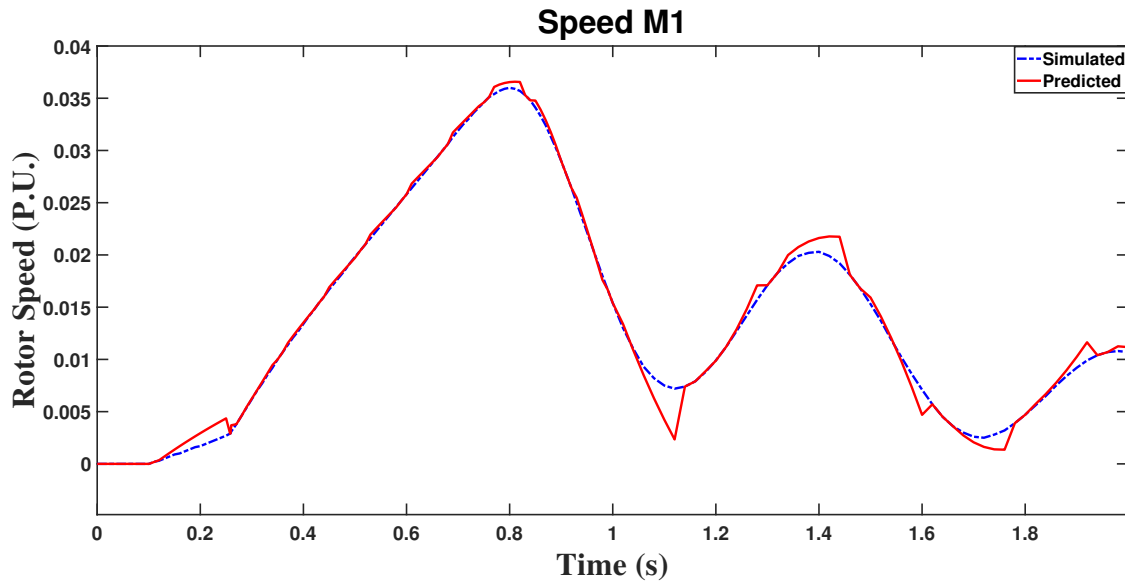
Figure 4.4: Actual and predicted rotor speed of G1 when $P_e(During\ Fault)$ is assumed to be zero - Fault on bus 2 - IEEE 9 bus test system.
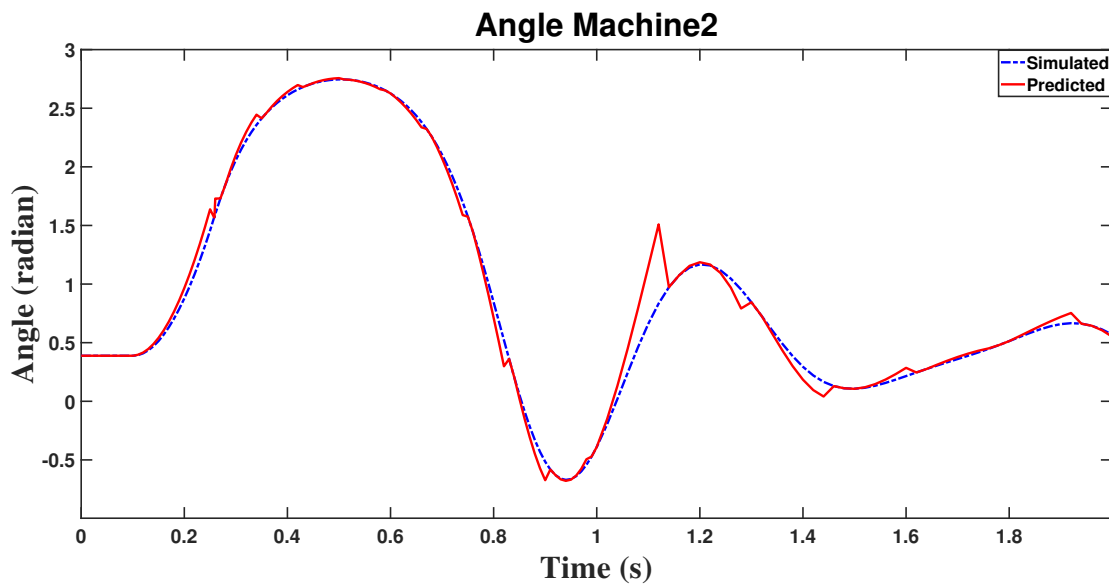
Figure 4.5: Actual and predicted rotor angle of G2 when $P_e(During\ Fault)$ is assumed to be zero - Fault on bus 2 - IEEE 9 bus test system.

4.2.2   Assumption 2: Generators Output Power During the Fault Is Constant

During the fault, generators electrical output, P_e, are considered constant and equal to their value of one moment after the fault happens ($P_e(During\ Fault) = P_e(t_{fault}^+)$). Table 4.2 shows maximum and average errors of predicting generators' rotor speed

Table 4.1: Absolute of prediction error(percent) when $P_e(During\ Fault)$ is assumed to be zero - Fault on bus 2 - IEEE 9 bus test system.

Variable	$\delta 2$	$\delta 3$	$\omega 1$	$\omega 2$	$\omega 3$	$Pe1$	$Pe3$
Maximum Error	12.3897	45.2952	72.8179	2.0025	67.7492	100	100
Mean Error	4.0723	10.1968	29.8803	0.3840	23.1830	50	50

and angle. Figures 4.6 and 4.7 depict the actual and predicted rotor speed and rotor angle for generators 1 and 2, respectively.

Table 4.2: Absolute of prediction error(percent) when $P_e(During\ Fault)$ is assumed to be equal to $P_e(t_{fault}^+)$ - Fault on bus 2 - IEEE 9 bus test system.

Variable	$\delta 2$	$\delta 3$	$\omega 1$	$\omega 2$	$\omega 3$	$Pe1$	$Pe3$
Maximum Error	16.0125	45.2952	16.2606	2.0025	10.7717	88.9390	32.0227
Mean Error	4.9704	4.3801	4.1981	0.3840	2.3184	14.6063	7.6442

4.2.3   Assumption 3: Generators Output Power During the Fault Is Approximated

In this scenario, generators electrical output power, P_e, during the fault, are predicted via Taylor Series ($P_e(During\ Fault) = $ Predicted P_e). Table 4.3 shows maxi-
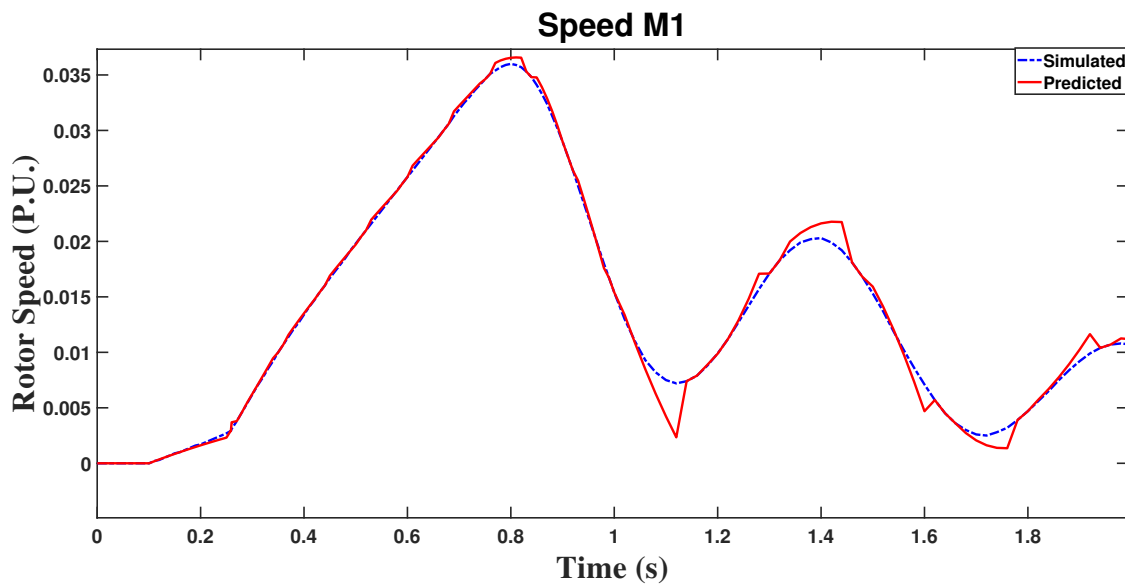
Figure 4.6: Actual and predicted rotor speed of G1 when $P_e(During\ Fault)$ is assumed to be equal to $P_e(t_{fault}^+)$ - Fault on bus 2 - IEEE 9 bus test system.
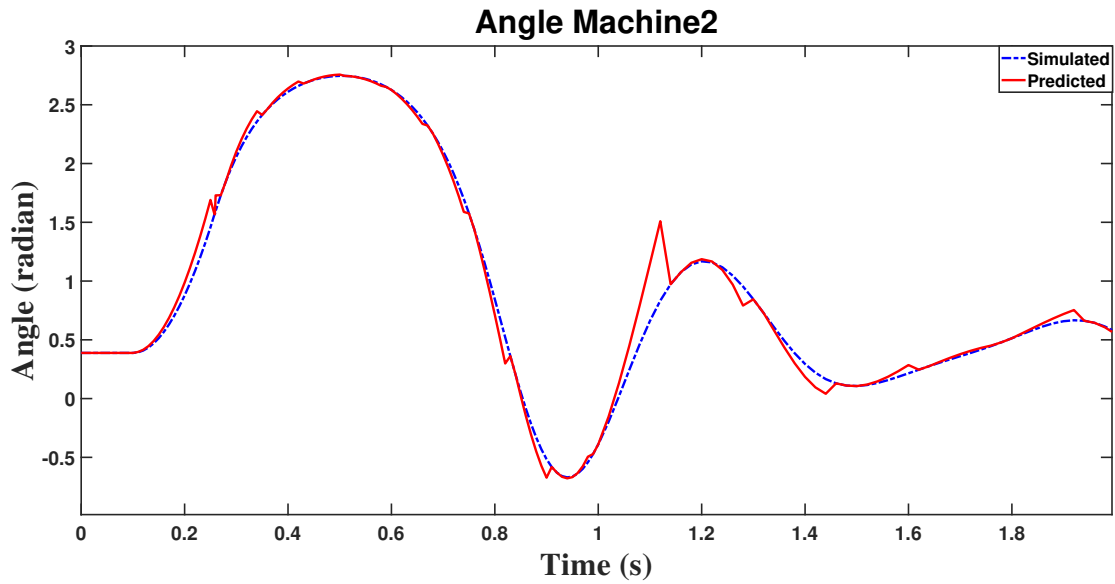
Figure 4.7: Actual and predicted rotor angle of G2 when $P_e(During\ Fault)$ is assumed to be equal to $P_e(t^+_{fault})$ - Fault on bus 2 - IEEE 9 bus test system.

mum and average errors of predicting generators' rotor speed and angle. Figures 4.8 and 4.9 depict the actual and predicted rotor speed and rotor angle for generators 1 and 2, respectively.
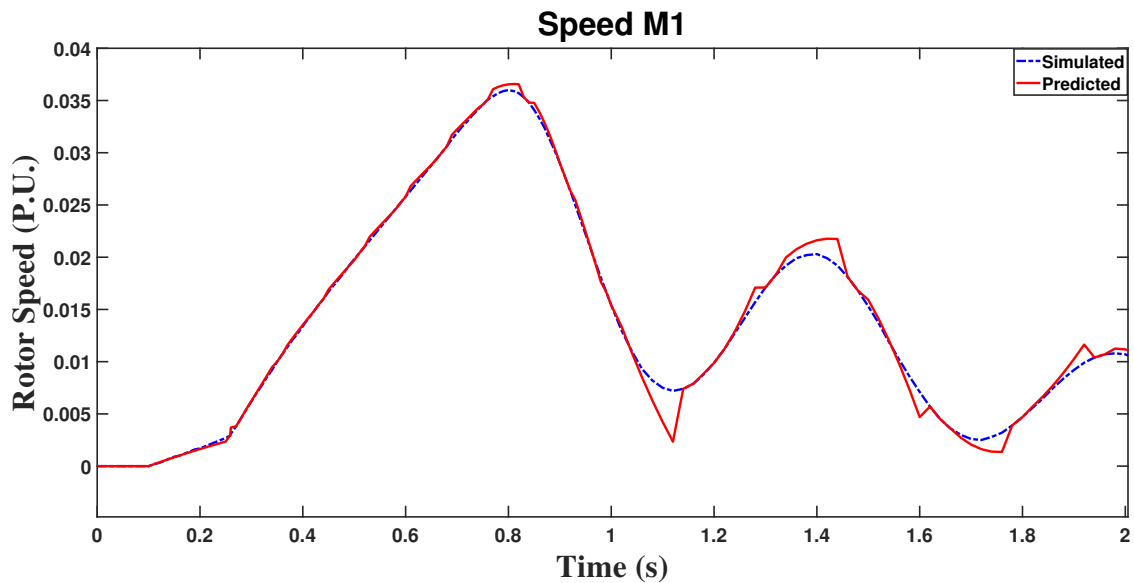
Figure 4.8: Actual and predicted rotor speed of G1 when $P_e(During\ Fault)$ is predicted - Fault on bus 2 - IEEE 9 bus test system.
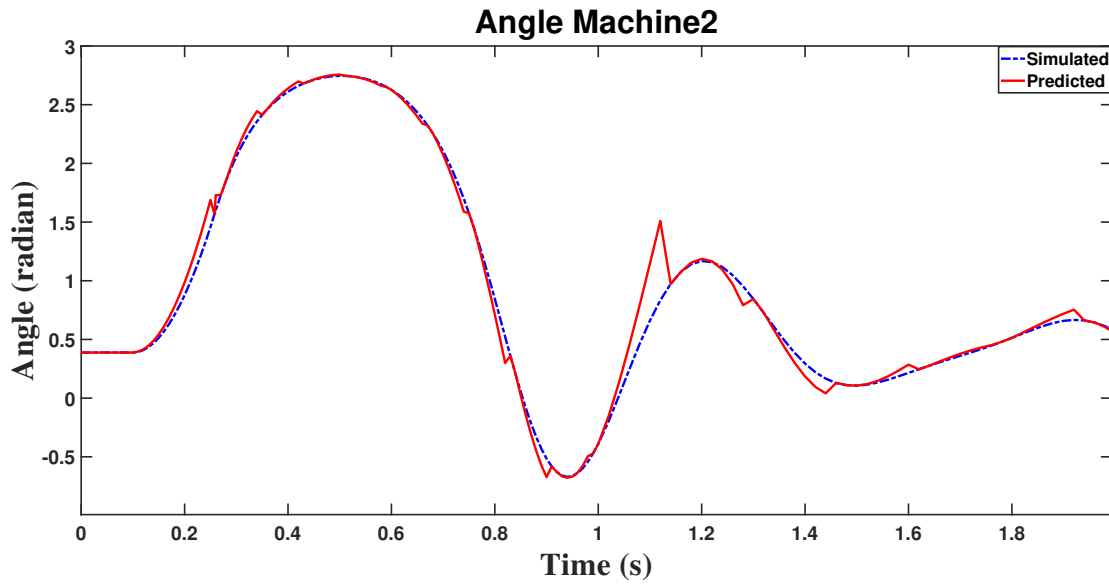
Figure 4.9: Actual and predicted rotor angle of G2 when $P_e(During\ \ Fault)$ is predicted - Fault on bus 2 - IEEE 9 bus test system.

Table 4.4 shows a comparison between the accuracy of prediction, based on the different assumptions that were discussed. As can be seen in table 4.4, minimum error belongs to the third scenario, where P_e during the fault were predicted. Therefore, in the following, predicting the behavior of the system is based on predicting P_e during the fault.

Table 4.3: Absolute of prediction error(percent) when $P_e(During\ \ Fault)$ is predicted - Fault on bus 2 - IEEE 9 bus test system.

Variable	$\delta2$	$\delta3$	$\omega1$	$\omega2$	$\omega3$	$Pe1$	$Pe3$
Maximum Error	15.8884	17.8510	16.2606	2.0025	9.3593	82.8961	28.7392
Mean Error During Fault	4.9495	4.2157	3.8519	0.4033	1.9940	13.2629	6.6263

Table 4.4: Mean percentage of prediction error for different assumption of generators output power - Fault on bus 2 - IEEE 9 bus test system.

Variable	$\delta 1$	$\delta 2$	$\delta 3$	$\omega 1$	$\omega 2$	$\omega 3$
$Pe = 0$	0	4.0723	10.1968	29.8803	0.3840	23.1830
$Pe = Pe(t_{fault}^{+})$	0	4.9704	4.3801	4.1981	0.3840	2.3184
$Pe = PredictingPe$	0	4.9495	4.2157	3.8519	0.4033	1.9940

4.3   Predicting Generators Behavior in IEEE 39 Bus Test System

To show the efficiency of the prediction method, two studies have been performed on the IEEE 39 bus test system [106]. One-line diagram and the features of the test system are presented in figure 4.10 and table 4.5. To create system dynamics, three-phase faults are applied on buses 16 and 18 one at a time.

During the fault, P_e is predicted. We must have the actual measured P_e for two time-steps after the fault in order to have an accurate and acceptable prediction. The first order approximation via Taylor series is used, and higher order terms are ignored.
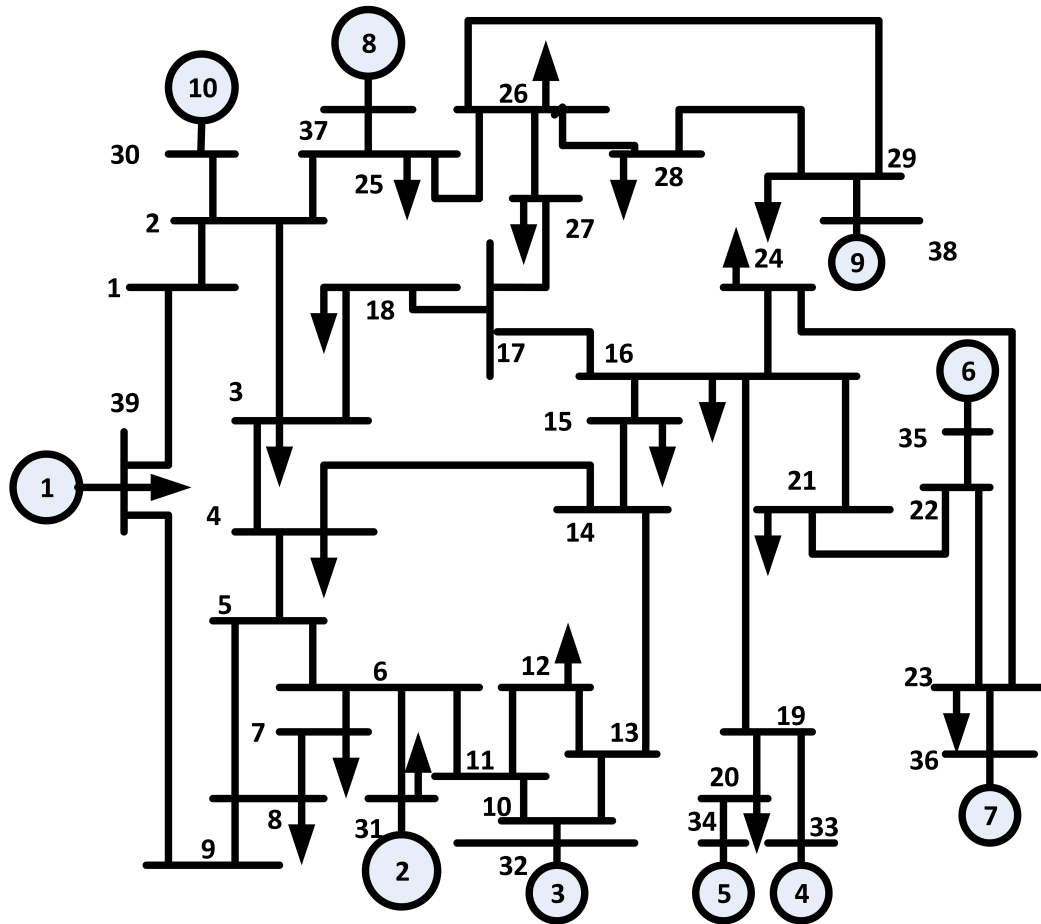
Figure 4.10: IEEE 39 bus test system one-line diagram.

Table 4.5: IEEE 39 bus system features.

Buses & Generators	39 Buses 10 Generators	Lines & Loads	46 Lines 19 Loads
Total Active Power Generation (MW)	6147.92	Total Active Load (MW)	6097.100
Total Reactive Power Generation (MVAR)	2487.332	Total Reactive Load (MVAR)	1409.100

4.3.1 Study 1: Symmetrical Fault on Bus 16 in IEEE 39 Bus System

A symmetrical fault is applied on bus 16 at $t = 0.1$ seconds. Fault is removed at $t = 0.285$ seconds. The system is critically stable in this scenario, meaning that the critical clearing time is 0.158 seconds.

The prediction for the system behavior during the fault is only based on the PMU data for two time-steps after the fault. However, the prediction for the post-fault system (after $t = 0.285$ sec) is corrected by updating the initial point in the related formulas every 8 time-steps (every 0.08 seconds). As a sample of generators behavior prediction, actual and predicted angle, speed, output power, and related errors for machine 4 are provided in Figures 4.11 to 4.16. The reason for choosing this machine is that the first machine that loses synchrony, for the mentioned transient scenario, is machine 4. Table 4.6 provides the maximum and average errors of speed, angle, and electrical power prediction, for fault occurrence on bus 16 of IEEE 39 bus system.symmetrical fault is applied on bus 16 at $t = 0.1$ seconds. Fault is removed at $t = 0.285$ seconds. The system is critically stable in this scenario, meaning that the critical clearing time is 0.158 seconds.
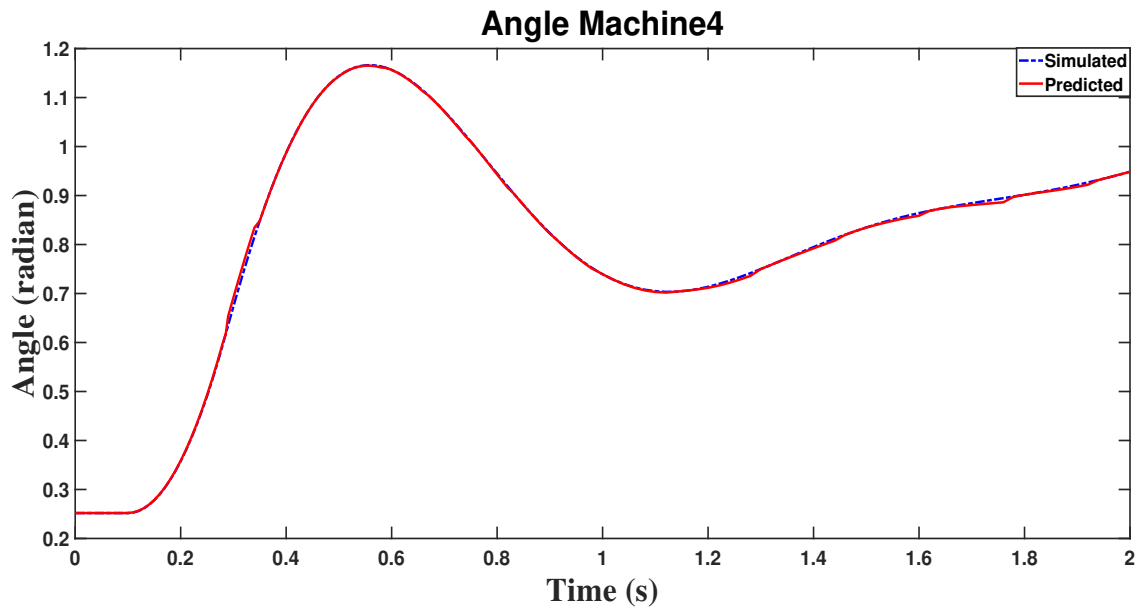
Figure 4.11: Actual and predicted rotor angle of G4 - Fault on bus 16 - IEEE 39 bus test system.
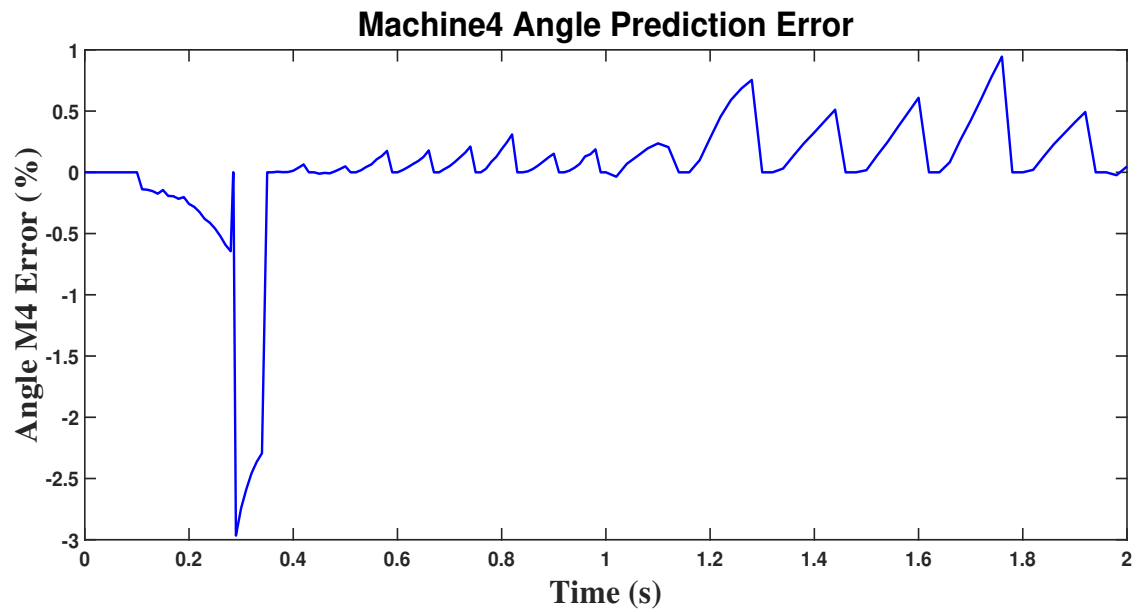
Figure 4.12: Error of G4 rotor angle prediction - Fault on bus 16 - IEEE 39 bus test system.
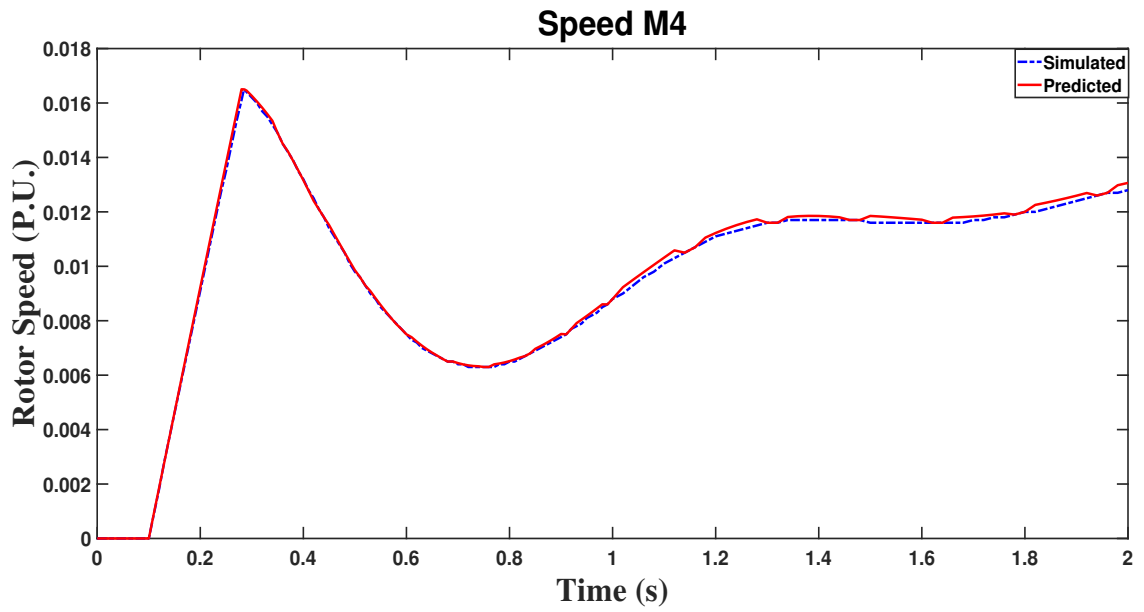
Figure 4.13: Actual and predicted rotor speed of G4 - Fault on bus 16 - IEEE 39 bus test system.
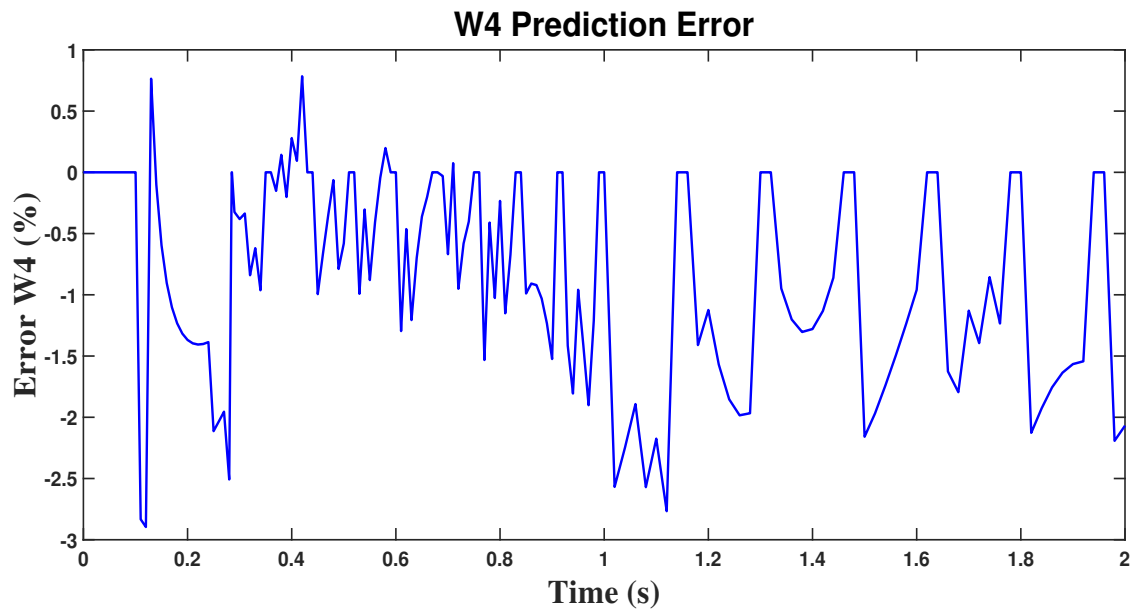
Figure 4.14: Error of G4 rotor speed prediction - Fault on bus 16 - IEEE 39 bus test system.
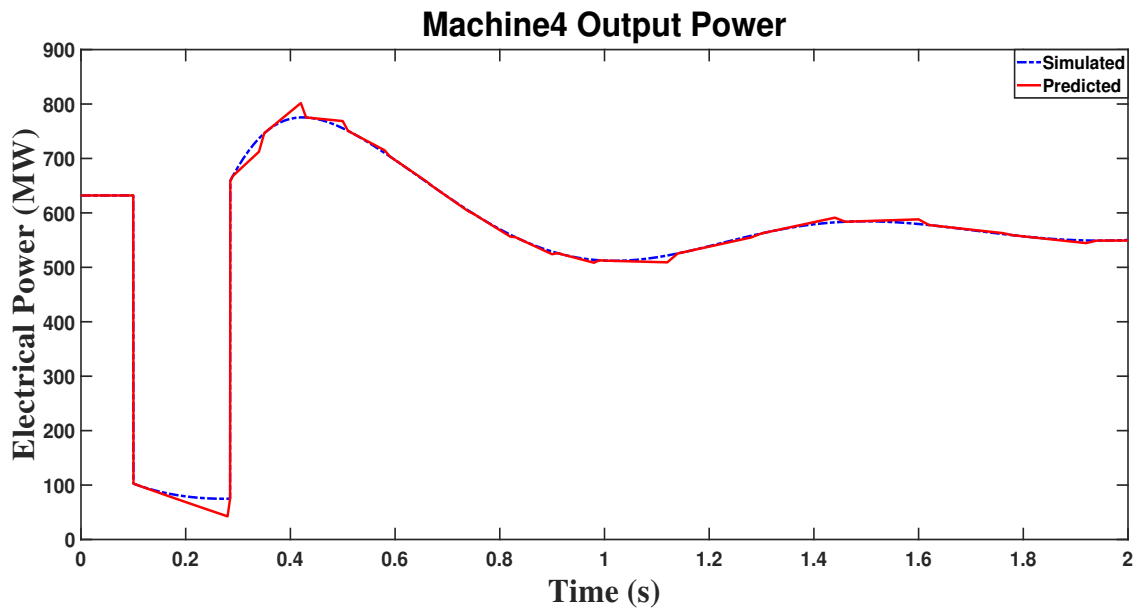
Figure 4.15: Actual and predicted electrical output of G4 - Fault on bus 16 - IEEE 39 bus test system.
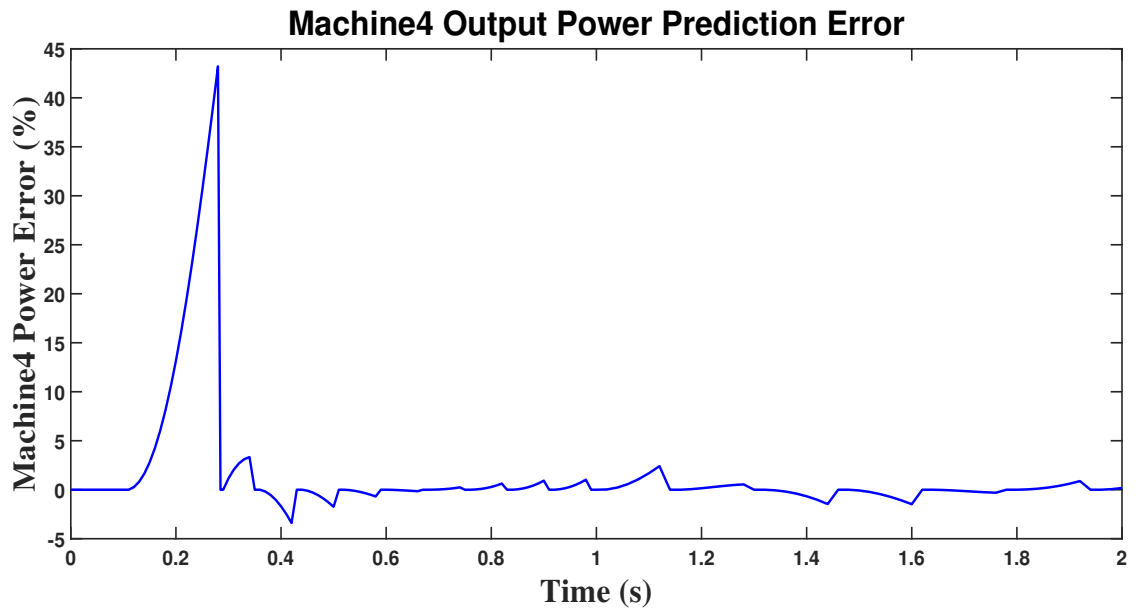
Figure 4.16: Error of G4 electrical output prediction - Fault on bus 16 - IEEE 39 bus test system.

Table 4.6: Electrical power, angle, and speed prediction error summary - Fault on bus 16 - IEEE 39 bus test system.

Variable	Maximum Error	Mean Error
$Pe1$	31.0983	6.0258
$Pe2$	6.5778	1.4300
$Pe3$	9.8255	2.3640
$Pe4$	43.2071	9.0200
$Pe5$	44.9937	9.1627
$Pe6$	118.5596	28.0595
$Pe7$	39.6288	7.7369
$Pe8$	4.2736	0.6794
$Pe9$	9.4758	2.1502
$Pe10$	4.9028e+03	306.1363

Variable	Maximum Error	Mean Error
$\delta1$	0.8925	0.1594
$\delta2$	0	0
$\delta3$	4.2746	0.9424
$\delta4$	0.6444	0.1752
$\delta5$	0.5775	0.2040
$\delta6$	1.9582	0.8554
$\delta7$	1.0643	0.3643
$\delta8$	2.1850	0.6977
$\delta9$	1.4799	0.2924
$\delta10$	0.4199	0.0514

Variable	Maximum Error	Mean Error
$\omega1$	36.9582	9.9729
$\omega2$	7.5957	1.6509
$\omega3$	5.2972	4.5763
$\omega4$	2.8957	0.7641
$\omega5$	3.8575	1.1778
$\omega6$	4.1434	0.7901
$\omega7$	2.2806	0.8683
$\omega8$	6.9979	1.4464
$\omega9$	5.0444	1.6391
$\omega10$	8.7904	2.4297

4.3.2 Study 2: Symmetrical Fault on bus 18 - IEEE 39 Bus System

A symmetrical fault is applied at bus 18 at $t = 0.1$ seconds. Fault is removed at $t = 0.375$ seconds. The system is critically stable in this scenario, meaning that the critical clearing time is 0.275 seconds.

Prediction for the system behavior during the fault is only based on the PMU data for two time-steps after the fault. However, the prediction for the post-fault system (after $t = 0.275$ sec) is corrected by updating the initial point in the related formulas every 8 time steps (every 0.08 seconds). As a sample of generators behavior prediction, actual and predicted angle, speed, output power, and related errors for machine 6 are provided in Figures 4.17 to 4.19. Table 4.7 provides the maximum and average errors of speed, angle, and electrical power prediction, for fault occurrence on bus 18 of IEEE 39 bus system.
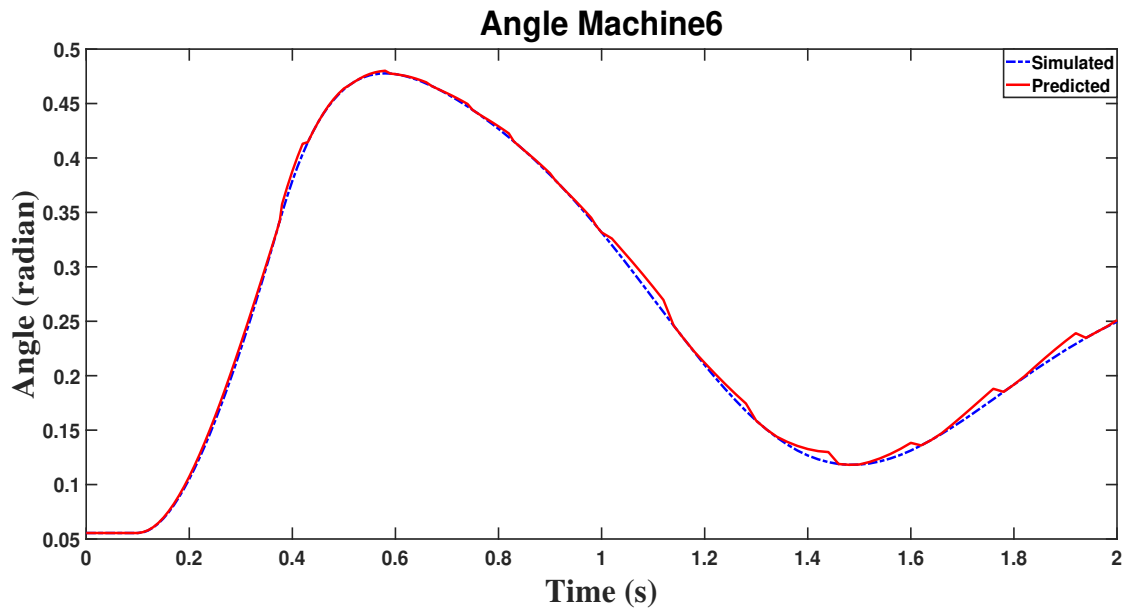
Figure 4.17: Actual and predicted rotor angle of G6 - Fault on bus 18 - IEEE 39 bus test system.
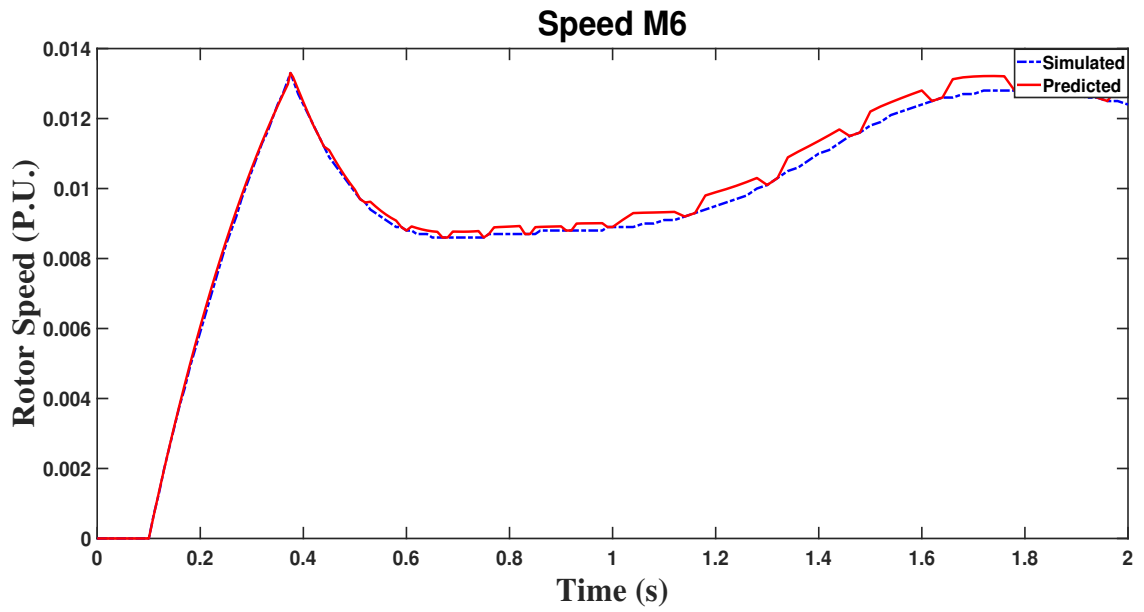
Figure 4.18: Actual and predicted rotor speed of G6 - Fault on bus 18 - IEEE 39 bus test system.
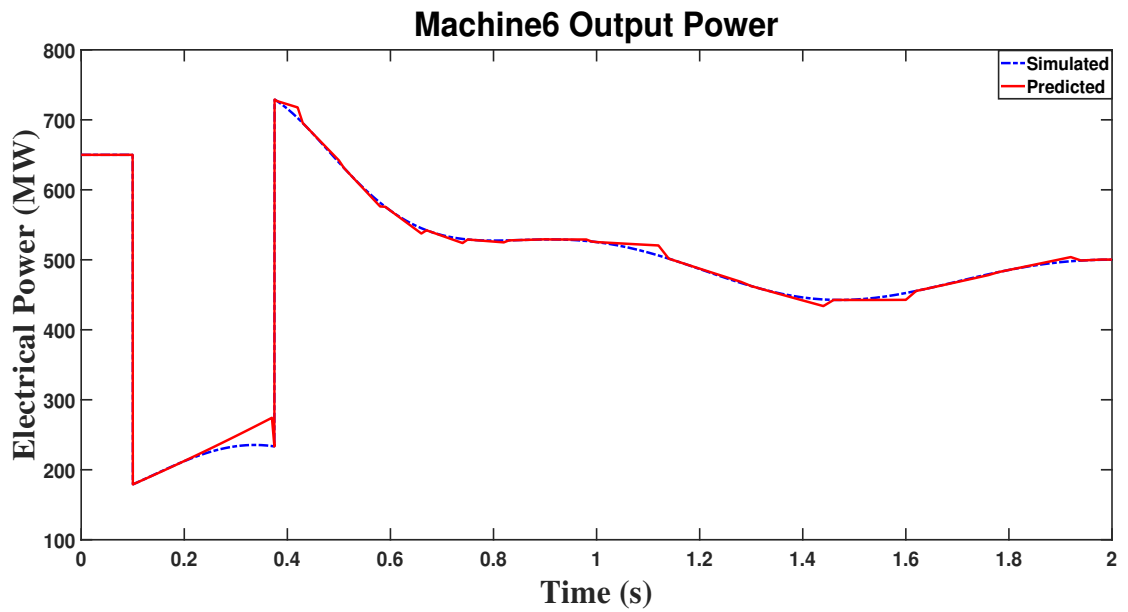
Figure 4.19: Actual and predicted output power of G6 - Fault on bus 18 - IEEE 39 bus test system.

Table 4.7: Electrical power, angle, and speed prediction error summary - Fault on bus 18 - IEEE 39 bus test system.

Variable	Maximum Error	Mean Error
$Pe1$	126.2268	23.6320
$Pe2$	5.6681	1.6861
$Pe3$	8.8298	3.2017
$Pe4$	31.9481	8.2226
$Pe5$	21.5576	4.6762
$Pe6$	17.2857	2.8054
$Pe7$	28.9100	7.0208
$Pe8$	15.8632	3.0326
$Pe9$	16.1102	4.6321
$Pe10$	2.3988e+4	821.3797

Variable	Maximum Error	Mean Error
$\delta1$	2.1283	0.4304
$\delta2$	0	0
$\delta3$	9.2962	2.3196
$\delta4$	4.6669	0.7988
$\delta5$	2.9087	0.4095
$\delta6$	2.7203	1.1315
$\delta7$	4.7063	0.9490
$\delta8$	8.9332	1.4584
$\delta9$	4.5886	0
$\delta10$	4.1767	0.6294

Variable	Maximum Error	Mean Error
$\omega1$	42.3082	15.3932
$\omega2$	8.1432	1.7233
$\omega3$	7.6034	2.8288
$\omega4$	9.5318	2.3376
$\omega5$	3.4790	0.8818
$\omega6$	3.3438	0.9697
$\omega7$	7.7984	2.2723
$\omega8$	7.5424	1.9274
$\omega9$	8.3451	2.6124
$\omega10$	17.8844	4.8999

4.4   Predicting Generators Behavior in North Carolina-South Carolina 500 Bus Synthetic System

Synthetic power systems are systems built from public information and statistical analysis of real power systems. They have no relation to the actual grids, except that generation and load profiles are similar to the real networks. More information about synthetic power systems can be found in [107]. Figure 4.20 shows a general view of this system.

In order to show the scalability of the proposed method, and provide some results showing the efficiency of the method in predicting generators behavior in relatively large systems, two studies have been performed on the North Carolina-South Carolina 500 bus synthetic system. In the first study, a three-phase fault is applied to the terminal of a generator, and the behavior of the active machines in the system are predicted and compared to their actual performance. The steady state voltage of the faulted bus is 13.8 kV. In the second scenario, the fault is applied on a non-generator bus. The behavior of the active machines in the system is predicted and compared to their actual performance. The steady state voltage of the faulted bus is 138 kV. The system under study is modeled in PSS/E, and MATLAB is used for prediction calculations.

4.4.1   Study 1: Symmetrical Fault on Bus 71 - 500 Bus Synthetic System

A symmetrical fault is applied on bus 71, which is a generator bus. The fault starts at $t = 0.1000$ seconds and is removed at $t = 0.3750$ seconds. Tables 4.8 and 4.9 show the maximum and average of rotor angles and speeds prediction. The results for maximum and the average error of predicting generators output powers are shown in table 4.10. Figures 4.21 to 4.27 depict the actual and predicted angles, speeds, and electrical output powers for generators with maximum and minimum errors in addition to the faulted machine.
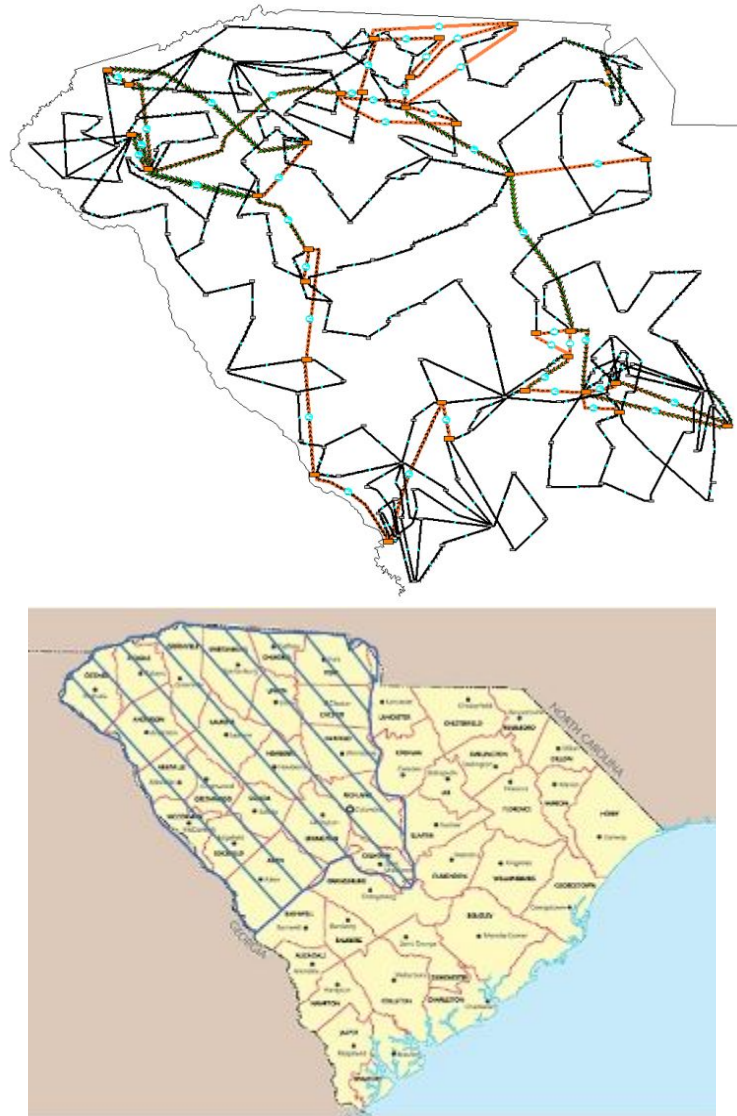
Figure 4.20: 500 bus synthetic system area.

Table 4.8: Angle, and speed prediction error summary - Fault on bus 71 - 500 bus system.

Row	Variable	Max Error	Mean Error	Variable	Max Error	Mean Error
1	$\delta 9$	32.0681	4.6908	$\omega 9$	71.2518	26.4629
2	$\delta 16$	30.6210	4.2849	$\omega 16$	30.2527	11.0781
3	$\delta 17$	0	0	$\omega 17$	113.7370	22.8771
4	$\delta 18$	43.0708	5.8895	$\omega 18$	24.508	9.6489
5	$\delta 49$	3.0986	0.3124	$\omega 49$	834.2463	104.6060
6	$\delta 50$	7.7463	0.9331	$\omega 50$	12631	748.1633
7	$\delta 71$	134.4775	7.0218	$\omega 71$	12.4149	1.3564
8	$\delta 72$	22.4233	3.1478	$\omega 72$	12.7745	5.6176
9	$\delta 73$	25.7077	3.0427	$\omega 73$	698.9226	96.2541
10	$\delta 82$	31.9027	4.2852	$\omega 82$	54.0125	11.8280
11	$\delta 127$	120.0203	13.8663	$\omega 127$	13.6037	3.5233
12	$\delta 128$	37.2061	5.1720	$\omega 128$	12.7324	4.0934
13	$\delta 144$	14.6212	1.8308	$\omega 144$	15.1175	4.5430
14	$\delta 145$	18.1544	2.5239	$\omega 145$	21.0440	8.2648
15	$\delta 167$	1.9235	0.2016	$\omega 167$	99.4237	22.0850
16	$\delta 168$	67.4328	9.8271	$\omega 168$	259.2769	49.1500
17	$\delta 169$	73.9847	9.8684	$\omega 169$	19.2068	5.3628
18	$\delta 197$	18.8964	2.7012	$\omega 197$	79.3254	17.9878
19	$\delta 198$	15.1736	2.0576	$\omega 198$	73.1954	22.8615
20	$\delta 222$	2.9588	0.5918	$\omega 222$	241.9405	52.8038
21	$\delta 223$	15.2567	2.0898	$\omega 223$	56.9263	18.2700
22	$\delta 224$	145.3434	14.4052	$\omega 224$	43.4312	10.3378
23	$\delta 225$	30.4601	4.2764	$\omega 225$	30.5038	8.9373
24	$\delta 231$	16.4338	2.3141	$\omega 231$	76.4635	27.5741
25	$\delta 258$	8.1006	1.0176	$\omega 258$	48.2300	14.6746
26	$\delta 301$	14.5336	1.9895	$\omega 301$	50.7095	15.9237
27	$\delta 302$	14.1782	1.9920	$\omega 302$	66.3536	22.8655
28	$\delta 305$	13.9523	3.3319	$\omega 305$	2921	272.3456

Table 4.9: Angle, and speed prediction error summary - Fault on bus 71 - 500 bus system.

Row	Variable	Max Error	Mean Error	Variable	Max Error	Mean Error
29	$\delta 306$	15.6742	2.2479	$\omega 306$	43.7622	15.3994
30	$\delta 319$	14.3949	1.9614	$\omega 319$	30.8230	10.1150
31	$\delta 350$	6.4688	0.8399	$\omega 350$	15.1251	2.8800
32	$\delta 351$	26.9002	3.5840	$\omega 351$	12418	887.1251
33	$\delta 352$	11.2908	1.5552	$\omega 352$	39.9707	11.4090
34	$\delta 353$	5.3618	0.6513	$\omega 353$	91.1781	21.4912
35	$\delta 410$	7.1314	0.9477	$\omega 410$	13.8784	5.3069
36	$\delta 411$	7.7947	1.0501	$\omega 411$	39.2143	12.9787
37	$\delta 412$	6.5370	0.8637	$\omega 412$	13.6871	2.3625
38	$\delta 413$	5.5702	0.7399	$\omega 413$	14.4234	3.4548
39	$\delta 430$	7.3916	1.6521	$\omega 430$	211.4979	56.8622
40	$\delta 431$	22.3538	3.4345	$\omega 431$	431.6999	83.1182
41	$\delta 432$	19.8405	2.7999	$\omega 432$	57.9313	19.7621
42	$\delta 433$	3.3609	0.6366	$\omega 433$	6662.6	400.0429
43	$\delta 434$	10.4829	1.4208	$\omega 434$	55.9027	18.7461
44	$\delta 437$	0.8914	0.2991	$\omega 437$	144.8353	35.2046
45	$\delta 438$	23.1551	3.2730	$\omega 438$	51.6110	18.4332
46	$\delta 439$	11.3424	1.5460	$\omega 439$	13.3520	3.0641
47	$\delta 455$	4.4881	0.5906	$\omega 455$	24.1285	4.6007
48	$\delta 456$	4.9169	0.6476	$\omega 456$	21.6221	4.6989
49	$\delta 458$	57.4235	6.4760	$\omega 458$	80.2558	31.9814
50	$\delta 480$	20.2655	2.8628	$\omega 480$	22.2373	4.2666
51	$\delta 481$	16.4358	2.2705	$\omega 481$	29.7171	9.6406
52	$\delta 482$	13.7253	1.8935	$\omega 482$	84.8017	35.1386
53	$\delta 483$	7.5123	1.0156	$\omega 483$	47.9544	13.0002
54	$\delta 484$	7.1131	0.9538	$\omega 484$	24.7822	6.9353
55	$\delta 497$	16.6367	2.2849	$\omega 497$	13.2052	2.9380
56	$\delta 498$	8.0804	2.3854	$\omega 498$	326.6866	100.0051

Table 4.10: Electrical output power prediction error summary - Fault on bus 71 - 500 bus system.

Row	Variable	Max Error	Mean Error	Row	Variable	Max Error	Mean Error
1	$Pe9$	3.6014	0.9717	29	$Pe306$	7.6978	3.1450
2	$Pe16$	3.6653	1.4326	30	$Pe319$	3.9727	0.8772
3	$Pe17$	18.6178	4.8721	31	$Pe350$	3.5275	0.6666
4	$Pe18$	1.9065	0.8273	32	$Pe351$	140.6296	33.2206
5	$Pe49$	20.8083	4.3009	33	$Pe352$	2.7459	0.9538
6	$Pe50$	105.3379	24.9071	34	$Pe353$	21.8052	6.0407
7	$Pe71$	55.2651	15.0971	35	$Pe410$	4.6026	0.8440
8	$Pe72$	10.4409	3.6321	36	$Pe411$	6.1214	1.8134
9	$Pe73$	133.4586	33.4963	37	$Pe412$	1.7332	0.2825
10	$Pe82$	6.2988	1.6838	38	$Pe413$	0.3122	0.0941
11	$Pe127$	4.7814	0.9855	39	$Pe430$	7.4589	2.9568
12	$Pe128$	1.9927	0.6123	40	$Pe431$	15.0050	4.7471
13	$Pe144$	0.9390	0.2284	41	$Pe432$	3.3916	1.2292
14	$Pe145$	2.2999	0.5028	42	$Pe433$	31.1942	7.2231
15	$Pe167$	14.9890	4.2511	43	$Pe434$	9.4336	2.6656
16	$Pe168$	26.2282	7.6815	44	$Pe437$	35.6044	9.4456
17	$Pe169$	1.4285	0.4336	45	$Pe438$	4.6386	1.5006
18	$Pe197$	6.0069	1.4923	46	$Pe439$	2.0311	0.3728
19	$Pe198$	6.0556	1.4027	47	$Pe455$	3.0640	0.4166
20	$Pe222$	9.7925	3.0882	48	$Pe456$	3.0800	0.4079
21	$Pe223$	8.4162	2.0078	49	$Pe458$	5.5723	1.3799
22	$Pe224$	4.3902	1.1069	50	$Pe480$	0.6370	0.0966
23	$Pe225$	2.9683	0.7699	51	$Pe481$	1.2083	0.3711
24	$Pe231$	13.9053	4.3884	52	$Pe482$	2.4696	0.7711
25	$Pe258$	4.1389	1.1811	53	$Pe483$	3.3700	0.8408
26	$Pe301$	6.5984	1.5410	54	$Pe484$	1.6982	0.4468
27	$Pe302$	2.8321	0.9705	55	$Pe497$	0.4441	0.0686
28	$Pe305$	3.5275	0.6666	56	$Pe498$	3.8164	1.6096
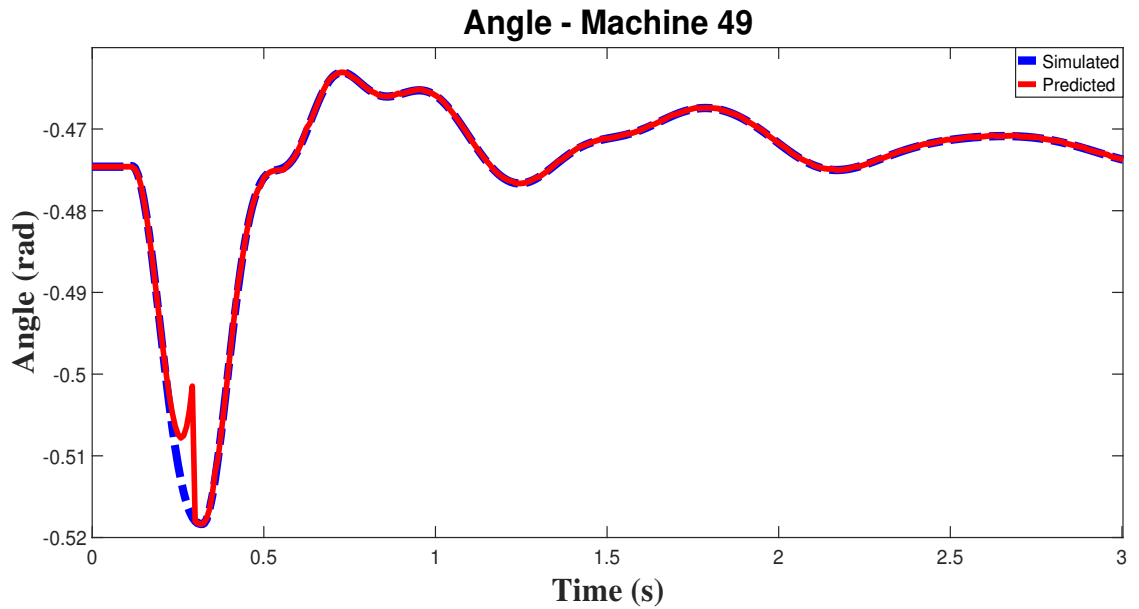
Figure 4.21: Actual and predicted rotor angle of G49 that has the minimum error - Fault on bus 71 - 500 bus system.
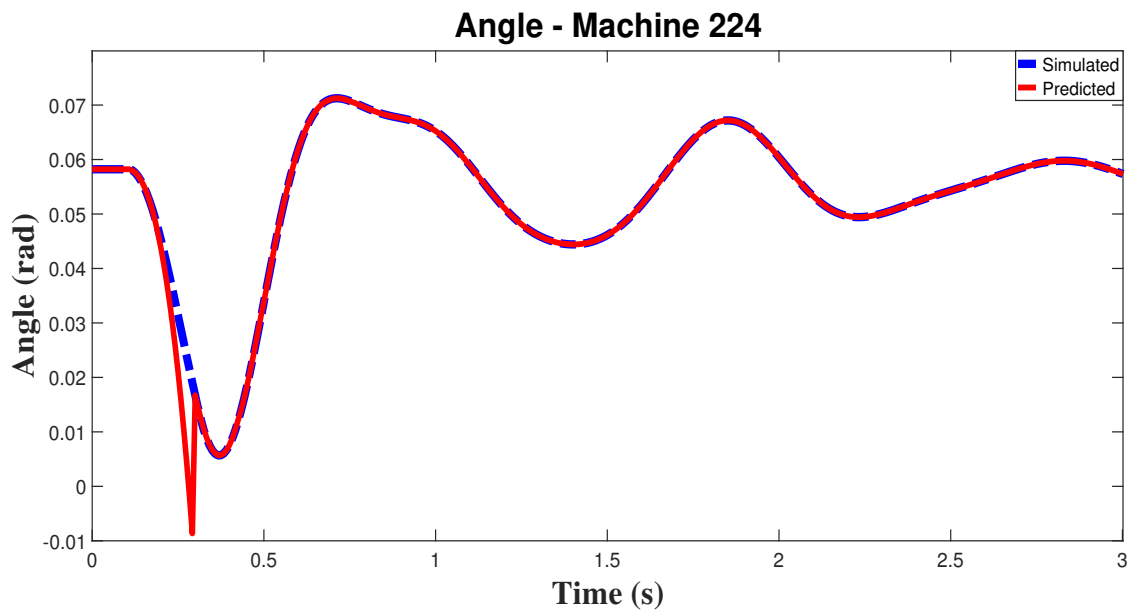
Figure 4.22: Actual and predicted rotor angle of G49 that has the maximum error - Fault on bus 71 - 500 bus system.

Figure 4.23: Actual and predicted rotor speed of G71 that has the minimum error - Fault on bus 71 - 500 bus system.

Figure 4.24: Actual and predicted rotor speed of G50 that has the maximum error - Fault on bus 71 - 500 bus system.

Figure 4.25: Actual and predicted rotor speed of G351 that has a relatively large error - Fault on bus 71 - 500 bus system.

Figure 4.26: Actual and predicted output power of G497 that has the minimum error - Fault on bus 71 - 500 bus system.

Figure 4.27: Actual and predicted output power of G73 that has the maximum error - Fault on bus 71 - 500 bus system.

4.4.2 Study 2: Symmetrical Fault on Bus 450 - 500 Bus Synthetic System

A symmetrical fault is applied on bus 450, which is a non-generator bus. The fault starts at $t = 0.1000s$ seconds and is removed at $t = 0.4000$ seconds. Tables 4.11 and 4.12 show the maximum and average of rotor angles and speeds prediction. The results for maximum and the average error of predicting generators output powers are shown in table 4.13. Figures 4.28 to 4.34 depict the actual and predicted angles, speeds, and electrical output powers for generators with maximum and minimum errors in addition to the faulted machine.
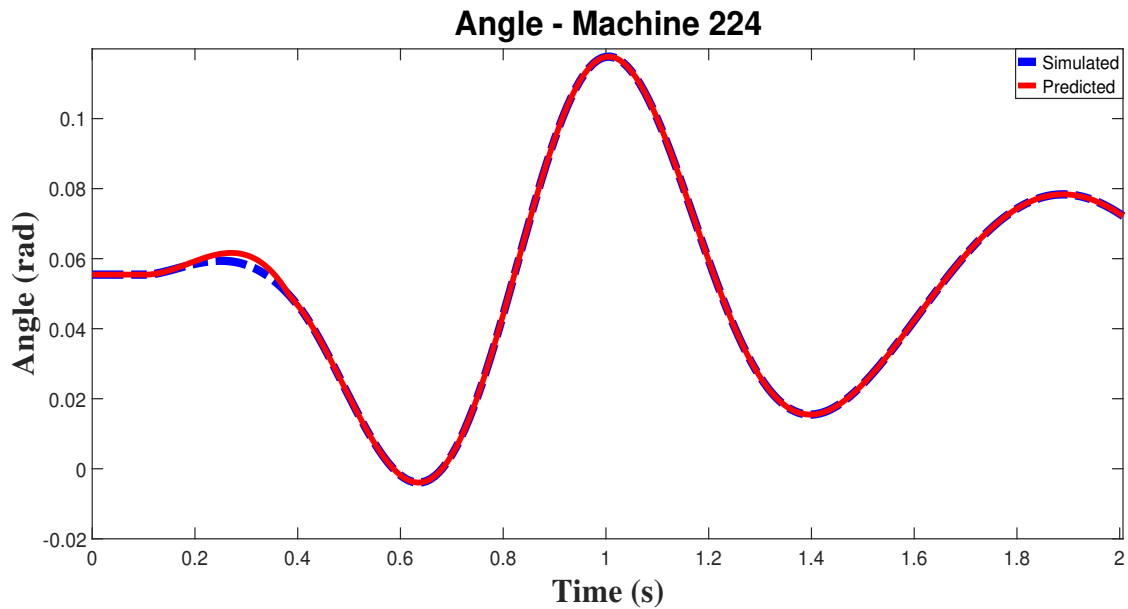

Figure 4.28: Actual and predicted rotor angle of G224 that has the minimum error - Fault on bus 450 - 500 bus system.

Table 4.11: Angle, and speed prediction error summary - Fault on bus 450 - 500 bus system.

Row	Variable	Max Error	Mean Error	Variable	Max Error	Mean Error	H
1	$\delta 9$	91.4625	15.9841	$\omega 9$	87.0353	43.1315	3.1915
2	$\delta 16$	148.8134	23.7692	$\omega 16$	49.8808	22.1091	3.5986
3	$\delta 17$	0	0	$\omega 17$	172.9712	42.9146	2.9752
4	$\delta 18$	232.2647	37.7936	$\omega 18$	49.2314	22.4254	2.5972
5	$\delta 49$	79.7514	10.7878	$\omega 49$	116760	2512.6	1.4139
6	$\delta 50$	23.7202	3.8971	$\omega 50$	48714	451.9091	5.7886
7	$\delta 71$	106.2970	14.7459	$\omega 71$	1916.1	258.7429	2.0026
8	$\delta 72$	43.7614	7.0553	$\omega 72$	1073.5	45.1104	8.9597
9	$\delta 73$	90.5423	13.6079	$\omega 73$	3890.9	401.7968	2.8385
10	$\delta 82$	79.7680	13.5353	$\omega 82$	29.9843	9.0961	2.7004
11	$\delta 127$	263.5726	55.7400	$\omega 127$	22.7407	6.7494	5.8911
12	$\delta 128$	130.3426	21.6864	$\omega 128$	13.3944	5.4345	6.2815
13	$\delta 144$	142.3040	19.3076	$\omega 144$	74.9406	19.6174	2.8511
14	$\delta 145$	57.0484	9.3430	$\omega 145$	13.5326	6.0887	3.7743
15	$\delta 167$	22.5512	3.0556	$\omega 167$	122.5394	34.0161	3.2120
16	$\delta 168$	261.5884	47.1354	$\omega 168$	355.8319	91.0237	2.3733
17	$\delta 169$	491.5222	77.9019	$\omega 169$	23.4214	8.8579	2.0596
18	$\delta 197$	12.9647	2.2141	$\omega 197$	218.2940	56.5397	2.8866
19	$\delta 198$	59.7912	9.7680	$\omega 198$	92.9216	41.7615	4.9960
20	$\delta 222$	173.3414	33.7263	$\omega 222$	755.7049	208.2877	1.8257
21	$\delta 223$	67.3032	11.2359	$\omega 223$	57.1363	22.3208	8.8882
22	$\delta 224$	4.8894	1.5819	$\omega 224$	188.3806	45.7805	3.1846
23	$\delta 225$	153.1567	25.4647	$\omega 225$	11.3583	3.4125	3.6203
24	$\delta 231$	71.6279	11.8682	$\omega 231$	94.9568	54.7302	6.5002
25	$\delta 258$	40.4970	6.0348	$\omega 258$	183950	3838.7	2.5311
26	$\delta 301$	53.4528	8.8000	$\omega 301$	59.2332	23.4262	9.5972
27	$\delta 302$	74.6226	12.8502	$\omega 302$	88.9512	43.8337	2.4814
28	$\delta 305$	108.7068	21.2238	$\omega 305$	423.6987	64.3792	1.2315

Table 4.12: Angle, and speed prediction error summary - Fault on bus 450 - 500 bus system.

Row	Variable	Max Error	Mean Error	Variable	Max Error	Mean Error	H
29	$\delta 306$	60.0691	9.9902	$\omega 306$	97.4561	56.0884	7.2081
30	$\delta 319$	57.0728	9.2876	$\omega 319$	34.8450	12.6185	7.2356
31	$\delta 350$	32.6801	5.2551	$\omega 350$	1095.8	59.1370	5.6549
32	$\delta 351$	42.7014	6.7976	$\omega 351$	18610	663.1148	3.5503
33	$\delta 352$	53.6746	8.8203	$\omega 352$	497.2981	72.1618	2.5354
34	$\delta 353$	40.2948	6.5456	$\omega 353$	22.3394	10.6109	6.3230
35	$\delta 410$	32.1924	5.1825	$\omega 410$	49.4975	25.7262	8.8158
36	$\delta 411$	37.5489	6.0908	$\omega 411$	591.3954	60.0138	3.6127
37	$\delta 412$	30.7344	4.9172	$\omega 412$	44.9364	23.3562	6.5338
38	$\delta 413$	27.1264	4.3285	$\omega 413$	50.9598	23.5125	6.4704
39	$\delta 430$	43938	1884.5	$\omega 430$	659.7413	207.8159	1.7846
40	$\delta 431$	34817	862.1905	$\omega 431$	4049.3	662.3740	1.3793
41	$\delta 432$	344.0998	57.8370	$\omega 432$	60.9430	26.0665	2.2978
42	$\delta 433$	297.8998	45.0795	$\omega 433$	56887	2166.5	4.9187
43	$\delta 434$	63.5577	10.1306	$\omega 434$	48.6328	19.1222	6.0258
44	$\delta 437$	12286	943.7844	$\omega 437$	562.7011	135.2771	5.4957
45	$\delta 438$	384.9362	52.2348	$\omega 438$	25.5708	13.5024	3.4301
46	$\delta 439$	54.3012	7.3048	$\omega 439$	83.3112	19.3674	3.2774
47	$\delta 455$	20.0996	3.1597	$\omega 455$	182.7913	11.8112	7.1662
48	$\delta 456$	21.5850	3.4032	$\omega 456$	43.7175	7.1831	6
49	$\delta 458$	133.4567	27.6421	$\omega 458$	96.5099	52.7808	5.9173
50	$\delta 480$	46.6683	7.8521	$\omega 480$	25.5261	8.6748	8.3071
51	$\delta 481$	38.4512	6.2633	$\omega 481$	74.9845	27.9497	3.0199
52	$\delta 482$	49.8761	8.4864	$\omega 482$	635.0478	61.0086	2.0289
53	$\delta 483$	22.0443	3.5844	$\omega 483$	109.7679	35.2278	3.5602
54	$\delta 484$	25.3580	4.0772	$\omega 484$	55.1835	19.7217	4.9387
55	$\delta 497$	56.7331	9.0754	$\omega 497$	12.8377	1.6214	3.3734
56	$\delta 498$	129.0264	31.9314	$\omega 498$	485.3784	187.4655	1.2305

Table 4.13: Electrical output power prediction error summary - Fault on bus 450 - 500 bus system.

| Row	Variable	Max Error	Mean Error	Row	Variable	Max Error	Mean Error
1	$Pe9$	12.6420	4.3416	29	$Pe306$	43.2194	13.1642
2	$Pe16$	11.7553	5.2532	30	$Pe319$	16.0694	4.5865
3	$Pe17$	42.1421	13.2646	31	$Pe350$	8.9228	3.5016
4	$Pe18$	7.6094	3.5723	32	$Pe351$	158.3749	44.0242
5	$Pe49$	89.2088	24.2342	33	$Pe352$	10.1872	4.3674
6	$Pe50$	218.5035	57.4605	34	$Pe353$	5.4156	2.1274
7	$Pe71$	149.2878	42.2225	35	$Pe410$	43.8586	9.0631
8	$Pe72$	21.3128	5.4871	36	$Pe411$	19.9390	7.7125
9	$Pe73$	208.9059	60.1185	37	$Pe412$	27.2669	6.2209
10	$Pe82$	5.9719	1.6012	38	$Pe413$	35.1213	7.5714
11	$Pe127$	15.3288	3.7803	39	$Pe430$	31.0499	14.4646
12	$Pe128$	3.7799	1.3198	40	$Pe431$	111.5046	43.9734
13	$Pe144$	14.9355	4.3382	41	$Pe432$	7.2465	3.9727
14	$Pe145$	4.5210	1.5027	42	$Pe433$	863.9895	229.4253
15	$Pe167$	33.5323	10.4374	43	$Pe434$	21.3448	9.0332
16	$Pe168$	55.9299	29.3133	44	$Pe437$	396.3185	160.5974
17	$Pe169$	3.4285	1.3617	45	$Pe438$	7.7057	2.8883
18	$Pe197$	34.7611	10.7811	46	$Pe439$	22.9125	8.2205
19	$Pe198$	24.6430	7.3251	47	$Pe455$	8.0641	3.3898
20	$Pe222$	56.3012	22.5412	48	$Pe456$	5.8205	1.8167
21	$Pe223$	30.6918	9.4638	49	$Pe458$	24.3975	6.8247
22	$Pe224$	40.6148	13.5207	50	$Pe480$	3.0531	1.2904
23	$Pe225$	2.7126	0.9836	51	$Pe481$	9.8293	3.1854
24	$Pe231$	40.7004	14.1230	52	$Pe482$	3.3278	1.2059
25	$Pe258$	114.9093	30.9099	53	$Pe483$	20.4200	6.0142
26	$Pe301$	34.2224	9.2704	54	$Pe484$	15.0988	4.2557
27	$Pe302$	9.3836	4.7064	55	$Pe497$	0.3433	0.1162
28	$Pe305$	28.7659	8.7850	56	$Pe498$	23.3208	9.3681
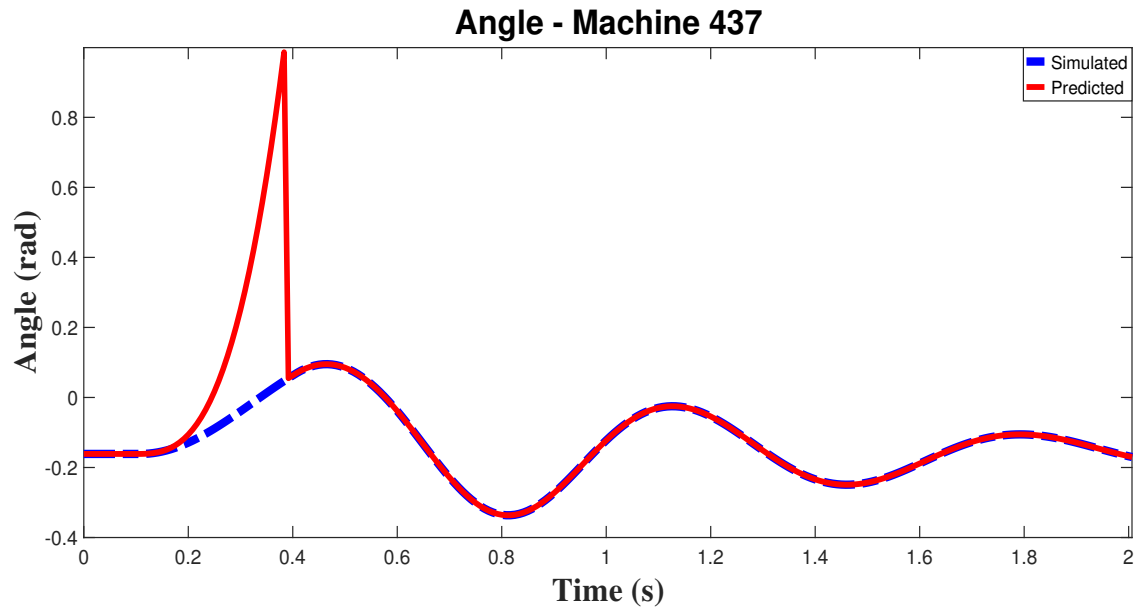
Figure 4.29: Actual and predicted rotor angle of G437 that has the minimum error - Fault on bus 450 - 500 bus system.
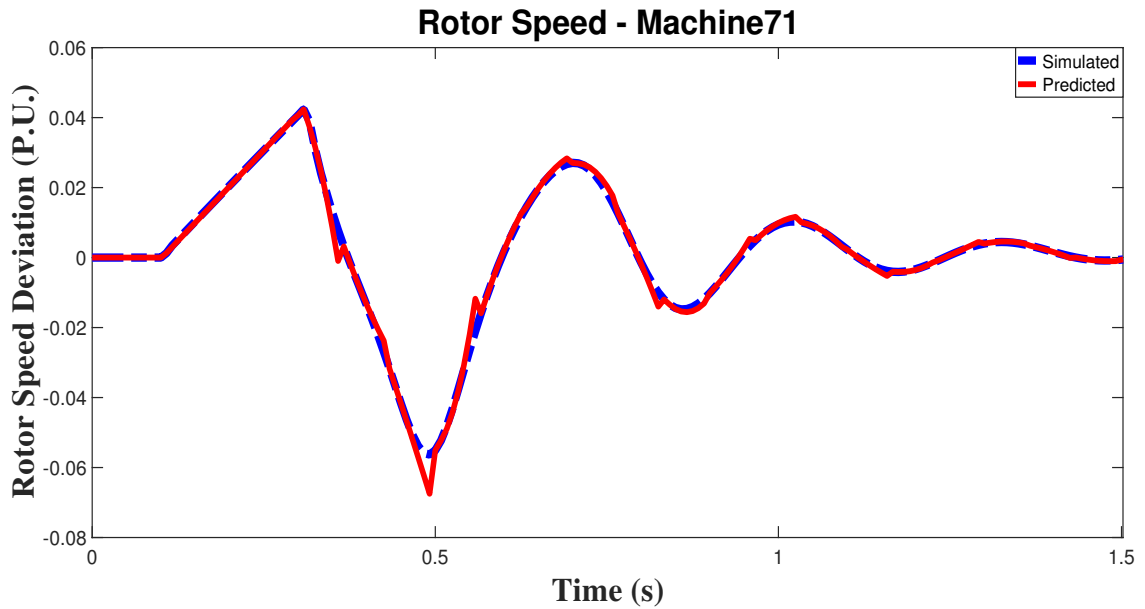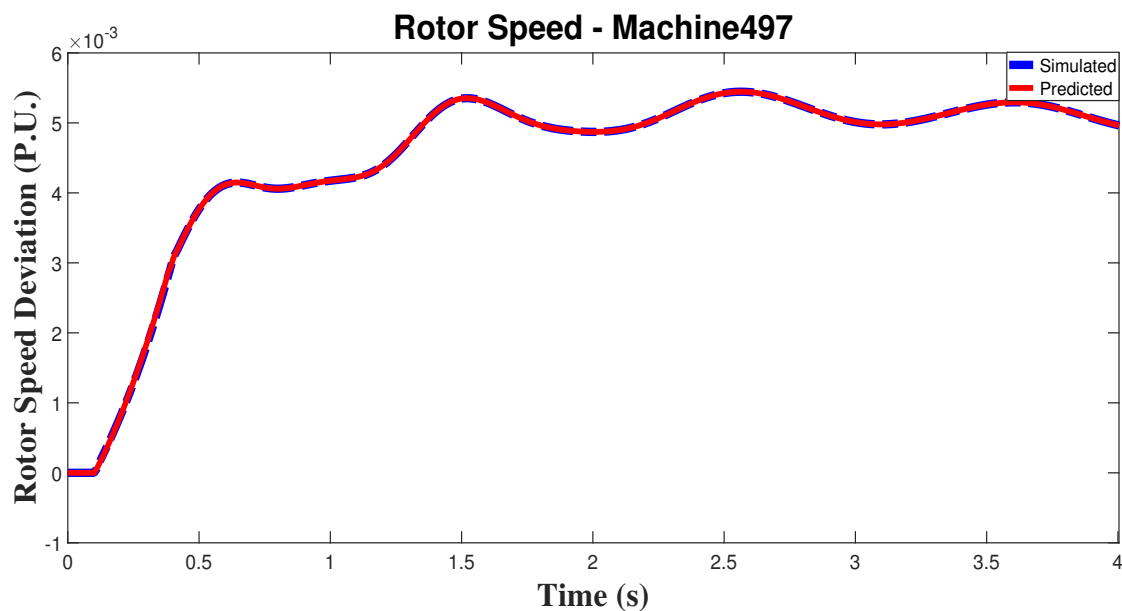

Figure 4.30: Actual and predicted rotor speed of G497 that has the minimum error - Fault on bus 450 - 500 bus system.
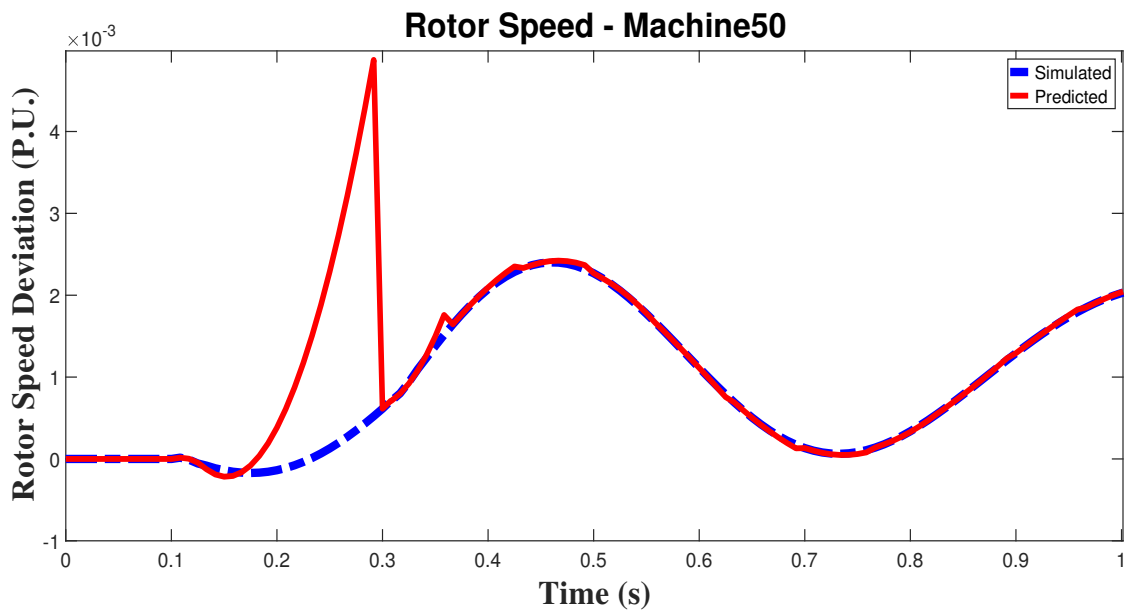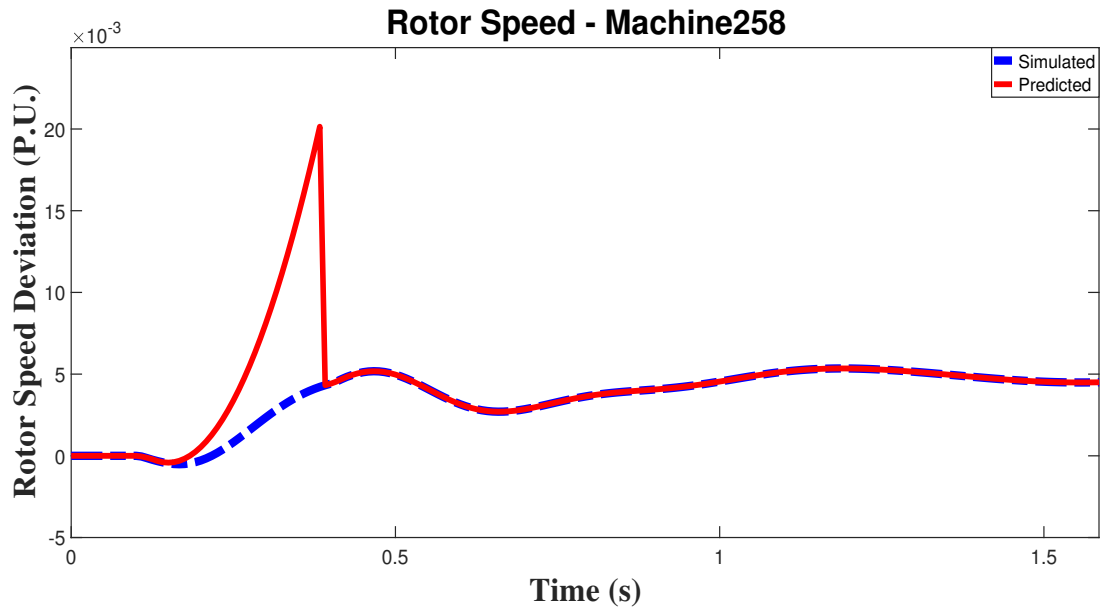
Figure 4.31: Actual and predicted rotor speed of G258 that has the maximum error - Fault on bus 450 - 500 bus system.
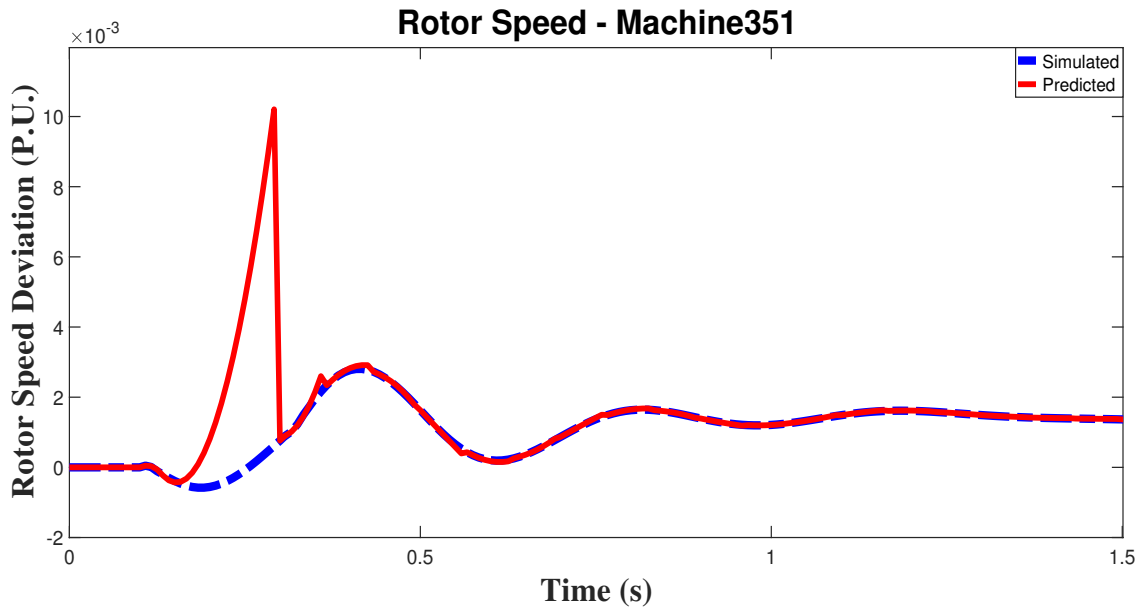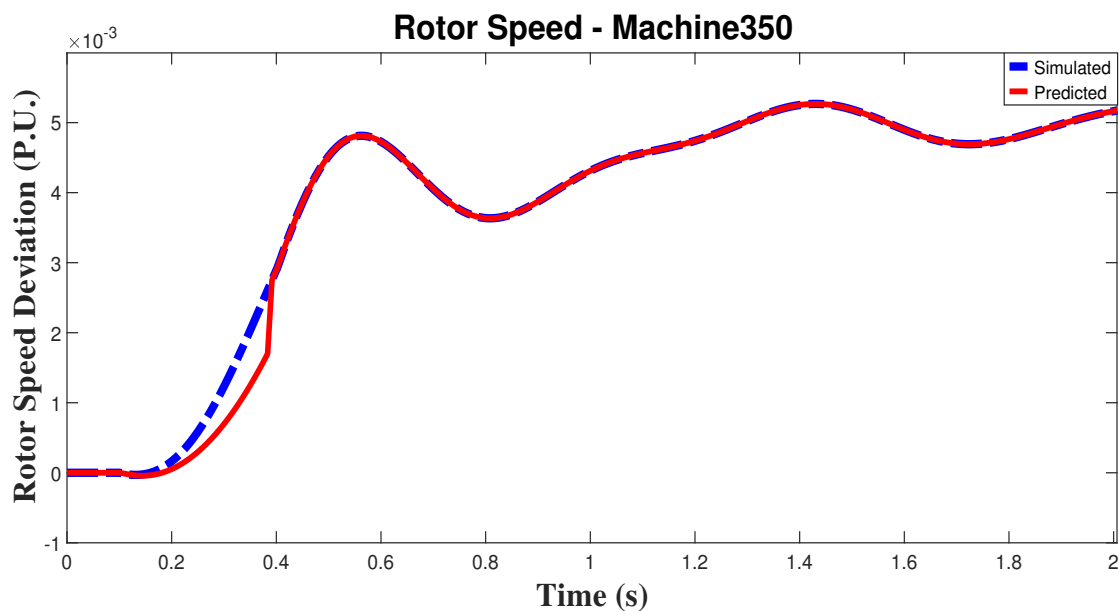

Figure 4.32: Actual and predicted rotor speed of G350 that has a relatively large error - Fault on bus 450 - 500 bus system.
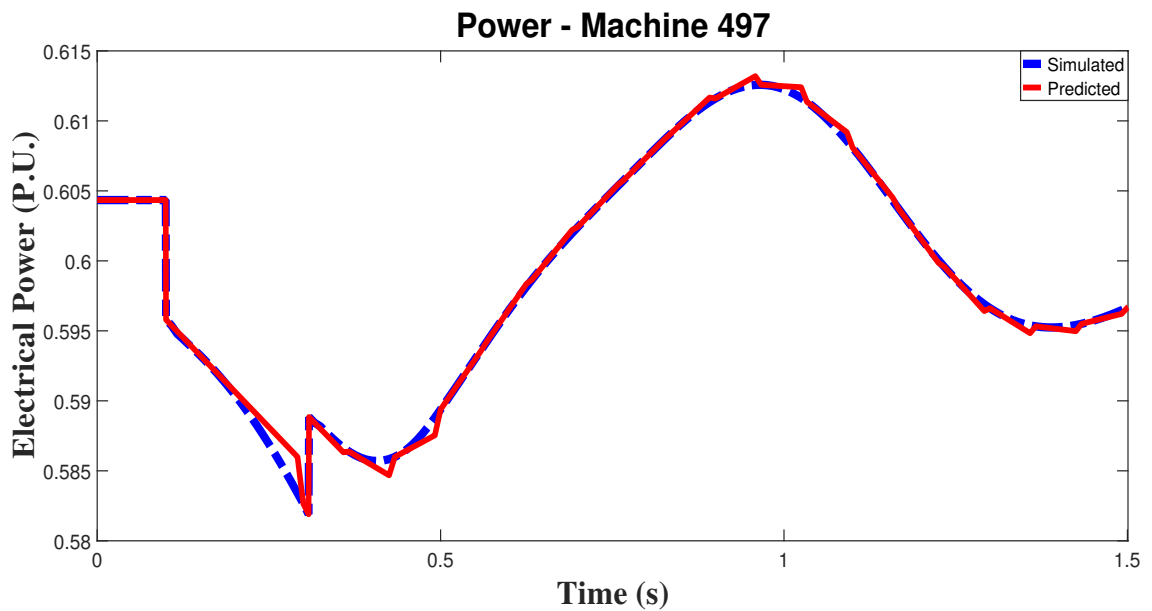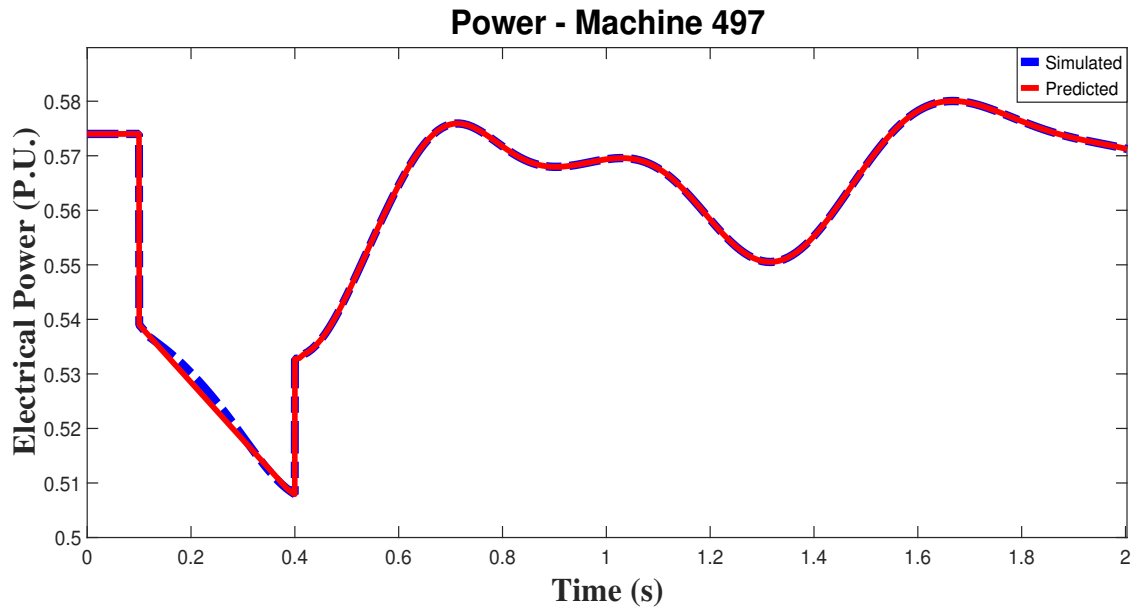
Figure 4.33: Actual and predicted output power of G497 that has the minimum error - Fault on bus 450 - 500 bus system.
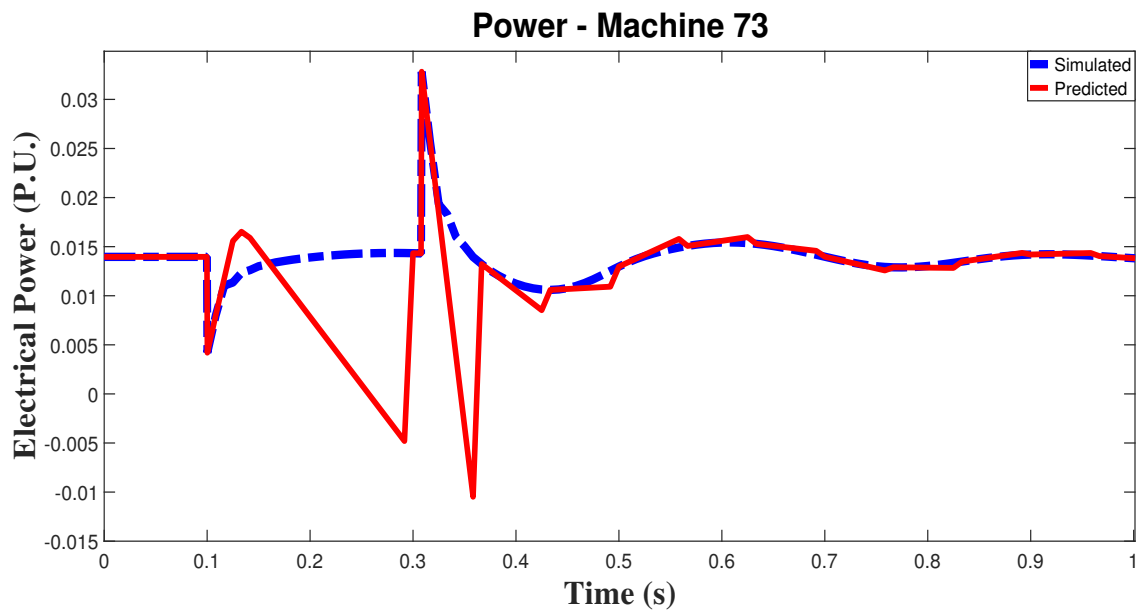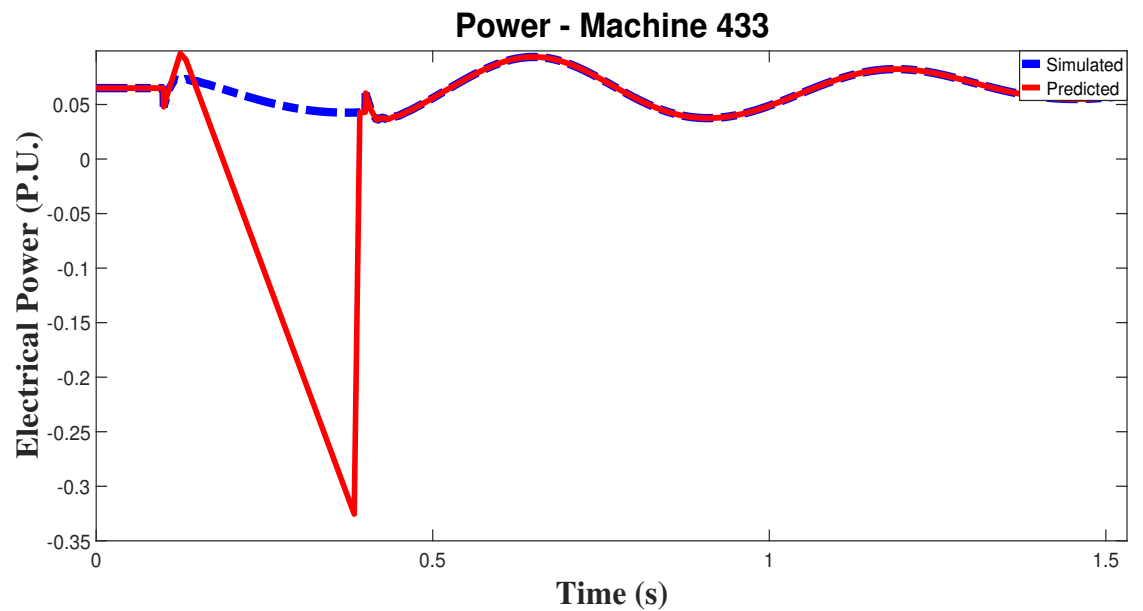

Figure 4.34: Actual and predicted output power of G433 that has the maximum error - Fault on bus 450 - 500 bus system.

4.5   Summary

In this chapter, it was presented how to use Taylor series-based prediction to predict the speed, angle, and output power of generators. The error of prediction was calculated and the results of testing this prediction method for different studies on IEEE 9 bus, IEEE 39 bus, and North Carolina - South Carolina 500 bus system were achieved.

In the next chapter, chapter 5, the energy function in a multi-machine power system and the proposed approach to use this concept in transient stability studies are discussed.

CHAPTER 5: Proposed Approach for Energy Function Problem in Power Systems

The main goal of using direct methods in power systems is to perform Transient Stability Assessment (TSA) without solving the dynamic equations numerically. Among all direct methods, the Lyapunov's idea associated with the LaSalle's Invariance Principle has been used to estimate the stability region of power systems [85].

5.1 Introduction

According to Lyapunov's theory, energy in a system converts from kinetic to potential form, when the system undergoes a disturbance. For a system to be stable, there should be a balance between energies, and the system should have the capacity to convert the kinetic into potential energy. Using Lyapunov's second method to assess the stability of a nonlinear system, a scalar energy function called a Lyapunov function should be constructed. This function should meet the Lyapunov's criteria. However, unfortunately, no general applicable way has been found yet to find or build Lyapunov functions [84, 108, 109]. The energy-based methods are a special case of, the more general, Lyapunov's second method, and are discussed in this chapter. The chapter is organized as follows: first, the energy function for a non-reduced system is driven. Then, it is explained how reducing the system can help to find a function closer to the Lyapunov function. Next, terms of the energy function are explained. The chapter ends with an illustrative example and some discussions about the problems of using direct methods in power system transient stability assessment.

5.2 Obtaining Energy Function for Power Systems

To better understand the concept of energy and leveraging it toward transient stability, the main power system equations and transient dynamics of the power

system should be elaborated. Consider a power network that has n buses. Equations 5.1 to 5.6 are used to perform a load flow on the power system at steady-state. These equations provide the pre-fault condition of the network, which is the initial condition for the during-the-fault dynamic studies.

$$[I] = [Y][V] \tag{5.1}$$

$$I_i = \sum_{j=1}^{n} y_{ij} V_j \tag{5.2}$$

$$S_i = V_i I_i^* \tag{5.3}$$

$$I_i = \sum_{j=1}^{n} Y_{ij} V_j = \sum_{j=1}^{n} |Y_{ij}| |V_j| (\Theta_{ij} + \delta_j) \tag{5.4}$$

$$P_{ei} = \sum_{j=1}^{n} |V_i| |V_j| |Y_{ij}| \cos(\Theta_{ij} - \delta_i + \delta_j) \tag{5.5}$$

$$Q_{ei} = -\sum_{j=1}^{n} |V_i| |V_j| |Y_{ij}| \sin(\Theta_{ij} - \delta_i + \delta_j) \tag{5.6}$$

where Y represents the transfer matrix of the network at steady-state. I_i, P_{ei}, and Q_{ei} are current, active power, and reactive power injected to the grid from bus i, respectively. V_i is the voltage of bus i, and δ_i is the angle of its voltage. Θ_{ij} is the angle of Z_{ij}, when Z_{ij} is the ijth element of $Zbus$.

Typically, the Lyapunov's idea associated with the LaSalle's Invariance Principle has been used to estimate the stability region of power systems [85]. Hence, the existence of an infinite bus is usually required, or alternatively a uniform damping hypothesis is made [110].

5.2.1 Energy Balance in a Non-Reduced Power Network

Assume that we have a system with n generators and m buses without generators. In order to analyze the transient behavior of the system, each generator is replaced with a constant voltage source behind its transient reactance. This results in having

$2n + m$ buses in the new system, where n buses are generator buses, and $n + m$ buses are considered as load buses. Equations 5.7 and 5.8 represent the classical dynamic model for generators i.

$$\frac{d^2 ffi_i}{dt^2} = \frac{\pi f}{H_i}(P_{m_i} - P_{e_i}) - D_i \frac{d\delta_i}{dt}, \quad i = 1, 2, \cdots, n \tag{5.7}$$

$$\frac{d\delta_i}{dt} = \omega_i, \quad i = 1, 2, \cdots, n \tag{5.8}$$

where δ_i is the generator angle with respect to synchronous frame, ω_s is the reference speed, ω_i is the speed of generator i, D_i is the damping factor, and H_i is the inertia constant of generator i. Replacing P_{ei} with Eq. 5.5 delivers Eq. 5.9:

$$\frac{d^2 ffi_i}{dt^2} = \frac{\pi f}{H_i}(P_{m_i} - \sum_{j=1}^{2n+m} |V_i| |V_j| |Y_{ij}| cos(\Theta_{ij} - \delta_i + \delta_j)) - D_i \frac{d\delta_i}{dt}, \quad i = 1, 2, \cdots, n \tag{5.9}$$

In order to achieve an energy function for a power system, integrating the swing equation is performed, since the time integration of power gives the energy [24]. Let $\frac{\pi f}{H_i} = M_i$, and multiply both sides of Eq. 5.9 by $\frac{d\delta_i}{dt}$. Then, perform a time integration. Integration steps are shown in what follows:

$$M_i \int_a^b \frac{d^2 \delta_i}{dt^2} * \frac{d\delta_i}{dt} dt = \int_a^b P_{m_i} \frac{d\delta_i}{dt} dt$$

$$- \int_a^b \sum_{j=1}^{2n+m} |V_i| |V_j| |Y_{ij}| cos(\Theta_{ij} - \delta_i + \delta_j)) \frac{d\delta_i}{dt} dt - \int_a^b D_i \frac{d\delta_i}{dt} \frac{d\delta_i}{dt} dt \tag{5.10}$$

$$M_i \int_a^b \frac{d^2 \delta_i}{dt^2} * \frac{d\delta_i}{dt} dt = \int_a^b (P_{m_i} - |V_i^2| |Y_{ii}| cos\Theta_{ii}) d\delta_i$$

$$- \int_a^b \sum_{j=1, j \neq i}^{2n+m} |V_i| |V_j| |Y_{ij}| cos(\Theta_{ij} - \delta_{ij}) d\delta_i - \int_a^b D_i (\frac{d\delta_i}{dt})^2 dt \tag{5.11}$$

$$M_i \int_a^b \frac{\mathrm{d}^2\delta_i}{\mathrm{d}t^2} * \frac{\mathrm{d}\delta_i}{\mathrm{d}t} dt = \int_a^b (P_{m_i} - |V_i^2| |Y_{ii}| cos\Theta_{ii}) d\delta_i$$

$$- \int_a^b \sum_{j=1,j\neq i}^{2n+m} |V_i| |V_j| |Y_{ij}| sin\Theta_{ij} sin\delta_{ij} \mathrm{d}\delta_i$$

$$- \int_a^b \sum_{j=1,j\neq i}^{2n+m} |V_i| |V_j| |Y_{ij}| cos\Theta_{ij} cos\delta_{ij} \mathrm{d}\delta_i - \int_a^b D_i (\frac{\mathrm{d}\delta_i}{\mathrm{d}t})^2 dt \tag{5.12}$$

$$|Y_{ij}| sin\Theta_{ij} = B_{ij} \tag{5.13}$$

$$|Y_{ij}| cos\Theta_{ij} = G_{ij} \tag{5.14}$$

$$M_i \int_a^b \frac{\mathrm{d}^2\delta_i}{\mathrm{d}t^2} * \frac{\mathrm{d}\delta_i}{\mathrm{d}t} dt = \int_a^b (P_{m_i} - |V_i^2| G_{ii}) d\delta_i$$

$$- \int_a^b \sum_{j=1,j\neq i}^{2n+m} |V_i| |V_j| B_{ij} sin\delta_{ij} \mathrm{d}\delta_i - \int_a^b \sum_{j=1,j\neq i}^{2n+m} |V_i| |V_j| G_{ij} cos\delta_{ij} \mathrm{d}\delta_i - \int_a^b D_i (\frac{\mathrm{d}\delta_i}{\mathrm{d}t})^2 dt$$

$$\tag{5.15}$$

$$|V_i| |V_j| B_{ij} = C_{ij} \tag{5.16}$$

$$|V_i| |V_j| G_{ij} = D_{ij} \tag{5.17}$$

$$M_i \int_a^b \frac{\mathrm{d}^2\delta_i}{\mathrm{d}t^2} * \frac{\mathrm{d}\delta_i}{\mathrm{d}t} dt = \int_a^b (P_{m_i} - |V_i^2| G_{ii}) d\delta_i$$

$$- \int_a^b \sum_{j=1,j\neq i}^{2n+m} C_{ij} sin\delta_{ij} \mathrm{d}\delta_i - \int_a^b \sum_{j=1,j\neq i}^{2n+m} D_{ij} cos\delta_{ij} \mathrm{d}\delta_i - \int_a^b D_i (\frac{\mathrm{d}\delta_i}{\mathrm{d}t})^2 dt \tag{5.18}$$

Substituting $\frac{\mathrm{d}\delta_i}{\mathrm{d}t}$ with ω_i, and assuming constant voltages during the fault, result in:

$$M_i \int_a^b \frac{\mathrm{d}\omega_i}{\mathrm{d}t} * \omega_i dt = \int_a^b (P_{m_i} - |V_i^2| G_{ii}) d\delta_i$$

$$-\int_a^b \sum_{j=1,j\neq i}^{2n+m} C_{ij} sin\delta_{ij} \mathrm{d}\delta_i - \int_a^b \sum_{j=1,j\neq i}^{2n+m} D_{ij} cos\delta_{ij} \mathrm{d}\delta_i - \int_a^b D_i (\frac{\mathrm{d}\delta_i}{\mathrm{d}t})^2 dt \qquad (5.19)$$

Considering that the integrands of second and third terms of the right side of the energy equation of a single machine depend on both δ_i and δ_j, it is not possible to find an explicit answer for those terms. Equation 5.19 holds true for each individual generator in the system. To find the energy of the entire system, the energy equation for all machines are summed up:

$$\sum_{i=1}^n M_i \int_a^b \frac{\mathrm{d}\omega_i}{\mathrm{d}t} * \omega_i dt = \sum_{i=1}^n \int_a^b (P_{m_i} - |V_i^2| G_{ii}) d\delta_i$$

$$-\sum_{i=1}^n \int_a^b \sum_{j=1,j\neq i}^{2n+m} C_{ij} sin\delta_{ij} \mathrm{d}\delta_i - \sum_{i=1}^n \int_a^b \sum_{j=1,j\neq i}^{2n+m} D_{ij} cos\delta_{ij} \mathrm{d}\delta_i - \sum_{i=1}^n \int_a^b D_i(\frac{\mathrm{d}\delta_i}{\mathrm{d}t})^2 dt \quad (5.20)$$

$$\sum_{i=1}^n M_i \int_a^b \omega_i \mathrm{d}\omega_i = \int_a^b \sum_{i=1}^n (P_{m_i} - |V_i^2| G_{ii}) d\delta_i$$

$$-\int_a^b \sum_{i=1}^n \sum_{j=1,j\neq i}^{2n+m} C_{ij} sin\delta_{ij} \mathrm{d}\delta_i - \int_a^b \sum_{i=1}^n \sum_{j=1,j\neq i}^{2n+m} D_{ij} cos\delta_{ij} \mathrm{d}\delta_i - \int_a^b \sum_{i=1}^n D_i(\frac{\mathrm{d}\delta_i}{\mathrm{d}t})^2 dt \quad (5.21)$$

It can be proved that [Appendix C]:

$$\sum_{i=1}^n \sum_{j=1,\neq i}^n C_{ij} Sin\delta_{ij} \dot{\delta}_i = \sum_{i=1}^{n-1} \sum_{j=i+1}^n C_{ij} Sin\delta_{ij} \dot{\delta}_{ij} \qquad (5.22)$$

$$\sum_{i=1}^n \sum_{j=1,\neq i}^n D_{ij} Cos\delta_{ij} \dot{\delta}_i = \sum_{i=1}^{n-1} \sum_{j=i+1}^n D_{ij} Cos\delta_{ij} (\dot{\delta}_i + \dot{\delta}_j) \qquad (5.23)$$

Substituting equations 5.22 and 5.23 in equation 5.20 results in:

$$\sum_{i=1}^n M_i \int_a^b \omega_i \mathrm{d}\omega_i = \int_a^b \sum_{i=1}^n (P_{m_i} - |V_i^2| G_{ii}) d\delta_i -$$

$$\int_a^b \sum_{i=1}^{n-1} \sum_{j=i+1}^{n} C_{ij} sin\delta_{ij} \mathrm{d}(\delta_i - \delta_j) - \int_a^b \sum_{i=1}^{n-1} \sum_{j=i+1}^{n} D_{ij} cos\delta_{ij} \mathrm{d}(\delta_i + \delta_j)$$

$$-\int_a^b \sum_{i=1}^{n} D_i (\frac{\mathrm{d}\delta_i}{\mathrm{d}t})^2 dt - \int_a^b \sum_{i=1}^{n} \sum_{j=n+1}^{2n+m} C_{ij} sin\delta_{ij} \mathrm{d}\delta_i - \int_a^b \sum_{i=1}^{n} \sum_{j=n+1}^{2n+m} D_{ij} cos\delta_{ij} \mathrm{d}\delta_i \quad (5.24)$$

$$\sum_{i=1}^{n} M_i \int_a^b \omega_i \mathrm{d}\omega_i = \int_a^b \sum_{i=1}^{n} (P_{m_i} - \left| V_i^2 \right| G_{ii}) d\delta_i$$

$$-\int_a^b \sum_{i=1}^{n-1} \sum_{j=i+1}^{n} C_{ij} sin\delta_{ij} \mathrm{d}\delta_{ij} - \int_a^b \sum_{i=1}^{n-1} \sum_{j=i+1}^{n} D_{ij} cos\delta_{ij} \mathrm{d}(\delta_i + \delta_j)$$

$$-\int_a^b \sum_{i=1}^{n} D_i (\frac{\mathrm{d}\delta_i}{\mathrm{d}t})^2 dt - \int_a^b \sum_{i=1}^{n} \sum_{j=n+1}^{2n+m} C_{ij} sin\delta_{ij} \mathrm{d}\delta_i - \int_a^b \sum_{i=1}^{n} \sum_{j=n+1}^{2n+m} D_{ij} cos\delta_{ij} \mathrm{d}\delta_i \quad (5.25)$$

$$\sum_{i=1}^{n} \frac{1}{2} M_i \omega_i^2]_{\omega_i^a}^{\omega_i^b} = \sum_{i=1}^{n} (P_{m_i} - \left| V_i^2 \right| G_{ii}) \delta_i]_{\delta_i^a}^{\delta_i^b}$$

$$+\sum_{i=1}^{n-1} \sum_{j=i+1}^{n} C_{ij} cos\delta_{ij}]_{\delta_{ij}^a}^{\delta_{ij}^b} - \int_a^b \sum_{i=1}^{n-1} \sum_{j=i+1}^{n} D_{ij} cos\delta_{ij} \mathrm{d}(\delta_i + \delta_j)$$

$$-\int_a^b \sum_{i=1}^{n} D_i (\frac{\mathrm{d}\delta_i}{\mathrm{d}t})^2 dt - \int_a^b \sum_{i=1}^{n} \sum_{j=n+1}^{2n+m} C_{ij} sin\delta_{ij} \mathrm{d}\delta_i - \int_a^b \sum_{i=1}^{n} \sum_{j=n+1}^{2n+m} D_{ij} cos\delta_{ij} \mathrm{d}\delta_i \quad (5.26)$$

As can be seen, on the right side of Eq. 5.26, there are path dependent terms that cannot be calculated without numerical methods, since the trajectory of the parameters during the fault is not known. In most of the researches, the system is considered loss-less, and D_{ij} is equal to zero. Also, the damping effect of the generators are usually neglected, and D_is are assumed to be zero. Hence, terms related to the resistance of the lines and damping of the generators are removed from Eq. 5.26, which delivers

Eq.5.27.

$$\sum_{i=1}^{n}\frac{1}{2}M_i\omega_i^2]_{\omega_i^a}^{\omega_i^b} = \sum_{i=1}^{n}(P_{m_i} - \left|V_i^2\right|G_{ii})\delta_i]_{\delta_i^a}^{\delta_i^b} + \sum_{i=1}^{n-1}\sum_{j=i+1}^{n}C_{ij}cos\delta_{ij}]_{\delta_{ij}^a}^{\delta_{ij}^b} - \int_{a}^{b}\sum_{i=1}^{n}\sum_{j=n+1}^{2n+m}C_{ij}sin\delta_{ij}\mathrm{d}\delta_i$$
$$(5.27)$$

In Eq. 5.27 there is still a path-dependent term. Trying to eliminate this term, leads to employing system reduction since the remaining path-dependent term represents the energy relation between generator buses and load buses. Reducing the network via Kron reduction is usually employed to remove this path-dependant term. Thus, energy balance in reduced networks is discussed in the following section.

5.2.2 Energy Balance in a Reduced Power Network

Assume that we have a system with n generators, and m buses without generators. In order to analyze the transient behavior of the system, each generator is replaced with a constant voltage source behind its transient reactance. This results in having $2n + m$ buses in the new system, where n buses are generator buses, and $n + m$ buses are considered as load buses. If the system is reduced by eliminating non-generator buses via Kron reduction, the reduced system will have only n buses, and all of them will be generator buses. Considering swing equation for each generator results in what follows:

$$\frac{\mathrm{d}^2\text{ffi}_i}{\mathrm{d}t^2} = \frac{\pi f}{H_i}(P_{m_i} - P_{e_i}) - D_i\frac{\mathrm{d}\delta_i}{\mathrm{d}t}, \quad i = 1, 2, \cdots, n \tag{5.28}$$

$$\frac{\mathrm{d}\delta_i}{\mathrm{d}t} = \omega_i, \quad i = 1, 2, \cdots, n \tag{5.29}$$

where δ_i is the generator angle with respect to synchronous frame, ω_s is the reference speed, ω_i is the speed of generator i, and D_i and H_i are the damping factor and inertia constant of the generator i, respectively. Replacing P_{ei} with the equivalent amount from Eq. 5.5 delivers Eq. 5.9 delivers:

$$\frac{\mathrm{d}^2\text{ffi}_i}{\mathrm{d}t^2} = \frac{\pi f}{H_i}(P_{m_i} - \sum_{j=1}^{n}\left|V_i\right|\left|V_j\right|\left|Y_{ij}\right|cos(\Theta_{ij} - \delta_i + \delta_j)) - D_i\frac{\mathrm{d}\delta_i}{\mathrm{d}t}, \quad i = 1, 2, \cdots, n \tag{5.30}$$

In order to achieve an energy function for a power system, integrating the swing equation is performed, because the time integration of power gives the energy [24]. Let $\frac{\pi f}{H_i} = M_i$, and multiply both sides of Eq. 5.30 by $\frac{d\delta_i}{dt}$. Then, perform a time integration. The integration steps are shown in what follows:

$$M_i \int_a^b \frac{d^2\delta_i}{dt^2} * \frac{d\delta_i}{dt} dt = \int_a^b P_{m_i} \frac{d\delta_i}{dt} dt$$

$$- \int_a^b \sum_{j=1}^n |V_i| |V_j| |Y_{ij}| \cos(\Theta_{ij} - \delta_i + \delta_j)) \frac{d\delta_i}{dt} dt - \int_a^b D_i \frac{d\delta_i}{dt} \frac{d\delta_i}{dt} dt \qquad (5.31)$$

$$M_i \int_a^b \frac{d^2\delta_i}{dt^2} * \frac{d\delta_i}{dt} dt = \int_a^b (P_{m_i} - |V_i^2| |Y_{ii}| \cos\Theta_{ii}) d\delta_i$$

$$- \int_a^b \sum_{j=1,j\neq i}^n |V_i| |V_j| |Y_{ij}| \cos(\Theta_{ij} - \delta_{ij}) d\delta_i - \int_a^b D_i (\frac{d\delta_i}{dt})^2 dt \qquad (5.32)$$

$$M_i \int_a^b \frac{d^2\delta_i}{dt^2} * \frac{d\delta_i}{dt} dt = \int_a^b (P_{m_i} - |V_i^2| |Y_{ii}| \cos\Theta_{ii}) d\delta_i$$

$$- \int_a^b \sum_{j=1,j\neq i}^n |V_i| |V_j| |Y_{ij}| \sin\Theta_{ij} \sin\delta_{ij} d\delta_i - \int_a^b \sum_{j=1,j\neq i}^n |V_i| |V_j| |Y_{ij}| \cos\Theta_{ij} \cos\delta_{ij} d\delta_i$$

$$- \int_a^b D_i (\frac{d\delta_i}{dt})^2 dt \qquad (5.33)$$

$$|Y_{ij}| \sin\Theta_{ij} = B_{ij} \qquad (5.34)$$

$$|Y_{ij}| \cos\Theta_{ij} = G_{ij} \qquad (5.35)$$

$$M_i \int_a^b \frac{d^2\delta_i}{dt^2} * \frac{d\delta_i}{dt} dt = \int_a^b (P_{m_i} - |V_i^2| G_{ii}) d\delta_i$$

$$- \int_a^b \sum_{j=1,j\neq i}^n |V_i| |V_j| B_{ij} \sin\delta_{ij} d\delta_i - \int_a^b \sum_{j=1,j\neq i}^n |V_i| |V_j| G_{ij} \cos\delta_{ij} d\delta_i - \int_a^b D_i (\frac{d\delta_i}{dt})^2 dt$$

$$(5.36)$$

$$|V_i|\,|V_j|\,B_{ij} = C_{ij} \tag{5.37}$$

$$|V_i|\,|V_j|\,G_{ij} = D_{ij} \tag{5.38}$$

$$M_i \int_a^b \frac{\mathrm{d}^2\delta_i}{\mathrm{d}t^2} * \frac{\mathrm{d}\delta_i}{\mathrm{d}t} dt = \int_a^b (P_{m_i} - |V_i^2|\,G_{ii})d\delta_i - \int_a^b \sum_{j=1,j\neq i}^n C_{ij} sin\delta_{ij}\mathrm{d}\delta_i$$
$$- \int_a^b \sum_{j=1,j\neq i}^n D_{ij} cos\delta_{ij}\mathrm{d}\delta_i - \int_a^b D_i(\frac{\mathrm{d}\delta_i}{\mathrm{d}t})^2 dt \tag{5.39}$$

Substituting $\frac{\mathrm{d}\delta_i}{\mathrm{d}t}$ with ω_i, based on Eq.5.29, and assuming that the magnitude of voltages remain constant during the fault, results in:

$$M_i \int_a^b \frac{\mathrm{d}\omega_i}{\mathrm{d}t} * \omega_i dt = \int_a^b (P_{m_i} - |V_i^2|\,G_{ii})d\delta_i - \int_a^b \sum_{j=1,j\neq i}^n C_{ij} sin\delta_{ij}\mathrm{d}\delta_i$$
$$- \int_a^b \sum_{j=1,j\neq i}^n D_{ij} cos\delta_{ij}\mathrm{d}\delta_i - \int_a^b D_i(\frac{\mathrm{d}\delta_i}{\mathrm{d}t})^2 dt \tag{5.40}$$

Considering that the integrands of second and third terms of the right side of the energy equation of each generator depend on both δ_i and δ_j, it is not possible to find an explicit answer for those terms. Equation 5.40 holds true for each individual generator in the system. To find the energy of the entire system, energy equations for all machines are summed up:

$$\sum_{i=1}^n M_i \int_a^b \frac{\mathrm{d}\omega_i}{\mathrm{d}t} * \omega_i dt = \sum_{i=1}^n \int_a^b (P_{m_i} - |V_i^2|\,G_{ii})d\delta_i - \sum_{i=1}^n \int_a^b \sum_{j=1,j\neq i}^n C_{ij} sin\delta_{ij}\mathrm{d}\delta_i$$
$$- \sum_{i=1}^n \int_a^b \sum_{j=1,j\neq i}^n D_{ij} cos\delta_{ij}\mathrm{d}\delta_i - \sum_{i=1}^n \int_a^b D_i(\frac{\mathrm{d}\delta_i}{\mathrm{d}t})^2 dt \tag{5.41}$$

$$\sum_{i=1}^n M_i \int_a^b \omega_i \mathrm{d}\omega_i = \int_a^b \sum_{i=1}^n (P_{m_i} - |V_i^2|\,G_{ii})d\delta_i - \int_a^b \sum_{i=1}^n \sum_{j=1,j\neq i}^n C_{ij} sin\delta_{ij}\mathrm{d}\delta_i$$

$$-\int_a^b \sum_{i=1}^n \sum_{j=1,j\neq i}^n D_{ij}cos\delta_{ij}\mathrm{d}\delta_i - \int_a^b \sum_{i=1}^n D_i(\frac{\mathrm{d}\delta_i}{\mathrm{d}t})^2 dt \qquad (5.42)$$

It can be proved that [Appendix C]:

$$\sum_{i=1}^n \sum_{j=1,\neq i}^n C_{ij}Sin\delta_{ij}\dot\delta_i = \sum_{i=1}^{n-1} \sum_{j=i+1}^n C_{ij}Sin\delta_{ij}\dot\delta_{ij} \qquad (5.43)$$

$$\sum_{i=1}^n \sum_{j=1,\neq i}^n D_{ij}Cos\delta_{ij}\dot\delta_i = \sum_{i=1}^{n-1} \sum_{j=i+1}^n D_{ij}Cos\delta_{ij}(\dot\delta_i + \dot\delta_j) \qquad (5.44)$$

substituting 5.43 and 5.44 in 5.42 results in:

$$\sum_{i=1}^n M_i \int_a^b \omega_i \mathrm{d}\omega_i = \int_a^b \sum_{i=1}^n (P_{m_i} - \left|V_i^2\right| G_{ii})d\delta_i - \int_a^b \sum_{i=1}^{n-1} \sum_{j=i+1}^n C_{ij}sin\delta_{ij}\mathrm{d}(\delta_i - \delta_j)-$$

$$-\int_a^b \sum_{i=1}^{n-1} \sum_{j=i+1}^n D_{ij}cos\delta_{ij}\mathrm{d}(\delta_i + \delta_j) - \int_a^b \sum_{i=1}^n D_i(\frac{\mathrm{d}\delta_i}{\mathrm{d}t})^2 dt \qquad (5.45)$$

$$\sum_{i=1}^n M_i \int_a^b \omega_i \mathrm{d}\omega_i = \int_a^b \sum_{i=1}^n (P_{m_i} - \left|V_i^2\right| G_{ii})d\delta_i - \int_a^b \sum_{i=1}^{n-1} \sum_{j=i+1}^n C_{ij}sin\delta_{ij}\mathrm{d}\delta_{ij}$$

$$-\int_a^b \sum_{i=1}^{n-1} \sum_{j=i+1}^n D_{ij}cos\delta_{ij}\mathrm{d}(\delta_i + \delta_j) - \int_a^b \sum_{i=1}^n D_i(\frac{\mathrm{d}\delta_i}{\mathrm{d}t})^2 dt \qquad (5.46)$$

$$\sum_{i=1}^n \frac{1}{2}M_i\omega_i^2]_{\omega_i^a}^{\omega_i^b} = \sum_{i=1}^n (P_{m_i} - \left|V_i^2\right| G_{ii})\delta_i]_{\delta_i^a}^{\delta_i^b} + \sum_{i=1}^{n-1} \sum_{j=i+1}^n C_{ij}cos\delta_{ij}]_{\delta_{ij}^a}^{\delta_{ij}^b}$$

$$-\int_a^b \sum_{i=1}^{n-1} \sum_{j=i+1}^n D_{ij}cos\delta_{ij}\mathrm{d}(\delta_i + \delta_j) - \int_a^b \sum_{i=1}^n D_i(\frac{\mathrm{d}\delta_i}{\mathrm{d}t})^2 dt \qquad (5.47)$$

As can be seen, on the right side of Eq. 5.47, there are path dependent terms that cannot be calculated without numerical methods, since the trajectory of the parameters during the fault is not known. In most of the researches, the system is considered

loss-less and accordingly, D_{ij} is equal to zero. Also, the damping effect of the generators is usually neglected, and D_i is assumed to be zero. Hence, terms related to the resistance of the lines and damping of the generators are removed from Eq. 5.26, which delivers Eq. 5.48:

$$\sum_{i=1}^{n} \frac{1}{2} M_i \omega_i^2]_{\omega_i^a}^{\omega_i^b} = \sum_{i=1}^{n} (P_{m_i} - |V_i^2| G_{ii}) \delta_i]_{\delta_i^a}^{\delta_i^b} + \sum_{i=1}^{n} \sum_{j=1, j \neq i}^{n} C_{ij} cos\delta_{ij}]_{\delta_{ij}^a}^{\delta_{ij}^b} \qquad (5.48)$$

5.2.3   Energy Function for Lossy Power Networks

Generally, the inclusion of transfer conductances in energy equations leads to twice nonlinearities compared to when they are neglected [111]. In 1984, Narasimhamurthi showed that the standard energy function of a lossless system cannot be extended in a general manner to a system with losses [110]. In 1989, Chiang studied the existence of energy functions for lossy power systems [84]. He proved that a general Lyapunov function does not exist when losses are considered in the power system model. In fact, Chiang proved the existence of a Lyapunov function for power systems considering transfer conductances, when they are not large enough. However, his result concerns with the existence only, and he did not exhibit such a function. When the transfer conductances are not neglected, the obtained energy function is not a Lyapunov function [85, 110]. Pai et al. found an expression for the energy function for lossy systems, but it was later shown that their derivation was applicable for only two machine systems [14, 66].

Stability analysis using Lyapunov functions for lossy power systems requires Lyapunov functions that are significantly different from those employed for lossless systems. Studies do not show if line losses have or have not induced instability in any actual system. A reason for this lack of knowledge is that oscillations induced by line losses are in the same frequency range as the electromechanical oscillation. Oscillations in this frequency range are classified as subsynchronous resonance oscillations,

Table 5.1: Summary of important findings of studying energy functions in lossy power systems.

Year Researcher(s)	Contribution
1984 Narasimhamurthi	- Proving that the standard energy function of a lossless system cannot be extended in a general manner to a system
1989 Pai	- Finding an energy function for lossy systems with two generators
1989 Chiang	- Proving that a general Lyapunov function does not exist when losses are considered in the power system model
Conclusion	No Lyapunov function can be found for lossy systems

which means oscillations induced by resonance between the electrical and mechanical systems. In conclusion, there is no general energy function for a system with losses. Table 5.1 provides a summary of important findings of studying energy functions in lossy power systems.

5.3 Interpretation of Power System Energy Balance Equation

In this section, each term of the energy function equation terms, calculated earlier, is discussed, and a definition for each term is provided. The energy balance equation for a non-reduced system was shown in Eq. 5.26. For ease of use, the equation is presented again in Eq. 5.49.

$$\sum_{i=1}^{n} \frac{1}{2} M_i \omega_i^2]_{\omega_i^a}^{\omega_i^b} = \sum_{i=1}^{n} (P_{m_i} - |V_i^2| G_{ii}) \delta_i]_{\delta_i^a}^{\delta_i^b} + \sum_{i=1}^{n-1} \sum_{j=i+1}^{n} C_{ij} cos\delta_{ij}]_{\delta_{ij}^a}^{\delta_{ij}^b}$$

$$- \int_a^b \sum_{i=1}^{n-1} \sum_{j=i+1}^{n} D_{ij} cos\delta_{ij} \mathrm{d}(\delta_i + \delta_j) - \int_a^b \sum_{i=1}^{n} D_i (\frac{\mathrm{d}\delta_i}{\mathrm{d}t})^2 dt$$

$$- \int_a^b \sum_{i=1}^{n} \sum_{j=n+1}^{2n+m} C_{ij} sin\delta_{ij} \mathrm{d}\delta_i - \int_a^b \sum_{i=1}^{n} \sum_{j=n+1}^{2n+m} D_{ij} cos\delta_{ij} \mathrm{d}\delta_i \qquad (5.49)$$

Equation 5.49 is also referred to as the energy-integral. It was first introduced by Aylett in 1958 and has been used as the Lyapunov function with minor modifications by a number of researchers [111]. Each term of Eq. 5.49 terms can be interpreted as

follows:

- Transient Kinetic Energy Stored in the mass of generators' rotors:

$$\sum_{i=1}^{n} \frac{1}{2} M_i \omega_i^2]_{\omega_i^a}^{\omega_i^b} = \sum_{i=1}^{n} \frac{1}{2} M_i (\omega_i^{b2} - \omega_i^{a2}) \tag{5.50}$$

Equation 5.50 shows the change in the kinetic energy of the rotor of all the generators when going from state a to b. Since we normally assume that the system is at a steady state before a disturbance, it is true to consider $\omega_i^a = 0$. Therefore, the kinetic energy stored in the rotor of each generator at its current state is defined as:

$$KE_i = \frac{1}{2} M_i \omega_i^2 \tag{5.51}$$

- Position Energy of generators' rotors:

$$\sum_{i=1}^{n} (P_{m_i} - |V_i^2| G_{ii}) \delta_i]_{\delta_i^a}^{\delta_i^b} = \sum_{i=1}^{n} [(P_{m_i} - |V_i^2| G_{ii})(\delta_i^b - \delta_i^a)] \tag{5.52}$$

- A disturbance makes generators' angles to swing from state a to b. During this transition, some of the mechanical power supplied to the generators is consumed by the loads that are directly connected to the generator buses, which is equal to $|V_i^2| G_{ii}$. Also, some power may be injected to the grid, which its effect is seen in another term of Eq. 5.49. The extra power that is injected by the turbine, but is not used by loads and grid, makes the generators' speeds to change, which is the causes of the change in generators' angles. The effect of changes in generators' rotor angles is considered in equation 5.52. This energy is usually called Rotor Potential Energy, and it is shown by P_r in this thesis. Therefore, the potential energy of the rotor of each generator at its current state is defined as:

$$P_{r_i} = (P_{m_i} - |V_i^2| G_{ii}) \delta_i \tag{5.53}$$

Magnetic Energy:

$$P_{Mag} = \sum_{i=1}^{n-1}\sum_{j=i+1}^{n} C_{ij}cos\delta_{ij}]_{\delta_{ij}^a}^{\delta_{ij}^b} - \int_a^b \sum_{i=1}^{n}\sum_{j=n+1}^{2n+m} C_{ij}sin\delta_{ij}\mathrm{d}\delta_i \qquad (5.54)$$

Equation 5.54 represents a relation for the energy transferred to the grid. It consists of two terms. The first term, which is path-independent, represents a relation for the energy transferred through the transmission lines that are directly connected to the generator buses. The second term, which is path-dependent, represents a relation for the energy injected to the grid through the lines that are connected between generator buses and load buses. The name "Magnetic Energy" is only a name and does not have any relation to the magnetic energy stored in the line inductances.

- Dissipated Energy:

$$P_{Loss} = -\int_a^b \sum_{i=1}^{n-1}\sum_{j=i+1}^{n} D_{ij}cos\delta_{ij}\mathrm{d}(\delta_i + \delta_j) - \int_a^b \sum_{i=1}^{n}\sum_{j=n+1}^{2n+m} D_{ij}cos\delta_{ij}\mathrm{d}\delta_i$$

$$- \int_a^b \sum_{i=1}^{n} D_i(\frac{\mathrm{d}\delta_i}{\mathrm{d}t})^2 dt \qquad (5.55)$$

Equation 5.55 represents a relation for the energy lost in the system. The first term in Eq. 5.55 represents the lost energy in the resistance of the lines that are directly connected to the generator buses. The second term shows the lost energy in the resistance of the lines that are connected between generator buses and load buses. The last term represents the energy lost because of the generators' damping.

In some papers, the dissipated energy in the lines is approximated by considering the fault trajectory linear. Hence, the following approximation is considered for

the energy dissipated in lines resistance of a reduced system:

$$\int_a^b \sum_{i=1}^{n-1} \sum_{j=i+1}^{n} D_{ij} cos\delta_{ij} \mathrm{d}(\delta_i + \delta_j) = D_{ij} \frac{\delta_i^b - \delta_i^a + \delta_j^b - \delta_j^a}{\delta_{ij}^b - \delta_{ij}^a}(sin\delta_{ij}^b - sin\delta_{ij}^a) \quad (5.56)$$

Considering the discussions above, it can be said that for machine i:

$$\frac{1}{2}M\omega_i^2|_{\omega_{i1}}^{\omega_{i2}} = P_{m_i}\delta_i|_{\delta_{i1}}^{\delta_{i2}} + Eei_{transferred}|_{t_1}^{t_2} + E_{Loss_i}|_{x_{i1}}^{x_{i2}} \quad (5.57)$$

In Eq. 5.57, ω_{i1} and ω_{i2} are the rotor speed at the beginning and end of the time frame of study, respectively. The rotor angles are shown with δ_{i1} and δ_{i2}, $Eei_{transferred}$ represents electrical power transferred from machine i. E_{Loss_i} shows the loss of the system, when the state of the system changes from x_{i1} to x_{i2}.

Equation 5.57 can be generalized in the following form for the entire system.

$$\sum \frac{1}{2}M\omega_i^2|_{\omega_{i1}}^{\omega_{i2}} = \sum P_{m_i}\delta_i|_{\delta_{i1}}^{\delta_{i2}} + \sum Eei_{transferred}|_{t_1}^{t_2} + \sum E_{Loss_i}|_{x_{i1}}^{x_{i2}} \quad (5.58)$$

Equations 5.57 and 5.58 are valid for the system before, during, and after a disturbance. However, appropriate values should be considered for each state.

According to what was presented above, the total Potential Energy (PE) of the system consists of three terms as follows:

$$PE = P_r + P_{Mag} + P_{Loss} \quad (5.59)$$

From Eq. 5.58 and Eq. 5.59, the kinetic energy change in generators between any two moments, during a fault for example, is equal to change in potential energy.

$$\Delta KE = \Delta PE \quad (5.60)$$

Next, an appropriate energy function for power systems is defined.

5.4 Defining the Energy Function for Power Systems

Conventionally, the energy function for the power system, V, has been derived in various ways as the difference between the transient Kinetic Energy (KE) and the total potential energy (PE):

$$V = KE - PE \tag{5.61}$$

Considering the conductance terms as zero, equations 5.26 and 5.47 has been shown to satisfy the required criteria (see [87]) to be a Lyapunov function in a region around the stable point. However, for nonzero conductance terms, only physical arguments can be used to show that the system energy function V is greater than zero. Independent of considering conductance or not, $\dot{V}$ is less than or equal to zero along the solution of swing equation [14]. This function has been used by researchers for the first swing stability studies in the time intervals of up to 1 second and has had acceptable performance. The peak of the first swing is reached typically in less than 0.5s.

To gain a better view of the concept of the energy, consider a SMIB system shown in Fig. 5.1. In this system, the synchronous machine is connected to an infinite bus through a line with an impedance of Z. Suppose that a three-phase symmetrical fault is applied on the line, and the fault is removed after about 0.3 seconds. No change happens in the network configuration following the fault, and the post-fault system is assumed stable.

Figures 5.2 and 5.3 depict the Potential Energy (PE) and Kinetic Energy (KE) before, during, and after the fault. During the fault, no electrical power is transferred from the generator. Hence, the mechanical power supplied to the machine makes the rotor to speed up and gain some kinetic energy. It can be seen that when the system is gaining extra energy during the fault, the potential energy is changing as well. After the fault, the conversion from kinetic to potential energy continues until

the system reaches its stable equilibrium point.
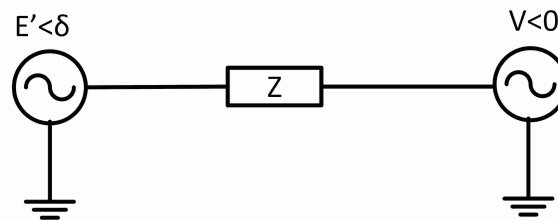
Figure 5.1: A simple single machine infinite bus system.
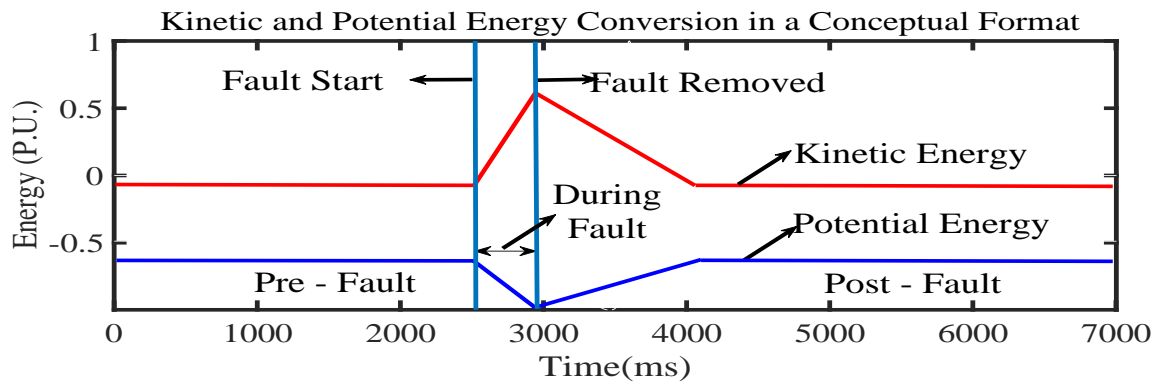
Figure 5.2: Potential and kinetic energy conversion concept.
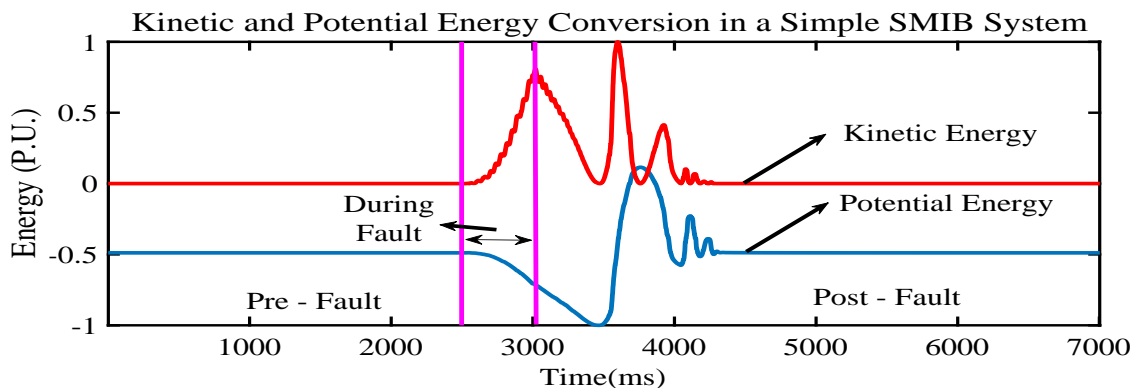
Figure 5.3: Potential and kinetic energy conversion for a SMIB system.

The kinetic energy gained by a power system during a transient is stored in the generators' rotors and can be calculated by using equation 5.50. Potential energy, however, is not always easy to calculate. Finding the system's potential energy in this example is simple, since the calculations only involve two machines, and energy conversion is not hard to follow. Complications occur while studying multi-machine

systems. In the rest of this chapter, the potential energy in a multi-machine system is discussed.

5.5   Potential Energy in a Multi-Machine System

Consider a power system operating at a steady state, related to a stable equilibrium point (SEP). If a fault happens, the generators accelerate due to a decrease in electric output power. During this fault-on period, the power system gains some kinetic energy (KE) and moves away from SEP, leading a change in the system's potential energy (PE). In studying multi-machine systems, it is necessary to determine: a) which generator will be pushed the hardest, b) how much of the available energy will go into pushing each of them, c) in which direction they will move, and d) how much energy they should get before they go unstable. Following clearing the fault, the kinetic energy is converted into potential energy again. The power system's capability to absorb the excess energy, gained during the disturbance, depends largely on its ability to convert the kinetic energy to the potential energy. This capability depends highly on the post-disturbance network configuration and the convergence area of the post-fault system.

Generally, depending on the fault location, the critically cleared (but unstable) trajectory exits the region of stability in the vicinity of an equilibrium point, which lies on the stability boundary as shown in Fig. 5.7 [14]. Potential energy varies along
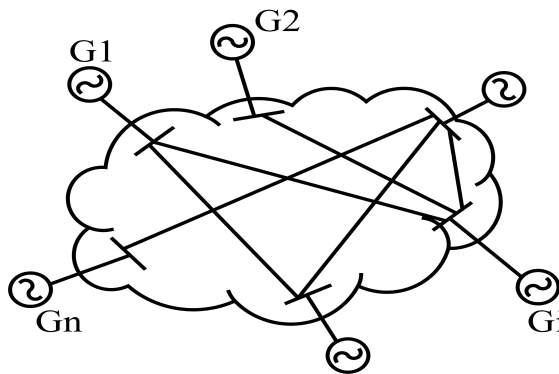
Figure 5.4: A multi-machine system schematic.

this post-disturbance trajectory [15]. If the fault is kept long enough for one machine (or more) to become critically unstable, the potential energy of the system and critical machines go through a maximum before the system goes unstable. This is shown in figures 5.5 and 5.6. In addition, this maximum value of the potential energy, along the post-disturbance trajectory, of a given machine is essentially independent of the duration of the disturbance. This value of potential energy represents the energy absorbing capacity of the network, and it is equal to V_{cr} along the trajectory. Thus,
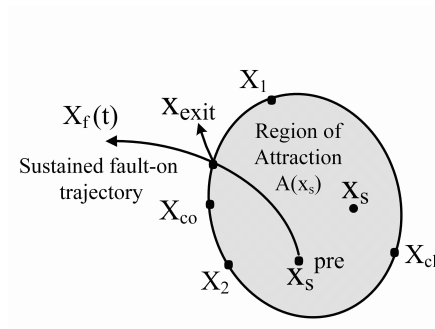
Figure 5.5: The sustained fault-on trajectory moves towards the stability boundary and intersects it at the exit point.
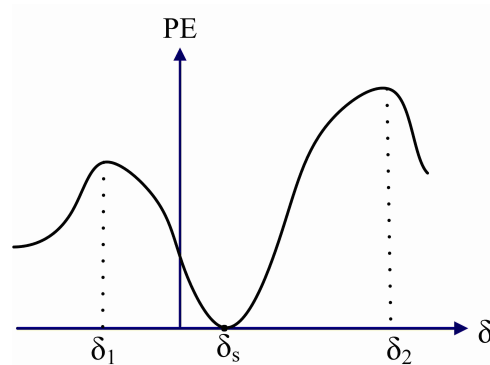
Figure 5.6: The potential energy function is only a function of δ and reaches its local maximum at UEPs $\delta1$ and $\delta2$.

the value of the energy function at the exit point, when the fault-on trajectory crosses the stable manifold of one of UEPs., is actually the true critical energy [84, 33]. Critical Energy is the amount of energy that should be injected into a system through a disturbance in order to make the post-disturbance system unstable. Since we do

not know the trajectory of the fault before it happens, different methods have been proposed for approximating the critical energy. Following, some of them are explained [14, 84]:

1. Lowest energy UEP method (Closest UEP method)

   The early approach of the direct method to find the critical energy of a system is the so-called closest UEP method, which is independent of the fault trajectory. In this method, critical energy is considered as the smallest amount of energy related to the UEPs of post-disturbance equations. In other words, $V_{cr} = V(x^u)$, where x^u is the unstable equilibrium point that gives the lowest amount of the defined energy function. Using this method needs calculating different UEPs of the post-fault system. Hence, a vast amount of computation is required. In addition, the lowest energy UEP gives conservative results, which depends completely on the chosen energy function, as can be seen in Figures 5.7 and 5.8 [14, 84].

2. Controlling UEP method
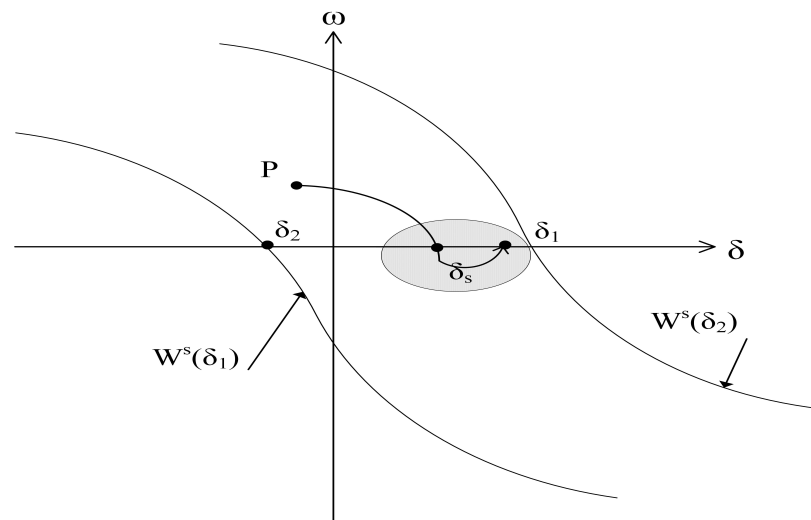
Figure 5.7: The post-fault trajectory starting from state P, which lies inside the stability region, is classified to be unstable by the closest UEP method, while in fact the resulting trajectory will converge to δ_s. Hence, it is stable.

Considering the fault-on trajectory, Kakimoto et al. and later Athay et al. in 1987, suggested a new method named "controlling UEP" method.

In this method, the closest UEP to the point that fault-on trajectory exits the region of stability of post-fault equations is found. If the exit point lies on the stable manifold of the closest UEP, the controlling UEP coincides with the closest UEP, as was shown in Fig. 5.5.

3. Potential Energy Boundary Surface [14, 15, 24, 84]:

The rim of potential energy surface contours is known as Principal Energy Boundary Surface (PEBS). This border has humps and dents and saddle points. In the PEBS method, by simulating a fault with a long duration (sustained fault), the potential energy is calculated for different time instants. The maximum value of potential energy related to different machines or groups of machines is calculated and will be considered as critical energy

$$V_{i_{cr}} = V_{PE}^{max} \tag{5.62}$$

At the PEBS, the system's potential energy is maximum and equal to the total energy of the system on the boundary of the region of stability. If the system's kinetic energy is totally converted to potential energy before reaching the PEBS, the system remains stable. However, when clearing time is bigger than the critical clearing time, the system trajectory crosses this ridge, and the system's stability is lost. The cross usually happens at some point other than the UEP but close to it.

Aylett studied a multi-machine system based on the classical model. For the multi-machine system, he obtained a set of differential equations in the inter-machine angle coordinates. In critical cases, the kinetic energy is equal to the potential energy $(KE = PE)$, in stable situations the kinetic energy is less than the potential energy
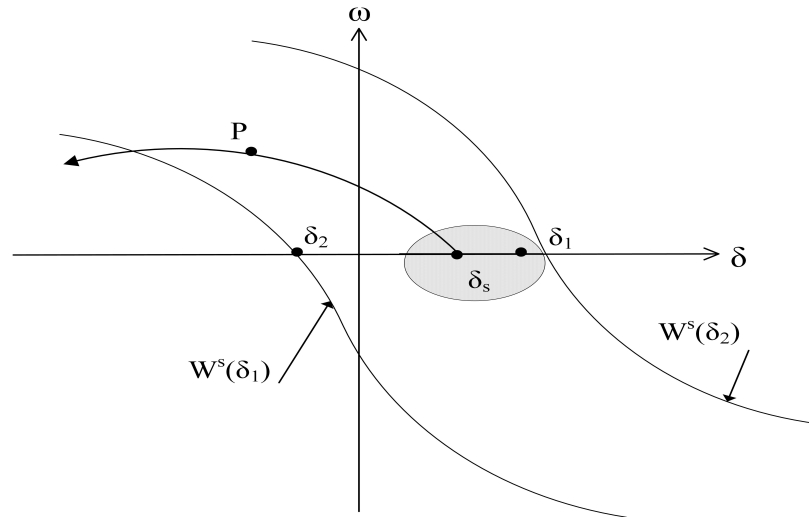
Figure 5.8: The closest UEP method gives considerable conservative stability assessments for those fault-on trajectories crossing the stability boundary through.

$(KE < PE)$, and instability occurs if the kinetic energy is greater than the potential energy $(KE > PE)$ [24, 92]. Following finding the unstable equilibrium point (UEP) via the mentioned methods, KE and PE can be found, and the stability of the system can be determined.

Based on the so far discussions regarding utilizing direct methods for TSA, it can be concluded that the success of direct methods depends upon [15, 33]:

- Determination of the region of stability more accurately, especially identifying the unstable equilibrium point (UEP) relevant to the post-disturbance trajectory.

- Better approximation of the system transient energy.

- Correct identification of the controlling UEP for the disturbance under consideration.

In the next section, it is discussed how to use the system behavior prediction for approximating energy balance in a network and find critical clearing time and angle.

5.6   Predicting Critical Clearing Time and Angles via Energy Balance

One of the interesting applications of using energy functions for transient stability assessment (TSA), is finding the critical clearing time. Finding t_{cr} includes the following steps [14, 84, 97, 112]:

1. Finding the stable equilibrium point (x_s) of the post-fault system.

2. Constructing an energy or Lyapunov function, $V(x)$, for the post-fault system.

3. Finding the critical value of $V(x)$, denoted by V_{cr}, for a given fault.

4. Integrating the faulted system equations until $V(x) = V_{cr}$, and obtaining critical clearing time (t_{cr}) by letting $V(x) = V_{cr}$ on the faulted trajectory.

While the mentioned steps are common in all methods, they differ from one another in finding V_{cr} and integrating the swing equations:

In the controlling UEP method, integration of during-the-fault dynamic equations for a short period of time is done. Then, a minimization problem is solved to get the controlling UEP, (x^u). An alternative approach for the latter is to integrate a reduced-order post-fault system after the PEBS is reached to a maximum of $V(x)$. Next, V_{cr} is calculated by solving $V(x^u) = V_{PE}(x^u)$, since V_{KE} is zero at an UEP. This is known as the BCU method. In the PEBS method, V_{cr} is computed via integrating the faulted trajectory (of during-the-fault dynamic equations) until the potential energy term of $V(x)$ reaches a maximum. This value is considered as critical energy in the PEBS method.

All the mentioned techniques need to be employed offline and are only useful for gaining some qualitative insight about system stability. To overcome this shortcoming, the energy concept combined with the prediction method, proposed in chapter 3, can be used. The importance of the proposed method is that by using two data samples after fault, the critical clearing time and angle can be predicted, and accord-

ingly, the necessary decisions can be made. Following, some discussions about the proposed method followed by case studies are provided.

It was shown in Eq. 5.60 that the change in the kinetic energy is equal to the change in potential energy. Also, it was explained earlier in this chapter that for a system to remain stable after a disturbance, the post-fault system should be able to convert the kinetic energy, gained during the fault, to potential form.

In fact, what determines the stability of the post-disturbance system, is the post-fault potential energy absorbing capacity. In the literature, it is common to calculate the energy gained during the fault with respect to the post-fault stable equilibrium point (SEP). Then, this energy is compared with the energy required to change the state of the post-fault system from SEP to the UEP. However, the post-fault system and its SEP are not usually unknown. As well, in order to use the common methods, it is required to change the reference of the pre-fault steady-state to the post-fault steady-state.

In the technique used in this thesis, the energy gained during the fault with respect to the pre-fault steady-state is compared with the energy required to make the post-fault system convey to its UEP. This, in fact, is inspired by the so-called equal area criterion. To make it more clear, further discussion is provided.

Let us define:

$$A1 = \left\{ PE(\delta^{cl}) - PE(\delta^{s.s.}) \right\}_{During the Fault} \tag{5.63}$$

$$A2 = \left\{ PE(\delta^{cl}) - PE(\delta^{UEP}) \right\}_{Post-Fault} \tag{5.64}$$

Where δ^{cl} is the generator angle at clearing time, δ^{UEP} is the generator angle at Unstable Equilibrium Point(UEP), and $\delta^{s.s.}$ is the generator angle at pre-fault steady-state. In calculating $A1$, the topology of the faulted system should be used for calculating the PE. Similarly, in finding $A2$, the post-fault configuration of the network should be assumed.

5.6.1   An Illustrative Example:

Finding Critical Clearing Time and Angle in a Single Machine - Infinite Bus System

via Energy Balance

Consider the same network, as shown in Fig. 5.9. Suppose that a symmetrical fault happens at $B3$ at $t = 0.1$ seconds. One time step after fault, the electrical output power going out from the generator is known. So, it is possible to find the accelerating power$(P_a = P_m - P_e)$.

Using the proposed method, it is shown how the critical clearing time and angle are found. It has been assumed that the network structure does not change after fault removal. The data from one instance after fault moment is used:

at $t = 0.1^+ sec$:
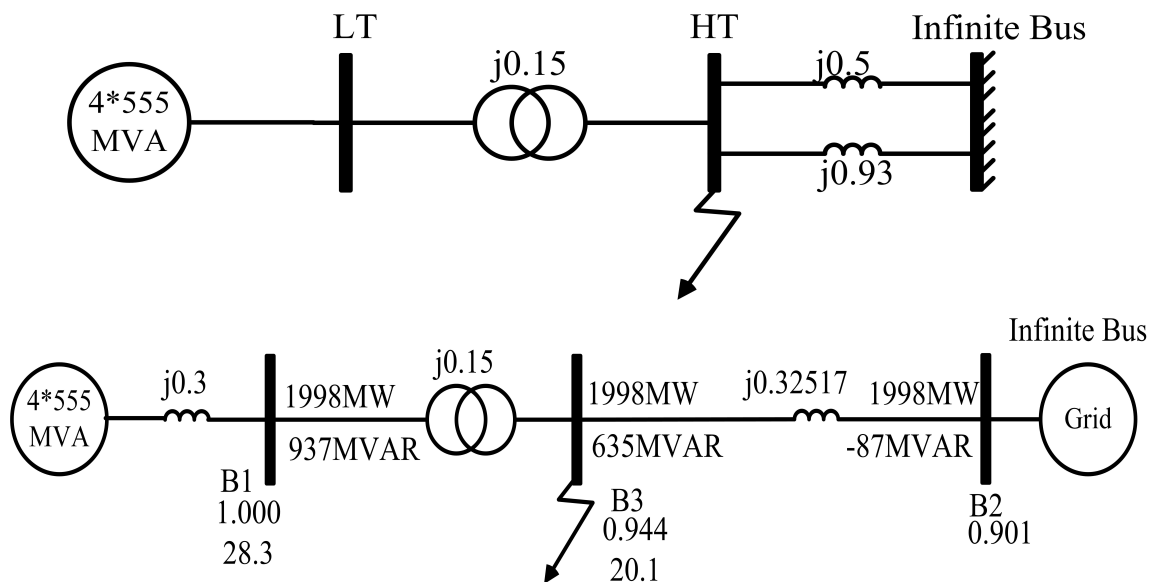
Figure 5.9: SMIB network for an illustrative example of predicting critical clearing time [1].

$Ang_{M1} = 41.77° = 0.72902 radian$

at critical clearing time, or being at critical clearing angle, $A1 = A2$:

$A1 = \left\{ PE(\delta^{cl}) - PE(\delta^{s.s.}) \right\}_{During the Fault} = \frac{1}{2} M \omega^2$

$A2 = \left\{ PE(\delta^{cl}) - PE(\delta^{UEP}) \right\}_{Post-Fault}$

letting $A1 = A2$ we have:

$A1 = A2 \Rightarrow 0.9 * \left\{ \frac{1}{2} * \frac{0.9}{7} * t^2 \right\} * 2 * \pi * 50 + 0.72902 - 1.1658 = \frac{7}{2} \left(\frac{0.9}{7} t^2 \right)$

So:

$\Rightarrow 18.1764 t^2 + 0.72902 - 1.1658 = 0.0579 t^2$

$\Rightarrow t^2 = 0.0241 sec \Rightarrow \Delta t = 0.1552 sec$

$Predicted \ \ Critical \ \ Clearing \ \ Time \ \ (PCCT) = 0.1552 sec$

$Critical \ \ Clearing \ \ Time \ \ from \ \ Simulation = 0.15 sec$

Using PCCT, the critical clearing angle can be predicted:

$\delta_{prediction}^{critical} = \left\{ \frac{1}{2} * \frac{0.9}{7} * (0.1552)^2 \right\} * 100 * \pi + 0.72902 = 1.2155 radian = 69.64°$

$\delta_{FromSimulation}^{critical} = 1.1836 radian = 67.82°$

$\omega_{prediction}^{critical} = \frac{0.9}{7} * 0.1552 = 0.02$

$\omega_{FromSimulation}^{critical} = 0.0193$

Using the equal area criteria for a SMIB system to find the critical clearing angle leads to Eq. 5.65:

$$\delta^{cr} = cos^{-1}(\pi - 2 * \delta^{s.s.}) * sin(\delta^{s.s.}) - cos(\delta^{s.s.}) \tag{5.65}$$

According to Eq.5.65 we have:

$\delta^{critical} = 1.1858 \ radian = 67.9386°$

$\delta_{From \ Simulation}^{critical} = 1.1836 \ radian = 67.82°$

$\delta_{prediction}^{critical}(if \ UEP = \pi - \delta^{s.s.}) = 1.2460 \ radian = 71.3927°$

$\delta_{prediction}^{critical}(if \ UEP = 132.4895°) = 1.1834 radian = 67.8056°$

Table 5.2 summarize the results for predicting Critical Clearing Time (CCT), Critical Clearing Angle (CCA), and UEP. Considering the numerical errors, the results are accurate. It is important to mention that the $UEP = 134.12°$ from simulation is different from $(\pi - \delta^{s.s.}) = 180 - 41.77 = 138.23°$, which shows the importance of finding the right exit-point (of the trajectory of the fault-on equation), or at least the

Table 5.2: Critical clearing time and angle of the SMIB used in the illustrative example of predictine clearing time and angle.

UEP_Simulated(Degree)	134.12
UEP_Predicted(Degree)	134.01
CCA_Simulated(Degree)	67.8056
CCA_Predicted(Degree)	67.82
CCT_Simulated(Time(s))	.25
CCT_Predicted(Time(s))	.2552

closest UEP to the exit-point. Figure 5.10 shows the steps of using predicted energy

for finding critical clearing time and angle.
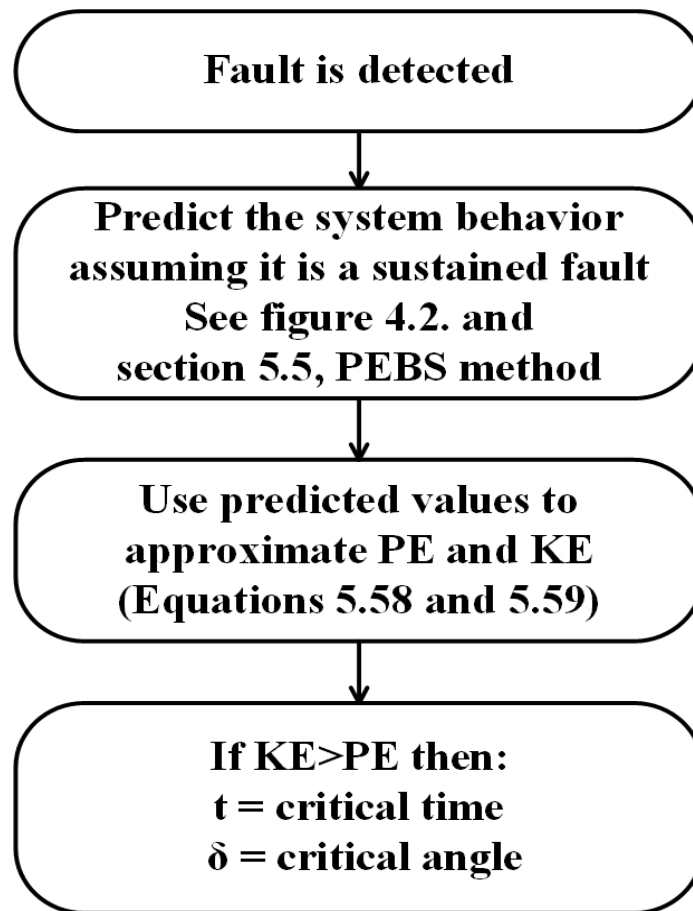
Figure 5.10: Flowchart showing the steps to use predicted energy for finding critical clearing time and angle.

5.6.2   Prediction Critical Clearing Time in IEEE 39 Bus System via Energy

Balance

In this study, the prediction method, combined with energy function is used to predict the critical clearing times and angles. A sustained fault at bus 16 is applied in order to find the critical values. The system is exactly the same as discussed in chapter 3. It is assumed that we have measurements unit on generator buses and the available data are the rotor angle, rotor speed, and the damping coefficients of each generator. The voltage of generators buses is known, and the voltage of non-generator buses is assumed to be 1 pu. Based on the available data, the related energy terms can be approximated via the following equations to provide us an index about the energy of the system. This approximation is useful because it reduces the calculation and process time and helps a faster response from control since one of the incentives of using energy functions is to have a fast screening tool and index.

$$PR_i = -P_{m_i}\delta_i \tag{5.66}$$

$$P_{Mag_i} = |V_i|\,|V_j|\,|Y_{ij}|\,sin\Theta_{ij}cos(\delta_i) \tag{5.67}$$

$$P_{Loss_i} = -D_i w_i^2 \Delta t \tag{5.68}$$

Using equations (5.66) to (5.68) the potential and kinetic energy of each generator is calculated. The summation of the kinetic and potential energy of all generators is considered as an approximation energy representative of the system's kinetic and potential energy. Table 5.3 and figures 5.11 to 5.16 provide the results.
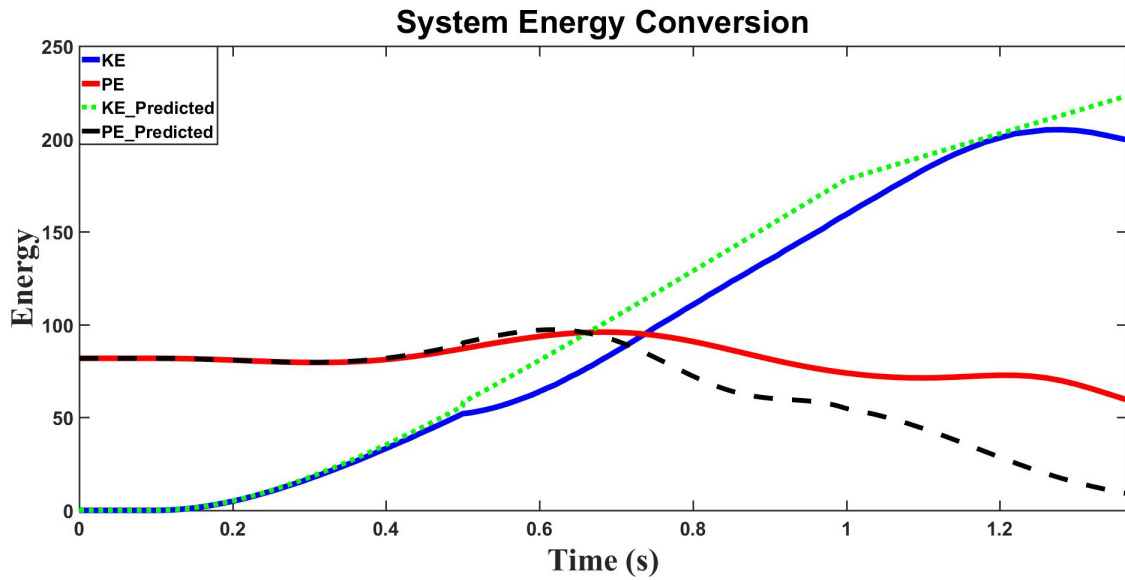
Figure 5.11: Energy conversion in generators of IEEE 39 bus system - Fault on bus 16.

Table 5.3: Generator critical energies for a three phase fault on bus 16 in IEEE 39 bus system.

Machine	Simulation				Prediction			
	PE	KE	CCT	CCA	PE	KE	CCT	CCA
G4	3.04	3.338	0.29	34.15	3.028	3.541	0.29	36.70
G5	2.403	2.511	0.3	33.3	2.407	2.452	0.3	34.9619
G7	3.32	3.609	0.32	31.8	3.3	3.834	0.32	34.59
G6	4.569	4.721	0.33	27.39	4.574	4.593	0.33	29.34
G9	3.763	3.864	0.47	38.99	3.892	4.165	0.43	37.76
G3	5.879	5.977	0.76	9.41	-	-	-	-
G2	6.018	6.076	0.81	N/A	6.018	6.061	0.96	N/A
G1	-	-	-	-	-	-	-	-
G8	-	-	-	-	-	-	-	-
G10	-	-	-	-	8.102	8.16	0.91	-49.55
System	94.78	95.64	0.737	-	94.88	97.38	0.67	-
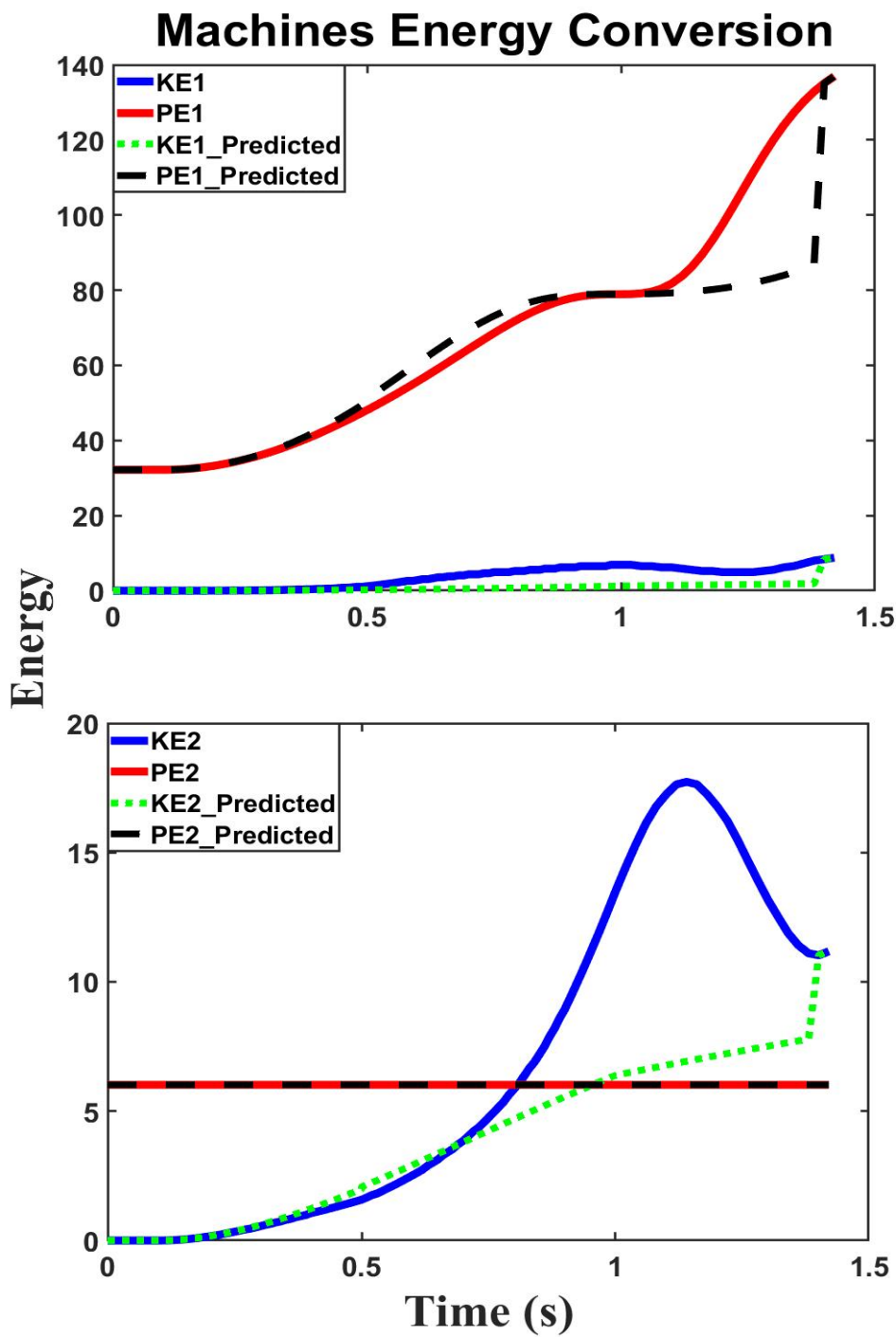
Figure 5.12: Energy conversion in G1 and G2 - IEEE 39 bus - Fault on bus 16.
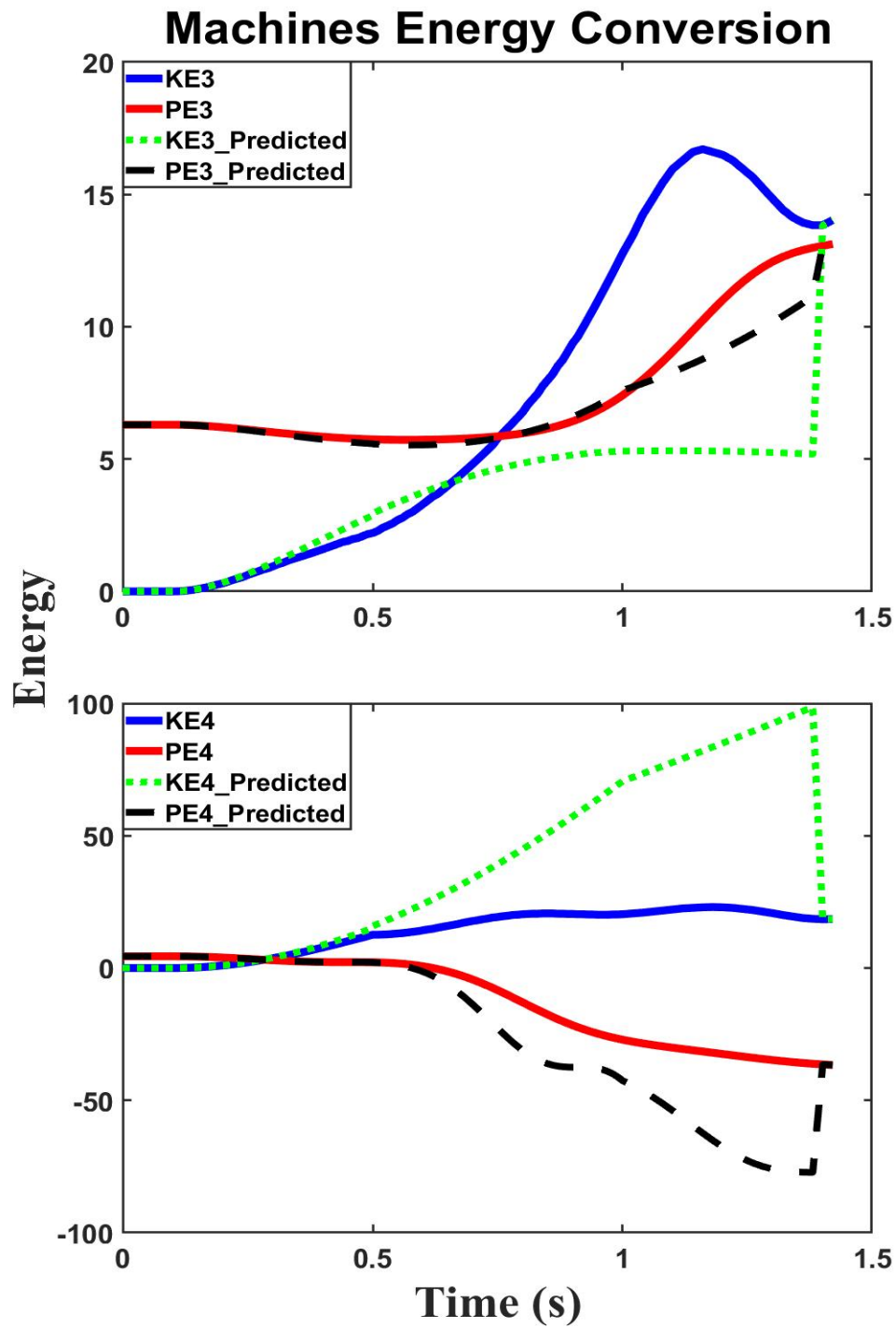
Figure 5.13: Energy conversion in G3 and G4 - IEEE 39 bus - Fault on bus 16.
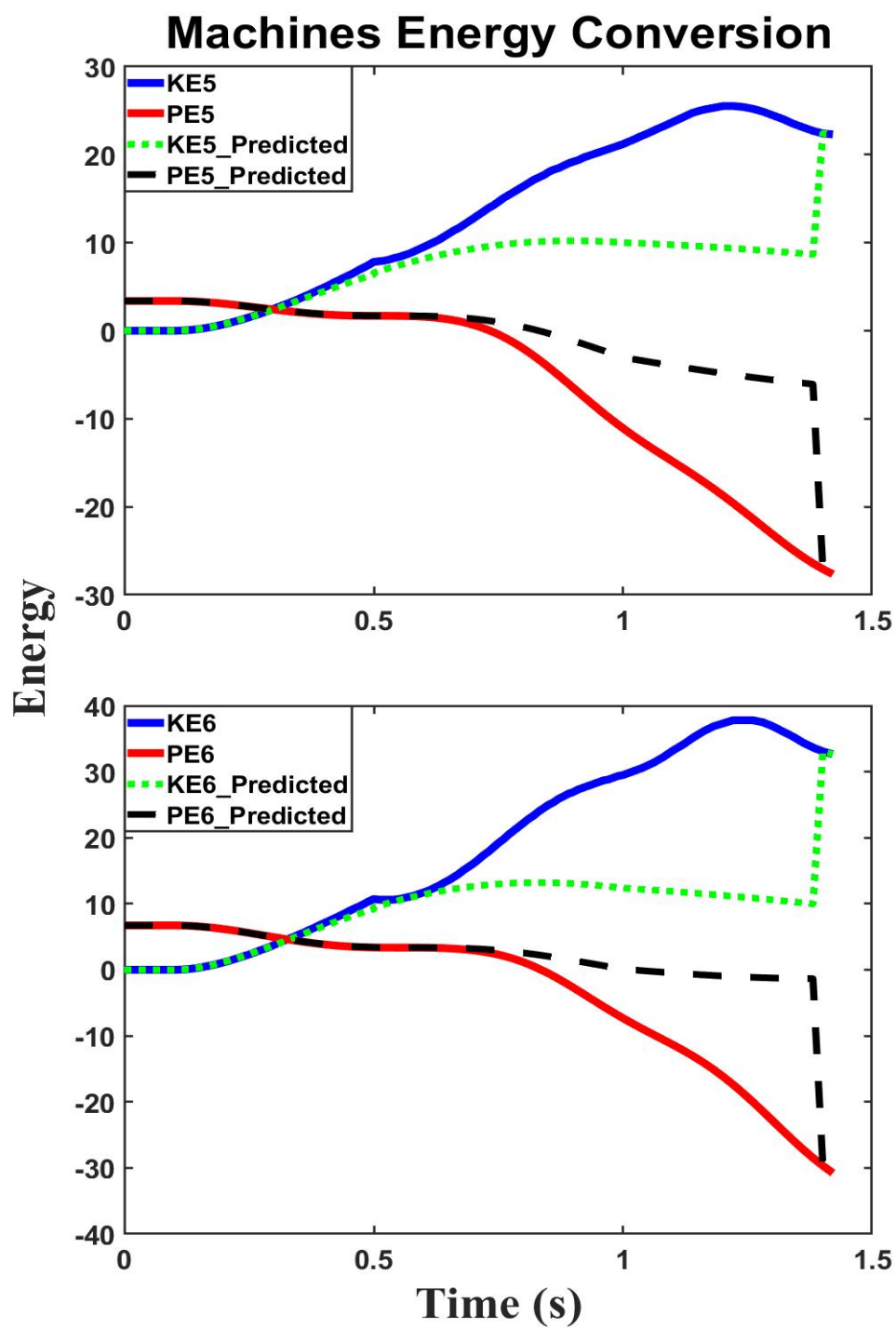
Figure 5.14: Energy conversion in G5 and G6 - IEEE 39 bus - Fault on Bus 16.
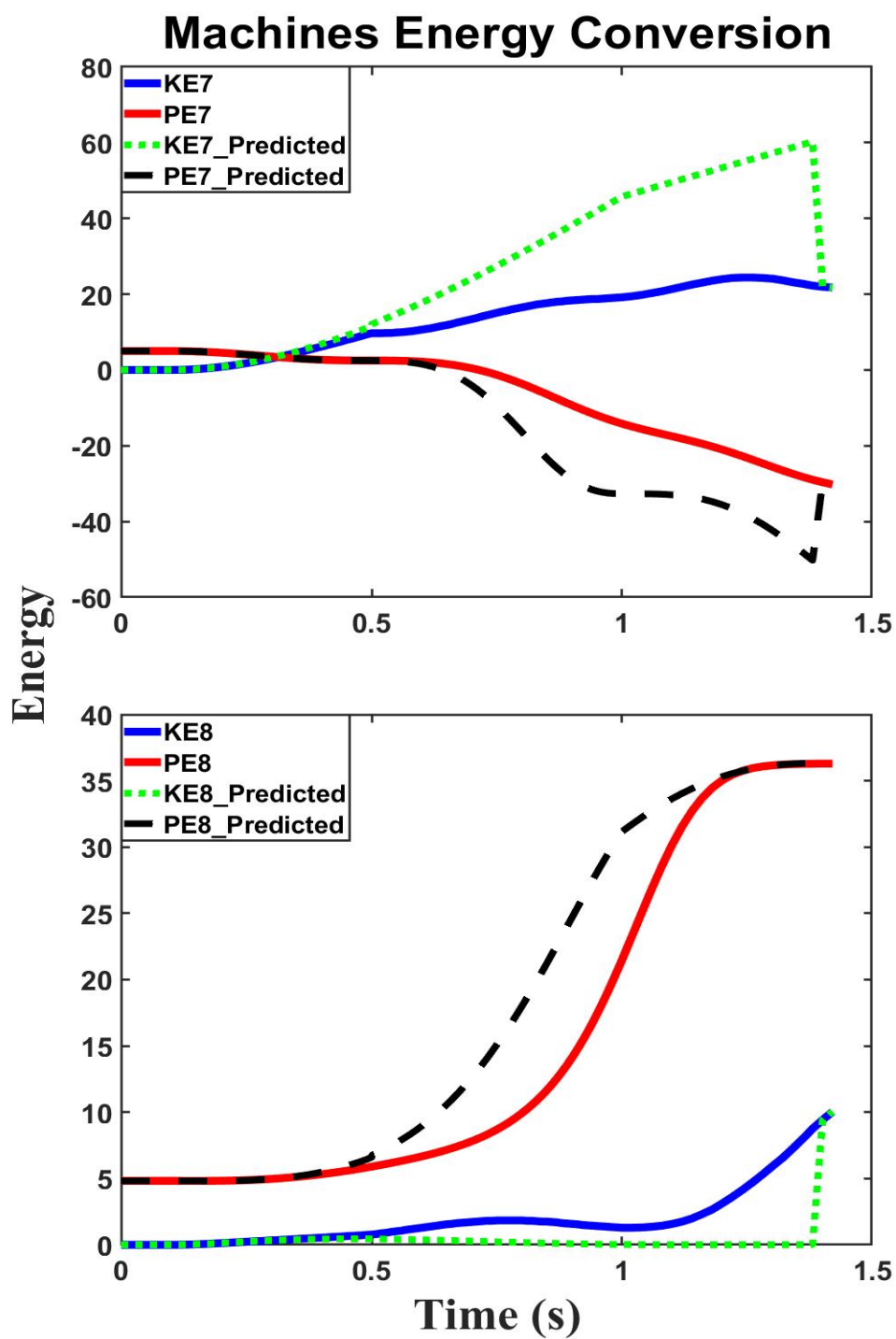
Figure 5.15: Energy conversion in G7 and G8 - IEEE 39 bus - Fault on bus 16.
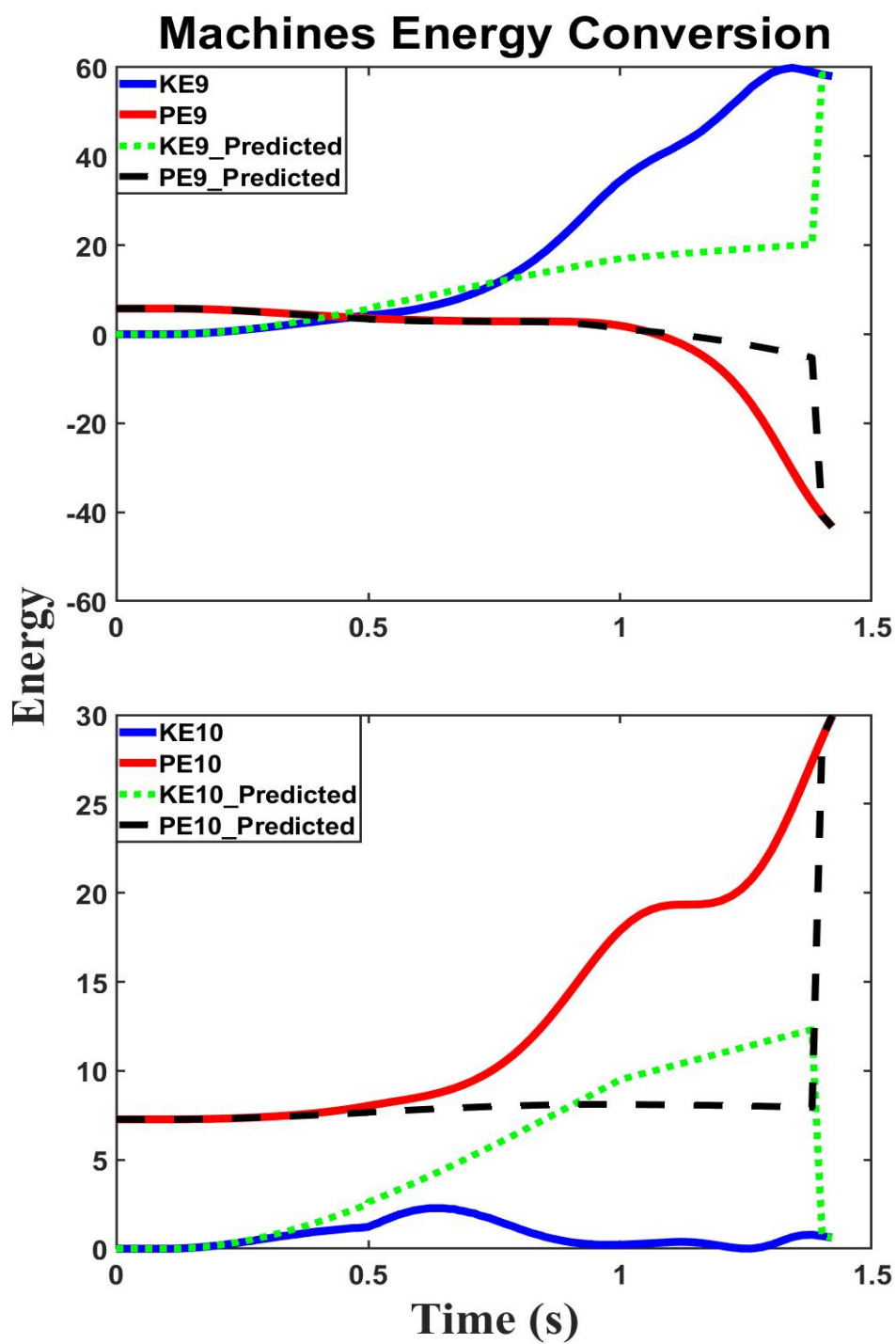
Figure 5.16: Energy conversion in G9 and G10 - IEEE 39 Bus - Fault on Bus 16.

5.7   Summary

In this chapter, the energy balance in reduced and non-reduced power systems was explained, and related mathematical equations were obtained. The effect of line resistances was explained, and an illustrative example was provided to make the energy balance concept more clear. Also, the definition and interpretation of each term of the energy balance equation were presented. In addition, the energy conversion in a multi-machine system, and the concept of fault trajectory, an unstable equilibrium point followed by the behavior of the potential energy of a power system was discussed. It was mentioned that the potential energy reaches a maximum when a disturbance happens. It was also expressed that the maximum of the potential energy does not depend on the fault duration. In the next chapter, the prediction method discussed in chapter 3, combined with the energy concept is used to predict the stability of a power system and take necessary control actions.

CHAPTER 6: Online Prediction-Based System Stability Assessment and

Enhancement

Energy supply without interruption is a must in power systems and one of the major expectations of customers. Several studies in planning, operating, and controlling fields endeavor directly to meet such an expectation in spite of frequent changes in operating conditions and load variations. In addition, a more accurate prediction and control of the behavior of modern interconnected power systems is an important issue due to the significant economic impacts and security consequences that might happen in case of a failure in power systems [69]. Natural or human-made causes such as adverse weather conditions, floods, trees connection to the power network, improper maintenance of electric components, and improper management of power systems are some of the reasons for this issue [6, 113].

6.1   Introduction

In chapters 3 and 4, it was discussed how the generators' behavior during a disturbance can be predicted via Taylor series. Hence, the energy of the system can be predicted using the equations obtained in chapter 5. In this chapter, it is explained how the prediction of generators' angle and speed combined with the concept of potential energy can be utilized for improving the transient stability.

6.2   Role of Potential Energy in Power System Transient Stability

Based on the concept of the energy, and with the focus on the potential energy in power systems, which was widely discussed in 5.5, a methodology is proposed to improve the transient stability of the power grid. In this approach, the potential energy absorbing capacity of the network is manipulated by using some pieces of equipment.

For example, potential energy can be increased via VAR injection, which causes an improvement in overall system stability. Finding an energy function, according to discussions in chapter 5, led to Eq. 5.26. So, for a lossy system, energy balance equation is presented again in Eq. 6.1:

$$\sum_{i=1}^{n} \frac{1}{2} M_i \omega_i^2 \big]_{\omega_i^a}^{\omega_i^b} = \sum_{i=1}^{n} (P_{m_i} - |V_i^2| G_{ii}) \delta_i \big]_{\delta_i^a}^{\delta_i^b} + \sum_{i=1}^{n-1} \sum_{j=i+1}^{n} C_{ij} cos\delta_{ij} \big]_{\delta_{ij}^a}^{\delta_{ij}^b}$$

$$- \int_a^b \sum_{i=1}^{n-1} \sum_{j=i+1}^{n} D_{ij} cos\delta_{ij} \mathrm{d}(\delta_i + \delta_j) - \int_a^b \sum_{i=1}^{n} D_i (\frac{\mathrm{d}\delta_i}{\mathrm{d}t})^2 dt - \int_a^b \sum_{i=1}^{n} \sum_{j=n+1}^{2n+m} C_{ij} sin\delta_{ij} \mathrm{d}\delta_i$$

$$- \int_a^b \sum_{i=1}^{n} \sum_{j=n+1}^{2n+m} D_{ij} cos\delta_{ij} \mathrm{d}\delta_i \tag{6.1}$$

Equation 6.1 can be rephrased as equation 6.2 for lossy systems, and rephrased as Eq. 6.3 for loss-less systems.

$$\sum_{i=1}^{n} \frac{1}{2} M_i \omega_i^2 \big]_{\omega_i^a}^{\omega_i^b} = \sum_{i=1}^{n} (P_{m_i} - |V_i^2| G_{ii}) \delta_i \big]_{\delta_i^a}^{\delta_i^b}$$

$$- \int_a^b \sum_{i=1}^{n} \sum_{j=1, j\neq i}^{2n+m} |V_i| |V_j| |Y_{ij}| cos(\Theta_{ij} - \delta_{ij}) \mathrm{d}\delta_i - \int_a^b \sum_{i=1}^{n} D_i (\frac{\mathrm{d}\delta_i}{\mathrm{d}t})^2 dt \tag{6.2}$$

$$\sum_{i=1}^{n} \frac{1}{2} M_i \omega_i^2 \big]_{\omega_i^a}^{\omega_i^b} = \sum_{i=1}^{n} (P_{m_i} - |V_i^2| G_{ii}) \delta_i \big]_{\delta_i^a}^{\delta_i^b} + \sum_{i=1}^{n-1} \sum_{j=i+1}^{n} C_{ij} cos\delta_{ij} \big]_{\delta_{ij}^a}^{\delta_{ij}^b}$$

$$- \int_a^b \sum_{i=1}^{n} \sum_{j=n+1}^{2n+m} C_{ij} sin\delta_{ij} \mathrm{d}\delta_i - \int_a^b \sum_{i=1}^{n} D_i (\frac{\mathrm{d}\delta_i}{\mathrm{d}t})^2 dt \tag{6.3}$$

As it was discussed earlier in this chapter , the kinetic energy stored in the rotor of each generator at its current state is defined as:

$$KE_i = \frac{1}{2} M_i \omega_i^2 \tag{6.4}$$

Hence, the total kinetic energy of the system generators would be:

$$KE^{Total} = \sum_{i=1}^{n} \frac{1}{2} M \omega_i^2 \qquad (6.5)$$

The total potential energy was derived as shown in Eq. 6.6,

$$PE^{Total} = P_r^{Total} + P_{Mag}^{Total} + P_{Loss}^{Total} \qquad (6.6)$$

where,

$$P_r^{Total} = \sum_{i=1}^{n} (P_{m_i} - \left|V_i^2\right| G_{ii}) \delta_i]_{\delta_i^a}^{\delta_i^b} = \sum_{i=1}^{n} [(P_{m_i} - \left|V_i^2\right| G_{ii})(\delta_i^b - \delta_i^a)] \qquad (6.7)$$

$$P_{Mag}^{Total} + P_{Loss}^{Total} = -\int_a^b \sum_{i=1}^{n} \sum_{j=1, j\neq i}^{2n+m} |V_i| |V_j| |Y_{ij}| \cos(\Theta_{ij} - \delta_{ij}) \mathrm{d}\delta_i - \int_a^b \sum_{i=1}^{n} D_i (\frac{\mathrm{d}\delta_i}{\mathrm{d}t})^2 dt$$
$$(6.8)$$

In a Loss-less system, the potential energy capacitance of the network consists of two terms, P_r, and P_{Mag}. No part of kinetic energy would be dissipated in the network. Therefore, the PE of the network depends on bus voltages and angles.

In a lossy system, PE consists of three terms, P_r, P_{Mag}, and P_{Loss}. P_{Loss} is a path-dependent term. Hence, there is no explicit way for calculating it. In 5.3, assuming a linear trajectory for the system, an approximation of P_{Loss} was provided, . In the lossy system, the PE of the system depends on the bus voltages and angles to some extent.

It was mentioned that the potential energy varies along the post-disturbance trajectory [15]. If the fault is kept long enough for one machine (or more) to become critically unstable, the potential energy of the critical machine goes through a maximum before the system goes unstable (Figure 6.1). In addition, this maximum value (of the potential energy along the post-disturbance trajectory) of a given machine is

essentially independent of the duration of the disturbance. This value of potential energy represents the energy absorbing capacity of the network, which is equal to V_{cr}.
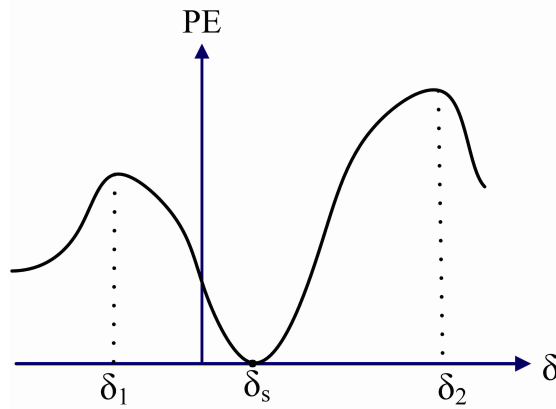
Figure 6.1: The potential energy function is only a function of δ and reaches its local maximum at UEPs $\delta 1$ and $\delta 2$.

6.2.1 Potential Energy Before and During the Fault

At steady-state, the system is settled at its Stable Equilibrium point (SEP). This is the point that PE of the system is at its minimum. To achieve this value, load-flow results of the system are used, and the potential energy is calculated.

Also, it has been proven that the KE of a system is at the lowest value [24]. During a fault, the KE gained by the rotors makes generator angles increase, which in turn change bus angles. Since the rotor energy depends on generator angles, the PE of the rotors increases. At the same time, the increase in angles makes the magnetic energy decrease, as it depends on the cosine of the angles.

6.2.2 Potential Energy after Fault Removal

When the fault is removed, a sudden change happens in the value of PE of the system, due to the immediate change that happens in the bus voltages and angles. The value of PE at the very moment of fault removal depends on the fault duration. Also, the increase in the generators angles continues, because the rotors still have

positive speed although with negative acceleration. It causes P_r to continue increasing. At the same time, the magnetic energy of network branches will decrease despite the voltage increase in the network. The reason is that the angles and corresponding cosines are increasing and decreasing, respectively. The increase in P_r and decrease in P_{Mag} continue until the speed deviation of the machines changes its direction, which happens simultaneously with a change in the direction of the magnetic energy. Therefore, it can be concluded that the magnetic energy reaches a minimum after the fault. From now on, the stability of the system depends mostly on the energy conversion between P_r and P_{Mag}. If the P_{Mag} goes lower than a certain limit, which means P_r is crossing an upper limit, the system will lose synchronism. Crossing the noted limits means the difference between some of the angles of buses and machines are so high that they are out of synchronism. Hence, by controlling the amount of PE at this moment, the stability of the system can be controlled. More discussion about the application of the potential energy manipulation is provided in chapter 6. Figure 6.2 shows a comparison between potential energy of a 9 bus system in critically stable and critically unstable cases.
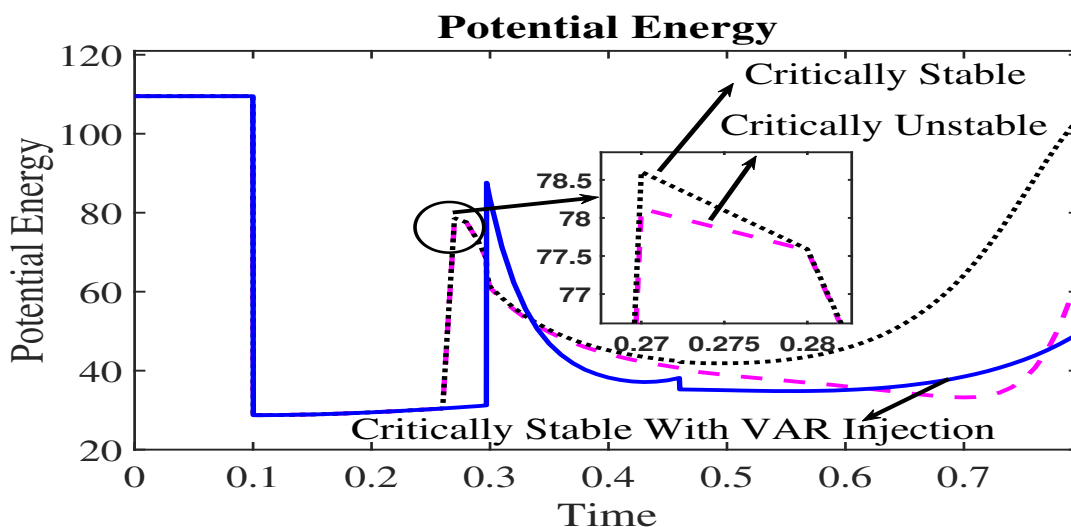
Figure 6.2: Potential energy comparison in a critically stable and a critically unstable system.

6.3   Utilizing Potential Energy for Transient Stability Improvement

According to discussions above, and the basic concepts discussed in chapter 5.5, if a system has a larger capacity to absorb the KE gained by generators during the fault, and can convert it to PE, that system is more stable against sudden changes. From the aforementioned analysis, it can be concluded that the system should be capable of absorbing the extra energy of rotors in order to remain stable. Hence, each system has a maximum of PE absorbing capacity, which depends on its SEP. The SEP depends on the configuration and initial condition of the post-fault network. For a system to be able to reach its maximum absorbing capacity, the deviation from the SEP should not be more than a certain value that is determined by PE.

The lower limit of the PE depends on the cosine of the bus angles and the voltage of buses. The angles are dictated by swing equations. Thus, to extend the limits of P_{Mag} and make the system more stable sudden voltage change can be employed. By increasing the voltages, P_{Mag} would increase according to Eq. 6.8. Consequently, the PE capacity of the network will increase, which helps the system become more stable. Using this method, the post-fault can absorb more KE injected into the grid during the fault, which in turn leads to a more stable post-fault network.

The amount of VAR that can be increased to raise the PE, and bus voltages, is limited. A huge amount of VAR injection to the grid can cause the generators to work in under-excitation mode, which can damage generators. Also, it will make such an increase in the voltage of buses that will endanger devices. Finally, a huge injection of reactive power increases the PE in a way that the system not only absorbs the extra KE gained during the fault but can also cause more KE absorption from the rotors, because the higher voltage causes an increase in voltage-dependent loads. This, in turn, brings about a decrease in generator speed, which can make the system lose its synchronism. Therefore, it is necessary to reduce the injected VAR as time passes after fault removal. Fig.6.3 depicts the flow-chart of the proposed method.

The maximum amount of VAR that can be injected to the grid without encountering the aforementioned problem, is equal to the amount of VAR that the system was generating before the fault happens when the voltages of the faulted systems are considered. The minimum amount of VAR required to improve the transient stability can be obtained by considering that the VAR source should supply the reactive loss of the pre-fault network.

$$Q_{min} = \frac{V_{BeforeFault}^2}{Q_{NetworkLoss}} < Q < Q_{max} = \frac{V_{Faulted}^2}{Q_{BeforeFault}} \tag{6.9}$$

To inject the reactive power equal to Q, the required lead impedance can be found using Eq. 6.10.

$$Q = \frac{|V_i|^2}{|Z_c|} \tag{6.10}$$

If Q is directly injected to the bus i, the new voltage of the bus i and other buses can be obtained using Eqs. (6.11)and (6.12) respectively.

$$V_i^{new} = \frac{V_i Z_c}{Z_{ii} + Z_c} \tag{6.11}$$

$$V_j^{new} = V_j - Z_{ij} * \frac{V_i}{Z_{ii} + Z_c} \tag{6.12}$$

where Z_{ii} is the Thevenin impedance seen from the bus i and Z_{ij} is the transfer impedance between buses i and j.

If we separate the real and imaginary parts of voltages and impedance as shown in equations (6.13), and (6.14), new voltages after VAR injection can be calculated using (6.15) and (6.16).

$$V_k < \delta_k = V_k^R + iV_k^I \tag{6.13}$$

$$Z_{ij} = R_{ij} + iX_{ij} \tag{6.14}$$

$$V_i^{new} = \frac{(V_i^I - iV_i^R)\sqrt{(V_i^I)^2 + (V_i^R)^2}}{Q * R_{ii} + i(Q * X_{ii} - |V_i|^2)} \tag{6.15}$$
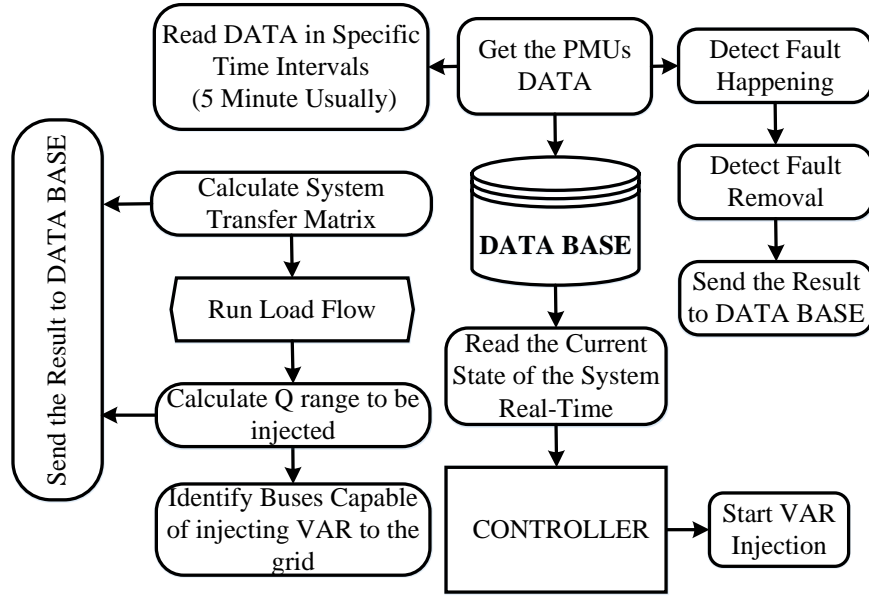
Figure 6.3: Proposed method flowchart for potential energy control.

$$V_j^{new} = \frac{(QR_{ii}V_j^R - V_j^I(QX_{ii} - |V_i|^2) - QR_{ij}V_i^R + QX_{ij}V_i^I)}{Q * R_{ii} + i(Q * X_{ii} - |V_i|^2)}$$

$$+i\frac{(QR_{ij}V_j^I + QX_{ii}V_j^R - V_j^R|V_i|^2 - QX_{ij}V_i^R - QR_{ij}V_i^I)}{Q * R_{ii} + i(Q * X_{ii} - |V_i|^2)} \tag{6.16}$$

Substituting new voltages in Eq. (6.8) delivers the new PE. It should be noted that the new energy can be used for calculating the required Q for a specific amount of PE change.

6.3.1 Case Study: Potential Energy Control for Improving IEEE 9 Bus System Stability

The proposed method is tested on IEEE 9 bus system. A three-phase symmetrical fault is applied on Bus 7 at $t = 0.1$ seconds. Without a voltage increase in the post-fault system, the critical clearing time obtained by numerical time-domain simulation is 0.158 seconds. Figures 6.6 and 6.7 present generator angles and bus voltages.

To illustrate the concept, a capacitor with 0.08 P.U susceptance, is placed at Bus 2 to increase the bus voltage. Time simulation shows if the capacitor is switched in at the moment of fault removal, the system can be survived from loss of synchronism for

a fault duration up to 0.31 seconds, which means the voltage increase has raised the critical clearing time from 0.158 seconds to 0.31 seconds. Figures 6.8 and 6.9 show the generator angles and bus voltages for this study. In order to avoid the rise in voltages and voltage-dependent loads, the capacitor is switched out at 0.4 seconds. Figure 6.10 shows the PE at the critically stable, critically unstable, and the critically stable system when the VAR is injected to bus 2 at the moment of fault removal. Tables 6.1 to 6.5 represent a comparison between different values of voltages and angles of system buses.
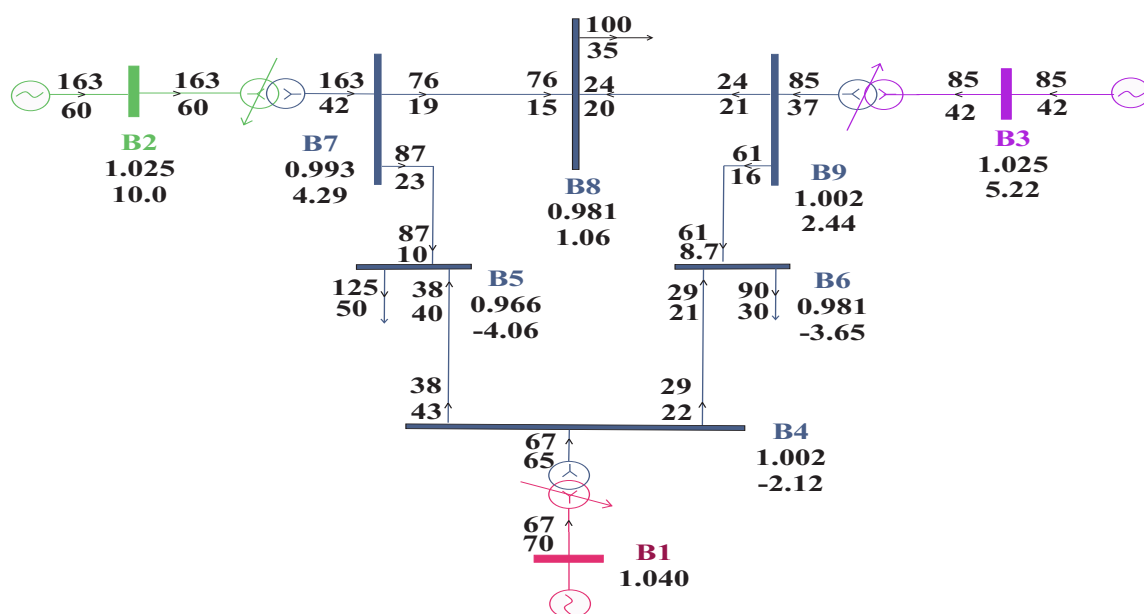
Figure 6.4: IEEE 9 bus system one-line diagram and its load flow result.

The capacitor is placed at different buses and the critical clearing time is found by numerical simulation. In all cases, the fault location is the same. The results are presented in table 6.6.
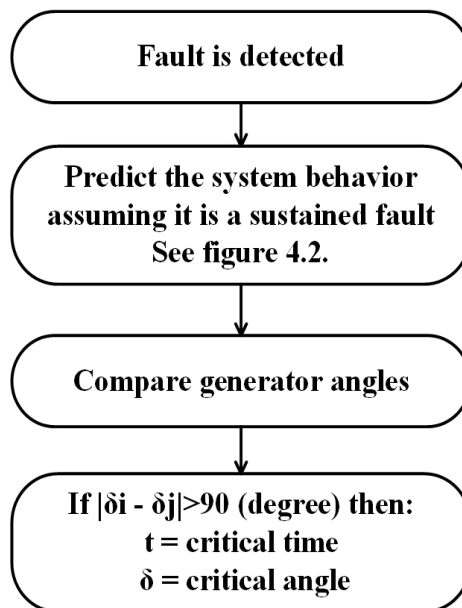
Figure 6.5: Flowchart showing the steps to use predicted angles for finding critical clearing time and angle.
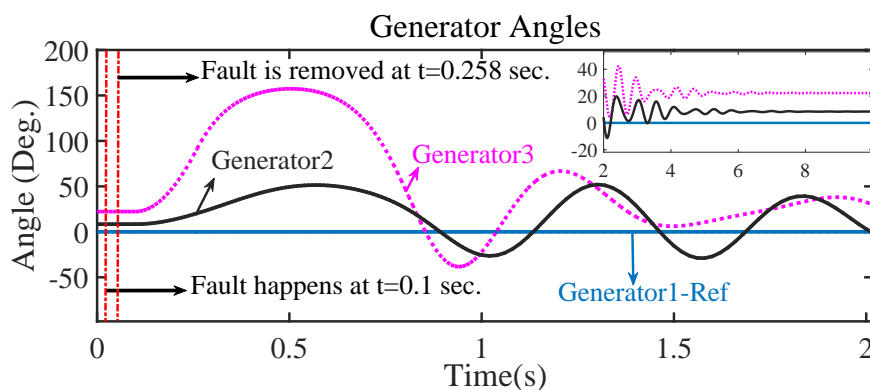
Figure 6.6: Generators 2 and 3 angles without potential energy increase - Fault on bus 2 - IEEE 9 bus system.
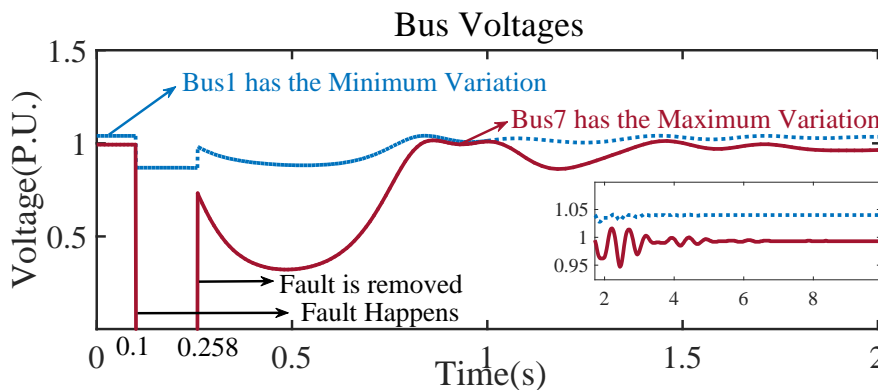
Figure 6.7: Bus1 and bus 7 Voltages without potential energy increase - Fault on bus 2 - IEEE 9 bus system.
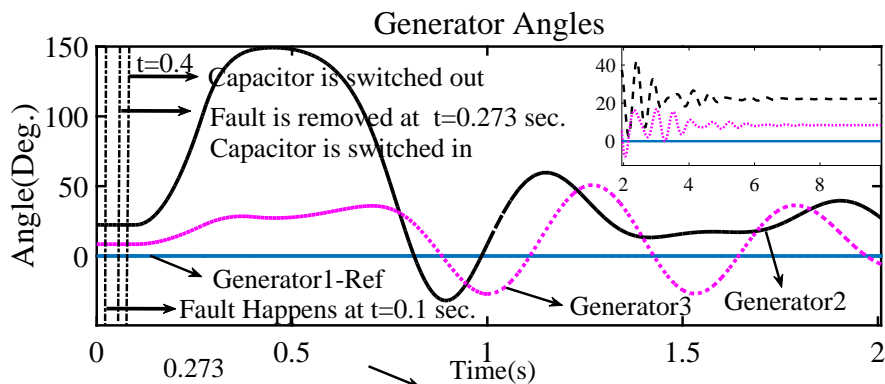
Figure 6.8: Generators 2 and 3 angles with potential energy increase - Fault on bus 2 - Capacitor switched in at fault removal - IEEE 9 bus system.
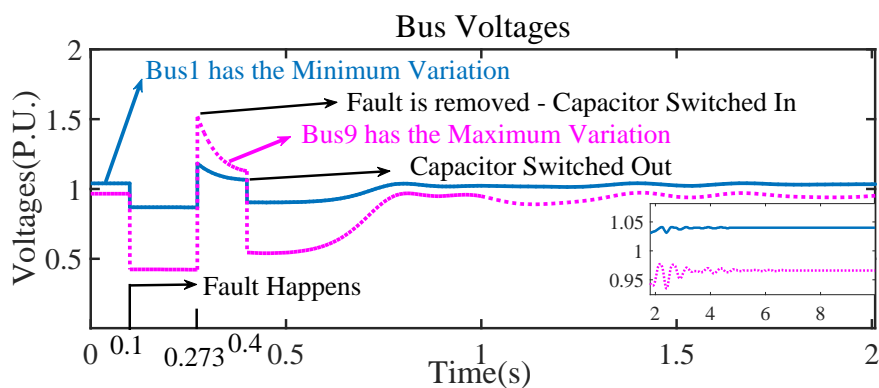
Figure 6.9: Bus1 and bus 9 Voltages with potential energy increase - Fault on bus 2 - Capacitor switched in at fault removal - IEEE 9 bus system.

Table 6.1: Steady State Voltages - Fault on bus 2 - IEEE 9 bus system.

Steady State Voltage (P.U.)			
Pre-Fault		Post-Fault	
Bus	Voltage	Without Proposed Method	With Proposed Method
Bus1	1.0400	1.0400	1.0400
Bus2	1.0250	1.0250	1.0250
Bus3	1.0250	1.0250	1.0250
Bus4	1.0020	1.0020	1.0020
Bus5	0.9660	0.9660	0.9660
Bus6	0.9810	0.9810	0.9810
Bus7	0.9930	0.9930	0.9930
Bus8	0.9810	0.9810	0.9810
Bus9	1.0020	1.0020	1.0020
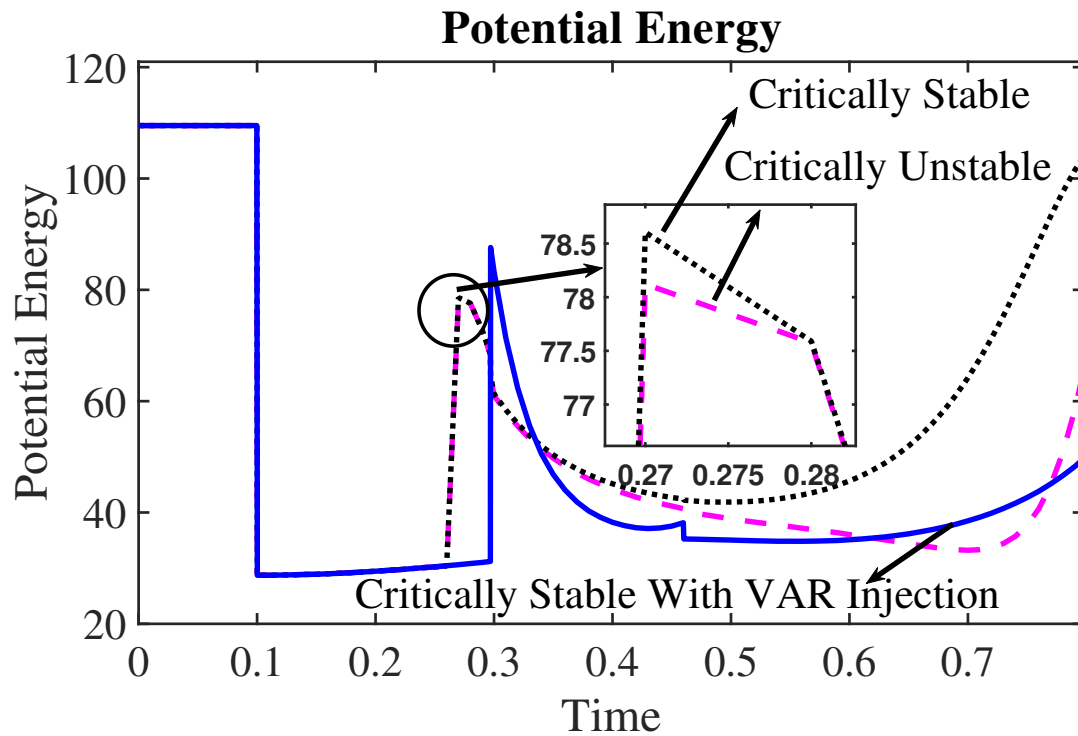
Potential Energy

Figure 6.10: Potential energy comparison - Fault on bus 2 - IEEE 9 bus system.

Table 6.2: Post-fault voltage extremum - Fault on bus 2 - IEEE 9 bus system.

Post Fault Voltage Peak (P.U.)				
	Without Proposed Method		With Proposed Method	
Busbars	Minimum	Maximum	Minimum	Maximum
Bus1	0.8680	1.0410	0.8680	1.1820
Bus2	0.2990	1.0540	0.2990	1.0530
Bus3	0.7190	1.0340	0.7180	1.0500
Bus4	0.6660	1.0060	0.6650	1.2770
Bus5	0.4220	0.9770	0.4220	1.5200
Bus6	0.6080	0.9870	0.6060	1.1650
Bus7	0	1.0160	0	1.0170
Bus8	0.2240	0.9990	0.2230	0.9990
Bus9	0.5460	1.0140	0.5450	1.0410

Table 6.3: Critical clearing time (mili-seconds) - Fault on bus 2 - IEEE 9 bus system.

Critical Clearing Time	
Without Proposed Method	With Proposed Method
158	173

Table 6.4: Steady state angles (Degree) - Fault on bus 2 - IEEE 9 bus system.

Steady State Angles (Degree)			
*Angles are with respect to synchronous frame		Post-Fault	
Pre - Fault		Without proposed method	With proposed method
Busbars	Steady State	Steady State	Steady State
Bus1	0	-138.7200	73.6100
Bus2	10.0400	-128.6900	83.6300
Bus3	5.2200	-133.5100	78.8300
Bus4	-2.1200	-140.8400	71.4900
Bus5	-4.0600	-142.7800	69.5500
Bus6	-3.6500	-142.3800	69.9500
Bus7	4.2900	-134.4300	77.8900
Bus8	1.0600	-137.6700	74.6600
Bus9	2.4400	-136.2800	76.0500
Generator2	22.2600	22.2500	22.2300
Generator3	8.4300	8.4200	8.4200

Table 6.5: Post-fault angles extremum with respect to synchronous frame (Degree) - Fault on bus 2 - IEEE 9 bus system.

Post Fault Angle Peak (Degree)				
	Without Proposed Method		With Proposed Method	
Busbars	Minimum	Maximum	Minimum	Maximum
Bus1	-178.7200	179.5600	-179.7500	176.5100
Bus2	-179.9200	179.4700	-179.3700	176.9300
Bus3	-179.7700	178.4100	-178.8000	179.6300
Bus4	-179.9700	178.4700	-179.5000	177.4700
Bus5	-179.7300	179.8500	-178.8100	178.3300
Bus6	-179.1200	179.9200	-177.9300	179.6100
Bus7	-178.1800	179.4700	-178.6500	178.2000
Bus8	-179.9500	178.3700	-178.9600	178.4700
Bus9	-179.3500	179.3900	-178.5800	179.7600
Generator2	-38.4200	157.3300	-31.9600	149.2000
Generator3	-28.9400	51.9800	-27.3400	50.7400

Table 6.6: Capacitor location effect on critical clearing cime - Fault on bus 2 - IEEE 9 bus system.

Capacitor Location Effect on Critical Clearing Time		
Capacitor Location	Fault Removed - Capacitor Switched In	Capacitor Switched out - Min time to keep the system Stable
No Capacitor	0.258	-
B1	0.264	0.35
B6	0.266	0.32
B4	0.268	0.36
B3	0.276	0.53
B9	0.279	0.45
B8	0.287	0.43
B7	0.292	0.49
B2	0.298	0.46

6.4   Application of Online Prediction of Power System Behavior

So far, it has been discussed how we can use the Taylor series to predict the generators' behavior. By using prediction and assuming that the fault is a sustained fault, generators that lose synchronism can be determined. Based on the obtained results, by manipulating potential energy, preventive actions can be done to prevent loss of synchronism between generators and as a result, the stability margin of the system will be increased. In using the prediction and calculations, a PC has been used with the following feature: CPU: Core i7-3770-3.4GHz, RAM:8GB. The following are the results of the case studies using the proposed technique.

6.4.1   IEEE 39 Bus Prediction and Stability Improvement

The following table shows the short circuit capacity (SCC) of all buses in the IEEE 39 bus system. Bus 39 has the highest SCC level. However, because of its large inertia constant, it is not the most vulnerable bus. The second highest SCC is for bus 16, which makes it experience the most severe transient effect on the grid. Hence, this bus has been chosen to study the system transient behavior. If a three-phase fault happens on bus 16, predicted critical clearing times (CCT) and critical clearing angles (CCA) for system machines are provided in the following tables. The simulation and prediction results are also compared. The fault and the prediction code have been simulated and developed in PASHA and MATLAB, respectively. Elapsed time for predicting the behavior of all generators and related energies is 0.078385 seconds. Since machines 1 and 4 are the first machines tending to lose synchrony with each other, the braking resistor has been switched in at bus 33, which is connected to the machine 4. Fault happens at $t = 0.1$ seconds, and prediction results are available at $t = 0.18$ seconds. The braking resistor is switched in at $t = 0.2$ seconds and switched out at $t = 0.7$ seconds. The fault is not cleared until $t = 0.315$ seconds. Hence, it shows that although the CCT for the original system is 0.285 seconds, being able to

predict the system behavior and taking a simple preventive action, helps saving the system even if the fault is not removed for a longer period than CCT.
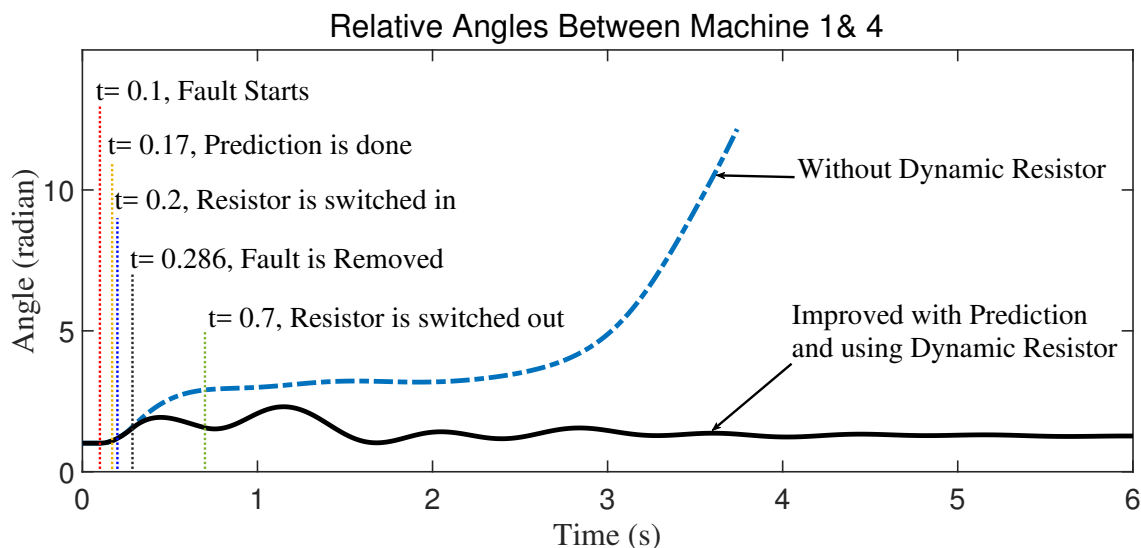
Figure 6.11: Relative angle between generators 4 and 1 - Fault on bus 16 - IEEE 39 bus system.
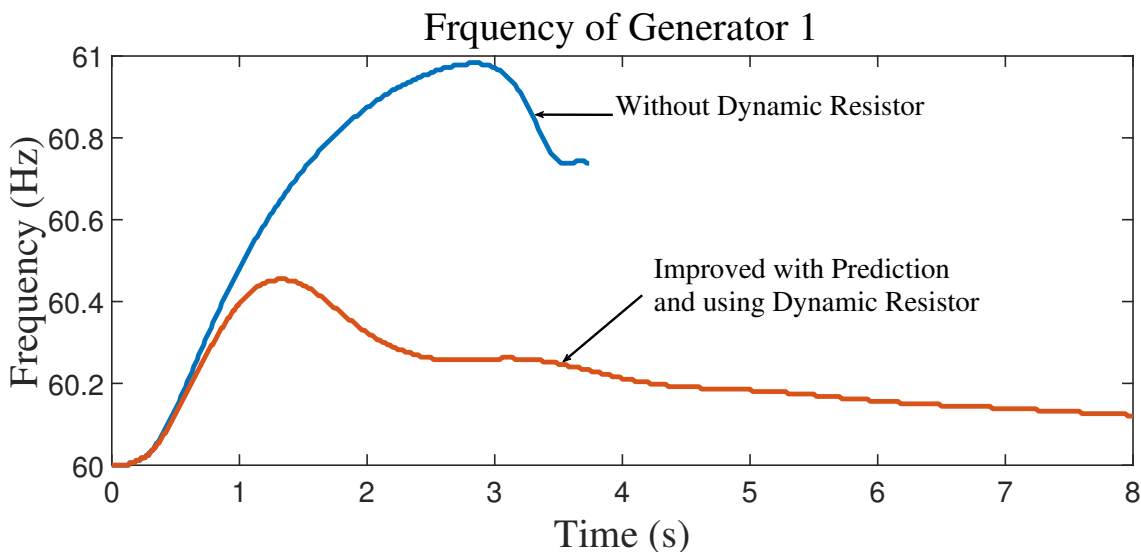
Figure 6.12: Frequency of generator 1 - Fault on bus 16 - IEEE 39 bus system.

6.4.2 North Carolina-South Carolina 500 Bus Synthetic System: Prediction and Stability Improvement

Figure 6.14 shows a schematic of the North Carolina-South Carolina 500 bus synthetic system. More information about synthetic systems is discussed in [107]. To
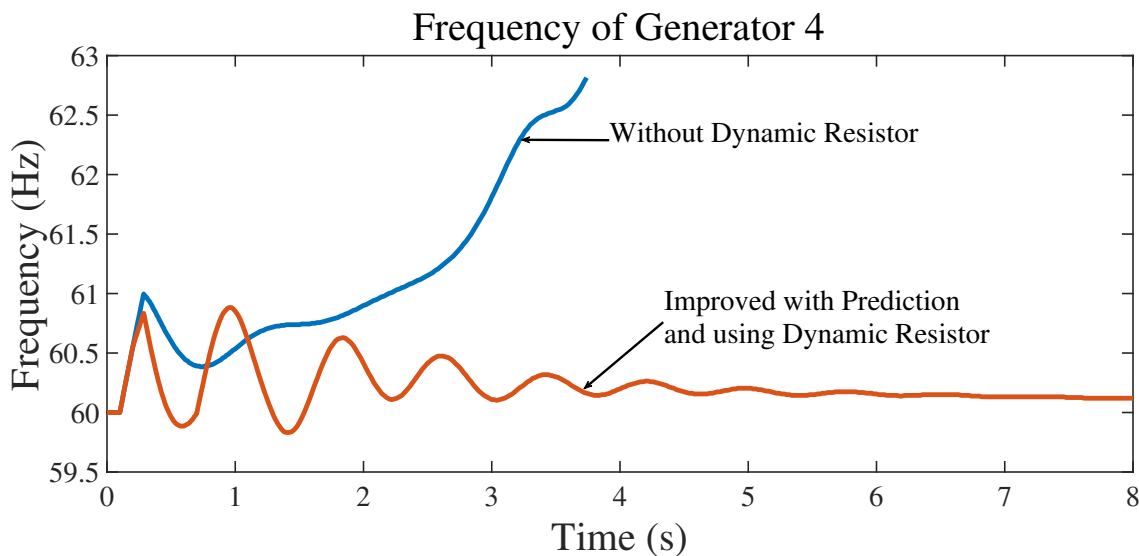
Figure 6.13: Frequency of Generator 4 - Fault on bus 16 - IEEE 39 bus system.

study the efficiency of the system, the results for two case studies are provided. One study is for a three-phase fault on a generator bus, and the other one is for a three-phase fault on a non-generator bus. PSS/E and MATLAB are employed for simulating the system's dynamics and prediction, respectively.

6.4.2.1   Three Phase Fault on Bus 71 of 500 Bus Synthetic System

In this study, a three-phase fault is applied to bus 71. This bus is a generator bus with a voltage of 13.8 kV. Inertia constant for this machine is $H = 2 seconds$. Fault starts at $t = 0.1$ seconds, and for the critically stable case, it must be removed at 0.3078 seconds.
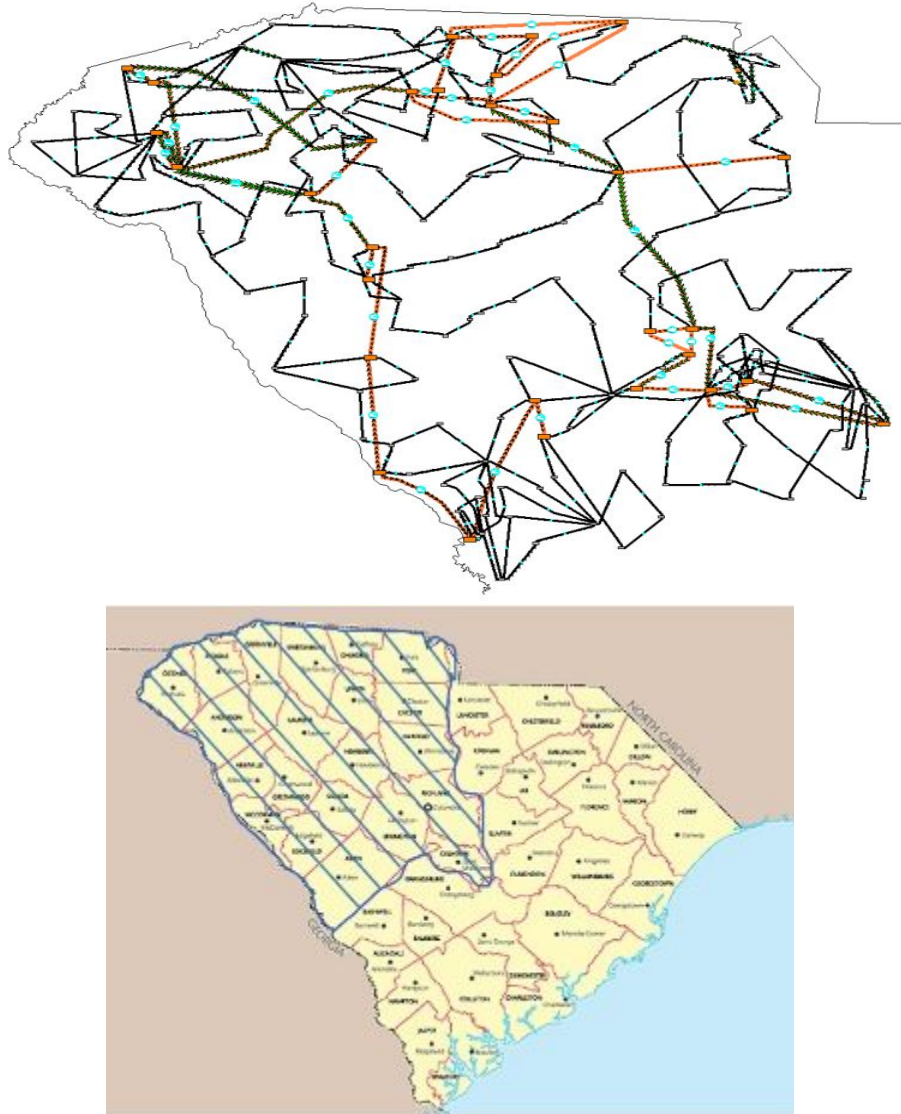
Figure 6.14: North Carolina-South Carolina 500 bus synthetic system

Table 6.7: Short circuit capacity of different buses in IEEE 39 bus system.

Bus Number	SCC (MVA)	Critica Clearing Time (s)
1	5058.9	0.854
2	7577.4	0.280
3	6651.9	0.285
4	6128.7	0.3000
5	6056.2	0.279
6	6148.1	0.267
7	5088.4	0.336
8	5309.8	0.329
9	4852.5	0.782
10	5629.2	0.284
11	5554	0.298
12	2539.1	0.756
13	5415.3	0.308
14	5833.1	0.304
15	5721.3	0.262
16	7613.1	0.185
17	6679.8	0.225
18	5843.3	0.275
19	5119.7	0.174
20	3552.7	0.194
21	5291.6	0.247
22	5504.2	0.229
23	5189.3	0.233
24	5798.5	0.230
25	6137.5	0.231
26	4620	0.165
27	4588.9	0.228
28	2751.5	0.161
29	3139.7	0.134
30	6260.2	0.513
31	3666.9	0.268
32	4143.8	0.278
33	4505.6	0.189
34	2717.6	0.188
35	4684	0.265
36	5027.9	0.247
37	4100	0.309
38	3200.9	0.124
39	19214	0.761

Table 6.8: CCT and CCA for IEEE 39 bus machine - Three phase fault at Bus16.

Machines	Prediction		Machines	Simulation	
	Critical Clearing Angle	Critical Clearing Angle		Critical Clearing Angle	Critical Clearing Angle
1,4	0.2800	-89.1800	1,4	0.2800	-89.8912
1,5	0.2900	-89.5500	1,5	0.2800	-87.1274
1,7	0.3000	-87.1100	1,7	0.2852	-88.1442
1,6	0.3200	-87.6100	1,6	0.3000	-88.5071
4,10	0.3300	87.6600	4,10	0.3100	87.6584
1,9	0.3400	-89.6500	1,9	0.3100	-89.0513
5,10	0.3600	89.2200	5,10	0.3500	89.5624
7,9	0.3700	89.4200	7,9	0.3500	89.2115
6,10	0.4000	89.0600	6,10	0.3900	88.5014
1,3	0.4300	-88.2800	1,3	0.3900	-88.3795
4,8	0.4500	89.5700	4,8	0.4100	85.0587
2,4	0.4500	-88.6400	2,4	0.4200	-86.5300

Table 6.9: Machines that lose syncronism - Three phase fault at bus 16 - IEEE 39 bus machine.

Machines that loose Syncronism	
Predictiom	Simulation
1,4 - 1,5 - 1,7 - 1,6 - 1,9 - 4,10 - 5,10 - 7,9 - 1,3 - 6,10 - 4,8 - 2,4 - 1,2 - 3,4 - 7,8 - 2,7 - 9,10 - 5,8 - 3,7 - 1,8 - 6,7 - 2,5 - 4,9 - 2,6 - 3,5 - 8,9 - 4,6 - 7,9 - 1,10 - 3,6 - (4,5) - (6,7) - (5,7) - 2,9 - 3,9 - 3,8 2,8 - (4,7) - 8,10 - (2,3) - 2,10 - (6,9)	1,4 - 1,5 - 1,7 - 1,6 - 4,10 - 1,9 - 5,10 - 7,9 - 6,10 - 1,3 - 4,8 - 2,4 - 3,4 - 7,8 - 9,10 - 2,7 - 1,2 - 5,8 - 2,5 - 1,8 - 3,7 - 6,8 - 3,5 - 2,6 - 4,9 - 3,6 - 7,9 - 8,9 - (5,9) - (3,10) - 1,10 - 2,9 - 2,10 - 3,9 - 4,6 - 2,8 - 3,8 - 8,10

Table 6.10: CCT and CCA for 500 bus machines - Three phase fault at Bus 71.

Row Number	Machines	Simulation		Prediction	
		Critical Clearing Time (s)	Critical Clearing Angle	Critical Clearing Time (s)	Critical Clearing Angle
1	351,455	0.23333	87.9532	0.23333	87.4267
2	351,456	0.25	89.7537	0.25	89.1773
3	351,413	0.25833	89.9	0.25833	89.3359
4	49,351	0.26667	-87.1025	0.26667	-87.7412
5	50,351	0.26667	-87.3952	0.26667	87.5541
6	73,351	0.26667	-89.5963	0.26667	87.0636
7	258,351	0.26667	-88.0698	0.275	-88.9755
8	351,411	0.26667	87.9568	0.275	-89.1608
9	351,412	0.26667	87.6602	0.275	-87.4438
10	71,351	0.275	-89.14	0.275	88.8385
11	351,410	0.275	89.4133	0.28333	87.0597
12	351,484	0.275	86.7177	0.28333	88.7177
13	350,351	0.28333	-86.7027	0.28333	89.5058
14	351,433	0.28333	87.9994	0.29167	-89.5685
15	351,434	0.28333	89.0702	0.29167	-86.6453
16	351,483	0.28333	86.7593	0.29167	-86.2303
17	72,351	0.29167	-87.1034	0.29167	-86.5609
18	231,351	0.29167	-86.3884	0.29167	-86.2485
19	302,351	0.29167	-86.8245	0.29167	-88.5117
20	306,351	0.29167	-86.4971	0.29167	85.9825
21	351,482	0.29167	86.1137	0.29167	89.3892
22	198,351	0.3	-86.7061	0.3	-86.3611
23	222,351	0.3	-88.3093	0.3	-85.9158
24	223,351	0.3	-86.3503	0.3	-87.2149
25	301,351	0.3	-87.6938	0.3	-89.9029
26	305,351	0.3	-89.7336	0.3	-86.262
27	319,351	0.3	-86.8086	0.3	86.6869
28	351,431	0.3	86.9413	0.3	88.9886
29	351,432	0.3	86.8115	0.30833	-85.7494
30	351,439	0.3	89.621	0.30833	-87.5763
31	16,351	0.30833	-85.9058	0.30833	-87.7579
32	145,351	0.30833	-88.0998	0.30833	-89.641
33	167,351	0.30833	-89.1417	0.30833	87.7425
34	351,430	0.30833	87.6226	0.30833	87.8483
35	351,437	0.30833	86.4005	0.30833	88.0527
36	351,438	0.30833	88.0123	0.31667	-87.2006

Table 6.11: CCT and CCA for 500 bus machines - Three phase fault at Bus 71.

Row Number	Machines	Simulation		Prediction	
		Critical Clearing Time (s)	Critical Clearing Angle	Critical Clearing Time (s)	Critical Clearing Angle
37	351,481	0.30833	86.6439	0.31667	-86.2696
38	351,497	0.30833	88.6557	0.31667	-87.2798
39	9,351	0.31667	-87.319	0.31667	89.5857
40	128,351	0.31667	-86.7644	0.31667	88.7922
41	168,351	0.31667	-86.0466	0.31667	88.7171
42	197,351	0.31667	-87.1645	0.31667	89.8108
43	225,351	0.31667	-87.8556	0.325	-87.4561
44	351,480	0.31667	89.4308	0.325	-87.2792
45	351,498	0.31667	87.9138	0.325	-87.9298
46	17,351	0.325	-86.5357	0.325	-89.2476
47	82,351	0.325	-89.0777	0.325	86.6618
48	169,351	0.325	-88.4051	0.325	89.5739
49	351,352	0.325	88.7113	0.33333	-89.1602
50	351,353	0.325	87.4905	0.33333	-87.2885
51	127,351	0.33333	-87.9095	0.33333	-87.214
52	224,351	0.33333	-88.4914	0.34167	-89.542
53	18,351	0.34167	-89.3861	0.34167	87.9172
54	351,458	0.34167	89.8316	0.34167	89.8537
55	144,351	0.35	-86.8835	0.35	-86.2291

6.5   Summary

In this chapter, the efficiency of the proposed methods and its application was tested on 39 bus and 500 bus systems. The prediction was used to find critical generators, and an appropriate method was employed to enhance the stability of the system and prevent the loss of synchronism.

CHAPTER 7: Conclusion and Future Works

A disturbance in a power system makes generators deviate from their stable oper-
ation states. In severe cases, they may lose synchronism, which leads to a local or
global blackout. Considering the effect of electricity loss on the economy and security
of the nations, it is vital to study the stability of systems. Among all sorts of stability
concerns in a power system, transient stability is the most important one. Hence, in
this research, a new technique for predicting the critical generators, critical clearing
times and angles are proposed. As a result, the transient stability prediction can be
performed, and via an appropriate preventive control strategy, the instability can be
prevented.

7.1 Conclusion Remarks

In this dissertation, the concept and importance of transient stability in power
systems were discussed. In the first two chapters, the dynamic equations of power
systems were explained and different approaches to cope with them were explained.
In chapter 3, a new method for online prediction of generators' behavior in a power
system was proposed. The efficiency of the proposed method was shown by proving
that the error is bounded and the method is convergent. Applying the method on
various networks, from a small single machine - infinite bus to a 500 bus system with
90 generators, which represents the North Carolina - South Carolina power system,
showed that the method is quite reliable and useful for industrial purposes. These
studies are discussed in chapter 4. Next, in chapter 5, the energy conversion in a power
system was discussed. It was mentioned that the potential energy of a system reaches
a maximum value before it goes unstable. Based on this concept, a new approach

for power system transient stability enhancement was introduced. In this approach, the stability of the system was improved by manipulating the potential energy of the system. This can be useful, specifically in cases that some of the energy sources do not have a moving part to use the kinetic energy for controlling the stability of the system. Chapter 6 showed the applications of the proposed methods in transient stability prediction and enhancement.

7.2   Direction For Future works

Continuing research in the area discussed in this dissertation, the followings can be investigated:

- Wind energy and photovoltaic resources are growing fast. With higher penetration of renewable energy resources, the role of inertia dynamics in the power system stability becomes more critical. The reason is that PV does not have inertia. It means that its contribution to the energy balance in the grid should be studied in a new way. It was shown that changes in the kinetic and potential energy are equal. Hence, by defining an appropriate energy function for renewable sources, their effects on a power system stability can be studied more efficiently.

- The energy function equations in a power system are very similar to the elements of the Jacobian and Hessian matrices. There is a great potential that the trend of the energy behavior of a power system can be assessed by studying these matrices.

- Finding a way to formulate the role of each element of the power grid in the dynamics of energy conversion provides a better understanding of direct methods and makes this approach more reliable for industrial applications.

REFERENCES

[1] *Power System Stability And Control.* EPRI power system engineering series, McGraw-Hill, 1994.

[2] H. Saadat, *Power System Analysis.* PSA Publishing, 2010.

[3] A. H. El-abiad and K. Nagappan, "Transient stability regions of multimachine power systems," *IEEE Transactions on Power Apparatus and Systems*, vol. PAS-85, pp. 169–179, Feb 1966.

[4] C. J. Tavora and O. J. M. Smith, "Stability analysis of power systems," *IEEE Transactions on Power Apparatus and Systems*, vol. PAS-91, pp. 1138–1144, May 1972.

[5] R. Yousefian, A. Sahami, and S. Kamalasadan, "Hybrid energy function based real-time optimal wide-area transient stability controller for power system stability," in *2015 IEEE Industry Applications Society Annual Meeting*, pp. 1–8, Oct 2015.

[6] A. Shokrollahi, H. Sangrody, M. Motalleb, M. Rezaeiahari, E. Foruzan, and F. Hassanzadeh, "Reliability assessment of distribution system using fuzzy logic for modelling of transformer and line uncertainties," in *2017 North American Power Symposium (NAPS)*, pp. 1–6, Sept 2017.

[7] Y. Zhang, M. E. Raoufat, and K. Tomsovic, *Remedial Action Schemes and Defense Systems.* John Wiley Sons, Ltd, 2016.

[8] A. Gajduk, M. Todorovski, and L. Kocarev, "Stability of power grids: An overview," *The European Physical Journal Special Topics*, vol. 223, pp. 2387–2409, Oct 2014.

[9] T. G. Magallones, J. G. Singh, and W. Pinthurat, "Small signal stability and transient stability analysis on the philippine-sabah power interconnection," in *2016 International Conference on Cogeneration, Small Power Plants and District Energy (ICUE)*, pp. 1–4, Sept 2016.

[10] J. K. Robinson, "Power system stability - computaton of critical clearing time and stability margin index.," *Thesis and Dissertations*, 1976.

[11] A. H. El-abiad and K. Nagappan, "Transient stability regions of multimachine power systems," *IEEE Transactions on Power Apparatus and Systems*, vol. PAS-85, pp. 169–179, Feb 1966.

[12] M. M. Hossain and M. H. Ali, "Transient stability improvement of doubly fed induction generator based variable speed wind generator using dc resistive fault current limiter," *IET Renewable Power Generation*, 2016.

[13] P. Kundur, J. Paserba, V. Ajjarapu, G. Andersson, A. Bose, C. Canizares, N. Hatziargyriou, D. Hill, A. Stankovic, C. Taylor, T. V. Cutsem, and V. Vittal, "Definition and classification of power system stability ieee/cigre joint task force on stability terms and definitions," *IEEE Transactions on Power Systems*, vol. 19, pp. 1387–1401, Aug 2004.

[14] M. A. Pai and P. W. Sauer, "Stability analysis of power systems by lyapunov's direct method," *IEEE Control Systems Magazine*, vol. 9, 1989.

[15] A. Michel, A. Fouad, and V. Vittal, "Power system transient stability using individual machine energy functions," *IEEE Transactions on Circuits and Systems*, vol. 30, pp. 266–276, May 1983.

[16] S. Sharma, S. Kulkarni, A. Maksud, S. R. Wagh, and N. M. Singh, "Transient stability assessment and synchronization of multimachine power system using kuramoto model," in *2013 North American Power Symposium (NAPS)*, pp. 1–6, Sept 2013.

[17] T. Chaiyatham and I. Ngamroo, "Improvement of power system transient stability by pv farm with fuzzy gain scheduling of pid controller," *IEEE Systems Journal*, vol. 11, pp. 1684–1691, Sept 2017.

[18] A. Vahidnia, G. Ledwich, and E. W. Palmer, "Transient stability improvement through wide-area controlled svcs," *IEEE Transactions on Power Systems*, vol. 31, pp. 3082–3089, July 2016.

[19] M. K. Musaazi, R. B. I. Johnson, and B. J. Cory, "Multimachine system transient stability improvement using transient power system stabilizers (tpss)," *IEEE Power Engineering Review*, Dec 1986.

[20] N. Ghanbari, H. Golzari, H. Mokhtari, and M. Poshtan, "Optimum location for operation of small size distributed generators," in *2017 IEEE 6th International Conference on Renewable Energy Research and Applications (ICRERA)*, pp. 300–303, Nov 2017.

[21] Y. Wang, D. J. Hill, R. H. Middleton, and L. Gao, "Transient stability enhancement and voltage regulation of power systems," *IEEE Transactions on Power Systems*, vol. 8, pp. 620–627, May 1993.

[22] M. M. Adibi, J. N. Borkoski, and R. J. Kafka, "Power system restoration???the second task force report," *IEEE Power Engineering Review*, vol. PER-7, pp. 36–36, Nov 1987.

[23] S. Chen and H. Glavitsch, "Stabilizing switching," *IEEE Transactions on Power Systems*, vol. 8, pp. 1511–1517, Nov 1993.

[24] A. Fouad and V. Vittal, *Power System Transient Stability Analysis Using the Transient Energy Function Method*. Pearson Education, 1991.

[25] M. Tajdinian, A. R. Seifi, and M. Allahbakhshi, "Calculating probability density function of critical clearing time: Novel formulation, implementation and application in probabilistic transient stability assessment," *International Journal of Electrical Power Energy Systems*, vol. 103, pp. 622 – 633, 2018.

[26] I. A. Hiskens and D. J. Hill, "Energy functions, transient stability and voltage behaviour in power systems with nonlinear loads," *IEEE Transactions on Power Systems*, vol. 4, pp. 1525–1533, Nov 1989.

[27] D. O'Kelly and G. Musgrave, "Improvement of power-system transient stability by phase-shift insertion," *Electrical Engineers, Proceedings of the Institution of*, vol. 120, pp. 247–252, February 1973.

[28] S. Geraee, M. Shafiei, A. R. Sahami, and S. Alavi, "Position sensorless and adaptive speed design for controlling brushless dc motor drives," in *2017 North American Power Symposium (NAPS)*, pp. 1–6, Sept 2017.

[29] A. Al-Subhi, S. Al-Alwani, and I. El-Amin, "Mathematical-based accurate prediction model of output ac power for grid-connected photovoltaic system," in *2017 Saudi Arabia Smart Grid (SASG)*, pp. 1–6, Dec 2017.

[30] M. Tajdinian, M. Z. Jahromi, M. Jalalpour, and S. M. Kouhsari, "Comprehensive and innovative method for dynamic phasor and frequency estimation," in *The 9th Power Systems Protection and Control Conference (PSPC2015)*, pp. 42–48, Jan 2015.

[31] M. T. Mehdi Zareian Jahromi and M. Jalalpour, "A secure-coordinated expansion planning of generation and transmission using game theory and minimum singular value," *International Journal of Electrical and Computer Engineering*, vol. 4, pp. 868 – 881, 2014.

[32] M. Mahmoudi and K. Tomsovic, "A distributed control design methodology for damping critical modes in power systems," in *2016 IEEE Power and Energy Conference at Illinois (PECI)*, pp. 1–6, Feb 2016.

[33] A. A. Fouad and S. E. Stanton, "Transient stability of a multi-machine power system. part ii: Critical transient energy," *IEEE Transactions on Power Apparatus and Systems*, vol. PAS-100, pp. 3417–3424, July 1981.

[34] K. Uemura, J. Matsuki, I. Yamada, and T. Tsuji, "Approximation of an energy function in transient stability analysis of power systems," *Electrical Engineering in Japan*, vol. 92, no. 6, pp. 96–100, 1972.

[35] M. Amini and M. Almassalkhi, "Investigating delays in frequency-dependent load control," in *Innovative Smart Grid Technologies-Asia (ISGT-Asia), 2016 IEEE*, pp. 448–453, IEEE, 2016.

[36] A. Thakallapelli, S. J. Hossain, and S. Kamalasadan, "Coherency based online wide area control of wind integrated power grid," in *2016 IEEE International Conference on Power Electronics, Drives and Energy Systems (PEDES)*, pp. 1–6, Dec 2016.

[37] C. Mishra, J. S. Thorp, V. A. Centeno, and A. Pal, "Stability region estimation under low voltage ride through constraints using sum of squares," in *2017 North American Power Symposium (NAPS)*, pp. 1–6, Sept 2017.

[38] A. A. Edris, "Enhancement of first-swing stability using a high-speed phase shifter," *IEEE Transactions on Power Systems*, vol. 6, pp. 1113–1118, Aug 1991.

[39] P. Kundur, M. Klein, G. J. Rogers, and M. S. Zywno, "Application of power system stabilizers for enhancement of overall system stability," *IEEE Transactions on Power Systems*, vol. 4, pp. 614–626, May 1989.

[40] A. A. Fouad and S. E. Stanton, "Transient stability of a multi-machine power system part i: Investigation of system trajectories," *IEEE Transactions on Power Apparatus and Systems*, July 1981.

[41] R. Yousefian, A. Sahami, and S. Kamalasadan, "Hybrid energy function based real-time optimal wide-area transient stability controller for power system stability," in *2015 IEEE Industry Applications Society Annual Meeting*, pp. 1–8, Oct 2015.

[42] A. R. Bergen and D. J. Hill, "A structure preserving model for power system stability analysis," *IEEE Transactions on Power Apparatus and Systems*, vol. PAS-100, pp. 25–35, Jan 1981.

[43] J. Machowski, S. Robak, J. W. Bialek, J. R. Bumby, and N. Abi-Samra, "Decentralized stability-enhancing control of synchronous generator," in *2000 Power Engineering Society Summer Meeting (Cat. No.00CH37134)*, vol. 2, pp. 923 vol. 2–, July 2000.

[44] H. Bagherpoor and F. R. Salmasi, "Robust model reference adaptive output feedback tracking for uncertain linear systems with actuator fault based on reinforced dead-zone modification," *ISA Transactions*, vol. 57, pp. 51 – 56, 2015.

[45] F. Salehi, A. Brahman, and R. K. and, "Reliability assessment of automated substation and functional integration," in *2016 IEEE Industry Applications Society Annual Meeting*, pp. 1–7, Oct 2016.

[46] G. G. Karady and J. Gu, "A hybrid method for generator tripping," *IEEE Transactions on Power Systems*, vol. 17, pp. 1102–1107, Nov 2002.

[47] Z. Mahmoodzadeh, N. Ghanbari, A. Mehrizi-Sani, and M. Ehsan, "Energy loss estimation in distribution networks using stochastic simulation," in *2015 IEEE Power Energy Society General Meeting*, pp. 1–5, July 2015.

[48] M. Gholizadeh, A. Yazdizadeh, and H. Mohammad-Bagherpour, "Fault detection and identification using combination of ekf and neuro-fuzzy network applied to a chemical process (cstr)," *Pattern Analysis and Applications*, Aug 2017.

[49] E. D. Tuglie, M. L. Scala, and P. Scarpellini, "Real-time preventive actions for the enhancement of voltage-degraded trajectories," *IEEE Transactions on Power Systems*, vol. 14, pp. 561–568, May 1999.

[50] A. E. Hammad, "Analysis of power system stability enhancement by static var compensators," *IEEE Transactions on Power Systems*, vol. 1, pp. 222–227, Nov 1986.

[51] V. Miranda, J. N. Fidalgo, J. A. P. Lopes, and L. B. Almeida, "Real time preventive actions for transient stability enhancement with a hybrid neural network-optimization approach," *IEEE Transactions on Power Systems*, vol. 10, pp. 1029–1035, May 1995.

[52] J. Renedo, A. Garcia-Cerrada, and L. Rouco, "Active power control strategies for transient stability enhancement of ac/dc grids with vsc-hvdc multi-terminal systems," *IEEE Transactions on Power Systems*, vol. 31, pp. 4595–4604, Nov 2016.

[53] L. Hui, D. Peiyong, W. Lin, and Y. Yu, "Neural network prediction methods of power consumption for gshp system with bilateral variable flow," in *2017 36th Chinese Control Conference (CCC)*, pp. 2023–2026, July 2017.

[54] S. Zhang, Y. Wang, M. Liu, and Z. Bao, "Data-based line trip fault prediction in power systems using lstm networks and svm," *IEEE Access*, vol. 6, pp. 7675–7686, 2018.

[55] Y. Zhou, H. Sun, Q. Guo, B. Xu, J. Wu, and L. Hao, "Data driven method for transient stability prediction of power systems considering incomplete measurements," in *2017 IEEE Conference on Energy Internet and Energy System Integration (EI2)*, pp. 1–6, Nov 2017.

[56] K. Venugopal, P. Madhusudan, and A. Amrutha, "Artificial neural network based fault prediction framework for transformers in power systems," in *2017 International Conference on Computing Methodologies and Communication (IC-CMC)*, pp. 520–523, July 2017.

[57] M. Z. Jahromi and S. M. Kouhsari, "A high-precision real-time approach to calculate closest unstable equilibrium points," *International Journal of Electrical Power Energy Systems*, vol. 89, pp. 82 – 93, 2017.

[58] M. Raoufat, K. Tomsovic, and S. M. Djouadi, "Virtual actuators for wide-area damping control of power systems," *IEEE Transactions on Power Systems*, vol. 31, pp. 4703–4711, Nov 2016.

[59] N. Ghanbari, H. Mokhtari, and S. Bhattacharya, "Optimizing operation indices considering different types of distributed generation in microgrid applications," *Energies*, vol. 11, no. 4, 2018.

[60] N. Ghanbari, M. Mobarrez, and S. Bhattacharya, "A review and modeling of different droop control based methods for battery state of the charge balancing in dc microgrids," in *IECON 2018 - 44th Annual Conference of the IEEE Industrial Electronics Society*, pp. 1625–1632, Oct 2018.

[61] N. Ghanbari, S. Bhattacharya, and M. Mobarrez, "Modeling and stability analysis of a dc microgrid employing distributed control algorithm," in *2018 9th IEEE International Symposium on Power Electronics for Distributed Generation Systems (PEDG)*, pp. 1–7, June 2018.

[62] R. Yousefian, R. Bhattarai, and S.Kamalasadan, "Direct intelligent wide-area damping controller for wind integrated power system," in *2016 IEEE Power and Energy Society General Meeting (PESGM)*, pp. 1–5, July 2016.

[63] A. Llamas, J. De La Ree Lopez, L. Mili, A. G. Phadke, and J. S. Thorp, "Clarifications of the bcu method for transient stability analysis," *IEEE Transactions on Power Systems*, vol. 10, pp. 210–219, Feb 1995.

[64] Y. Tang, F. Li, Q. Wang, and Y. Xu, "Hybrid method for power system transient stability prediction based on two-stage computing resources," *IET Generation, Transmission Distribution*, vol. 12, no. 8, pp. 1697–1703, 2018.

[65] T. Athay, R. Podmore, and S. Virmani, "A practical method for the direct analysis of transient stability," *IEEE Transactions on Power Apparatus and Systems*, vol. PAS-98, pp. 573–584, March 1979.

[66] A. Pai, *Energy Function Analysis for Power System Stability*. Power Electronics and Power Systems, Springer US, 1989.

[67] S. Geraee, H. Mohammadbagherpoor, M. Shafiei, M. Valizadehdeh, F. Montazeri, and M. R. Feyzi, "A modified dtc with capability of regenerative braking energy in bldc driven electric vehicles using adaptive control theory," *CoRR*, vol. abs/1710.01873, 2017.

[68] S. M. Mazhari, A. Sahami, and S. M. Kouhsari, "A large-change sensitivity based approach for distributed harmonic resonance assessment in multi-area interconnected power systems," in *2018 IEEE Power and Energy Conference at Illinois (PECI)*, pp. 1–8, Feb 2018.

[69] A. Sahami and S. M. Kouhsari, "Making a dynamic interaction between two power system analysis software," in *2017 North American Power Symposium (NAPS)*, pp. 1–6, Sept 2017.

[70] F. Salehi, I. B. M. Matsuo, and W. Lee, "Detection of sub-synchronous control interaction (ssci) using modal identification analysis and fft," in *2018 North American Power Symposium (NAPS)*, pp. 1–5, Sep. 2018.

[71] H. K. Nia, F. Salehi, M. Sahni, N. Karnik, and H. Yin, "A filter-less robust controller for damping ssci oscillations in wind power plants," in *2017 IEEE Power Energy Society General Meeting*, pp. 1–1, July 2017.

[72] R. Yousefian, R. Bhattarai, and S. Kamalasadan, "Transient stability enhancement of power grid with integrated wide area control of wind farms and synchronous generators," *IEEE Transactions on Power Systems*, vol. 32, pp. 4818–4831, Nov 2017.

[73] M. Pavella, "Generalized one-machine equivalents in transient stability studies," *IEEE Power Engineering Review*, vol. 18, pp. 50–52, Jan 1998.

[74] M. Tajdinian, A. R. Seifi, and M. Allahbakhshi, "Sensitivity-based approach for real-time evaluation of transient stability of wind turbines interconnected to power grids," *IET Renewable Power Generation*, vol. 12, no. 6, pp. 668–679, 2018.

[75] M. J. Al-Khishali, "Comparison between fast direct methods for transient stability assessment," in *2012 IEEE Electrical Power and Energy Conference*, pp. 233–236, Oct 2012.

[76] L. G. W. Roberts, A. R. Champneys, K. R. W. Bell, and M. di Bernardo, "Analytical approximations of critical clearing time for parametric analysis of power system transient stability," *IEEE Journal on Emerging and Selected Topics in Circuits and Systems*, vol. 5, pp. 465–476, Sep. 2015.

[77] R. Yousefian, A. Sahami, and S.Kamalasadan, "Hybrid transient energy function-based real-time optimal wide-area damping controller," *IEEE Transactions on Industry Applications*, pp. 1506–1516, 2017.

[78] "Proposed terms and definitions for power system stability task force on terms amp; definitions system dynamic performance subcommittee power system engineering committee," *IEEE Power Engineering Review*, vol. PER-2, pp. 28–28, July 1982.

[79] C. J. Tavora and O. J. M. Smith, "Characterization of equilibrium and stability in power systems," *IEEE Transactions on Power Apparatus and Systems*, vol. PAS-91, pp. 1127–1130, May 1972.

[80] M. Tajdinian, A. R. Seifi, and M. Allahbakhshi, "Transient stability of power grids comprising wind turbines: New formulation, implementation, and application in real-time assessment," *IEEE Systems Journal*, pp. 1–12, 2018.

[81] T. L. Vu and K. Turitsyn, "Lyapunov functions family approach to transient stability assessment," *IEEE Transactions on Power Systems*, vol. 31, pp. 1269–1277, March 2016.

[82] M. Watanabe, Y. Mitani, and K. Tsuji, "A numerical method to evaluate power system global stability determined by limit cycle," *IEEE Transactions on Power Systems*, vol. 19, pp. 1925–1934, Nov 2004.

[83] N. Yorino, A. Priyadi, H. Kakui, and M. Takeshita, "A new method for obtaining critical clearing time for transient stability," *IEEE Transactions on Power Systems*, vol. 25, pp. 1620–1626, Aug 2010.

[84] H.-D. Chiang, F. Wu, and P. Varaiya, "Foundations of direct methods for power system transient stability analysis," *IEEE Transactions on Circuits and Systems*, vol. 34, pp. 160–173, Feb 1987.

[85] N. G. Bretas and L. F. C. Alberto, "Energy function for power systems with transmission losses: extension of the invariance principle," in *PowerCon 2000. 2000 International Conference on Power System Technology. Proceedings (Cat. No.00EX409)*, vol. 1, pp. 145–150 vol.1, 2000.

[86] T. Chen, H. Pourbabak, and W. Su, "A game theoretic approach to analyze the dynamic interactions of multiple residential prosumers considering power flow constraints," in *2016 IEEE Power and Energy Society General Meeting (PESGM)*, pp. 1–5, July 2016.

[87] K. Ogata, *Discrete-Time Control Systems*. Prentice-Hall International Editions, Prentice-Hall, 1987.

[88] Q. Jiang and Z. Huang, "An enhanced numerical discretization method for transient stability constrained optimal power flow," *IEEE Transactions on Power Systems*, vol. 25, pp. 1790–1797, Nov 2010.

[89] V. Vittal, S. Rajagopal, A. A. Fouad, M. A. El-Kady, E. Vaahedi, and V. F. Carvalho, "Transient stability analysis of stressed power systems using the energy function method," *IEEE Transactions on Power Systems*, vol. 3, pp. 239–244, Feb 1988.

[90] P. Magnusson, *The Transient-energy Method of Calculating Stability ...* American Institute of electrical engineers, 1946.

[91] P. C. Magnusson, "The transient-energy method of calculating stability," *Transactions of the American Institute of Electrical Engineers*, vol. 66, pp. 747–755, Jan 1947.

[92] P. Aylett, "The energy-integral criterion of transient stability limits of power systems," *Proceedings of the IEE - Part C: Monographs*, vol. 105, pp. 527–536(9), September 1958.

[93] C. J. Tavora and O. J. M. Smith, "Equilibrium analysis of power systems," *IEEE Transactions on Power Apparatus and Systems*, vol. PAS-91, pp. 1131–1137, May 1972.

[94] K. Uemura, J. Matsuki, I. Yamada, and T. Tsuji, "Approximation of an energy function in transient stability analysis of power systems," *Electrical Engineering in Japan*, vol. 92, no. 6, pp. 96–100, 1972.

[95] C. L. Gupta and A. H. El-Abiad, "Determination of the closest unstable equilibrium state for liapunov methods in transient stability studies," *IEEE Transactions on Power Apparatus and Systems*, vol. 95, pp. 1699–1712, Sep. 1976.

[96] H. Chiang, *Direct Methods for Stability Analysis of Electric Power Systems: Theoretical Foundation, BCU Methodologies, and Applications*. Wiley, 2011.

[97] A. Bose, "Application of direct methods to transient stability analysis of power systems system dynamic performance subcommittee," *IEEE Power Engineering Review*, vol. PER-4, pp. 33–34, July 1984.

[98] M. Doostan and B. H. Chowdhury, "Power distribution system equipment failure identification using machine learning algorithms," pp. 140 – 147, 2017.

[99] A. Pal, C. Mishra, A. K. S. Vullikanti, and S. S. Ravi, "General optimal substation coverage algorithm for phasor measurement unit placement in practical systems," *IET Generation, Transmission Distribution*, vol. 11, no. 2, pp. 347–353, 2017.

[100] J. Sun, H. Zheng, C. L. DeMarco, and Y. Chai, "Energy function-based model predictive control with upfcs for relieving power system dynamic current violation," *IEEE Transactions on Smart Grid*, vol. 7, pp. 2933–2942, Nov 2016.

[101] D. L. Lubkeman and G. T. Heydt, "The application of dynamic programming in a discrete supplementary control for transient stability enhancement of multimachine power systems," *IEEE Transactions on Power Apparatus and Systems*, vol. PAS-104, pp. 2342–2348, Sept 1985.

[102] E. Kreyszig and E. Norminton, *Mathematica Computer Manual for Seventh Edition Advanced Engineering Mathematics, Erwin Kreyszig*. Wiley, 1995.

[103] E. Kreyszig, *Advanced Engineering Mathematics: Maple Computer Guide*. New York, NY, USA: John Wiley & Sons, Inc., 8th ed., 2000.

[104] M. MiloÅ¡eviÄ and M. JovanoviÄ, "An application of taylor series in the approximation of solutions to stochastic differential equations with time-dependent delay," *Journal of Computational and Applied Mathematics*, vol. 235, no. 15, pp. 4439 – 4451, 2011.

[105] M. Eslahchi and M. Dehghan, "Application of taylor series in obtaining the orthogonal operational matrix," *Computers Mathematics with Applications*, vol. 61, no. 9, pp. 2596 – 2604, 2011.

[106] A. Sahami and S. Kamalasadan, "Prediction and enhancement of power system transient stability using taylor series," in *2018 North American Power Symposium (NAPS)*, pp. 1–6, Sep. 2018.

[107] A. B. Birchfield, T. Xu, K. M. Gegner, K. S. Shetye, and T. J. Overbye, "Grid structural characteristics as validation criteria for synthetic networks," *IEEE Transactions on Power Systems*, vol. 32, pp. 3258–3265, July 2017.

[108] A. CIFCI and Y. Uyaroglu, "Energy function analysis of a two-machine infinit-bus power syatem y lyapunovâs second method," *IEEE Transactions on Power Apparatus and Systems*, vol. II, July 1981.

[109] *Power System Stability And Control*. EPRI power system engineering series, McGraw-Hill, 1994.

[110] F. H. J. R. Silva, L. F. C. Alberto, and G. Bretas, "Extended lyapunov function for power systems with transmission losses," in *2003 IEEE Bologna Power Tech Conference Proceedings,*, vol. 3, pp. 6 pp. Vol.3–, June 2003.

[111] N. Narasimhamurthi, "On the existence of energy function for power systems with transmission losses," *IEEE Transactions on Circuits and Systems*, vol. 31, pp. 199–203, Feb 1984.

[112] P. Sauer and M. Pai, *Power System Dynamics and Stability*. Prentice Hall, 1998.

[113] E. Nechadi, M. Harmas, A. Hamzaoui, and N. Essounbouli, "A new robust adaptive fuzzy sliding mode power system stabilizer," *International Journal of Electrical Power Energy Systems*, vol. 42, no. 1, pp. 1 – 7, 2012.

APPENDIX A: Power Series in Function Approximation

A.1 Power Series Defenition

The power series method is a standard method for solving linear ODEs with variable coefficients. It pro solutions in the form of power series. These series can be used for computing values, graphing curves, proving formulas, and exploring properties of solutions.

A power series in powers of $(z - z_0)$ is a series of the following form:

$$\sum_{n=0}^{\infty} a_n (z - z_0)^n = a_0 + a_1(z - z_0) + a_2(z - z_0)^2 + \cdots \tag{A.1}$$

where z is a complex variable, $a_0, a_1, \cdots$ are complex (or real) constants, called the coefficients of the series, and z_0 is a complex (or real) constant, called the center of the series. As a particular case, if $z_0 = 0$, we obtain a power series of z:

$$\sum_{n=0}^{\infty} a_n z^n = a_0 + a_1 z + a_2 z^2 + \cdots \tag{A.2}$$

A.1.1 Convergence of a power Series

Consider the smallest circle with center z_0 that includes all the points at which a given power series, Eq. A.1, converges. Let R denote its radius. The circle $|z - z_0| = R$ is called the circle of convergence and its radius R the radius of convergence of equation A.1. The following is worth reminding while studying the convergence of a power series:

1. Every power series (Eq. A.1) converges at the center z_0

2. If Eq. A.1 converges at a point $z = z_1 \neq z_0$, it converges absolutely for every z closer to z_0 than z_1, that is $|z - z_0| < |z_1 - z_0|$. See figure A.1.

3. If Eq. A.1 diverges at $z = z_2$, it diverges for every z farther away from z_0 than
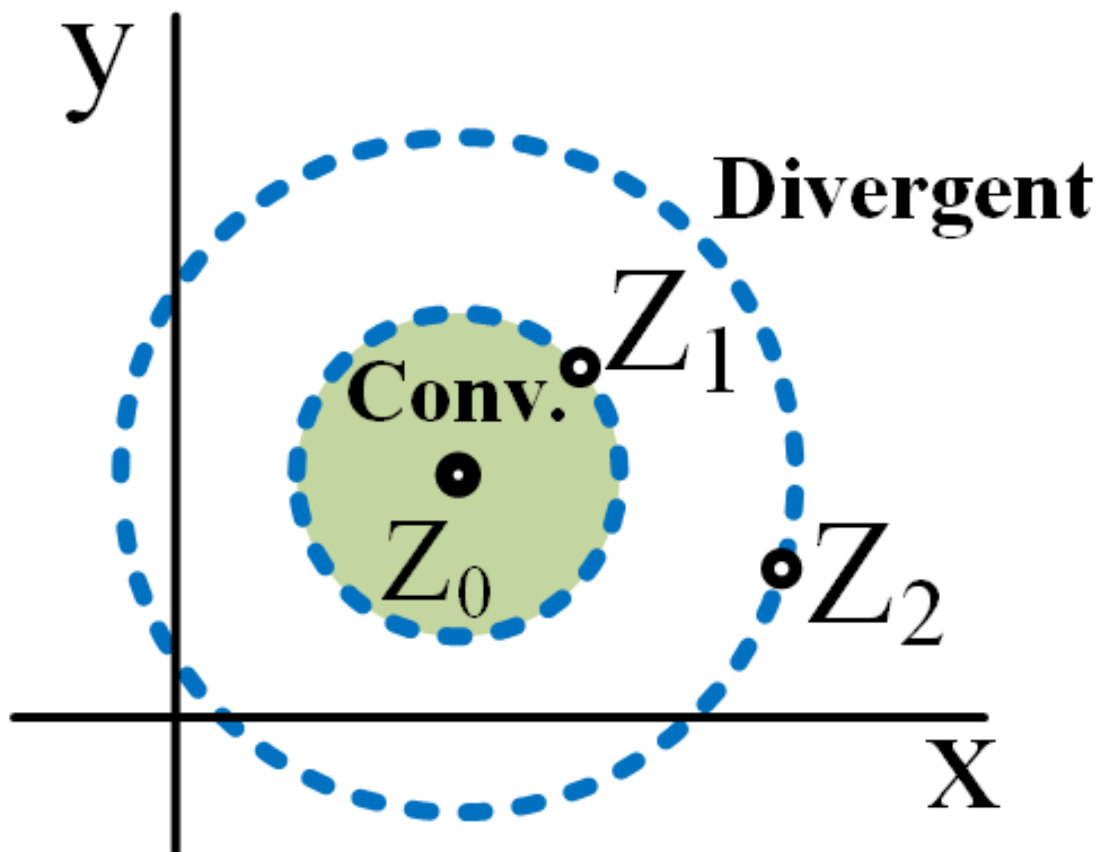
z_2 (see figure A.1).

Figure A.1: Region of convergence of a power series.

A.2   Taylor and Maclaurin Series

The Taylor series of a function $f(z)$, is:

$$f(z) = \sum_{n=1}^{\infty} a_n(z - z_0)^n \tag{A.3}$$

where

$$a_n = \frac{1}{n!} f^{(n)}(z_0)$$

or

$$a_n = \frac{1}{2\pi i} \oint_C \frac{f(z^*)}{(z^* - z_0)^{n+1}} dz^* \tag{A.4}$$

In Eq. A.4 we integrate counterclockwise around a simple closed path C that contains z_0 in its interior and is such that $f(z)$ is analytic in a domain containing C and every point inside C. A Maclaurin series is a Taylor series with center $z_0 = 0$.

The *nth* partial sum of Eq. A.1 is defined as Eq. A.5:

$$S_n(z) = a_0 + a_1(z - z_0) + a_2(z - z_0)^2 + \cdots + a_n(z - z_0)^n \tag{A.5}$$

Where $n = 0, 1, \cdots$. If we omit the terms of S_n from Eq. A.1, the remaining expression would be like Eq. A.6:

$$R_n(z) = a_{n+1}(z - z_0)^{n+1} + a_{n+2}(z - z_0)^{n+2} + \cdots \tag{A.6}$$

This expression is called the remainder of Eq. A.1 after the term $a_n(z - z_0)^n$.

In this way we have now associated with Eq. A.1 the sequence of the partial sums $S_0(z), S_1(z), S_2(z), \cdots$. If for some $z = z_1$ this sequence converges, say, $\lim_{n\to\infty} S_n(z_1) = S(z_1)$, then the series Eq. A.1 is called converged at $z = z_1$, the numbers $S(z_1)$ is called the value of sum of Eq. A.1 at z_1, and we can write

$S(z_1) = \sum_{m=0}^{\infty} a_m(z_1 - z_0)^m$

Then we have for every n,

$$S(z_1) = S_n(z_1) + R_n(z_1) \tag{A.7}$$

If that sequence diverges at $z = z_1$, the series A.1 is called divergent at $z = z_1$.

In the case of convergence, for any positive ϵ, there will be an N (depending on ϵ) such that, by Eq. A.7:

$$|R_n(z_1)| = |S(z_1) - S_n(z_1)| < \epsilon, \forall n > N \tag{A.8}$$

The remainder of the Taylor series A.3 after the term $a_n(z - z_0)^n$ can be found via equation A.9:

$$R_n(z) = \frac{(z - z_0)^{n+1}}{2\pi i} \oint_C \frac{f(z^*)}{(z^* - z_0)^{n+1}(z^* - z)} dz^* \tag{A.9}$$

Writing out the corresponding partial sum of A.3, we thus have:

$$f(z) = f(z_0) + \frac{z - z_0}{1!} f'(z_0) + \frac{(z - z_0)^2}{2!} f''(z_0) + \cdots$$

$$+ \frac{(z - z_0)^n}{n!} f^n(z_0) + R_n(z) \tag{A.10}$$

This is called Taylor's formula with the remainder. We see that the Taylor series are power series. From section 3.2.1 we know that power series represent analytic functions. Now, we show that every analytic function can be represented by power series, namely, by Taylor series (with various centers). This makes the Taylor series a crucial tool in complex analysis. Indeed, they are more fundamental in complex analysis than their real counterparts are in calculus.

APPENDIX B: Calculating the Error of Approximating the Answer of a Set of

Dependant First Order Differential Equations of Functions f and g

B.1   Scenario 1:

When f' Is Always Accurate and Independent of Prediction

Assume that we have the initial points of a function, we have the accurate value of f' at every point, and the derivatives of the function $(f^{(n)}, \forall n \in N)$ are independent of the prediction. It means that the error of prediction will not be affected by the error from approximating f at each time step or iteration. Also, assume that we have derivatives of function g as a coefficient of function f. Mathematically it means:

$$
\begin{cases}
f^{(n)}(x) & \textit{Always Accurate} \\
\\
g^{(n)}(x) = & a f^{(n-1)}
\end{cases}
\qquad \forall n \in N
\tag{B.1}
$$

Hence, the derivatives of function g will be accurate as well except for $g' = g^{(1)} = f$, which cause the equation to include the error from approximating f.

Iteration 1:

$$
f(t_0 + h) = f(t_0) + \frac{h^1}{1!} f'(t_0) + \frac{h^2}{2!} f''(t_0) + \frac{h^3}{3!} f^{(3)}(t_0) + \cdots
\tag{B.2}
$$

$$
f(t_0 + h) = f(t_0) + \sum_{n=1}^{N} \frac{h^n}{n!} f^{(n)}(t_0) + \sum_{n=N+1}^{\infty} \frac{h^n}{n!} f^{(n)}(t_0)
\tag{B.3}
$$

$$
f(t_0 + h) = \tilde{f}(t_0 + h) + R_1^f
\tag{B.4}
$$

where

$$
\tilde{f}(t_0 + h) = f(t_0) + \sum_{n=1}^{N} \frac{h^n}{n!} f^{(n)}(t_0)
\tag{B.5}
$$

is the Nth order of approximation of function f at $t = t_0 + h$ and

$$Error_1^f = R_1^f = \sum_{n=N+1}^{\infty} \frac{h^n}{n!} f^{(n)}(t_0) \tag{B.6}$$

is the error of this approximation. However, we do not have f. Therefore, it is not possible to find the exact value of the error. Finding a limit for the error will be discussed later.

For predicting function g:

$$g(t_0 + h) = g(t_0) + \frac{h^1}{1!} g'(t_0) + \frac{h^2}{2!} g''(t_0) + \frac{h^3}{3!} g^{(3)}(t_0) + \cdots \tag{B.7}$$

$$g(t_0 + h) = g(t_0) + \sum_{n=1}^{N} \frac{h^n}{n!} g^{(n)}(t_0) + \sum_{n=N+1}^{\infty} \frac{h^n}{n!} g^{(n)}(t_0) \tag{B.8}$$

$$g(t_0 + h) = g(t_0) + \sum_{n=1}^{N} \frac{h^n}{n!} a f^{(n-1)}(t_0) + \sum_{n=N+1}^{\infty} \frac{h^n}{n!} f^{(n-1)}(t_0) \tag{B.9}$$

$$g(t_0 + h) = g(t_0) + ahf(t_0) + \sum_{n=2}^{N} \frac{h^n}{n!} a f^{(n-1)}(t_0) \tag{B.10}$$

$$+ \sum_{n=N+1}^{\infty} \frac{h^n}{n!} f^{(n-1)}(t_0) \tag{B.11}$$

$$g(t_0 + h) = \tilde{g}(t_0 + h) + R_1^g \tag{B.12}$$

where

$$\tilde{g}(t_0 + h) = g(t_0) + ahf(t_0) + \sum_{n=2}^{N} \frac{h^n}{n!} g^{(n)}(t_0) \tag{B.13}$$

is the Nth order of approximation of function f at $t = t_0 + h$ and

$$Error_1^g = R_1^g = \sum_{n=N+1}^{\infty} \frac{h^n}{n!} g^{(n)}(t_0) \tag{B.14}$$

Iteration 2:

Let us predict the value at the moment of $t = t_0 + 2h$

$$f(t_0 + 2h) = f(t_0 + h) + \sum_{n=1}^{\infty} \frac{h^n}{n!} f^{(n)}(t_0 + h) \tag{B.15}$$

$$f(t_0 + 2h) = f(t_0 + h) + \sum_{n=1}^{N} \frac{h^n}{n!} f^{(n)}(t_0 + h)$$

$$+ \sum_{n=N+1}^{\infty} \frac{h^n}{n!} f^{(n)}(t_0 + h) \tag{B.16}$$

$$f(t_0 + 2h) = f(t_0 + h) + \sum_{n=1}^{N} \frac{h^n}{n!} f^{(n)}(t_0 + h) + R_2^f(t_0 + h) \tag{B.17}$$

With the same logic, if we have the exact value of $f(t_0+h)$, the error in approximating $f(t_0 + 2h)$ can be found like previous steps. However, if we do not know the exact value of $f(t_0+h)$, we can use the approximation of it from Eq. B.69. Hence, the first term of Eq. B.78 has an error from the previous approximation step, which will be added to the current approximation error. It means that we are replacing $f(t_0 + h)$ with $\tilde{f}(t_0 + h)$ in Eq. B.78:

$$f(t_0 + 2h) = \tilde{f}(t_0 + h) + \sum_{n=1}^{N} \frac{h^n}{n!} f^{(n)}(t_0 + h) + R_2^f \tag{B.18}$$

To be able to compare it to the situation that we have f, we can replace $\tilde{f}(t_0 + h)$ with $f(t_0 + h) - R_1^f$ from Eq. B.69. So,

$$f(t_0 + 2h) = f(t_0 + h) - R_1^f + \sum_{n=1}^{N} \frac{h^n}{n!} f^{(n)}(t_0 + h) + R_2^f(t_0 + h) \tag{B.19}$$

$$f(t_0 + 2h) = f(t_0 + h) + \sum_{n=1}^{N} \frac{h^n}{n!} f^{(n)}(t_0 + h)$$

$$+R_2^f(t_0 + h) - R_1^f(t_0) \tag{B.20}$$

So:

$$f(t_0 + 2h) = \tilde{f}(t_0 + 2h) + Error_2^f \tag{B.21}$$

where

$$\tilde{f}(t_0 + 2h) = f(t_0 + h) + \sum_{n=1}^{N} \frac{h^n}{n!} f^{(n)}(t_0 + h) \tag{B.22}$$

$$R_2^f(t_0 + h) = \sum_{n=N+1}^{\infty} \frac{h^n}{n!} f^{(n)}(t_0 + h) \tag{B.23}$$

$$Error_2^f = R_2^f(t_0 + h) - R_1^f(t_0) \tag{B.24}$$

With the same logic and procedure we have:

$$g(t_0 + 2h) = g(t_0 + h) - R_1^g + \sum_{n=1}^{N} \frac{h^n}{n!} g^{(n)}(t_0 + h) + R_2^g \tag{B.25}$$

$$g(t_0 + 2h) = g(t_0 + h) - R_1^g + ha(f(t_0 + h) - Error_1^f)$$
$$+ \sum_{n=2}^{N} \frac{h^n}{n!} a f^{(n-1)}(t_0 + h) + R_2^g \tag{B.26}$$

$$Error_2^g = R_2^g - R_1^g - ha Error_1^f \tag{B.27}$$

Iteration 3:

Let's find the next step:

$$f(t_0 + 3h) = f(t_0 + 2h) + \sum_{n=1}^{N} \frac{h^n}{n!} f^{(n)}(t_0 + 2h) + R_3^f(t_0 + 2h) \tag{B.28}$$

we are replacing $f(t_0 + 2h)$ with $\tilde{f}(t_0 + 2h)$

$$f(t_0 + 2h) = \tilde{f}(t_0 + 2h) + \sum_{n=1}^{N} \frac{h^n}{n!} f^{(n)}(t_0 + 2h) + R_3^f(t_0 + 2h) \tag{B.29}$$

To be able to compare it to the situation that we have f, we can replace $\tilde{f}(t_0 + 2h)$ with $f(t_0 + 2h) - Error_2^f$ from Eq. . So,

$$f(t_0 + 3h) = f(t_0 + 2h) - Error_2^f + \sum_{n=1}^{N} \frac{h^n}{n!} f^{(n)}(t_0 + 2h)$$

$$+ R_3^f(t_0 + 2h) \tag{B.30}$$

$$f(t_0 + 3h) = f(t_0 + 2h) + \sum_{n=1}^{N} \frac{h^n}{n!} f^{(n)}(t_0 + 2h)$$

$$+ R_3^f - Error_2^f \tag{B.31}$$

So:

$$f(t_0 + 3h) = \tilde{f}(t_0 + 3h) + Error_3^f \tag{B.32}$$

where

$$\tilde{f}(t_0 + 3h) = f(t_0 + h) + \sum_{n=1}^{N} \frac{h^n}{n!} f^{(n)}(t_0 + 2h) \tag{B.33}$$

$$R_3^f(t_0 + h) = \sum_{n=N+1}^{\infty} \frac{h^n}{n!} f^{(n)}(t_0 + 2h) \tag{B.34}$$

$$Error_3^f = R_3^f(t_0 + 2h) - Error_2^f \tag{B.35}$$

$$Error_3^f = R_3^f(t_0 + 2h) - R_2^f(t_0 + h) + R_1^f(t_0) \tag{B.36}$$

Similarly, for function g, we have:

$$g(t_0 + 3h) = g(t_0 + 2h) - Error_2^g + ha(f(t_0 + 2h) - Error_2^f) \tag{B.37}$$

$$+ \sum_{n=2}^{N} \frac{h^n}{n!} a f^{(n-1)}(t_0 + 2h) + R_3^g \tag{B.38}$$

$$Error_3^g = R_3^g - R_2^g + R_1^g + ha Error_1^f - ha Error_2^f \tag{B.39}$$

In the same way, we have the followings for functions f and g. The equations are presented only for function f, while the same holds by changing superscripts to g:

$$f(t_0 + h) = \tilde{f}(t_0 + h) + Error_1^f \tag{B.40}$$

$$f(t_0 + 2h) = \tilde{f}(t_0 + 2h) + Error_2^f \tag{B.41}$$

$$\vdots$$

$$f(t_0 + kh) = \tilde{f}(t_0 + kh) + Error_k^f \tag{B.42}$$

where,

$$\tilde{f}(t_0 + kh) = f(t_0 + (k-1)h) + \sum_{n=1}^{N} \frac{h^n}{n!} f^{(n)}(t_0 + (k-1)h) \tag{B.43}$$

$$Error_k^f = \sum_{i=1}^{k} (-1)^{k-i} R_i^f \tag{B.44}$$

$$R_i^f = \sum_{n=N+1}^{\infty} \frac{h^n}{n!} f^{(n)}(t_0 + (i-1)h) \tag{B.45}$$

$$Error_k^g = \sum_{i=1}^{k} R_i^g - ha \sum_{i=1}^{k-1} Error_i^f \tag{B.46}$$

$$R_i^g = \sum_{n=N+1}^{\infty} \frac{h^n}{n!} a f^{(n-1)}(t_0 + (i-1)h) \tag{B.47}$$

Since we do not have f, we cannot find the exact amount of error at each step. However, We can find a range for the error.

In order to find the amount of this error, assume:

$$max(|f^{(n)}(t_0 + (i-1)h)|) = C_i^f, n, i \in N \tag{B.48}$$

So:

$$\left| \sum_{n=N+1}^{\infty} \frac{h^n}{n!} f^{(n)}(t_0 + (i-1)h) \right| \leq \sum_{n=N+1}^{\infty} \frac{h^n}{n!} \left| f^{(n)}(t_0 + (i-1)h) \right| \tag{B.49}$$

$$0 \leq \sum_{n=N+1}^{\infty} \frac{h^n}{n!} \left| f^{(n)}(t_0 + (i-1)h) \right| \leq C_i^f * \sum_{n=N+1}^{\infty} \frac{h^n}{n!} \tag{B.50}$$

So,

$$\left| R_i^f = \sum_{n=N+1}^{\infty} \frac{h^n}{n!} f^{(n)}(t_0 + (i-1)h) \right| \leq C_i^f * \sum_{n=N+1}^{\infty} \frac{h^n}{n!} \tag{B.51}$$

On the other hand, we know that the Taylor expansion for exponential function is

:

$$e^x = \sum_{n=0}^{\infty} \frac{x^n}{n!} \tag{B.52}$$

so

$$C_i^f * \sum_{n=N+1}^{\infty} \frac{h^n}{n!} = C_i(e^h - \sum_{n=0}^{N} \frac{h^n}{n!}) \tag{B.53}$$

Therefore,

$$\left| R_i^f \right| \leq C_i^f (e^h - \sum_{n=0}^{N} \frac{h^n}{n!}), i \in \left\{ 1, 2, \cdots, k \right\} \tag{B.54}$$

if

$$C_m^f = max(C_i), , i \in \left\{ 1, 2, \cdots, k \right\} \tag{B.55}$$

then,

$$\left| R_i^f \right| \leq C_m^f (e^h - \sum_{n=0}^{N} \frac{h^n}{n!}), i \in \left\{ 1, 2, \cdots, k \right\} \tag{B.56}$$

So far, the maximum error of R_i^f is found. However, since the error is cumulative, the $Error_k^f$ should be found. $Error_k^f$ can be found via Eq. B.113, which is repeated:

$$\left| Error_k^f \right| = \left| \sum_{i=1}^{k} (-1)^{k-i} R_i^f \right| \tag{B.57}$$

$$\left| Error_k^f \right| \leq \sum_{i=1}^{k} \left| R_i^f \right| \tag{B.58}$$

From equation B.56 and B.57 it is concluded that:

$$\left|Error_k^f\right| \leq k * C_m^f(e^h - \sum_{n=0}^{N} \frac{h^n}{n!}) \tag{B.59}$$

For 1st order approximation:

$$\left|Error_k^f\right| \leq k * C_m^f(e^h - 1 - h) \tag{B.60}$$

Similarly, for function g it can be said that:

$$|Error_k^g| \leq \sum_{i=1}^{k} |R_i^g| + h\,|a| \left|\sum_{i=1}^{k-1} Error_i^f\right| \tag{B.61}$$

$$\sum_{i=1}^{k} |R_i^g| \leq k * C_m^g(e^h - \sum_{n=0}^{N} \frac{h^n}{n!}) \tag{B.62}$$

$$|Error_k^g| \leq k * C_m^g(e^h - \sum_{n=0}^{N} \frac{h^n}{n!})$$

$$+ h\,|a|\,(k-1)^2 * C_m^f(e^h - \sum_{n=0}^{N} \frac{h^n}{n!}) \tag{B.63}$$

$$C_m^g = aC_m^f \tag{B.64}$$

$$|Error_k^g| \leq (k + h(k-1)^2) * |a|\,C_m^f(e^h - \sum_{n=0}^{N} \frac{h^n}{n!}) \tag{B.65}$$

In power system equations, the maximum change happens in the beginning of a disturbance, hence, in equation B.55, $C_m^f = C_1^f$.

The limits that are found for R_i^f and $Error_i^f$ are based on the worst case scenario. Hence, it is guaranteed that the error will not exceed the mentioned limits. In reality, however, the error will be less than these limits.

B.2   Scenario 2:

When f' Is Not Accurate and Depends on Predicted Value for f

Assume that we have the initial points of a function and the derivative of this function as a function that depends on its value. Then, we want to predict this function and a second function, while the derivative of the second function depends on the first function. In mathematical expression:

$$
\begin{cases}
f^{(n)}(t) = q(t) - bf^{(n-1)}(t) \\[2em]
g^{(n)}(t) = af^{(n-1)}(t)
\end{cases}
\qquad \forall n \in N \qquad (B.66)
$$

where $q(t)$ is a function that is unlimited times differentiable.

$$
f(t_0 + h) = f(t_0) + \sum_{n=1}^{N} \frac{h^n}{n!} f^{(n)}(t_0) + \sum_{n=N+1}^{\infty} \frac{h^n}{n!} f^{(n)}(t_0) \qquad (B.67)
$$

$$
f(t_0 + h) = \tilde{f}(t_0 + h) + R_1^f \qquad (B.68)
$$

where

$$
\tilde{f}(t_0 + h) = f(t_0) + \sum_{n=1}^{N} \frac{h^n}{n!} f^{(n)}(t_0) \qquad (B.69)
$$

is the Nth order of approximation of the function f at $t = t_0 + h$ and

$$
Error_1^f = R_1^f = \sum_{n=N+1}^{\infty} \frac{h^n}{n!} f^{(n)}(t_0) \qquad (B.70)
$$

is the error of this approximation.

$$
g(t_0 + h) = g(t_0) + \sum_{n=1}^{N} \frac{h^n}{n!} g^{(n)}(t_0) + \sum_{n=N+1}^{\infty} \frac{h^n}{n!} g^{(n)}(t_0) \qquad (B.71)
$$

$$
g(t_0 + h) = g(t_0) + \sum_{n=1}^{N} \frac{h^n}{n!} af^{(n-1)}(t_0) + \sum_{n=N+1}^{\infty} \frac{h^n}{n!} af^{(n-1)}(t_0) \qquad (B.72)
$$

$$g(t_0 + h) = g(t_0) + ahf(t_0) + \sum_{n=2}^{N} \frac{h^n}{n!} af^{(n-1)}(t_0) \tag{B.73}$$

$$+ \sum_{n=N+1}^{\infty} \frac{h^n}{n!} af^{(n-1)}(t_0) \tag{B.74}$$

$$g(t_0 + h) = \tilde{g}(t_0 + h) + R_1^g \tag{B.75}$$

where

$$\tilde{g}(t_0 + h) = g(t_0) + ahf(t_0) + \sum_{n=2}^{N} \frac{h^n}{n!} g^{(n)}(t_0) \tag{B.76}$$

is the Nth order approximation of function f at $t = t_0 + h$ and

$$Error_1^g = R_1^g = \sum_{n=N+1}^{\infty} \frac{h^n}{n!} g^{(n)}(t_0) \tag{B.77}$$

Iteration 2:

Let us predict the value at the moment of $t = t_0 + 2h$

$$f(t_0 + 2h) = f(t_0 + h) + \sum_{n=1}^{\infty} \frac{h^n}{n!} f^{(n)}(t_0 + h) \tag{B.78}$$

$$f(t_0 + 2h) = f(t_0 + h) + \sum_{n=1}^{N} \frac{h^n}{n!} f^{(n)}(t_0 + h)$$

$$+ \sum_{n=N+1}^{\infty} \frac{h^n}{n!} f^{(n)}(t_0 + h) \tag{B.79}$$

$$f(t_0 + 2h) = f(t_0 + h) + \sum_{n=1}^{N} \frac{h^n}{n!} f^{(n)}(t_0 + h) + R_2^f(t_0 + h) \tag{B.80}$$

$$f'(t_0 + h) = q'(t_0 + h) - bf(t_0 + h) + bError_1^f \tag{B.81}$$

$$Error^{f'(t_0+h)} = bError_1^f \tag{B.82}$$

$$f''(t_0 + h) = q''(t_0 + h) - bf'(t_0 + h) + b^2 Error_1^f \tag{B.83}$$

$$Error^{f''(t_0+h)} = b^2 Error_1^f \qquad (B.84)$$

$$f^{(3)}(t_0 + h) = q^{(3)}(t_0 + h) - bf''(t_0 + h) + b^3 Error_1^f \qquad (B.85)$$

$$Error^{f^{(3)}(t_0+h)} = b^3 Error_1^f \qquad (B.86)$$

$$\vdots$$

$$f^{(i)}(t_0 + h) = q^{(i)}(t_0 + h) - bf^{(i-1)}(t_0 + h) + b^i Error_1^f \qquad (B.87)$$

$$Error^{f^{(i)}(t_0+h)} = b^i Error_1^f \qquad (B.88)$$

$$\left| Error^{f^{(i)}(t_0+h)} \right| = |b|^i Error_1^f \qquad (B.89)$$

With the same logic, if we have the exact value of $f(t_0 + h)$, the error in approximating $f(t_0 + 2h)$ can be found like previous step. However, if we do not know the exact value of $f(t_0 + h)$, we can use its approximation from Eq. B.69. Hence, the first term of Eq. B.78 has an error from the previous approximation step, which will be added to the current approximation error. It means that we are replacing $f(t_0 + h)$ with $\tilde{f}(t_0 + h)$ in Eq. B.78:

$$f(t_0 + 2h) = \tilde{f}(t_0 + h) + \sum_{n=1}^{N} \frac{h^n}{n!} f^{(n)}(t_0 + h) + R_2^f \qquad (B.90)$$

To be able to compare it to the situation that we have f, we can replace $\tilde{f}(t_0 + h)$ with $f(t_0 + h) - Error_1^f$ from Eq. B.69. So,

$$f(t_0 + 2h) = f(t_0 + h) - Error_1^f + \sum_{n=1}^{N} \frac{h^n}{n!} q^{(n)}(t_0 + h)$$

$$- \sum_{n=1}^{N} \frac{h^n}{n!} bf^{(n-1)}(t_0 + h) + R_2^f(t_0 + h) \qquad (B.91)$$

SO:

$$f(t_0 + 2h) = f(t_0 + h) - Error_1^f + \sum_{n=1}^{N} \frac{h^n}{n!} q^{(n)}(t_0 + h)$$

$$-hbf(t_0 + h) + hbError_1^f - \frac{h^2}{2!} bf'(t_0 + h) + \frac{h^2}{2!} b^2 Error_1^f$$

$$\cdots - \frac{h^N}{(N)!} bf^{(N-1)}(t_0 + h) + \frac{h^N}{(N)!} b^N Error_1^f$$

$$+R_2^f(t_0 + h) \tag{B.92}$$

So:

$$f(t_0 + 2h) = \tilde{f}(t_0 + 2h) + Error_2^f \tag{B.93}$$

where

$$\tilde{f}(t_0 + 2h) = f(t_0 + h) + \sum_{n=1}^{N} \frac{h^n}{n!} f^{(n)}(t_0 + h) \tag{B.94}$$

$$R_2^f(t_0 + h) = \sum_{n=N+1}^{\infty} \frac{h^n}{n!} f^{(n)}(t_0 + h) \tag{B.95}$$

$$Error_2^f = R_2^f - Error_1^f + \sum_{n=1}^{N} \frac{(hb)^n}{n!} Error_1^f \tag{B.96}$$

With the same logic and procedure we have:

$$g(t_0 + 2h) = g(t_0 + h) - R_1^g + \sum_{n=1}^{N} \frac{h^n}{n!} g^{(n)}(t_0 + h) + R_2^g \tag{B.97}$$

$$g(t_0 + 2h) = g(t_0 + h) - R_1^g + ha(f(t_0 + h) - Error_1^f)$$

$$+ \sum_{n=2}^{N} \frac{h^n}{n!} af^{(n-1)}(t_0 + h) + R_2^g \tag{B.98}$$

$$Error_2^g = R_2^g - R_1^g - haError_1^f \tag{B.99}$$

Iteration 3:

Let's find the next step:

$$f(t_0 + 3h) = f(t_0 + 2h) - Error_2^f + \sum_{n=1}^{N} \frac{h^n}{n!} q^{(n)}(t_0 + 2h)$$

$$- \sum_{n=1}^{N} \frac{h^n}{n!} bf^{(n-1)}(t_0 + 2h) + R_3^f(t_0 + 2h) \tag{B.100}$$

SO:

$$f(t_0 + 3h) = f(t_0 + h) - Error_2^f + \sum_{n=1}^{N} \frac{h^n}{n!} q^{(n)}(t_0 + 2h)$$

$$- hbf(t_0 + 2h) + hbError_2^f - \frac{h^2}{2!} bf'(t_0 + 2h) + \frac{h^2}{2!} b^2 Error_2^f$$

$$\cdots - \frac{h^N}{(N)!} bf^{(N-1)}(t_0 + 2h) + \frac{h^N}{(N)!} b^N Error_2^f$$

$$+ R_3^f(t_0 + 2h) \tag{B.101}$$

So:

$$f(t_0 + 3h) = \tilde{f}(t_0 + 3h) + Error_3^f \tag{B.102}$$

where

$$\tilde{f}(t_0 + 3h) = f(t_0 + 2h) + \sum_{n=1}^{N} \frac{h^n}{n!} f^{(n)}(t_0 + 2h) \tag{B.103}$$

$$R_3^f(t_0 + 2h) = \sum_{n=N+1}^{\infty} \frac{h^n}{n!} f^{(n)}(t_0 + 2h) \tag{B.104}$$

$$Error_3^f = R_3^f - Error_2^f + \sum_{n=1}^{N} \frac{(hb)^n}{n!} Error_2^f \tag{B.105}$$

Similarly, for function g, we have:

$$g(t_0 + 3h) = g(t_0 + 2h) - Error_2^g + ha(f(t_0 + 2h) - Error_2^f) \tag{B.106}$$

$$+ \sum_{n=2}^{N} \frac{h^n}{n!} af^{(n-1)}(t_0 + 2h) + R_3^g \tag{B.107}$$

$$Error_3^g = R_3^g - R_2^g + R_1^g + haError_1^f - haError_2^f \tag{B.108}$$

In the same way, we have the followings for functions f and g. The equations are presented only for function f, while the same holds by changing superscripts to g:

$$f(t_0 + h) = \tilde{f}(t_0 + h) + Error_1^f \tag{B.109}$$

$$f(t_0 + 2h) = \tilde{f}(t_0 + 2h) + Error_2^f \tag{B.110}$$

$$\vdots$$

$$f(t_0 + kh) = \tilde{f}(t_0 + kh) + Error_k^f \tag{B.111}$$

where,

$$\tilde{f}(t_0 + kh) = f(t_0 + (k-1)h) + \sum_{n=1}^{N} \frac{h^n}{n!} f^{(n)}(t_0 + (k-1)h) \tag{B.112}$$

$$Error_k^f = R_k^f - Error_{k-1}^f + \sum_{n=1}^{N} \frac{(hb)^n}{n!} Error_{k-1}^f \tag{B.113}$$

$$\sum_{n=1}^{N} \frac{(hb)^n}{n!} = \beta \tag{B.114}$$

$$\left| \sum_{n=1}^{N} \frac{(hb)^n}{n!} Error_{k-1}^f \right| \leq \beta \left| Error_{k-1}^f \right| \tag{B.115}$$

$$\left| Error_k^f \right| \leq \left| R_k^f \right| + \left| (1-\beta)Error_{k-1}^f \right| \tag{B.116}$$

$$\left| Error_k^f \right| \leq \sum_{i=1}^{k} (|1-\beta|)^{k-i} R_i^f \tag{B.117}$$

$$R_i^f \leq C_m^f (e^h - 1 - \alpha) \tag{B.118}$$

$$\left| Error_k^f \right| \leq C_m^f (e^h - 1 - \alpha) \sum_{i=0}^{k-1} (|1-\beta|)^i \tag{B.119}$$

According to geometric progression, if $\alpha\beta \neq 0$, which impose $b \neq 0$, it can be said:

$$\sum_{i=0}^{k-1}(|1-\beta|)^i = \frac{1-(|1-\beta|)^k}{1-(|1-\beta|)} \tag{B.120}$$

$$\left|Error_k^f\right| \leq C_m^f(e^h - 1 - \alpha) * \frac{1-(|1-\beta|)^k}{1-(|1-\beta|)} \tag{B.121}$$

If $|1-\beta| > 1$, the error will increase in an unacceptable rate after some iterations. However, if $|1-\beta| \leq 1$, we can say:

$$\sum_{i=0}^{k-1}(|1-\beta|)^i \leq \sum_{i=0}^{k-1} 1 = k \tag{B.122}$$

Hence:

$$\left|Error_k^f\right| \leq k * C_m^f(e^h - 1 - \alpha) \tag{B.123}$$

$$\tag{B.124}$$

$$\tag{B.125}$$

$$R_i^f = \sum_{n=N+1}^{\infty} \frac{h^n}{n!} f^{(n)}(t_0 + (i-1)h) \tag{B.126}$$

$$Error_k^g = \sum_{i=1}^{k} R_i^g - ha \sum_{i=1}^{k-1} Error_i^f \tag{B.127}$$

$$R_i^g = \sum_{n=N+1}^{\infty} \frac{h^n}{n!} a f^{(n-1)}(t_0 + (i-1)h) \tag{B.128}$$

Similarly, for function g it can be said that:

$$|Error_k^g| \leq \sum_{i=1}^{k} |R_i^g| + h\,|a| \left|\sum_{i=1}^{k-1} Error_i^f\right| \tag{B.129}$$

$$\sum_{i=1}^{k} |R_i^g| \leq k * C_m^g(e^h - \sum_{n=0}^{N} \frac{h^n}{n!}) \tag{B.130}$$

$$\left| \sum_{i=1}^{k-1} Error_i^f \right| \leq \sum_{i=1}^{k-1} k * C_m^f(e^h - 1 - \alpha) \tag{B.131}$$

$$\left| \sum_{i=1}^{k-1} Error_i^f \right| \leq k(k-1) * C_m^f(e^h - 1 - \alpha) \tag{B.132}$$

Using features of geometric progression, when $\alpha\beta \neq 0$:

$$|Error_k^g| \leq \sum_{i=1}^{k} |R_i^g| + h\,|a| \left| \sum_{i=1}^{k-1} Error_i^f \right| \tag{B.133}$$

$$|Error_k^g| \leq k * C_m^g(e^h - 1 - \alpha)$$

$$+ h\,|a| * k * (k-1)C_m^f(e^h - 1 - \alpha) \tag{B.134}$$

$$|Error_k^g| \leq k * |a|\,C_m^f(e^h - 1 - \alpha)$$

$$+ h\,|a| * k * (k-1)C_m^f(e^h - 1 - \alpha) \tag{B.135}$$

$$|Error_k^g| \leq k\,|a|\,C_m^f(e^h - 1 - \alpha) * [1 + h(k-1)] \tag{B.136}$$

APPENDIX C: Mathematical Proof of Relations used in finding Energy Function

Following, the mathematical proof for equations 5.22, 5.23, 5.43, and 5.44, which are used in sections 5.2.1 and 5.2.2 is provided.

For ease of understanding, noted equations are provided again:

$$\sum_{i=1}^{n}\sum_{j=1,\neq i}^{n} C_{ij}Sin\delta_{ij}\dot{\delta}_i = \sum_{i=1}^{n-1}\sum_{j=i+1}^{n} C_{ij}Sin\delta_{ij}\dot{\delta}_{ij}$$

and,

$$\sum_{i=1}^{n}\sum_{j=1,\neq i}^{n} D_{ij}Cos\delta_{ij}\dot{\delta}_i = \sum_{i=1}^{n-1}\sum_{j=i+1}^{n} D_{ij}Cos\delta_{ij}(\dot{\Theta}_i + \dot{\delta}_j)$$

Proof:

$$\sum_{i=1}^{n}\sum_{j=1,\neq i}^{n} C_{ij}Sin\delta_{ij}\dot{\delta}_i =$$

$$\sum_{i=1}^{n} C_{i1}Sin\delta_{i1}\dot{\delta}_i + C_{i2}Sin\delta_{i2}\dot{\delta}_i + \cdots + C_{ii}Sin\delta_{ii}\dot{\delta}_i + \cdots + C_{in}Sin\delta_{in}\dot{\delta}_i - C_{ii}Sin\delta_{ii}\dot{\delta}_i =$$

$$\underline{C_{11}Sin\delta_{11}\dot{\delta}_1} + C_{12}Sin\delta_{12}\dot{\delta}_1 + \cdots + C_{13}Sin\delta_{13}\dot{\delta}_1 + \cdots + C_{1n}Sin\delta_{1n}\dot{\delta}_1 \underline{- C_{11}Sin\delta_{11}\dot{\delta}_1} +$$

$$C_{21}Sin\delta_{21}\dot{\delta}_2 + \underline{C_{22}Sin\delta_{22}\dot{\delta}_2} + \cdots + C_{23}Sin\delta_{23}\dot{\delta}_2 + \cdots + C_{2n}Sin\delta_{2n}\dot{\delta}_2 \underline{- C_{22}Sin\delta_{22}\dot{\delta}_2} +$$

$$C_{31}Sin\delta_{31}\dot{\delta}_3 + C_{32}Sin\delta_{32}\dot{\delta}_3 + \underline{C_{33}Sin\delta_{33}\dot{\delta}_3} + \cdots + C_{3n}Sin\delta_{3n}\dot{\delta}_3 \underline{- C_{33}Sin\delta_{33}\dot{\delta}_3} +$$

$$\vdots \qquad\qquad \vdots \qquad\qquad \vdots \qquad\qquad \vdots \qquad :C_{n1}Sin\delta_{n1}\dot{\delta}_n + C_{n2}Sin\delta_{n2}\dot{\delta}_n +$$

$$C_{n3}Sin\delta_{n3}\dot{\delta}_n + \cdots + \underline{C_{nn}Sin\delta_{nn}\dot{\delta}_n} \underline{- C_{nn}Sin\delta_{nn}\dot{\delta}_n} =$$

$$[C_{12}Sin\delta_{12}\dot{\delta}_1 + C_{21}Sin\delta_{21}\dot{\delta}_2] + [C_{13}Sin\delta_{13}\dot{\delta}_1 + C_{31}Sin\delta_{31}\dot{\delta}_3] + \cdots + [C_{1n}Sin\delta_{1n}\dot{\delta}_1 + C_{n1}Sin\delta_{n1}\dot{\delta}_n] +$$

$$[C_{23}Sin\delta_{23}\dot{\delta}_2 + C_{32}Sin\delta_{32}\dot{\delta}_3] + [C_{24}Sin\delta_{24}\dot{\delta}_2 + C_{42}Sin\delta_{42}\dot{\delta}_4] + \cdots + [C_{2n}Sin\delta_{2n}\dot{\delta}_2 + C_{n2}Sin\delta_{n2}\dot{\delta}_n] +$$

$[C_{34}Sin\delta_{34}\dot\delta_3+C_{43}Sin\delta_{43}\dot\delta_4]+[C_{35}Sin\delta_{35}\dot\delta_3+C_{53}Sin\delta_{53}\dot\delta_5]+\cdots+[C_{3n}Sin\delta_{3n}\dot\delta_3+C_{n3}Sin\delta_{n3}\dot\delta_n]+$

$$\vdots \qquad\qquad \vdots \qquad\qquad \vdots \qquad\qquad \vdots \qquad :[C_{(n-1)n)}Sin\delta_{(n-1)n}\dot\delta_{(n-1)} +$$

$C_{n(n-1)}Sin\delta_{n(n-1)}\dot\delta_n]=$

$$C_{12}Sin\delta_{12}\dot\delta_{12} + C_{13}Sin\delta_{13}\dot\delta_{13} + \cdots + C_{1n}Sin\delta_{1n}\dot\delta_{1n}+$$

$$C_{23}Sin\delta_{23}\dot\delta_{23} + C_{24}Sin\delta_{24}\dot\delta_{24} + \cdots + C_{2n}Sin\delta_{2n}\dot\delta_{2n}+$$

$$C_{34}Sin\delta_{34}\dot\delta_{34} + C_{35}Sin\delta_{35}\dot\delta_{35} + \cdots + C_{3n}Sin\delta_{3n}\dot\delta_{3n}+$$

$$\vdots \qquad\qquad \vdots \qquad\qquad \vdots \qquad\qquad \vdots \qquad \vdots$$

$$C_{(n-1)n}Sin\delta_{(n-1)n}\dot\delta_{(n-1)n}$$

$=$

$$\sum_{i=1}^{n-1}\sum_{j=i+1}^{n} C_{ij}Sin\delta_{ij}\dot\delta_{ij}$$

$$\Rightarrow \sum_{i=1}^{n}\sum_{j=1,\neq i}^{n} C_{ij}Sin\delta_{ij}\dot\delta_i = \sum_{i=1}^{n-1}\sum_{j=i+1}^{n} C_{ij}Sin\delta_{ij}\dot\delta_{ij}$$

Considering that $Cos(\delta_i - \delta_j) = Cos(\delta_j - \delta_i)$, in the same way, it can be proved that:

$$\sum_{i=1}^{n}\sum_{j=1,\neq i}^{n} D_{ij}Cos\delta_{ij}\dot\delta_i = \sum_{i=1}^{n-1}\sum_{j=i+1}^{n} D_{ij}Cos\delta_{ij}(\dot\delta_i + \dot\delta_j)$$